TID--25438

R-6914-925

AJA

A STUDY OF EARTHQUAKE INPUT MOTIONS FOR SEISMIC DESIGN

by

Stuart D. Werner

June 1970

Contract No. AT(49-5)-3012

Prepared for

UNITED STATES ATOMIC ENERGY COMMISSION
Division of Reactor Standards
Washington, D.C.

AGBABIAN-JACOBSEN ASSOCIATES
Los Angeles, California

DISCLAIMER

R-6914-925

LEGAL NOTICE

R-6914-925

A STUDY OF EARTHQUAKE INPUT MOTIONS FOR SEISMIC DESIGN

by

Stuart D. Werner

June 1970

Contract No. AT(49-5)-3012

Prepared for

UNITED STATES ATOMIC ENERGY COMMISSION
Division of Reactor Standards
Washington, D.C.

THIS REPORT SUMMARIZES THE STATE OF
THE ART AND SHOULD NOT BE USED AS
THE BASIS FOR ENGINEERING DESIGN

AGBABIAN-JACOBSEN ASSOCIATES
Los Angeles, California

FOREWORD

This study of earthquake input motions for seismic design was performed for the United States Atomic Energy Commission, Division of Reactor Standards, by Agbabian-Jacobsen Associates under Contract No. AT(49-5)-3012. The purpose of this study was to investigate the various parameters that affect earthquake ground motions at a specific site. S. D. Werner was Principal Investigator for this study and wrote the final report. Major contributions to the study were made by S. A. Adham, M. S. Agbabian, and G. A. Young. In addition, D. P. Reddy and H. S. Ts'ao contributed extensively to the preparation of the appendixes. P. C. Jennings of the California Institute of Technology served as consultant, and provided valuable guidance throughout the study.

Acknowledgement is made to D. F. Lange of the United States Atomic Energy Commission for his assistance and direction throughout the course of this study.

AJA

CONTENTS

CONTENTS (CONTINUED)

ILLUSTRATIONS

ILLUSTRATIONS (CONTINUED)

AJA

ILLUSTRATIONS (CONTINUED)

ILLUSTRATIONS (CONTINUED)

TABLES

SECTION 1

OBJECTIVES AND SCOPE

1.1 OBJECTIVES OF STUDY

Nuclear energy is becoming increasingly important as a source of energy for generating electric power. Currently, nearly 100 nuclear power plants are in operation, under construction, or are in the planning stage in the United States. During the past five years (1965-69) these plants have provided 38 percent of all new steam generating capacity announced.

Nuclear power plants have a special safety requirement because of the possibility of the release of fission products during accidents or during naturally occurring disasters, such as earthquakes, tornadoes, and floods. Great care must, therefore, be exercised in their design to ensure that those features necessary to shut down the reactor and maintain the plant in a safe condition remain functional at all times.

Earthquake ground motions are of critical importance because of the magnitudes of the displacements and dynamic forces induced in critical structures and equipment of nuclear power plants. The design of the facility must give special consideration to these effects, and must be based on reasonable and reliable estimates of the earthquake effects. If these effects are overestimated, the expense of the design may render the project uneconomical, but if underestimated, the health and safety of the public may be endangered. A much more sophisticated prediction and analytical design procedure is, therefore, required than is normally used on more conventional structures.

This report deals with one aspect of the earthquake problem, namely, the estimation of seismic ground motions in the vicinity of the nuclear power plant. It is known that the characteristics of earthquake motions at a nuclear power plant are dependent on the seismicity and fault patterns of the region, the soil properties of the site, and on the interaction effects between the soil and structure. However, due to the scarcity of earthquake ground motion records and the lack of dynamic soil-structure interaction measurements, the basic manner in which these and other parameters combine to affect the earthquake motions at a facility is only partially understood. Therefore, procedures and analysis techniques that consider these parameters in an approximate manner must be used, together with sound engineering judgment, to estimate seismic ground motions at the site of a nuclear power plant. The purpose of this study is to investigate these procedures, and to provide some guidance regarding the effects of various physical parameters on the earthquake motions at a site.

The specific objectives of the study can be summarized as follows:

- To provide a basis for developing guidelines which the engineer can use to select design levels of seismic input at a given site
- To investigate the dynamic response of a layered site and the manner in which it may affect the earthquake ground motions at a particular site
- To provide a discussion of state-of-the-art soil-structure interaction techniques suitable for use in nuclear reactor response analyses

1.2 BACKGROUND

The estimation of earthquake ground motions at a potential site of a nuclear reactor must be based on seismological and geological studies, as well as a careful investigation of the static and dynamic properties of the soil layers that comprise the site. The information obtained from these studies can then be used as input into an analysis technique that calculates the seismic motions. A brief description of these various investigations is provided for general background.

The objective of the geological investigation is to establish the lithologic, stratigraphic, and structural geological conditions of the potential site and the general region surrounding the site, complete with geological history. Tectonic structures underlying the region are identified as well as any physical evidence of behavior during prior earthquakes. The seismological investigation is closely related to the geological investigation and frequently starts with a listing of all earthquakes of record which may have affected the general area of the site. The magnitude of these earthquakes, epicenter locations, dynamic characteristics, and durations of the resulting ground motion are determined, or estimated. Epicenters within about 250 miles of the proposed site are of particular significance. Geological structures within this approximate radius and greater than one mile in length which are capable of causing surface faulting may need to be studied if it appears that these structures could cause severe earthquake motions at the site. From the length of the geological structures, their relationship to regional tectonic structures, and the geological history of displacements along the structures, experienced seismologists can make predictions of the magnitudes of potential earthquakes.

All nuclear power plant projects require a thorough investigation of the subsurface soil conditions to provide information for construction and design. Among the potential construction problems that should be considered in the soils investigation are slope stability, dewatering, swelling, and volume change of the surrounding soil. The soils investigation should also consider such structure design problems as (1) the method of support and foundation arrangement to control settlement and (2) foundation vibrations that might occur when the structure supports vibrating equipment. In addition, due to the potential hazards involved, the study of subsurface soil conditions for a nuclear power plant should provide information that will permit evaluation of the behavior of the soil during an earthquake. The field and laboratory tests that are needed for this evaluation are as follows:

Geophysical Studies. These studies consist of seismic refraction, bore hole resistivity, magnetometer surveys, etc., and can give a gross picture of the subsurface conditions depending upon specific site conditions. The refraction and bore hole surveys are of low energy and yield only *limiting* dynamic (elastic) soil parameters for earthquake response studies. Under earthquake loads, soils frequently experience nonlinear behavior, which at present can only be estimated from the results of laboratory tests.

Laboratory Tests. Many of the properties used to describe dynamic soil behavior are provided by laboratory tests. Those most frequently used to provide information for earthquake response studies include cyclic triaxial tests, vibration tests, sonic velocity tests, compression tests, and relative density tests.

Evaluation of Results. An evaluation of the quantitative results from the above elements of the investigation permits the engineer to make decisions on siting and foundation design, and to select soil parameters that are suitable for use as input to a mathematical model of the response of the site profile under earthquake loading. In all cases, soil parameters selected require the interpretation of test results by experienced soils engineers.

When the sources of potential earthquakes and the properties of the site have been established by the geological, seismological, and soil profile investigations, the characteristics of the seismic ground motions at the proposed nuclear power plant site can be estimated. The significant characteristics of these motions are (1) the peak acceleration, spectrum intensity, and root-mean-square acceleration of the earthquake, (2) the predominate frequencies of motion, and (3) the duration of strong motion.

The free-field soil motions along the depth of the site profile can be estimated using a mathematical model of the profile. This model considers the dynamic behavior of the soil and can serve to estimate the degree of amplification or attenuation of the boundary input motions by the soil mass. Procedures of this type are still in their formative stage and involve many uncertainties in estimating the input motions and soil parameters. However, it is anticipated that these uncertainties will be minimized by technical advances of the future; therefore, procedures of this type should be considered to be an extremely promising approach for estimating the severity of the earthquake environment for a nuclear power plant.

The presence of a stiff structure having significant mass, such as a nuclear power plant containment structure, may substantially modify the ground motions near the structure from those of the free field. Therefore, dynamic soil-structure interaction should be considered when estimating earthquake effects for a nuclear power plant. Mathematical models of the soil and structure, which use input motions based on the free-field calculations indicated above, can serve to estimate these interaction effects.

1.3 SCOPE OF WORK

The scope of the work for this study encompassed the following basic tasks:

- Task 1--Guidelines for Calculating Site-Dependent Earthquake Ground Motions
- Task 2--Soil-Structure Interaction Analysis Techniques
- Task 3--First-Level Approach to Defining Seismic Input
- Task 4--Summary Recommendations and Procedures for Estimating Seismic Motions.

The relationship and content of these tasks is depicted in Figure 1-1 and is discussed below.

Task 1 deals with procedures feasible for use in a detailed investigation of the effects of local soil conditions on earthquake ground motions at a nuclear reactor site. This task has received the major emphasis of this study, and the results of Task 1 are presented in Section 4.

A review of some representative state-of-the-art techniques for evaluating the effects of soil-structure interaction on the response of a nuclear reactor is presented in Task 2. The advantages and disadvantages of the various techniques are summarized, and recommendations are made regarding the use of these techniques. The results of this task are contained in Section 5.

Task 3 consists of a simplified, first-level approach to defining seismic input at a site and is described in Appendix A. Although this task represents only a small portion of the total effort, it is considered to be important since it serves as a basis for comparison with the more detailed procedures studied in Task 1.

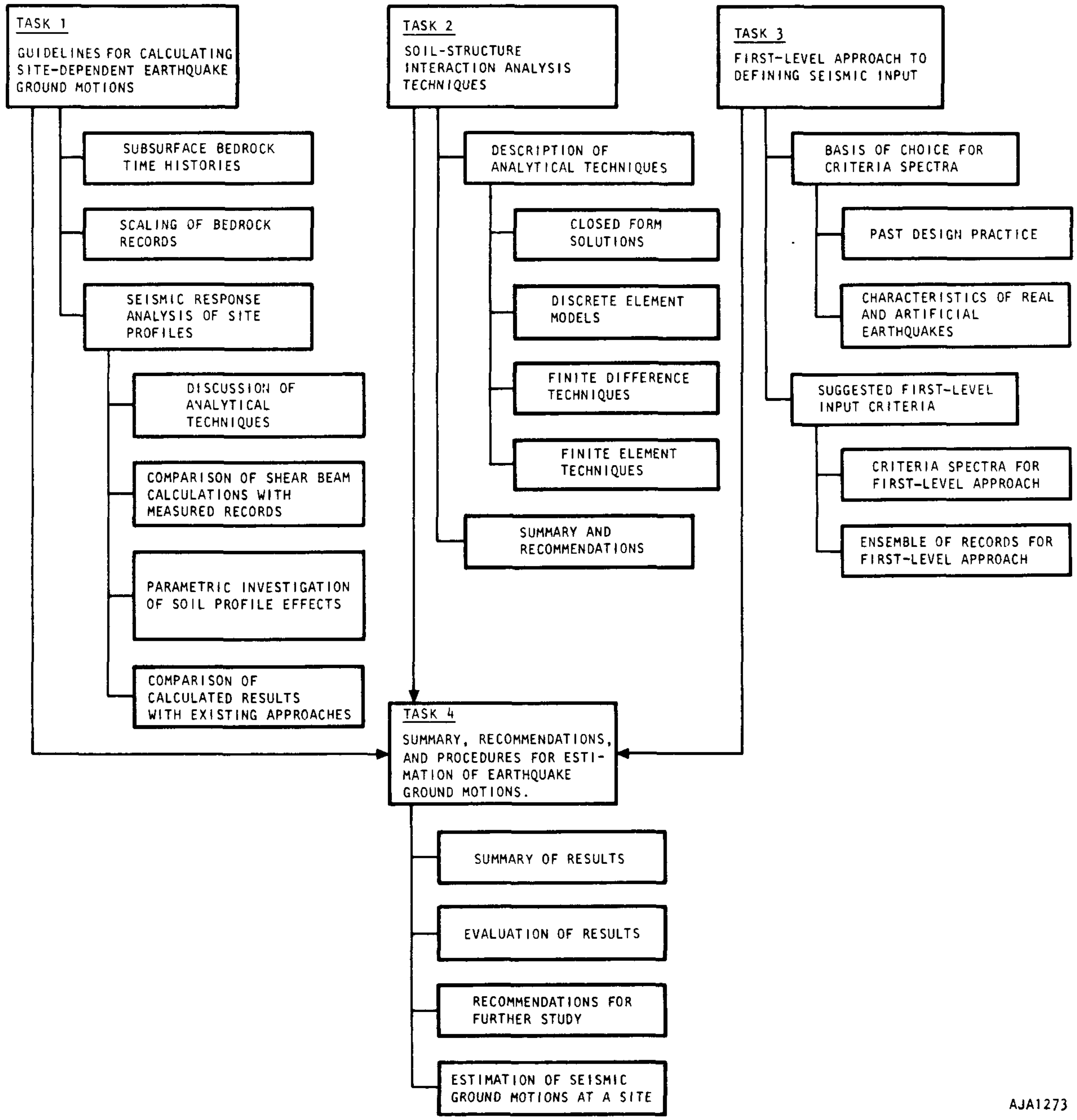

FIGURE 1-1. SCOPE OF WORK--SEISMIC INPUT STUDY

In Task 4, the results of Tasks 1 through 3 are summarized and, based on the present state of the art, some approaches to the problems of selecting seismic input at a nuclear reactor site are discussed. Also, because of scope limitations of this study, there are aspects of the tasks discussed above that warrant additional investigation. Recommendations for further study have been made as part of this task effort. The summary of the results of this study and the recommendations for further study are contained in Section 2, and general procedures for estimation of seismic ground motions at a site are described in Section 3.

SECTION 2

SUMMARY AND RECOMMENDATIONS

This report describes an investigation of procedures for determining seismic input for use in the analysis and design of nuclear power plants. As indicated in Section 1, the study has consisted of three primary tasks: (1) procedures for the determination of site-dependent earthquake ground motions, (2) a survey and assessment of existing soil/structure interaction analysis techniques, and (3) a first-level approach to the representation of earthquake ground motions in a region. The results of the investigations contained under each of these tasks are described in detail in Sections 4 and 5 and in Appendix A of this report and are summarized and evaluated in this section. In addition, this section contains some recommendations for further study.

2.1 SUMMARY OF RESULTS

2.1.1 GUIDELINES FOR CALCULATING SITE-DEPENDENT GROUND MOTIONS--TASK 1

At a specific site, the characteristics of the ground motion resulting from an earthquake are dependent upon several variables. Among these are the epicentral distance, the earthquake magnitude, the depth of the center of energy release, the length and duration of fault movement, local geology, and the properties of the soil layers at the site under consideration. Analytical procedures that adequately consider the effects of all of these important parameters have not as yet been developed. However, the rapid increase in recent years of the use of the digital computer has resulted in the development of many types of mathematical models of a material continuum. These models are readily adaptable to the prediction of the earthquake response of a soil profile, provided that input motions at the boundaries of the mathematical model can be defined in terms of the seismicity and geology of the region. The objective of this task has been: (1) to investigate techniques for estimating subsurface bedrock motions appropriate for use as input at the base of a mathematical model of the site profile, (2) to describe mathematical models that can be used to calculate seismic ground motions, and (3) to provide sample computations that illustrate trends regarding the effects of various site characteristics on the earthquake ground motions.

2.1.1.1 Subsurface Bedrock Motions

Ideally, seismic input motions at the site of a nuclear power plant should be estimated from measured records of strong earthquake motions at the subsurface bedrock level. At present, however, there are no records of strong motion at the subsurface bedrock level, and the few existing records on bedrock at the ground surface are not necessarily representative of strong earthquake motions that would occur at the subsurface level. Therefore, until strong earthquake motions are recorded in rock-like material below the ground surface, estimates of the dynamic characteristics of earthquake records at the subsurface bedrock level of the soil must be inferred from surface records and based on engineering judgment.

Because of the absence of measurements of subsurface earthquake motions, records of band-limited white noise (i.e., records which contain equal contributions from all frequencies within a defined frequency range) were used in this study to represent subsurface bedrock motions. The advantages of using this type of random process are: (1) ensembles of band-limited white noise are simple to generate and use in a dynamic analysis, (2) segments of white noise, although simple, have been shown to have the basic characteristics of strong motion earthquakes, and (3) the uniform level of frequency content inherent in a white noise process seems more appropriate, in view of the lack of measured data for comparison, than more refined estimates of subsurface bedrock motion. Additional discussion of subsurface bedrock time histories is provided in Subsection 4.2.

The important parameters that define the characteristics of a band-limited white noise record are its strength* and duration. Procedures have been investigated for scaling these quantities in terms of the earthquake magnitude and the minimum distance of the site from a potential causative fault.** For sites in close proximity to known surface fault patterns, the causative fault distance can be selected from a study of the seismicity and geology of the region. However, for sites located in areas that do not exhibit surface faulting (such as many regions in the Eastern United States), the strength and duration of the band-limited white noise bedrock records must be estimated from available information regarding previous earthquakes in the region. It is noted that the highly seismic regions of the United States generally contain active surface faults, whereas the regions without surface faulting generally exhibit lower seismicity characteristics.

---

* The strength of an earthquake is a measure of its damage potential, and is often described by the peak acceleration of the record. However, other descriptions of the strength of the earthquake, such as the root-mean-square (rms) acceleration are often more appropriate. The rms acceleration is especially useful for measuring the strength of motion represented by band-limited white noise, because it is the single measure needed for the application of random vibration theory to earthquake response analysis based on this type of input.

**When estimating seismic input for a nuclear power plant site, it is conservative to assume the region of energy release to be located at the point along the fault that is closest to the site. In this study, the "minimum distance to the causative fault" corresponds to this assumed location of the zone of energy release.

G. W. Housner studied the duration of strong motion for a number of earthquake records, and found the duration to be generally dependent on the magnitude of the shock (Reference 2-1). A plot of duration of the strong shaking phase versus Richter magnitude was obtained and is shown in Subsection 4.3.2, Figure 4-2. Although this plot was obtained for surface motions, the same relation has been assumed in this study to hold for subsurface bedrock records. Also, since the duration of the strong phase of shaking can be distinguished only for ground motions recorded relatively close to the causative fault, there are relatively few data points in the curve of Figure 4-2. The effect of causative fault distance on duration is thought to be minor, and cannot be specified until more precise measurements at sites far from a causative fault become available.

A set of illustrative curves that relate the rms acceleration of subsurface bedrock motions to the causative fault distance and the earthquake magnitude were generated as part of this task. The curves were obtained by: (1) using a set of curves of the same functional form and relative position as those of Seed, et al., (Reference 2-2); and (2) making use of engineering judgment and some one-dimensional calculations of the El Centro site to modify the ordinates of the curves of Reference 2-2 to correspond to rms acceleration (rather than peak acceleration). These curves were generated solely for the purpose of illustrating trends in the parametric study of site-dependent earthquake motions contained in this study, and are not recommended for general use in scaling bedrock motions at an actual site.

The techniques described in this study for scaling the strength and duration of subsurface bedrock records in terms of the magnitude and causative fault distance illustrate the type of approach that may eventually be used by the practicing engineer. However, because there are no strong motion records at the subsurface bedrock level, the degree of conservatism inherent in these particular scaling methods is not readily evaluated. Therefore, definitive techniques for scaling the strength and duration of subsurface bedrock records cannot be recommended until additional studies of the problem have been made.

More detailed information regarding the investigation of the scaling of subsurface bedrock motions is provided in Subsections 4.2 and 4.3.

2.1.1.2 Mathematical Models for Calculating Site-Dependent Ground Motions

The effects of the site profile on the strength and frequency characteristics of the earthquake motions can be obtained through the use of a mathematical model of the site. Mathematical models suitable for use on the digital computer in analyzing the seismic response of a soil profile, are based on the assumption that the inertia characteristics of the soil are concentrated at a number of discrete mass points in the model. The location of these mass points and the mass concentrated at each point should reflect the mass distribution of the continuous site profile being modeled. The discrete mass points are interconnected by one-dimensional or two-dimensional stiffness elements whose characteristics represent the properties of the soil at the corresponding location in the profile. Three-dimensional stiffness elements are also possible but are largely in the developmental stage.

For simplicity, most available mathematical models simulate the nonlinear, hysteretic material properties of the site by an equivalent linear viscoelastic representation. One of the major problems in the use of a model of this type is the determination of a suitable viscous damping mechanism to represent the actual hysteretic energy dissipation characteristics of typical properties of the soil at the corresponding location in the profile. Three-dimensional stiffness elements are also possible but are largely in the developmental stage.

A vertically oriented one-dimensional shear beam model is feasible for analyzing the earthquake response of sites where the motions induced by a seismic excitation at the base result from shear waves propagating vertically through the profile. This will be true of horizontally layered sites subjected to a deep-focus earthquake, or of sites subjected to a shallow-focus earthquake in which the half-wavelength of incoming waves is large compared to the lateral extent of the soil layers.

If a deposit has irregular or sloping boundaries, or is subjected to a shallow-focus earthquake for which the response of the site is essentially two-dimensional, the shear beam model is no longer valid, and a more complex analytical procedure is required. A technique often used for this purpose is the finite element approach, in which a continuum is idealized as an assemblage of compatible two-dimensional elements of appropriate sizes and shapes. The material properties of each of these elements corresponds to those of the continuum at that location.

Section 4.4 provides a detailed discussion of mathematical models that are appropriate for use in the calculation of earthquake motions at a site. Examples of correlation between computed ground motions and measured earthquake records are also presented.

2.1.1.3 Investigation of the Effects of Site Properties on Earthquake Ground Motions

One of the objectives of this study was to investigate the effects of local soil properties on seismic ground motions. To achieve this objective within the scope and budget of the study, a shear beam analysis was employed. The linear viscoelastic model described in Reference 2-3 was used, since this approach provides a means of determining the parameters of the mathematical model directly from the soil properties of each layer. However, as discussed in Subsection 4.4.3, the damping mechanism in this model has some inherent limitations.

The first set of calculations made during the course of this study is described in Subsection 4.5, and is based on the seismic characteristics and site properties of the 1940 El Centro earthquake. The purpose of these calculations was to determine the sensitivity of the computed results to variations in soil properties and input motions, at a site where measured records are available.

The results of these calculations indicated that variations of ±30 percent in the material parameters for this particular shear beam model of the El Centro site resulted in substantial variations in the rms accelerations and low period spectral characteristics of the resulting computed ground motions. The longer period components of the computed motions (greater than about 1 sec) were more dependent on the charactertistics of the input base motions and were not strongly influenced by these variations in soil properties.

Only a limited number of shear beam calculations were made for the El Centro site using band-limited white noise as input base motion. Therefore, no definitive statements can be made regarding the overall correlation of this approach with measured data. The few calculations made using band-limited white noise as input showed that reasonable comparisons with the rms acceleration level of the measured records could be obtained. However, this same white noise input produced spectra that fell below the average of the spectra from the two horizontal components measured at El Centro, especially in the long period regions. It is noted that the spectra of the two measured horizontal components of the 1940 El Centro earthquake differ considerably; therefore, factors not related to the local site properties considered in the shear beam analysis may be affecting the dynamic characteristics of the measured records.

A second set of calculations using the shear beam model is described in Subsection 4.6 and provides some trends regarding the effects of variations in the Richter magnitude, causative fault distance, and soil properties on the strength and frequency characteristics of earthquake ground motions. Two profiles were considered in this set of calculations, namely, a soft site with relatively low fundamental frequency, and a stiff site with a relatively high fundamental frequency. For each site, a high-magnitude earthquake (7.5) and a moderate-magnitude earthquake (5.5) have been considered. Each of these magnitudes has been investigated for a site location near a causative fault (5 miles) and farther from a causative fault (50 miles). The input at the subsurface bedrock level was a segment of band-limited white noise whose duration and strength level was determined from the illustrative scaling curves given in Subsection 4.3. For each of these cases, the dynamic characteristics of the ground surface response have been obtained in terms of acceleration time histories, rms accelerations, and pseudo-velocity spectra. The results of this parametric study can be summarized as follows:

a. The degree of amplification of the subsurface bedrock motions by the soil profile was dependent on: (1) the magnitude of the earthquake and the distance from the site to the region of energy release (i.e., causative fault), and (2) the material properties of the site.

b. The frequency range over which the bedrock response spectrum is amplified was seen to be dependent on the soil properties and on the strength level of the input motions.

c. As the earthquake magnitude increased and/or the distance from the site to the earthquake source decreased, the strain-dependent soil moduli and damping factors appeared to be the prime reason for observed reductions in the amplification of input base motions by the overlying soil profile.

2.1.1.4 Evaluation of Results--Site-Dependent Ground Motions

This study has used a linear viscoelastic shear beam model to calculate ground motions at various sites for both high-intensity and low-intensity earthquakes. The manner in which these results and procedures should be used by the design engineer in selecting seismic input at an actual reactor site is discussed below.

Assuming that the linear viscoelastic shear beam model is applicable for the site conditions under consideration, three major items must be specified before calculations such as those in Section 4 can be performed for any given nuclear reactor site. These are:

- A basic model for bedrock motions.
- Scaling rules for estimating the strength and duration of subsurface bedrock motions.
- Material properties for use in the mathematical model. For the linear viscoelastic material model, these will consist of equivalent elastic moduli and damping coefficients for each layer. These equivalent parameters are usually obtained from soil tests and are dependent on the peak strain level in the soil.

The technique used in this study appears capable of providing a self-consistent method for approximating the effect of soil properties on ground surface motions. With the proper choice of parameters, the method produces results which agree quantitatively with the surface motions recorded at sites of actual earthquakes. The technique has the further advantage that it is well within the analytical capabilities of most engineering firms that might be involved in the design of nuclear reactor structure.

There are two main drawbacks in the technique. First, the relative scarcity of ground surface records and the complete lack of subsurface records for strong earthquakes make it almost impossible at this point to assess the validity of the basic model for bedrock motion and the scaling rules for this motion. Second, both the theoretical and experimental bases for the damping coefficients are not as firm as would be desirable in a technique that might have status as a guideline for design. The damping is particularly important because the primary effects of the soil in amplifying or reducing the subsurface bedrock motions are dependent on the damping in the modes of vibration of the mathematical model. The actual damping mechanisms, the magnitude of the damping, and the experimental determination of damping values for various soil types need further study.

It is noted that overall magnitude of the damping values and the scaling of the subsurface bedrock motions are related in the final results. For example, if the damping in the model were reduced, the same strength level of the ground surface motions could be obtained by decreasing the strength level of the bedrock motions. Without subsurface records and extensive soil tests, the true levels of the bedrock motion and the damping cannot be specified.

In view of the above uncertainties, the shear beam model and the bedrock motion scaling techniques discussed in Section 4 should be viewed as a first attempt at the development of a definitive approach to the calculation of site-dependent earthquake motions. Considerable analytical and experimental development work, in addition to deployment of subsurface earthquake motion instrumentation, is needed to provide the basis for development of improved techniques for the prediction of the earthquake response of a a soil profile.

2.1.2 SOIL-STRUCTURE INTERACTION ANALYSIS TECHNIQUES--TASK 2

The analysis of earthquake ground motions discussed in Subsection 2.1.1 and in Section 4 has been based on free-field effects only, i.e., the presence of a structure has not been considered. However, the presence of a stiff structure, such as the containment structure of a nuclear power plant, in the soil will modify the ground motions in the vicinity of the structure. The modification of the free-field ground motions due to the presence of a structure is termed soil-structure interaction, and the effects of this interaction should be considered in any analysis of the dynamic response of a nuclear power plant subjected to an earthquake.

A number of state-of-the-art techniques for evaluating the effects of soil-structure interaction on the earthquake response of a nuclear reactor have been reviewed and evaluated. To facilitate this review, the soil-structure interaction techniques have been categorized as (1) closed-form solutions, (2) discrete element representations of interaction effects at the soil-structure interface, (3) finite difference techniques, and (4) finite element methods. Under each of these general categories, representative analysis techniques have been described to illustrate the capabilities of these approaches in predicting interaction effects.

From this review it was concluded that finite difference and finite element methods are the most promising for representing the soil-structure system realistically and, therefore, should be used in detailed analytical studies of interaction effects in nuclear reactor structures. Closed-form solutions and discrete element (spring-dashpot) models are considerably simpler than the finite difference or finite element approaches and treat the three-dimensional aspects of the problem in some cases. However, these approaches do not provide as refined a simulation of the profile characteristics. Therefore, closed-form solutions and discrete element models are most appropriate for use in parametric studies and in the preliminary stages of the analysis and design of a nuclear power plant.

The details of this review and assessment of soil-structure interaction prediction techniques are provided in Section 5.

2.1.3 FIRST-LEVEL APPROACH TO DEFINING SEISMIC INPUT--TASK 3

A simplified procedure for selecting earthquake ground motions has been provided, based on existing strong motion earthquake measurements. This procedure provides a basis of comparison with the results of the site-dependent calculations described in Subsection 2.1.1 and in Section 4.

This approach is based on the scaling of existing real and/or artificial earthquake records to correspond to a spectrum that is estimated to describe the dynamic characteristics of representative earthquake motions of the region. Two sets of spectra were originally considered for this purpose, namely, those of Housner (Reference 2-4) and of Newmark and Hall (Reference 2-5). The following general comparisons were made of these two sets of spectra:

a. Housner's spectra are based on the *average* dynamic characteristics of strong earthquake motions on competent soil, and otherwise are independent of the soil properties at a site. The Newmark-Hall spectra are based on the spectra *envelopes* from strong motion earthquakes and have foundation amplification factors that should be used only in the absence of more reliable soils data.

b. The upper bound and lower bound spectra of Newmark and Hall are more intense than those of Housner. This follows from the fact that the Newmark-Hall spectra represent an envelope of existing earthquake records, whereas the Housner spectra correspond to an average.

c. The ratio of the peak spectral acceleration to the zero period spectral acceleration is greater in the Newmark-Hall spectra than in the Housner spectra.

Either envelope spectra or average spectra appear to provide a reasonable basis for selection of input in this approach, as long as this choice is consistent with structure and equipment design stresses and with earthquake strength levels selected for the region. In this study, the average (i.e., Housner) spectra were selected, along with peak acceleration levels that are intended to correspond to *average* strength levels in regions of high, moderate, low, and minimal seismicity. These acceleration levels are provided in Table A-5 of Appendix A.

To use this approach for obtaining spectra and ground motions at a site, a study of the seismic and geologic characteristics of the site should be made by qualified geologists and engineers. From this study, the site may be classified into one of the four seismicity categories indicated in the preceding paragraph. A set of spectra can then be obtained for the site by scaling the Housner spectra to correspond to the peak acceleration level defined for that particular seismicity. These spectra provide representative, rather than maximum, conditions for a region, and are shown in Figure A-8 of Appendix A.

Since the spectra in the first-level approach are based on the average of spectra from the existing strong motion records indicated above, a corresponding ensemble of ground motion time histories can consist of these strong motion records. This ensemble can be supplemented by artificial earthquake records whose dynamic characteristics are modeled by the Housner spectra (References 2-6, 2-7). The real and/or artificial time history records in the ensemble can be scaled to correspond to the scaled spectra indicated in the previous paragraph.

A detailed description of this first-level approach is provided in Appendix A.

2.2 RECOMMENDATIONS FOR FURTHER STUDY

2.2.1 REPRESENTATION OF SUBSURFACE BEDROCK RECORDS

No subsurface measurements of strong earthquake motions are presently available. This information is needed to provide (1) a better understanding of the propagation of earthquake waves through the soil medium and (2) a vehicle for verification and refinement of existing analytical techniques. To obtain this information, instrumentation located at various depths below the ground surface in regions of high earthquake potential is recommended.

Until a sufficient number of subsurface records are obtained, the strength and duration of subsurface bedrock motions must be estimated in terms of the seismicity and geology of the site. Additional calculations are needed to provide procedures for estimating these subsurface records that correspond to existing strong motion surface records. For example, a one-dimensional model with nonlinear, hysteretic stress strain law could be used to represent the soil profile at sites for which surface strong motion records have been obtained during an earthquake of known magnitude and epicentral location. An ensemble of band-limited white noise records could be scaled so that when used as input at the base of the one-dimensional model, the dynamic characteristics of the resulting ensemble of calculated ground surface motions correspond statistically to the measured records at that site. This should be repeated for a sufficient number of measured earthquake records to define a series of curves relating the strength of the subsurface bedrock motion to the earthquake magnitude and distance from the site to the causative fault.

Another approach to the determination of the dynamic characteristics of earthquake motions is to provide a number of recording stations located at various distances from a planned explosion. At each of these stations, accelerometers could be located at the ground surface, at various depths below the ground surface, and at the bedrock level. Practical considerations might limit the size of the explosion and hence the resulting ground accelerations might be below those of a strong motion earthquake. However, these measurements could provide valuable information regarding the effect of the distance from the energy source on the strength level, frequency characteristics, and duration of strong motion of the bedrock motions. In addition, the records obtained at various depths at any one station would provide a means for verifying a mathematical model of the soil profile (since the input base motions at that station are known).

Another problem is the determination of horizontal and vertical records that are usable as input for a two-dimensional analysis of free-field ground motions. This includes the determination of an appropriate ratio of the strengths of the horizontal and vertical record, and the effect of the phasing of the horizontal and vertical input motion.

2.2.2 ANALYSIS TECHNIQUES FOR DETERMINATION OF EARTHQUAKE GROUND MOTIONS

As indicated in Subsection 4.4.3, there are inherent limitations in the damping mechanism of the shear beam approach utilized in this study. These limitations arise from the use of an approximate Raleigh damping mechanism to simulate all energy dissipation effects that might exist at a site. In view of this, it appears reasonable to investigate other damping mechanisms, including a nonlinear one-dimensional model, in which hysteresis effects and radiation damping are modeled directly.

The use of finite-element techniques to predict earthquake ground motions at sites whose response is essentially two-dimensional should be investigated further. In particular, the seismic response of soil deposits predicted by the finite-element technique should be compared with measured earthquake data and with other analytical techniques.

As indicated in Subsection 4.5, uncertainties in estimating soil properties at a site can have a significant effect on the predicted earthquake-induced ground motions for that site. Therefore, to reduce these uncertainties, improved procedures should be investigated for (1) extracting soil samples from the field and (2) testing these samples in the laboratory. In addition, soil properties that can be measured in a laboratory often do not correlate with those required for input to a seismic ground motion calculation for a site. Therefore, testing and analysis procedures that provide increased correlation between these two sets of properties should be investigated.

2.2.3 SOIL-STRUCTURE INTERACTION ANALYSIS TECHNIQUES

Field measurements are needed for determining soil-structure interaction effects in the vicinity of a nuclear power plant. To obtain additional insight into this problem, it is recommended that instrumentation be placed in the soil near existing nuclear facilities in highly seismic regions. Also, instrumentation could be placed in the vicinity of a structure located in a region where a planned explosion will be set off (as indicated in the discussion of Subsection 2.2.2).

As noted in Subsection 5.3.4, no dynamic three-dimensional analysis techniques appropriate for predicting soil-structure interaction are available, although some two-dimensional analyses have been used to estimate three-dimensional effects in an approximate manner. The eventual formulation of three-dimensional finite-element (or finite difference) analysis techniques should be encouraged.

REFERENCES

2-1. Housner, G. W., "Intensity of Earthquake Ground Shaking Near a Causative Fault," *Proc. of the Third World Conference on Earthquake Engineering*, Aukland and Wellington, New Zealand, January, 1965.

2-2. Seed, H. B., et al., *Characteristics of Rock Motions During Earthquakes*, Report No. EERC 68-5, College of Engineering, University of California, Berkeley, California, September, 1968.

2-3. Idriss, I. M. and H. B. Seed, "Seismic Response of Soil Deposits," *Journal of the Soil Mechanics Division, ASCE*, Vol. 96, No. SM2, March, 1970.

2-4. Housner, G. W., "Behavior of Structures During Earthquakes," *Journal of the Engineering Mechanics Division, ASCE*, Vol. 85, No. 4, October, 1959.

2-5. Newmark, N. M., and W. J. Hall, "Seismic Design Criteria for Nuclear Reactor Facilities," *Fourth World Conference on Earthquake Engineering*, Santiago, Chile, January 1969.

2-6. Housner, G. W., and P. C. Jennings, "Generation of Artificial Earthquakes," *Engineering Mechanics Division, Proc. of American Society of Civil Engineers*, Vol. 90, No. EM1, February, 1964.

2-7. Jennings, P. C., G. W. Housner, and N. C. Tsai, "Simulated Earthquake Motions for Design Purposes," *Fourth World Conference on Earthquake Engineering*, Santiago, Chile, January, 1969.

SECTION 3

PROCEDURE FOR ESTIMATING SEISMIC GROUND MOTIONS

In this section, a procedure is described for estimating seismic ground motions at the site of a nuclear power plant. This procedure is based on the investigations carried out during the course of this study and is intended to illustrate a *general* type of approach that can be used to select seismic input at a site. However, at present, some aspects of this procedure are still in their formative stage and will require additional studies before they can be considered to represent definitive techniques for estimating earthquake ground motions.

A general procedure for selecting seismic input is outlined in Figure 3-1. Each of the items shown on the flow chart are briefly discussed below.

3.1 DESCRIPTION OF PROCEDURE

3.1.1 EVALUATION OF SEISMICITY, TECTONICS, AND SOIL PROPERTIES OF SITE (ITEM (1), FIGURE 3-1)

A review of the seismic history of the region in which the site is located should be made by qualified geologists and engineers for the purposes of statistically estimating the possibility of earthquake activity of a given strength level (References 3-1 and 3-2). In conjunction with this seismicity study, the characteristics of both regional and local geology should be investigated. Such a study would consider both regional and local faulting, including the size, location, and history of recent tectonic activity. The seismicity and tectonics of highly seismic regions such as Southern California have been studied in some detail (References 3-3 and 3-4); however, detailed investigations of this type are not available in less active regions. Guidelines which set forth the principal seismic and geologic considerations at a site are provided in Reference 3-5.

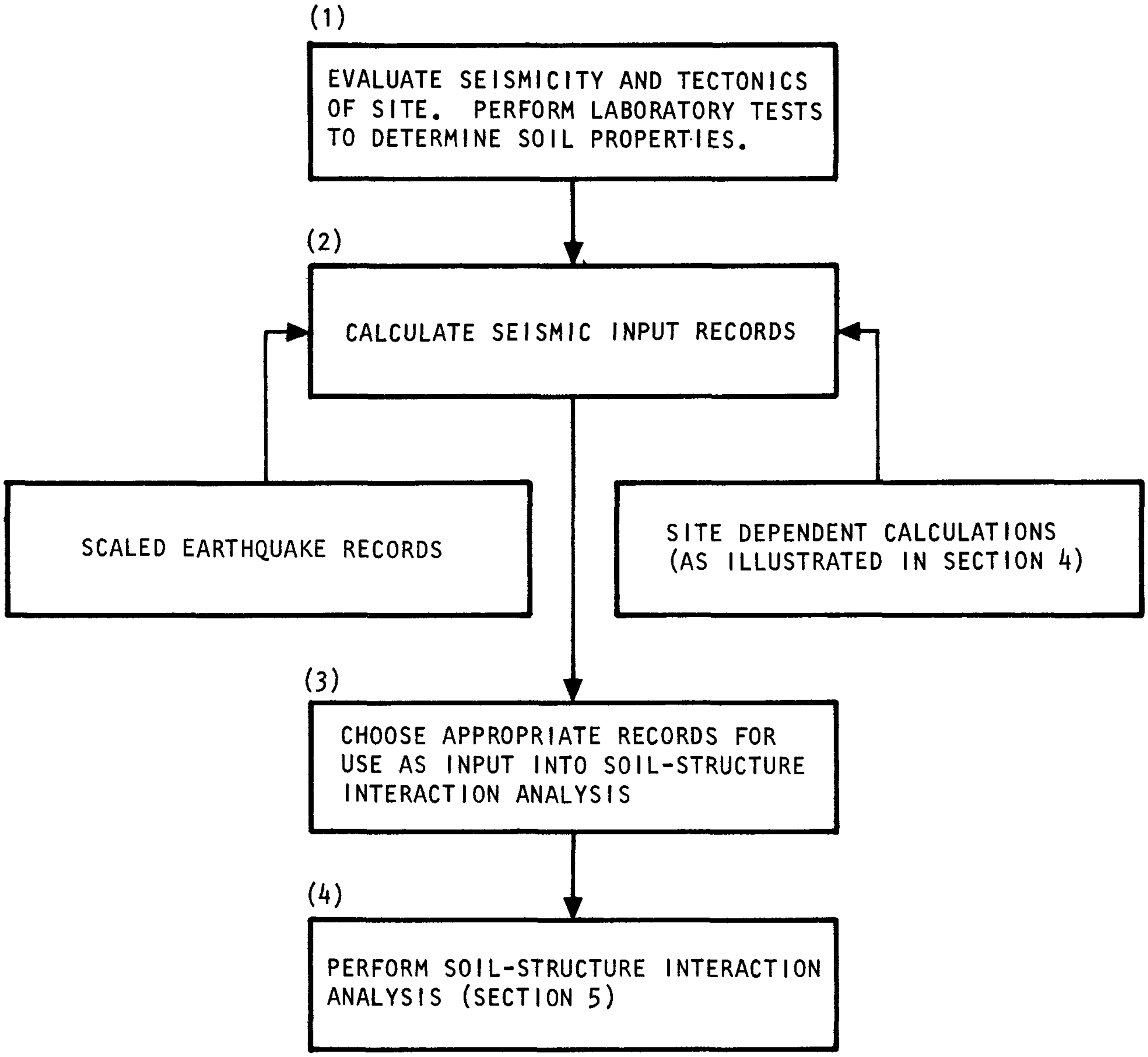

FIGURE 3-1. PROCEDURE FOR SELECTING SEISMIC GROUND MOTIONS AT A SITE

On the basis of the seismic history and geology of a region, combinations of earthquake magnitude and causative fault distance appropriate to an Operating Basis Earthquake (OBE) and a Design Basis Earthquake (DBE) would be selected. For sites in regions with no surface faulting, the magnitudes and corresponding strength levels appropriate to an OBE and a DBE must be estimated from available information regarding previous earthquakes that have occurred in the vicinity. The OBE defines an earthquake which might realistically be experienced by a structure during its economic life, whereas the DBE defines the most severe earthquake that might be conceived as occurring at the site at any time in the future. As noted in Reference 3-6, the determination of the DBE strength levels may be a difficult task, since this earthquake may never have occurred within the period of recorded history.

Due to the dynamic nature of the applied earthquake motions, it is important to determine dynamic and static soil properties at peak strain levels responding to the design earthquake. This requires laboratory tests of soil samples obtained from a number of representative borings located in the vicinity of the nuclear power plant site. These tests could include the determination of compressional and shear wave velocities for the purpose of computing dynamic elastic moduli and other dynamic properties. Mass densities, moisture contents, static stress strain properties, and Poisson's ratios should also be determined. In addition, soil tests that simulate the behavior of the soil materials to earthquake loading cycles (such as cyclic load tests, etc.) should be considered. Also, potential tendencies of the profile toward liquefaction should be investigated.

3.1.2 CALCULATION OF SEISMIC INPUT RECORDS (ITEM (2), FIGURE 3-1)

Earthquake ground motions for use as input into response analyses of nuclear power plants should be obtained through consideration of existing strong motion records and from the results of site-dependent calculations that consider the effects of local soil properties on the earthquake motions at a site.

The site-dependent earthquake motions utilize an ensemble of estimated subsurface bedrock time-motion records as the basic input. A suitable mathematical model is used to introduce the modifying effect of the overlying soil profile at the site. An ensemble of time histories of soil motions along the profile is predicted, and the ensemble average of response spectra and strength levels of the calculated soil motions at appropriate depths is computed.

At present, there are no measurements of strong earthquake motions at the subsurface bedrock level. Therefore, reasonable estimates of bedrock motions should be obtained by appropriate scaling of real earthquake ground surface records, artificial earthquake records, or band-limited white noise.* Also, reasonable estimates of upper bound and lower bound soil properties should be made, so as to provide bounds on the results of the calculations. The scaling of bedrock motions and the selection of material parameters should be performed by experienced engineers and geologists who are thoroughly familiar with the state-of-the-art information contained in the various references cited in this report.

For purposes of comparison with the site-dependent calculations, an ensemble of real and/or artificial strong motion earthquake records, and the associated spectra of these records, should be scaled by qualified geologists and engineers to correspond to strength levels estimated to be consistent with the seismicity of the region. An average of these scaled spectra would then be compared to the ensemble average spectra of the soil motions computed as described in the preceding paragraphs. As described in the next subsection, the purpose of this comparison is to select suitable soil motions for input into the analysis of the nuclear power plant.

*Band-limited white noise is used to represent subsurface bedrock motions in the site-dependent calculations described in Section 4.

3.1.3 CHOICE OF INPUT INTO SOIL-STRUCTURE INTERACTION ANALYSIS (ITEM (3), FIGURE 3-1)

The next phase of the procedure consists of evaluating the results obtained using each of the procedures indicated under Item (2) of Figure 3-1 and choosing the ensemble of ground motion for use as input into the soil-structure interaction analysis of the power plant.

The choice of appropriate seismic input should be based on a comparison of the ensemble average spectra obtained from the site-dependent calculations and from the scaled earthquake records. This comparison should consider the frequency characteristics of the containment structure, as well as of any internal components of the reactor that are mounted on the foundation base slab.

It is noted that the structure response, including the effects of interaction with the soil, is dependent on motions in the soil adjacent to and below the structure. Therefore, if the scaled earthquake records (which provide only surface motions), are selected for use as input into the interaction analysis, the dynamic characteristics of corresponding motions at finite depths below the ground surface will have to be estimated. The results of the site-dependent calculations may provide guidance in making these estimates.

3.1.4 SOIL-STRUCTURE INTERACTION ANALYSIS (ITEM (4), FIGURE 3-1)

The final step in the procedure is the calculation of dynamic soil-structure interaction effects. These effects are generally dependent on the dynamic properties of (1) the structure, (2) the soil in the vicinity of the structure, and, in some cases, (3) the deeper soil or rock. Procedures for calculating dynamic soil-structure interaction effects are reviewed and evaluated in Section 5.

3.2 EXAMPLE PROBLEM

An example problem for the selection of seismic motions at the site of a nuclear power plant is provided in this subsection. This problem is intended only to illustrate the general procedures described in Subsection 3.1, and the particular analysis techniques used in this example do not necessarily exclude other analytical methods that might be used.

3.2.1 STATEMENT OF PROBLEM

Given: A potential site of a nuclear power plant.

Required: Determine seismic input motions for a Design Basis Earthquake whose strength, duration, and frequency characteristics are representative of the seismicity, tectonics, and soil properties of the site.

Approach: The approach to be used is outlined in Figure 3-1 and is discussed in detail in Section 4 and in Appendix A.

3.2.2 STEP-BY-STEP PROCEDURE

3.2.2.1 Evaluation of Seismicity, Tectonics, and Soil Properties of a Site (Item 1, Figure 3-1)

a. A study of the seismic history of the region and the characteristics of both regional and local geology is made by qualified geologists and engineers in accordance with Reference 3-5. For this example problem, it is assumed that these studies indicate that (1) the site is in a region of moderate seismicity, and (2) a Richter magnitude of 7.5 and a distance from the site to a causative fault of 5 miles is representative of the Design Basis Earthquake that could occur at the site.

b. It is assumed for this example problem that static and dynamic tests of soil samples from representative borings at the site indicate that the site profile has the material properties and layering characteristics shown in Figure 3-2. Also, no problems arising from liquefaction of the site are anticipated.

3.2.2.2 Calculation of Seismic Input Records (Item 2, Figure 3-1)

This procedure consists of the determination of an ensemble of ground motions that are appropriate for use as input into a soil-structure interaction analyses of the nuclear power plant. These motions are based on a comparison of the results of site-dependent calculations with suitably scaled records from strong motion earthquakes. Only horizontal ground motions have been compared in this illustrative example; however, the vertical ground motions, although usually less severe than the horizontal motions, may have a significant effect on the structure response, and should also be estimated.

Site-Dependent Calculations

a. It is assumed, in this example, that the free-field earthquake motions of the site are due primarily to the vertical propagation of seismic waves to the surface by means of shear deformations induced in the soil layers by a seismic excitation at the subsurface bedrock level. For this case, the earthquake response of the site profile can be analyzed using a one-dimensional shear beam model that extends vertically from the ground surface to the subsurface bedrock level. (Note that other methods, such as finite element calculations, may also be used.)

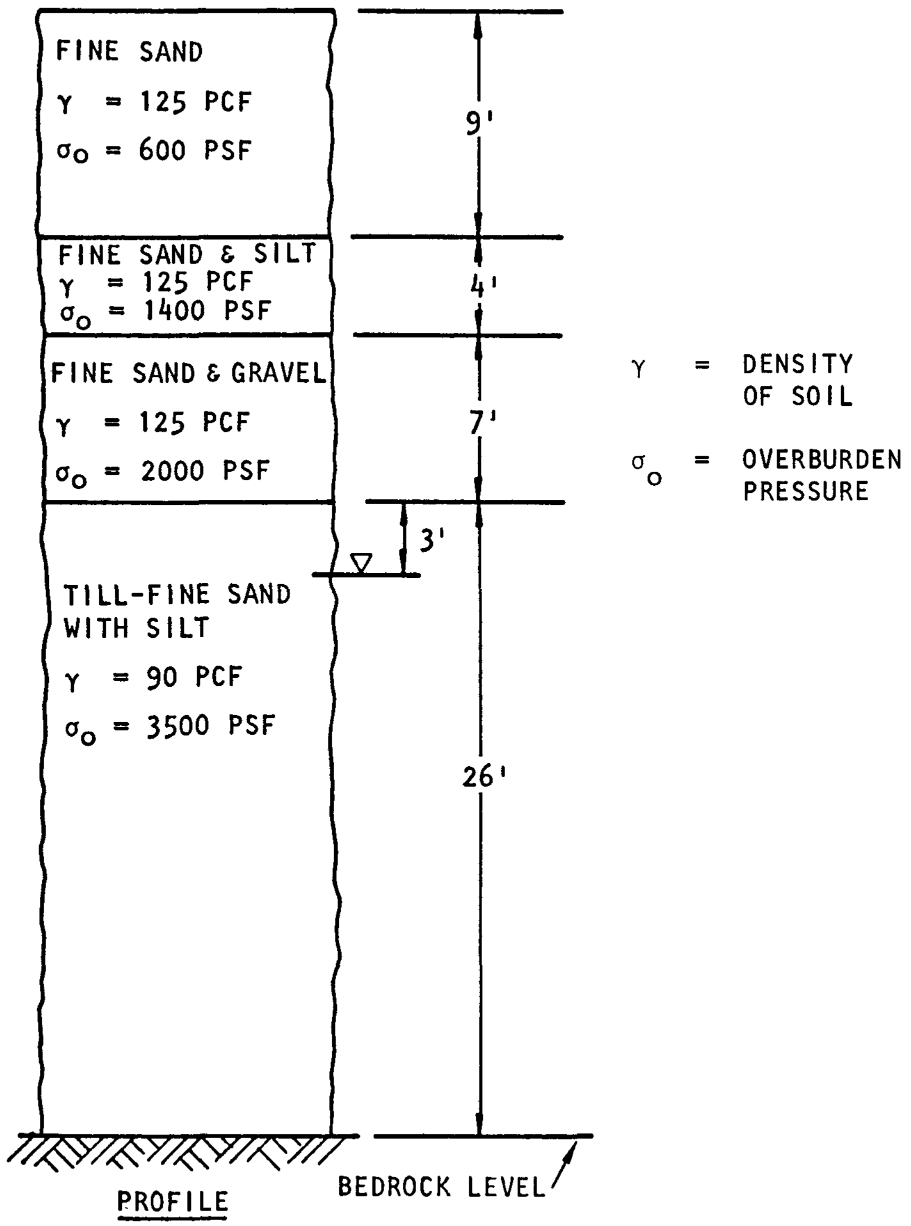

FIGURE 3-2. SITE PROFILE ASSUMED FOR EXAMPLE PROBLEM

b. An ensemble of band-limited white noise records are used in this example to represent subsurface bedrock input motions. The rms acceleration and the duration of these records are estimated from the Richter magnitude of the Design Basis Earthquake and from the minimum distance of the site to a potential causative fault. At present, considerable uncertainties are inherent in the estimation of subsurface bedrock motions.

c. To account for the statistical nature of the earthquake problem, the average response characteristics of the site when subjected to scaled versions of an *ensemble* of band-limited white noise records should be considered. However, in this illustrative example problem, the input to the site-dependent calculations has consisted of *only one* band-limited white noise record, namely White Noise No. 2 shown in Figure 4-1 of Section 4. The rms acceleration of this record is 0.81 g.

d. Figure 4-2 of Subsection 4.3.2 has been used in this example to scale the duration of the subsurface bedrock input motions to correspond to the Richter magnitude of 7.5 (as obtained from the seismic and geologic study of the site). For a magnitude 7.5 earthquake, this figure indicates that the bedrock record should have a duration of 30 sec.

e. A discussion of the feasibility of scaling the strength of subsurface bedrock motions is provided in Subsection 4-3. Based on the use of estimated scaling curves and on engineering judgment, it is assumed in this example that, for a Richter magnitude of 7.5 and a causative fault distance of 5 miles, the rms acceleration of the bedrock accelerograms should be about 4 ft/sec^2. Since the rms acceleration of White Noise No. 2 is 0.81 g, the scale factor is

$$\frac{4.0/32.2}{0.81} = 0.153$$

Therefore, all acceleration amplitudes in the unscaled White Noise No. 2 should be multiplied by 0.153 to correspond to the earthquake Richter magnitude and the causative fault distance of the example site. The scaled and unscaled white noise records are shown in Figure 3-3.

f. The shear beam program described in Subsection 4.4.3 is used to model the site profile in this example problem. The scaled white noise record shown in Figure 3-3 is used as input at the base of this shear beam model. The acceleration time history at the ground surface is calculated at the ground surface mass point, as illustrated in Figure 3-4.

g. The response spectra of the ensemble of calculated time histories should next be obtained. The spectrum of the single surface record calculated in this illustrative example is compared to that of the subsurface bedrock input record in Figure 3-5 to indicate the frequency range over which the base motion has been amplified. The selection of the oscillator damping ratio of 5 percent has been based on the damping factors set forth in Reference 3-8.

Scaled Earthquake Records

a. The first-level approach described in Appendix A is used in this illustrative example to provide spectra and motion time histories from existing earthquake records. These spectra and time histories are scaled to represent average conditions for a region of moderate seismicity; hence, within the region, these records will be overly severe for some sites and not severe enough for other sites.

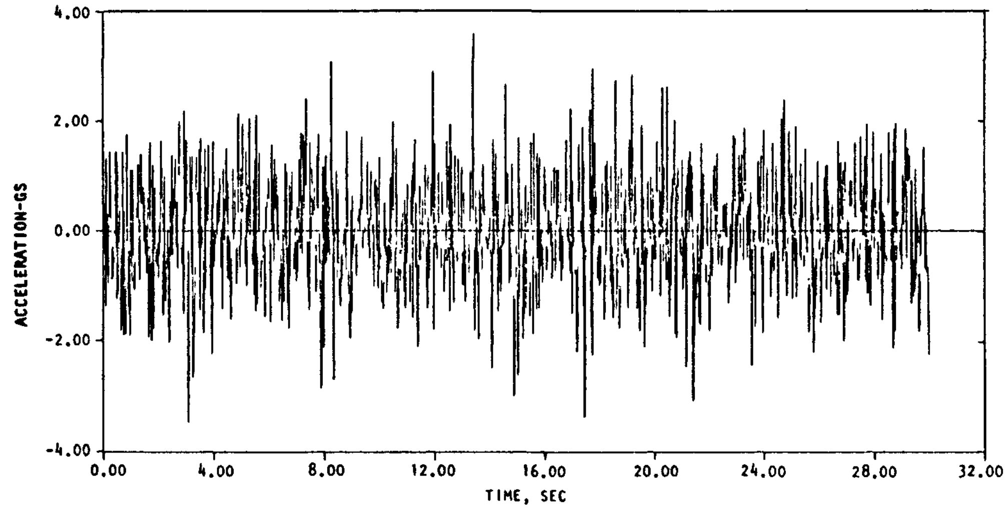

(a) UNSCALED WHITE NOISE NO. 2 (FROM FIGURE 4-1(b), SECTION 4)

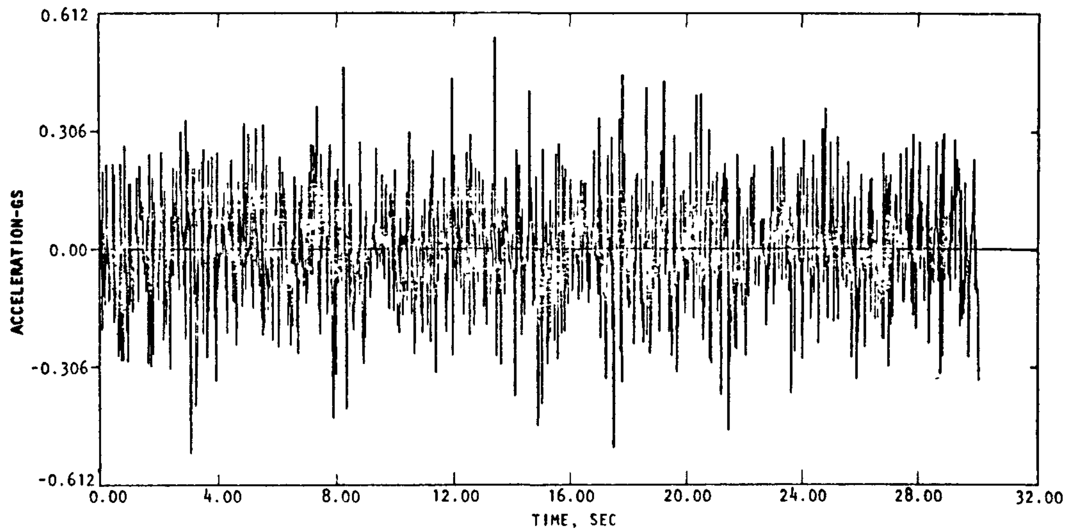

(b) SCALED WHITE NOISE NO. 2 (CORRESPONDING TO A MAGNITUDE 7.5 EARTHQUAKE AND A SITE LOCATED 5 MILES FROM THE CAUSATIVE FAULT)

FIGURE 3-3. SCALING OF SUBSURFACE BEDROCK RECORD FOR EXAMPLE PROBLEM

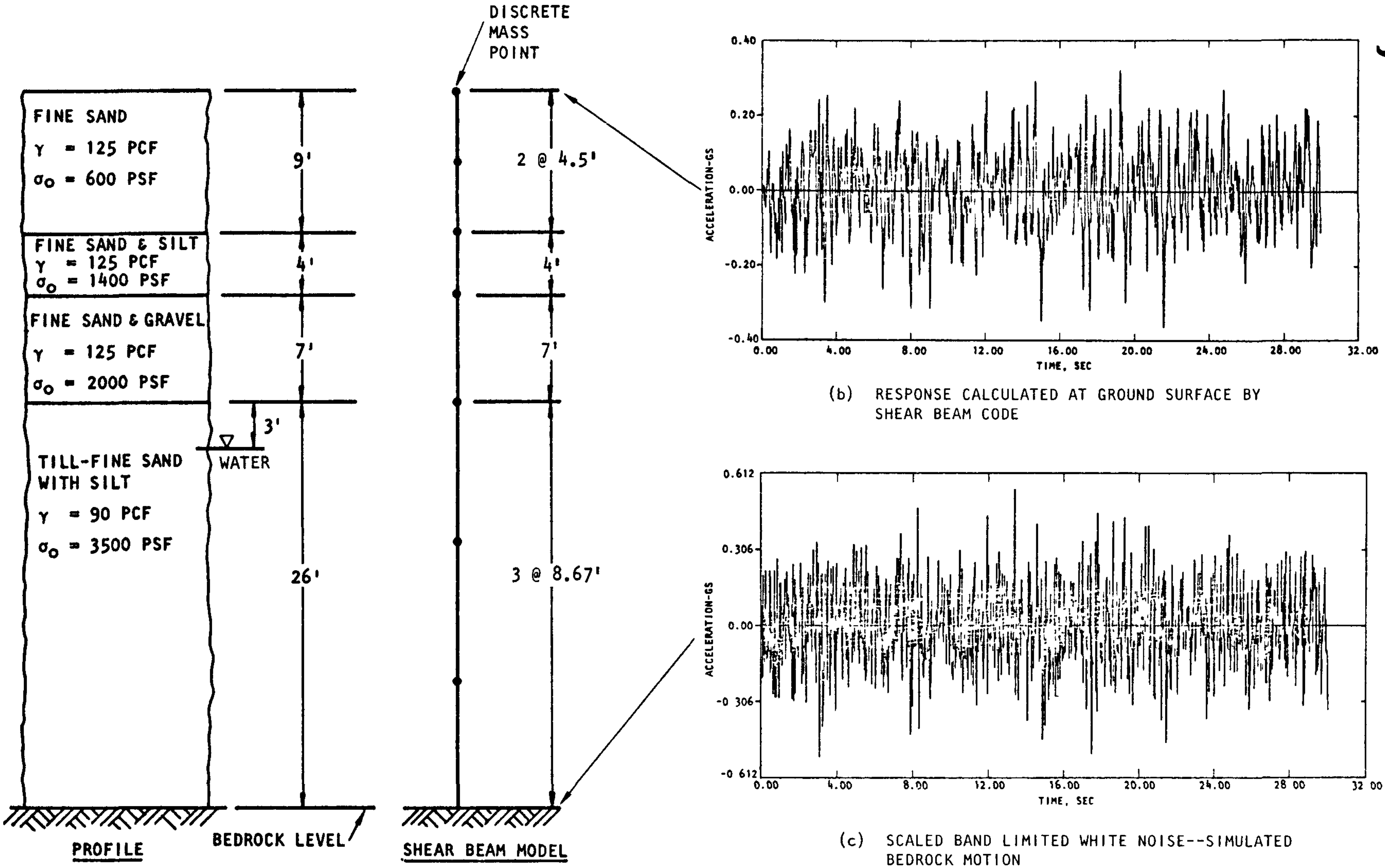

(a) SITE PROFILE

(b) RESPONSE CALCULATED AT GROUND SURFACE BY SHEAR BEAM CODE

(c) SCALED BAND LIMITED WHITE NOISE--SIMULATED BEDROCK MOTION

FIGURE 3-4. CALCULATED SURFACE MOTIONS IN EXAMPLE PROBLEM

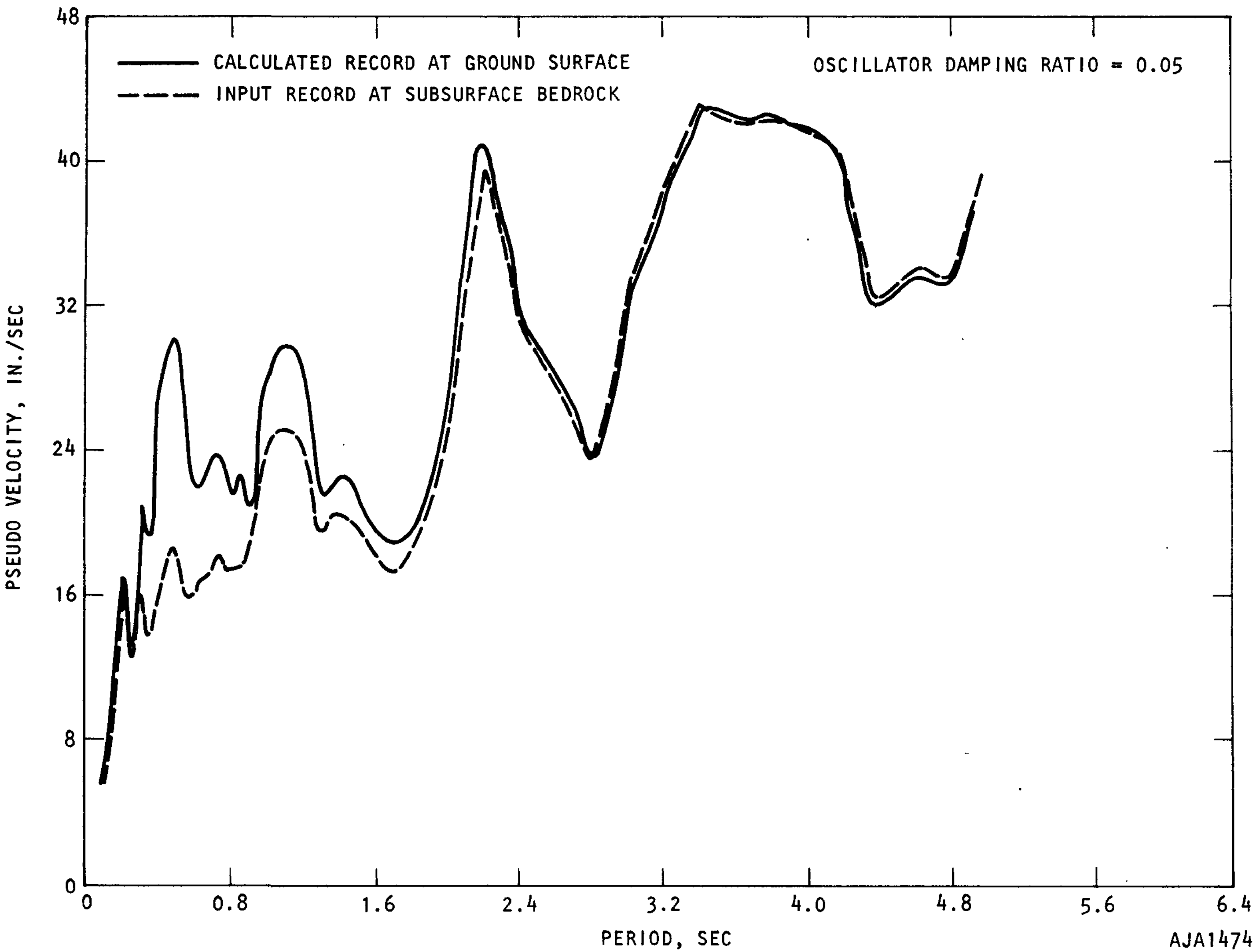

FIGURE 3-5. COMPARISON OF SPECTRA AT GROUND SURFACE AND AT BEDROCK FOR EXAMPLE PROBLEM

R-6914-925

b. The first-level approach is based on the use of the *average* spectra for strong motion earthquakes as determined by G. W. Housner (Reference 3.7). Other spectra have been formulated based on an *envelope* of strong motion spectral characteristics (Reference 3-6). In general, the use of an average spectrum or envelope spectrum for defining seismic input should be consistent with the allowable stress levels, damping factors, and peak earthquake acceleration levels used in the structure analysis and design.

c. The strong motion spectrum shown in Figure A-4 of Appendix A, for an oscillator damping of 5 percent, is used in this example. As in the site-dependent calculations, the oscillator damping of 5 percent has been based on damping factors set forth in Reference 3-8.

d. This spectrum is scaled according to an estimate of the strength of seismic input at the site. This estimate is based on the geologic and seismic investigations indicated in Subsection 3.2.2.1. It is assumed that these geologic and seismic investigations have indicated that the site is in a region of moderate seismicity. As indicated in Table A-5, this corresponds to a DBE peak acceleration of 0.33 g. Therefore, the strong motion acceleration spectrum of Figure A-4, Appendix A, is scaled so that its spectral acceleration at the origin of the period scale (4 ft/sec^2), which corresponds to the maximum ground acceleration, is equal to 0.33 g. This scale factor is calculated as

$$\frac{0.33}{4/32.2} = 2.66$$

and is applied to both the acceleration spectrum and velocity spectrum, as indicated in Figure 3-6.

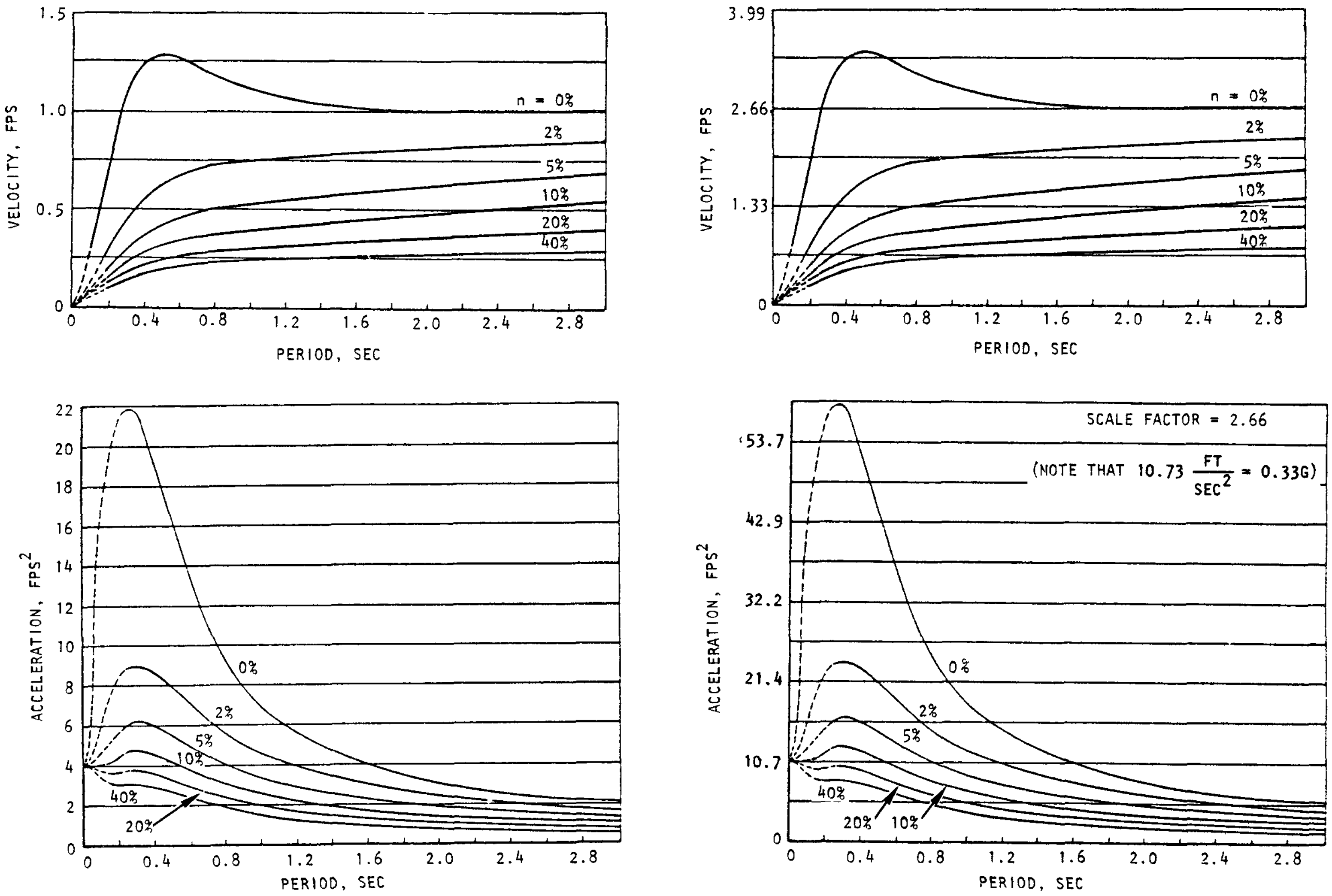

(a) ORIGINAL STRONG MOTION SPECTRA (FIGURE A-6 OF APPENDIX A)

(b) SCALED STRONG MOTION SPECTRA (TO CORRESPOND TO A PEAK GROUND ACCELERATION OF 0.33G)

FIGURE 3-6. SCALED STRONG MOTION SPECTRA FOR EXAMPLE PROBLEM

e. An ensemble of earthquake records that corresponds to the scaled spectra of Figure 3-6 is next obtained. The spectrum intensity of the 5 percent damped velocity spectrum (as defined in Table 3-1) was used as the basis of comparison between these existing records and the scaled spectra. The scaling procedure is described in Table 3-1, and the ensemble of scaled records used for this example problem is shown in Figure 3-7.

3.2.2.3 Choice of Ensemble of Records for Input Into Soil-Structure Interaction Analysis (Item 3, Figure 3-1)

a. The spectra corresponding to the single site-dependent calculation and to the scaled earthquake records are compared in Figure 3-8. As previously indicated, this illustrative example contains only a single soil-motion time history and spectrum, rather than an ensemble of time histories and ensemble average spectra. It is noted that an average spectrum from an ensemble of calculated surface motions will be relatively smooth and will not contain the peaks and valleys inherent in the spectrum from the single calculation.

b. As discussed in Subsection 3.2.2.2, the spectra from the first-level approach correspond to representative conditions in a region of moderate seismicity, whereas a magnitude 7.5 earthquake at a site 5 miles from a potential causative fault represents conditions that are more severe than the average in a moderate seismicity region. Therefore, it is consistent for the results of the site-dependent calculation, based on a magnitude 7.5 earthquake and a causative fault distance of 5 miles, to yield a more severe spectrum than that resulting from the scaled earthquake records in a region of moderate

TABLE 3-1. PROCEDURE FOR OBTAINING ENSEMBLE OF SCALED EARTHQUAKE RECORDS FOR EXAMPLE PROBLEM

Earthquake Record	Spectrum Intensity of 5 Percent Damped Spectra, in.	Scale Factor
1940 El Centro, NS Component	50.2	0.80
1934 El Centro, EW Component	21.6	1.85
1949 Olympia, S10E Component	33.0	1.21
1952 Taft, S69E Component	27.0	1.48

Procedure:

1. The spectrum intensity (SI) is defined as the area under the velocity spectrum, S_v, in the period range from T = 0.1 sec to 2.5 sec. For example,

$$SI = \int_{0.1}^{2.5} S_v(t)\,dT$$

2. The 5 percent damped spectrum is considered in this example as the basis for scaling the above records. The spectrum intensity of the scaled 5 percent damped velocity spectrum of Figure 3-6 is computed to be 40 in.

3. The scaled factor for each record is computed as the spectrum intensity of the scaled spectrum of Figure 3-6 divided by the spectrum intensity of the record. For example, the scale factor for the NS component of the 1940 El Centro earthquake (whose spectrum intensity is 50.2 in.) is

$$\frac{40}{50.2} \approx 0.8$$

4. The ensemble of earthquake records can consist of either existing strong motion measurements or of artificial earthquakes having dynamic characteristics similar to strong motion measurements. For this example problem, an ensemble was chosen that consists of scaled versions of the following records: (1) 1940 El Centro, NS Component, (2) 1934 El Centro, EW Component, (3) 1949 Olympia, S10E Component, and (4) 1952 Taft, S69E Component. These scaled records are shown in Figure 3-7.

AJA2060

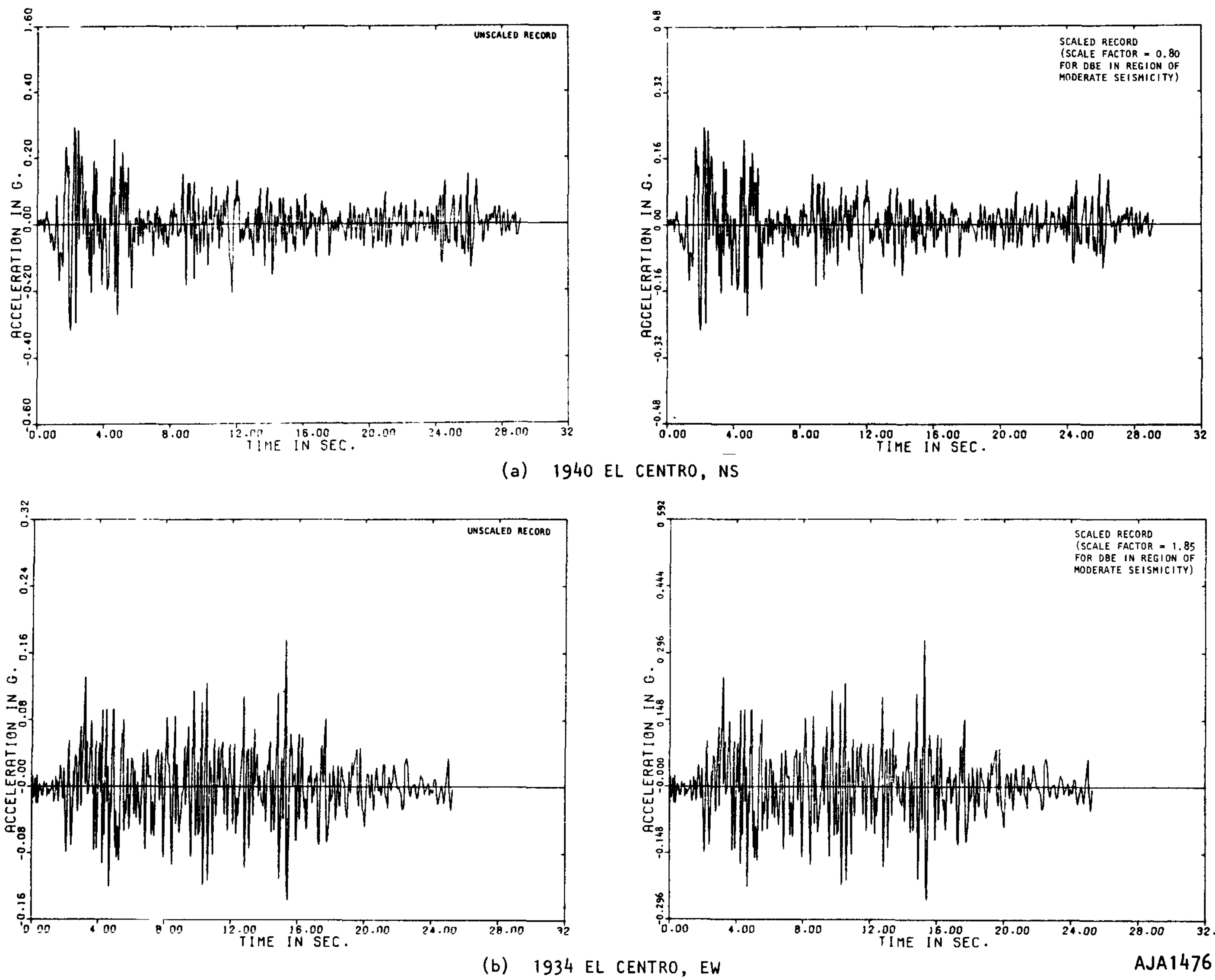

FIGURE 3-7. SCALED ENSEMBLE OF RECORDS FOR EXAMPLE PROBLEM
(SEE TABLE 3-1 FOR SCALE FACTORS)

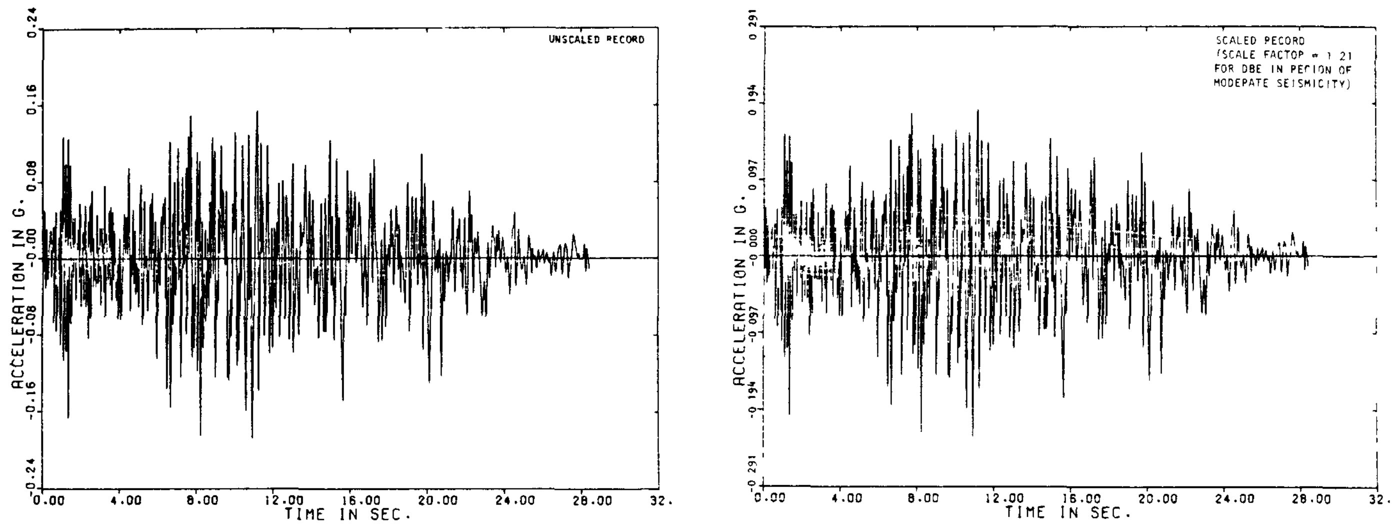

(c) 1949 OLYMPIA, S10E

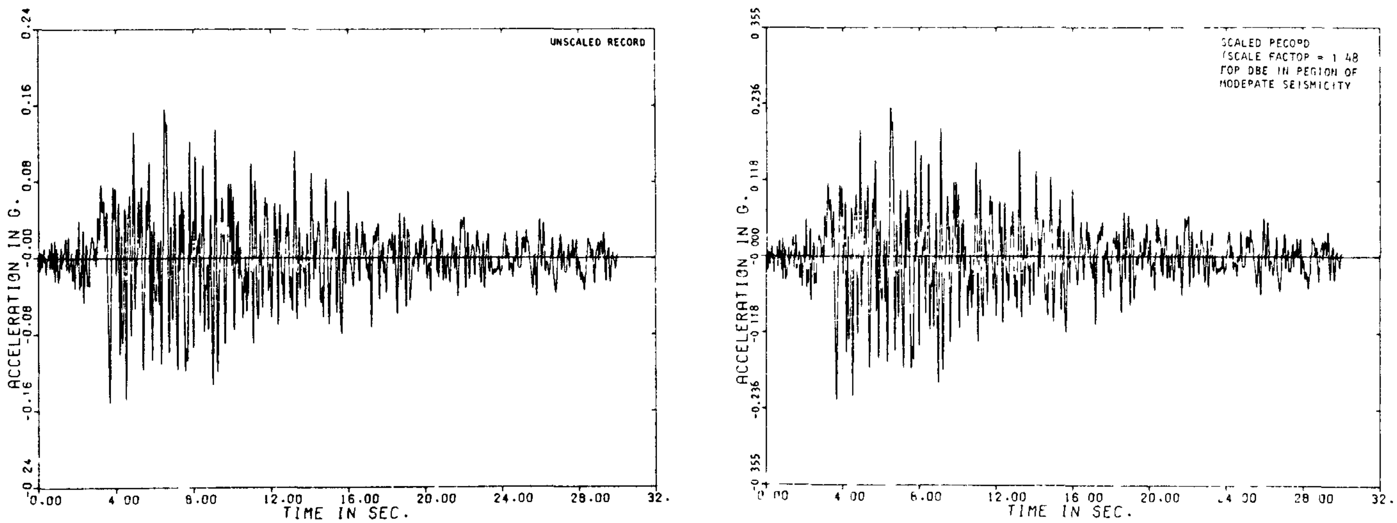

(d) 1952 TAFT, S69E

AJA1477

FIGURE 3-7. (CONTINUED)

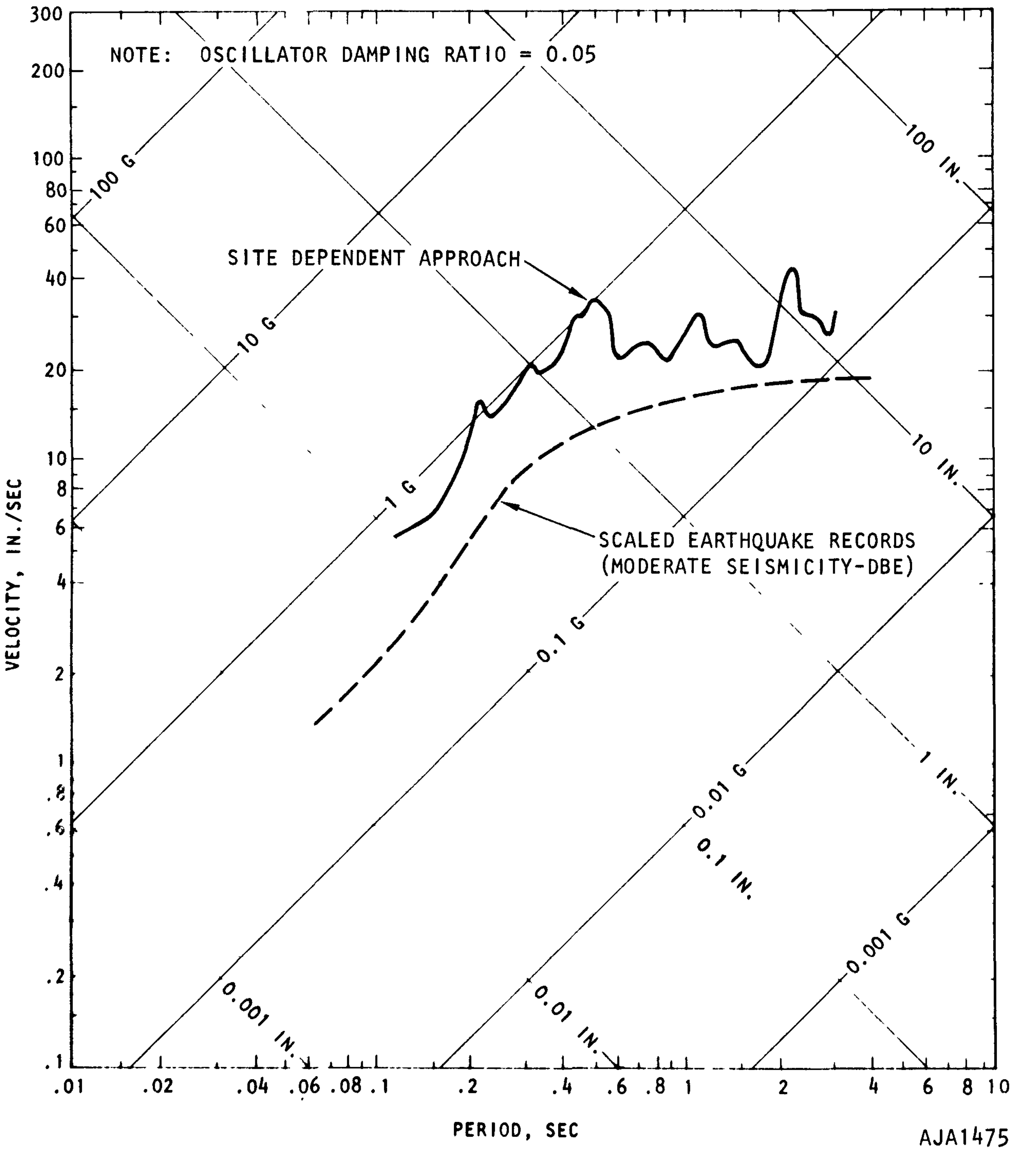

FIGURE 3-8. COMPARISON OF SPECTRA OBTAINED FROM SITE DEPENDENT CALCULATIONS AND FROM SCALED EARTHQUAKE RECORDS FOR EXAMPLE PROBLEM

seismicity. Therefore, in this example, the results of the site-dependent calculations appear appropriate for use as input into a soil-structure interaction analysis of the nuclear power plant.

3.2.2.4 <u>Soil-Structure Interaction Analysis (Item 4, Figure 3-1)</u>

a. The final step in the procedure is the calculation of dynamic soil-structure interaction effects using the ground motions computed above, as input to the analysis.

b. These effects are generally dependent on the dynamic properties of the structure, of the soil in the vicinity of the structure, and of the deeper soil and rock in some cases.

c. Techniques for calculating dynamic soil-structure interaction effects are reviewed and evaluated in Section 5.

d. A numerical example can be carried out only if the structure properties as well as the soil properties are defined.

REFERENCES

3-1. Fischer, J. A., and W. J. Murphy, "Selection of Design Earthquakes for Nuclear Reactor Facilities," *Fourth World Conference on Earthquakes Engineering*, Santiago, Chile, January 1969.

3-2. John A. Blume and Associates, Engineers, *Summary of Current Seismic Design Practice for Nuclear Reactor Facilities*, San Francisco, California, Report No. TID-25021, September 1967.

3-3. Allen, C. R., et al., "Relationship Between Seismology and Geologic Structure in the Southern California Region," *Bulletin of the Seismological Society of America*, Vol. 55, No. 4, August 1965.

3-4. Housner, G. W., "Engineering Estimates of Ground Shaking and Maximum Earthquake Magnitude," *Fourth World Conference on Earthquake Engineering*, Santiago, Chile, January 1969.

3-5. *Seismic and Geologic Siting and Design Criteria for Nuclear Power Plants*, Atomic Energy Commission Tentative Regulatory Criteria, March 1969, (to be published).

3-6. Newmark, N. M., and W. J. Hall, "Seismic Design Criteria for Nuclear Reactor Facilities," *Fourth World Conference on Earthquake Engineering*, Santiago, Chile, January 1969.

3-7. Housner, G. W., "Behavior of Structures During Earthquakes," *Engineering Mechanics Division, Proceedings of the American Society of Civil Engineers*, Vol. 85, No. EM4, October 1959.

3-8. *Seismic Design Criteria for Nuclear Power Units*, Atomic Energy Commission Regulatory Criteria, February 1970, (to be published).

SECTION 4

GUIDELINES FOR CALCULATING SITE-DEPENDENT EARTHQUAKE GROUND MOTIONS

4.1 PURPOSE AND SCOPE

The purpose of this task was to investigate procedures for estimating earthquake motions, based on the seismicity, geology, and soil properties of a given site. The effort was divided into the following subtasks:

a. Modeling of subsurface bedrock time histories

b. Scaling of bedrock records

c. Analysis of seismic response of site profiles

The behavior of soil deposits during earthquakes can often be assessed with the aid of appropriate analyses of their response to the motions developed in underlying rock formations. Therefore, it is necessary to develop suitable representations of subsurface bedrock motions for use as input into soil profile analyses. The modeling of subsurface bedrock motions is investigated under Subtask a, and an ensemble of time histories appropriate for this purpose is compiled. The uncertainties arising from the lack of recorded earthquake subsurface motions and the results of previous studies dealing with this problem have been considered. This work is described in Subsection 4.2.

Procedures for scaling subsurface bedrock records to correspond to a given nuclear reactor site are examined in Subtask b. In this subtask, the strength and duration of the subsurface bedrock record are related to the magnitude of the potential earthquake and to the minimum distance of the site from the causative fault. Subsection 4.3 presents the results of this subtask.

Subtask c consists of an investigation of procedures for analyzing the seismic response of a soil profile subjected to motions in the underlying bedrock; the results of this investigation are presented in Subtions 4.4 through 4.6. One-dimensional and two-dimensional techniques for predicting earthquake ground motions at a site are discussed in Subsection 4.4. Subsection 4.5 contains the results of a number of one-dimensional analyses of ground motions at the site of the recording instrument in the 1940 El Centro earthquake. In this, the characteristics of the calculated records are compared with those of the actual measurements. In Subsection 4.6, a parametric study of two sites with significantly different frequency characteristics identifies trends regarding the effects of the site profiles on surface earthquake ground motions. Response spectra calculated in this parametric study are compared to spectra obtained from other existing procedures for estimating seismic ground motions of a site.

4.2 SUBSURFACE BEDROCK TIME HISTORIES

This subsection contains a discussion of the modeling of subsurface bedrock motions for use as input at the base of a mathematical model of a soil profile at a nuclear reactor site.

Although some subsurface rock measurements have been made for some small earthquake motions in Japan (Reference 4-1), there are no known subsurface measurements of strong motion earthquakes. In addition, the relatively few records of strong motion obtained on or near the surface of rock outcroppings (e.g., at Helena, Montana, and at Golden Gate Park, San Francisco), do not necessarily have the same dynamic characteristics as subsurface records. These differences can be attributed to confinement of the subsurface bedrock by the overlying soil, interaction between the subsurface bedrock and the soil, and possible differences in the mechanical properties of the subsurface bedrock as compared to those of near-surface rock outcroppings due to relative weathering effects (Reference 4-2).

In summary, there are no pertinent subsurface earthquake measurements, and the few surface records obtained on rock are not necessarily representative of earthquake motions that occur at the subsurface bedrock level. Therefore, until some strong earthquake motions have been recorded on subsurface bedrock, reasonable estimates of the dynamic characteristics of earthquake motions at the subsurface bedrock level must be based on engineering judgment.

Two approaches to the problem of modeling bedrock motions have been considered herein, namely:

a. Scaling of peak accelerations, frequency content, and duration of real and/or artificial surface motions as functions of the distance from the causative fault and the earthquake magnitude, according to the empirical relationships given by H. B. Seed, et al., in Reference 4-3.

b. Use of band-limited white noise for bedrock motions, based on comparative analyses at sites where surface records are available.

From physical reasons, subsurface bedrock records should contain some frequency bias, because as the distance of a site from the focal point of an earthquake is increased, the degree of filtering of the high-frequency content of an earthquake record at that site is also increased. Therefore, the curves contained in Reference 4-3, in which the time scale of the bedrock motion at a site is modified according to an earthquake magnitude and assumed minimum distance of that site from a causative fault, is qualitatively reasonable.* However, the quantitative manner in which these records are scaled is an extremely complex problem, and will, in general, be dependent on the energy dissipation mechanisms inherent in the bedrock, and on the geologic profile between the site and the earthquake epicenter. Also, as is discussed in Subsection 4.5, one-dimensional calculations of the earthquake response of a firm site (El Centro) have indicated that the frequency content of the resulting surface motions will be distorted if the time scale of the bedrock record is modified according to the procedure of Reference 4-3. Therefore, in view of the considerable uncertainties presently involved in scaling the frequency content of the bedrock motions, it appears reasonable to use a simple band-limited white noise process, with constant frequency content over the range of interest, to simulate subsurface bedrock motions. The advantages of using this type of random process are summarized as follows:

a. Ensembles of band-limited white noise are simple to generate and use in a dynamic analysis.

*The minimum distance of a site from a potential causative fault can be used as a scaling parameter only in regions where surface fault patterns exist. As discussed in Subsection 4.3.1, the strength and duration of subsurface bedrock motions in regions with no surface fault patterns must be estimated from available seismic information for the surrounding area.

b. Segments of white noise, although simple, have the basic dynamic properties of a strong ground motion. This was shown by G. N. Bycroft (Reference 4-4), who demonstrated that the response spectra of band-limited white noise samples correlate closely with the average earthquake spectra calculated by G. W. Housner (Reference 4-5). Also, in Reference 4-6, Housner and P. C. Jennings used band-limited white noise samples, as input to a mathematical filter, to generate an ensemble of artificial earthquakes having dynamic characteristics like recorded motions of strong earthquakes. In addition, filtered white noise was used by S. H. Liu and D. P. Jhaveri to simulate actual earthquake records at the ground surface (Reference 4-7).

c. The uniform level of frequency content inherent in a white noise process seems more appropriate, in view of the lack of data for comparison, than more refined estimates of sub-surface bedrock motion. The approximate nature of the estimated frequency content is clearly evident. The possible overabundance of high-frequency content in the band-limited white noise model for bedrock motion is not a serious problem, inasmuch as these components (which err conservatively, if overestimated) are greatly reduced by subsequent filtering through the model of the soil profile.

An ensemble of four white noise records suitable for use as subsurface bedrock accelerograms are shown in Figure 4-1. Each of these white noise records has a duration of 30 sec. The 120 numbers which form each record have a zero mean and a variance of 1. In addition, each record is considered to be piecewise linear with a mean square of 0.667. In Reference 4-6, the spectral density function of these white noise segments is given as

$$G(\omega) \approx \frac{\sigma_n^2 \Delta h}{\pi} \left[1 - \frac{(\omega \Delta h)^2}{6}\right] \tag{4-1}$$

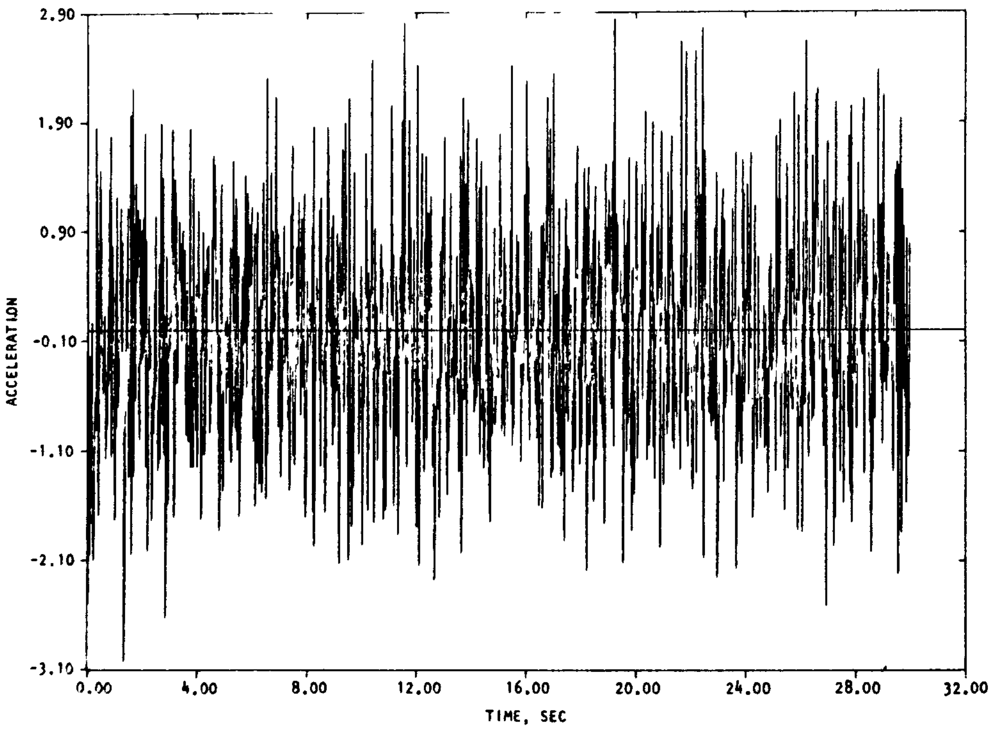

(a) WHITE NOISE NO. 1

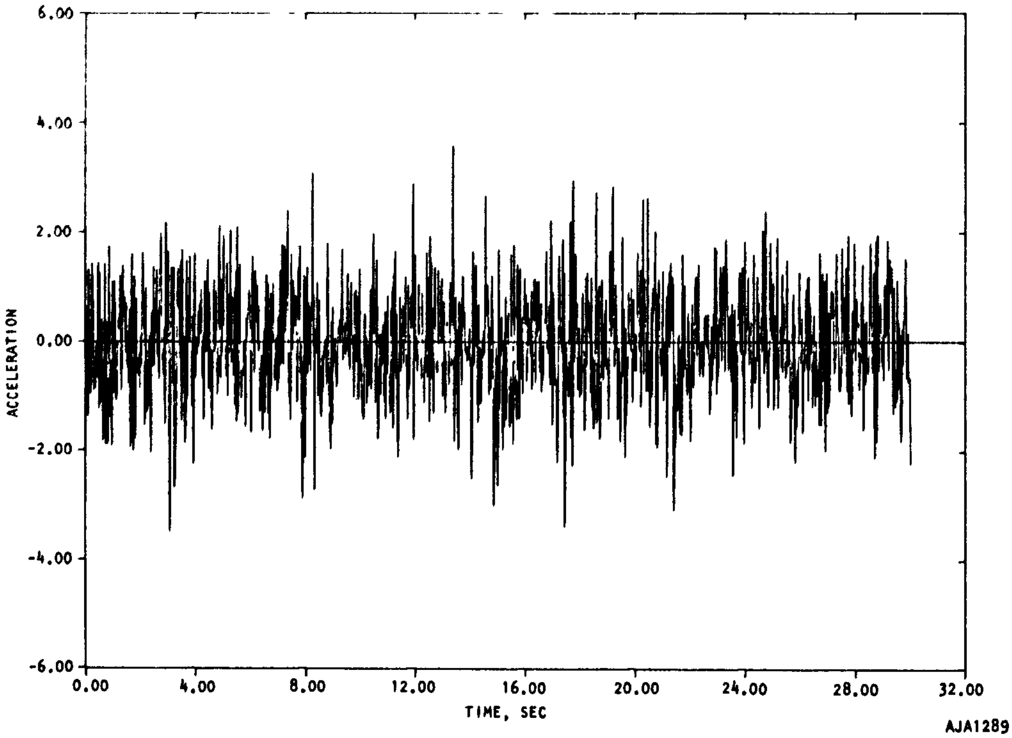

(b) WHITE NOISE NO. 2

FIGURE 4-1. ENSEMBLE OF RECORDS FOR SEISMIC MOTIONS AT SUBSURFACE BEDROCK LEVEL (NOTE DIFFERENT SCALES)

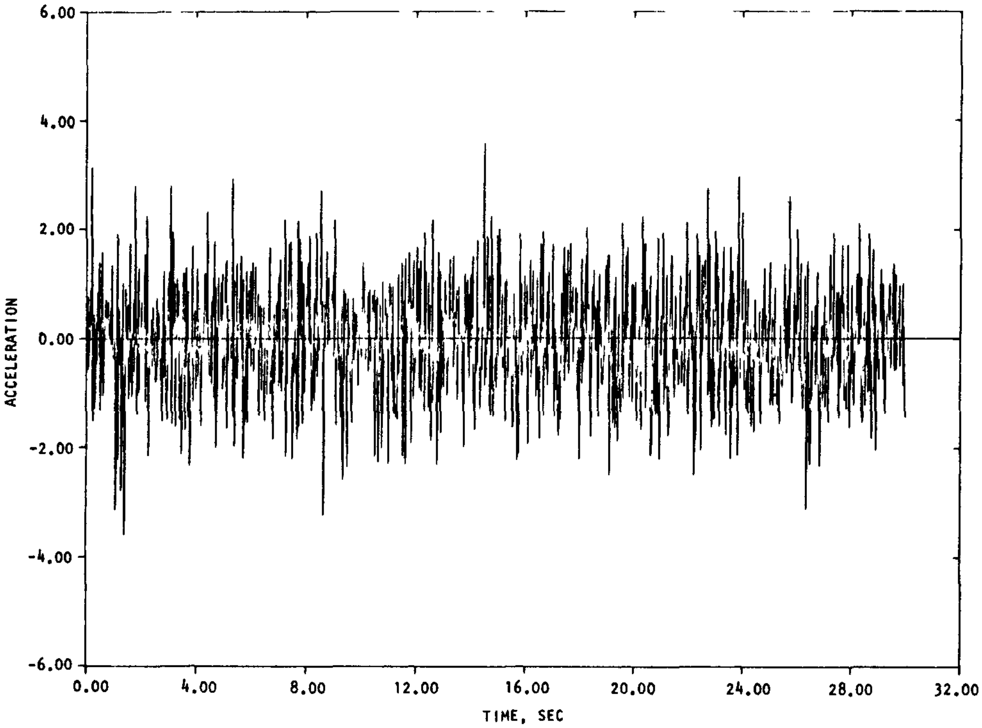

(c) WHITE NOISE NO. 3

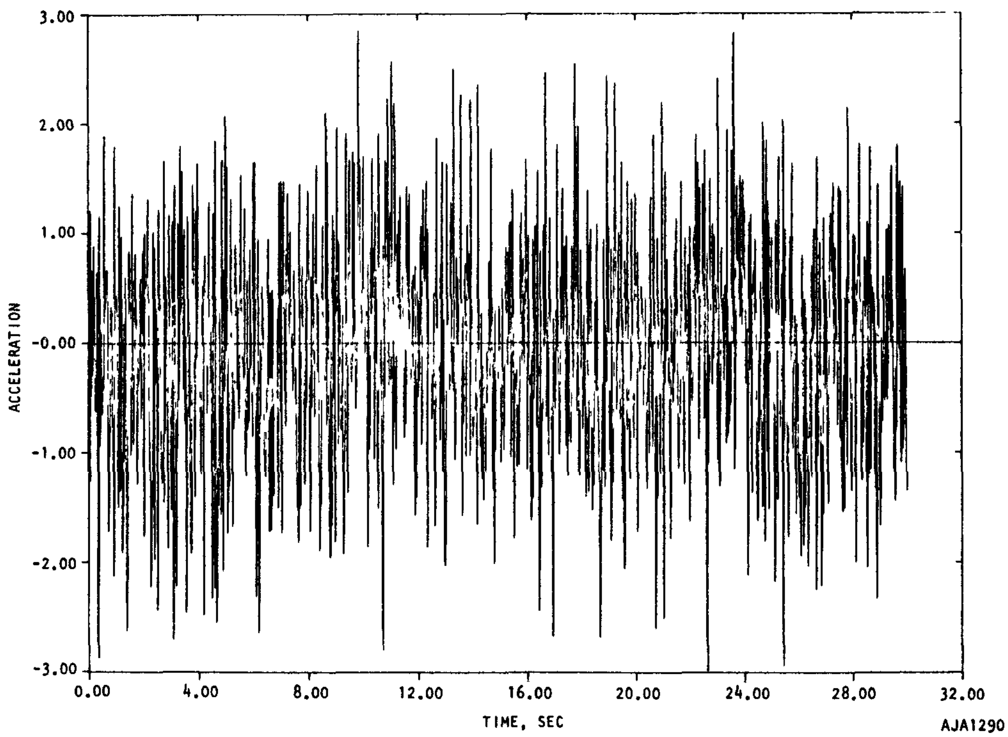

(d) WHITE NOISE NO. 4

FIGURE 4-1. (CONTINUED)

for small values of $\omega\Delta h$, where σ_n^2 is the variance of the Gaussian, uncorrelated numbers used to form the record, ω is the circular frequency, and Δh is the time interval between successive numbers in the digitized record. For $\Delta h = 0.025$ sec, Equation 4-1 indicates that for $\omega \leq 31$ rad/sec, $G(\omega)$ is constant to within 10 percent; and for $\omega \leq 21$ rad/sec, $G(\omega)$ is constant to within 5 percent.

The ensemble of records shown in Figure 4-1 represents only one of many possible white noise ensembles that might be used as subsurface bedrock motions. All that is required to construct additional records is a sequence of normally distributed uncorrelated numbers; generation of such sequences is well within the capabilities of most computer facilities. Procedures for scaling the strength and duration of an ensemble of band-limited white noise records to simulate subsurface bedrock motions are discussed in the next section.

4.3 SCALING OF BEDROCK RECORDS

To model subsurface bedrock motions, the strength and duration of white noise segments should be specified. Relating the strength and duration to the distance from the site to a potential fault and to the Richter magnitude of the earthquake appears to be a feasible approach.

4.3.1 GENERAL SCALING CONSIDERATIONS

The size of an earthquake is commonly measured by its magnitude on the Gutenberg-Richter scale; this magnitude is an indication of the amount of energy released when slippage occurs along a given fault. In general, the greater magnitude earthquakes result from the larger lengths of fault rupture. Therefore, the Gutenberg-Richter magnitude of the earthquake is an important parameter for measuring the strength level and duration of subsurface bedrock motions that might occur during an earthquake.

The dynamic characteristics of subsurface bedrock motions are strongly dependent on the fault patterns and geology of the region. This can often be characterized by an assumed distance from the site to a potential causative fault in regions where surface fault patterns can be observed. Therefore, in these regions, the distance to a causative fault is a reasonable parameter for scaling subsurface bedrock motions. However, many parts of the eastern United States do not exhibit surface fault patterns, and the relatively few earthquakes that have occurred in these regions can generally be attributed to a subsurface source mechanism. Therefore, in these regions, the minimum distance to a potential causative fault cannot be used as a parameter for scaling subsurface bedrock motions. Instead, the strength and duration of subsurface bedrock motions must be estimated from available information regarding any previous earthquakes that have occurred in the region.

The greatest number of earthquake records in the United States have had shallow focal points and have occurred in regions containing surface fault patterns (such as California, for example). The scaling techniques for subsurface bedrock motion described in this subsection will be based on these critical earthquake regions. As indicated in the preceding paragraph, the strength and duration of subsurface bedrock motions for the generally less severe earthquake regions that do not exhibit surface fault patterns (such as in many areas of the Eastern United States) should be estimated from available regional seismic information, rather than from the scaling procedures described in this subsection.

The significant distance from a site to a causative fault can be represented by the distance to the epicenter (the position in plan where the earthquake starts) or to the hypocenter (the actual point below the surface at which the fault break begins). However, the use of the epicentral distance as a measure of the distance to the zone of energy release may be misleading for the case of a long fault break and a site near a causative fault. For this case, the site can be relatively far from the epicenter, but only a short distance from the zone of energy release when the break has progressed along the fault and toward the location of the site. The location of the hypocenter may be important for sites located near a fault; however, since many known earthquakes (in California, for example) have relatively shallow focal depths, the hypocentral distance and epicentral distance may not differ significantly for sites located at moderate distances from a fault (Reference 4-3).

When estimating seismic input motions for a nuclear power plant site, it is conservative to assume the region of energy release to be located at the point along the fault that is closest to the site. In this study, the term "distance to the causative fault" corresponds to this assumed location of the zone of energy release.

In summary, it is important to relate the strength level and duration of the subsurface bedrock motions to the size of the earthquake and to the fault patterns of the surrounding region. The size of the earthquake can be represented by the Gutenberg-Richter magnitude, whereas the fault patterns can be represented by the minimum distance from the site to a potential causative fault. In regions where no surface faults can be observed, the characteristics of the subsurface records should be estimated from available seismic information of the surrounding area.

Due to the absence of subsurface earthquake motion measurements, the scaling techniques presented in the remainder of this subsection represent only first approximations for estimating the strength and duration of subsurface bedrock motions at a site. Considerable experimental and analytical programs should be initiated to provide improved representations of the dynamic characteristics of these subsurface motions.

4.3.2 DURATION OF STRONG MOTION OF BEDROCK RECORDS

Housner studied the duration of strong motion for a number of earthquake records, and found the duration to be dependent on the magnitude of the shock (Reference 4-8). From these studies, a plot of duration of the strong shaking phase versus Richter magnitude was obtained, and is shown in Figure 4-2. Although this plot was obtained for surface

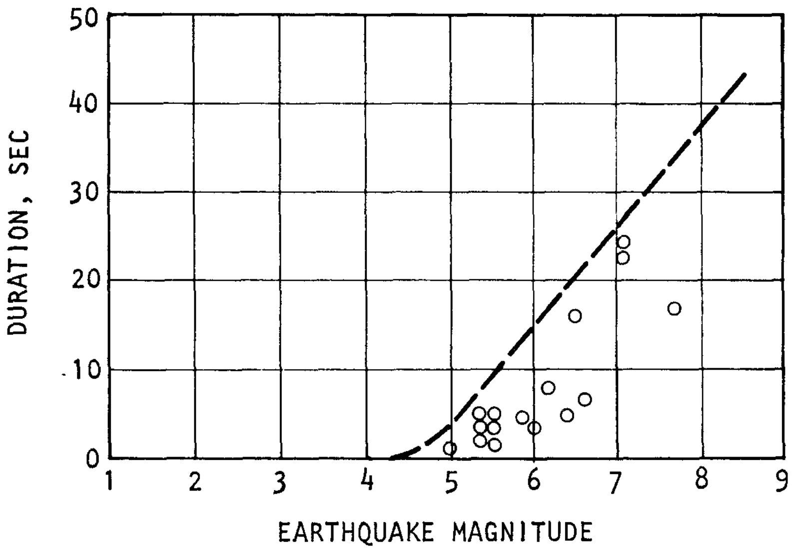

FIGURE 4-2. DURATION OF STRONG SHAKING VS EARTHQUAKE MAGNITUDE (REFERENCE 4-8)

motions, the same relation was assumed herein to hold for subsurface bedrock records. Also, Housner found that the duration of strong shaking can be distinguished only for ground motions recorded relatively close to the causative fault. Therefore, the duration of strong motion was assumed in this study to be dependent on earthquake magnitude only. The effect of causative fault distance on duration is thought to be minor and cannot be specified until more precise measurements at sites far from a causative fault become available.

4.3.3 STRENGTH OF SUBSURFACE BEDROCK RECORDS

The strength of an earthquake may be defined in terms of one of the following parameters (see Liu, Reference 4-9):

a. Peak amplitude of ground acceleration

b. Peak amplitude of ground displacement

c. Spectrum intensity

d. Time-averaged root-mean-square acceleration of the earthquake record

The peak acceleration or the peak displacement can be used to define a scale factor for a specific earthquake record, but they do not lead to good correlation between the relative strengths of different earthquakes. Also, these quantities are not good measures of the frequency content of the motion, nor are they particularly meaningful for the response of most structures. Furthermore, the peak displacement is inaccurately known because of errors involved in doubly integrating earthquake acceleration records.

The spectrum intensity of an earthquake has been defined by Housner to be the area under its pseudo-velocity spectrum between periods of 0.1 to 2.5 sec (Reference 4-5). This definition correlates the earthquake strength to the peak response of an oscillator in a period range common to many structures.

The root-mean-square (rms) acceleration of an earthquake record is defined as

$$\text{rms} = \left[\frac{1}{T}\int_{0}^{T} \ddot{y}^{2}(t)dt\right]^{\frac{1}{2}}$$

where $\ddot{y}(t)$ is the earthquake record having a duration of strong motion T. The primary advantage of the rms acceleration as a measure of the strength of an earthquake record is that it is easily calculated and is applicable for both deterministic and nondeterministic earthquake response analyses. It is dependent only on the input record, as contrasted with the spectrum intensity, which is dependent on the transfer characteristics of the structure as well as the input record. However, these two measures of earthquake strength lead to nearly the same results when applied to strong earthquake motions (Reference 4-6).

Some insight into the problems of choosing a meaningful earthquake strength definition has been provided by Housner in Reference 4-10. In this, the dynamic characteristics of an accelerogram recorded near the epicenter of the 1966 Parkfield earthquake were compared to those of the 1940 El Centro record. Records taken at the Parkfield earthquake showed that high peak accelerations, such as that shown in Figure 4-3(a), occurred within a few miles of the fault but did not typify the acceleration levels at distances greater than about 6 miles. However, near the causative fault, the Parkfield accelerograms indicated peak accelerations of about 0.5 g as compared to a peak acceleration of 0.33 g for the El Centro record. Also, as indicated in Figure 4-3(c), the ordinates of the response spectrum for the Parkfield accelerogram are seen to be consistently greater than those of the El Centro shock, which is usually considered to be the most severe ground motion yet recorded. However, the Parkfield earthquake did almost no damage to the structures located near the fault.

This apparent paradox is resolved when it is observed that the duration of strong motion in the Parkfield record is about 1 sec, as compared to a strong motion duration of 15 sec for the El Centro record.

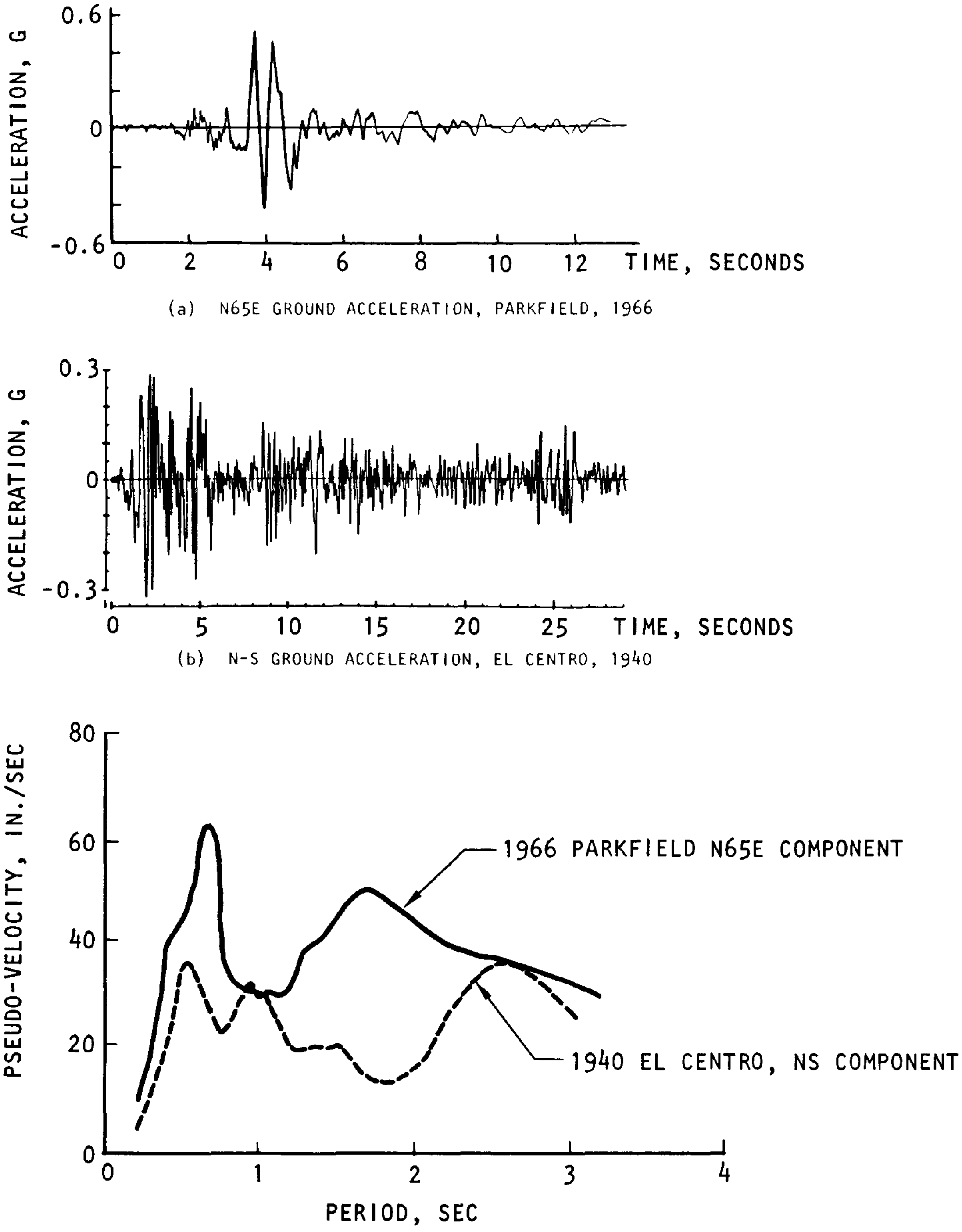

(a) N65E GROUND ACCELERATION, PARKFIELD, 1966

(b) N-S GROUND ACCELERATION, EL CENTRO, 1940

(c) COMPARISON OF VELOCITY SPECTRA

FIGURE 4-3. COMPARISON OF PARKFIELD AND EL CENTRO EARTHQUAKE CHARACTERISTICS

Housner concluded in his study that an earthquake excitation of strong motion with a short duration is not as damaging as might be inferred from its peak acceleration and response spectrum.

The above discussion indicates that the duration of strong motion in an earthquake record is an important measure of its potential damage to existing structures in the area. Also, because the rms acceleration of the strong shaking and the spectrum intensity give similar results, the above paragraphs indicate that no single measure of the strength of earthquake ground motion is going to be satisfactory for all applications. The potentially most damaging earthquakes are the larger shocks, however, and these will usually govern the structure and equipment design. For these larger shocks, which have strong motion durations of several seconds, the spectrum intensity of rms acceleration averaged over the duration of strong motion are judged to be the best measures of the strength of ground shaking.

The rms acceleration has additional advantages that render it desirable for use as a definition of earthquake strength in this study. First, it is easily calculated directly from the record. Second, the rms acceleration is especially appropriate for measuring the strength of motion modeled by band-limited white noise, because it is the single measure needed for the application of random vibration theory to earthquake response analysis, based on this type of input. For these reasons, the rms acceleration has been adopted in this study as the measure of the subsurface bedrock motion strength.

It remains to discuss methods for scaling the strength of the subsurface bedrock motion to correspond to a particular site location. Housner, in Reference 4-8, has developed curves for scaling the peak acceleration of surface motions in terms of (1) the distance of the site to the fault and (2) the earthquake magnitude. A comparison of these curves with recorded data is shown in Figure 4-4(a), and indicates the scatter involved in using these curves. It is apparent that a considerably greater degree of uncertainty is involved in developing scaling procedures for bedrock motions, due to the complete lack of measurements of strong motion in subsurface

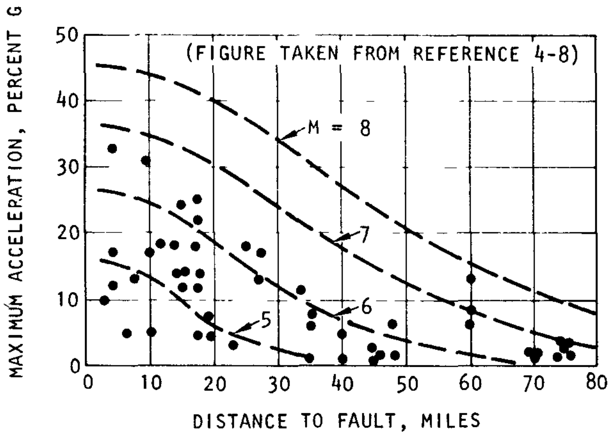

Strong Motion Records	Magnitude	Distance to Fault, Miles	Peak Acceleration, Percent g
1940 El Centro (NS)	7.0	10-15	0.33
1949 Olympia (N10W)	7.1	25	0.18
1962 Taft (N69W)	7.7	40	0.18
1934 El Centro (EW)	6.5	35	0.16

NOTE: COMPARISON OF PEAK ACCELERATIONS OF RECORDS IN TABLE TO THOSE INDICATED BY CURVES IN FIGURE INDICATES SCATTER INVOLVED IN USING CURVES OF THIS TYPE.

(a) ILLUSTRATION OF SCATTER IN MEASUREMENTS OF PEAK ACCELERATIONS OF GROUND SURFACE MOTIONS

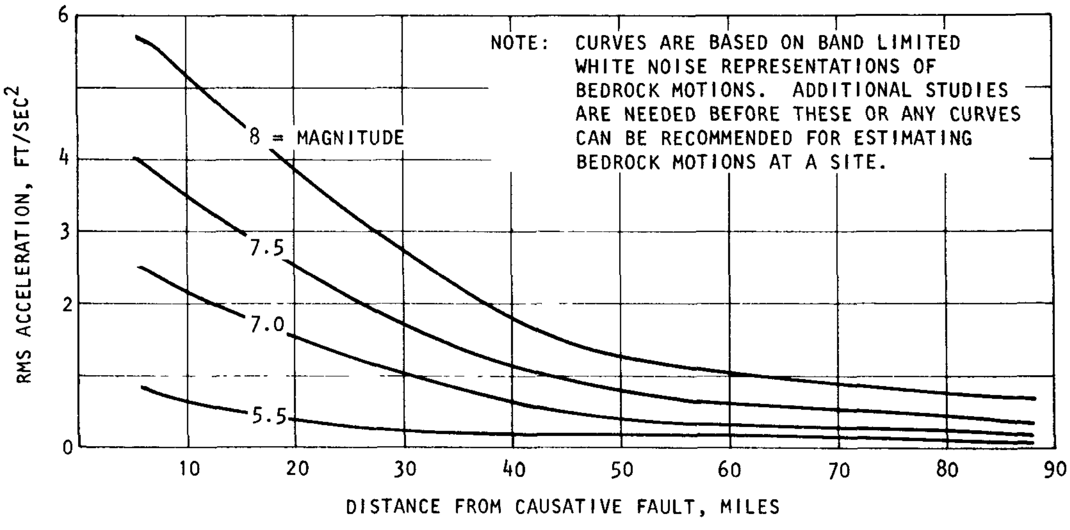

(b) ILLUSTRATIVE SCALING CURVES FOR SCALING OF RMS ACCELERATION OF SUBSURFACE BEDROCK MOTION--FOR USE IN PARAMETRIC STUDY OF SUBSECTION 4-6

AJA1399

FIGURE 4-4. ILLUSTRATIVE CURVES FOR SCALING STRENGTH LEVELS OF SURFACE MOTIONS AND OF SUBSURFACE BEDROCK MOTIONS bedrock on which to base a scaling approach. In order to resolve this difficulty, considerable investigation, beyond the scope of this study, is required and is discussed in Subsection 2.2.

A set of illustrative curves for scaling the strength level of subsurface bedrock motions are shown in Figure 4-4(b), and have been developed for use in the parametric investigation contained in Subsection 4.6. These curves have the same functional form as those of Seed, et al., who, in Reference 4-3, used weighted averages of empirical formulae to obtain a set of curves relating the peak acceleration of bedrock motion to the causative fault distance and the earthquake magnitude. To be more appropriate for use in scaling band-limited white noise records, the ordinates of these curves have been changed to rms acceleration by: (1) maintaining the shapes and relative positions of the original curves of Reference 4.3, and (2) making use of the limited number of one-dimensional calculations at the site of the 1940 El Centro earthquake described in Subsection 4.5.

The curves of Figure 4-4(b) are not intended to represent a completely definitive procedure for scaling bedrock motions; rather, they represent a set of illustrative approximate curves that were obtained within the time and budget limitations of the study. It is emphasized that the development of subsurface bedrock motions involves many uncertainties that can be cleared up only by means of additional studies of the type recommended in Subsection 2.2. Therefore, the curves provided in Figure 4.4(b) are intended only to provide trends in the parametric study of Subsection 4.6, and are *not recommended for general use* in scaling bedrock motions. Also, this figure is based on a band-limited white noise model of bedrock motions, and may have to be modified if other representations of bedrock records are used.

4.4 INVESTIGATION OF ANALYTICAL TECHNIQUES FOR CALCULATING EARTHQUAKE MOTIONS

In this subsection, techniques for computing the effect of the soil profile properties on earthquake ground motions are discussed. This information is intended to provide background information for the calculations described in Subsections 4.5 and 4.6.

A number of mathematical models based on a one-dimensional or two-dimensional representation of the site profile are suitable for use on the digital computer in analyzing the seismic response of the profile to input base motions. Three-dimensional programs are also possible but are largely in the development stage at this time.

The mathematical models assume the inertia characteristics of the soil to be concentrated at a number of discrete mass points. The location of these mass points and the mass concentrated at each point reflect the mass distribution of the continuous soil profile. The discrete mass points are interconnected by stiffness elements whose characteristics represent the material properties of the soil at the corresponding locations in the profile.

For simplicity, many available mathematical models simulate the nonlinear, hysteretic, energy dissipation characteristics of the soil by an equivalent linear-viscoelastic representation. The determination of a suitable set of viscous damping coefficients for this purpose is one of the major problems in the use of a model of this type. An improved estimate of the energy dissipation characteristics of soils can be attained by models that consider stiffness elements with nonlinear material properties; however, the use of these models often involves significantly increased computer run times.

4.4.1 ONE-DIMENSIONAL AND TWO-DIMENSIONAL MODELS

A vertical shear beam model is feasible for application to sites where the significant ground motions induced by seismic excitation result from shear waves propagating vertically through the profile. As indicated in

Reference 4-11, this is true of sites for which the following conditions are valid:

- All boundaries of the site are essentially horizontal in extent; hence, the soil profile may be treated as a series of semi-infinite layers.

- Seismic waves propagate vertically to the surface by means of shear deformations induced in the soil layers by a seismic excitation at the subsurface bedrock level. This will generally be true for deep-focus earthquakes and will not be true for estimating ground motions near the source of a shallow-focus earthquake. However, for shallow-focus earthquakes in which the site under consideration is far away from the epicenter, the significant seismic waves may approach the local subsoils horizontally. For this case, the response of these local subsoils can be predicted by the shear beam model only if the half-wave length of incoming waves is large compared to the lateral extent of the layers (Figure 4-5).

- The energy dissipation mechanisms inherent in soil profiles, such as hysteresis effects in the layers and radiation damping in the subsurface bedrock, can be simulated by a linear visco-elastic model of the profile.

Several investigators have made comparisons of calculated results using various shear beam models with measured earthquake induced ground motions. Extensive comparisons by Seed and Idriss (References 4-12 through 4-14), as given in the sample results of Figures 4-6 and 4-7, have generally shown reasonable comparisons between measured and computed results, although the theoretical basis for the damping mechanism in their mathematical model may require further investigation (Subsection 4.4.3).

N. C. Tsai has made some shear beam calculations at the site of the Union Bay earthquake of 1967 (Reference 4-11). A seismometer layout at this site is shown in Figure 4-8, and ground motions that occurred during this tremor were measured by each of the instruments shown. The procedure

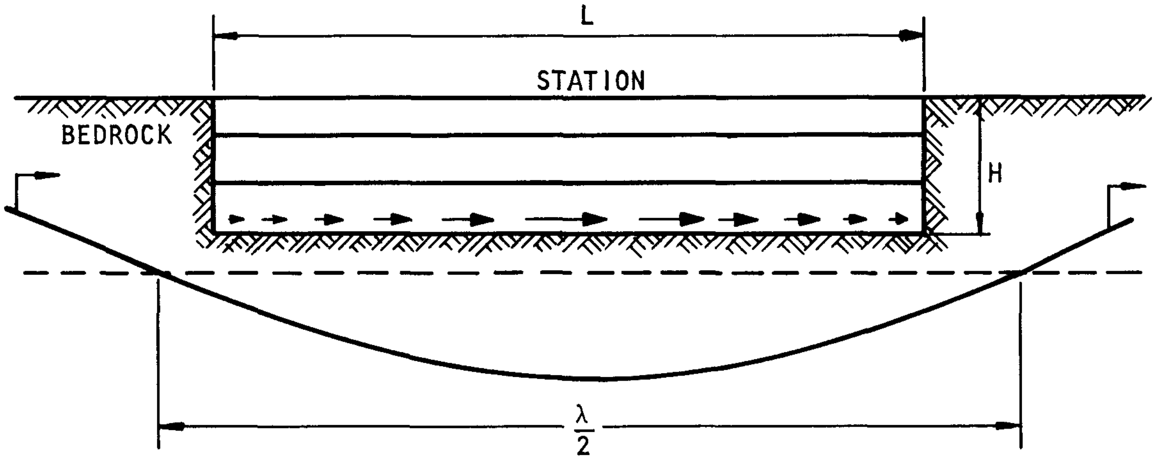

(a) $\frac{\lambda}{2} \geq L$ (SHEAR BEAM THEORY APPLICABLE)

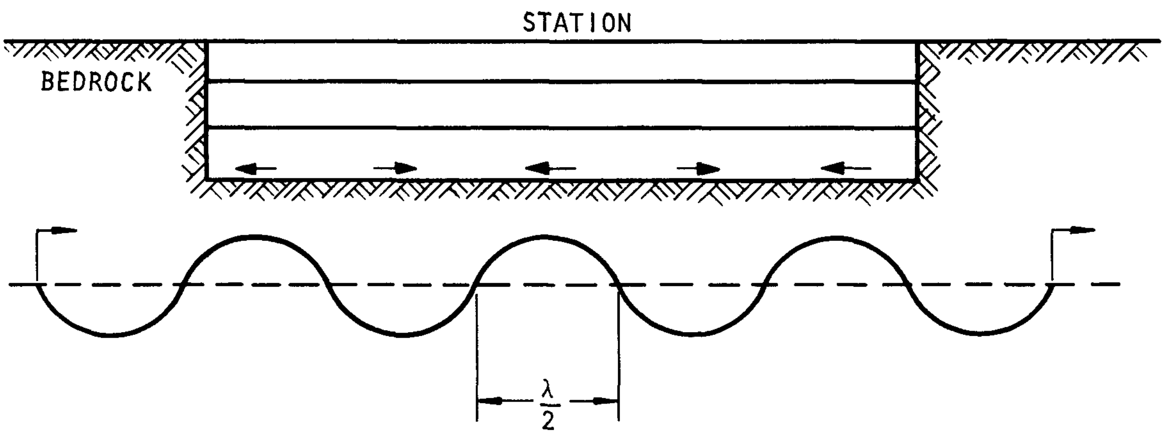

(b) $\frac{\lambda}{2} < L$ (SHEAR BEAM THEORY NOT APPLICABLE)

AJA1078

FIGURE 4-5. RESPONSE OF IDEALIZED LOCAL GROUND LAYERS TO WAVE COMPONENTS ARRIVING HORIZONTALLY FROM SHALLOW FOCUS EARTHQUAKES (REFERENCE 4-11)

AJA

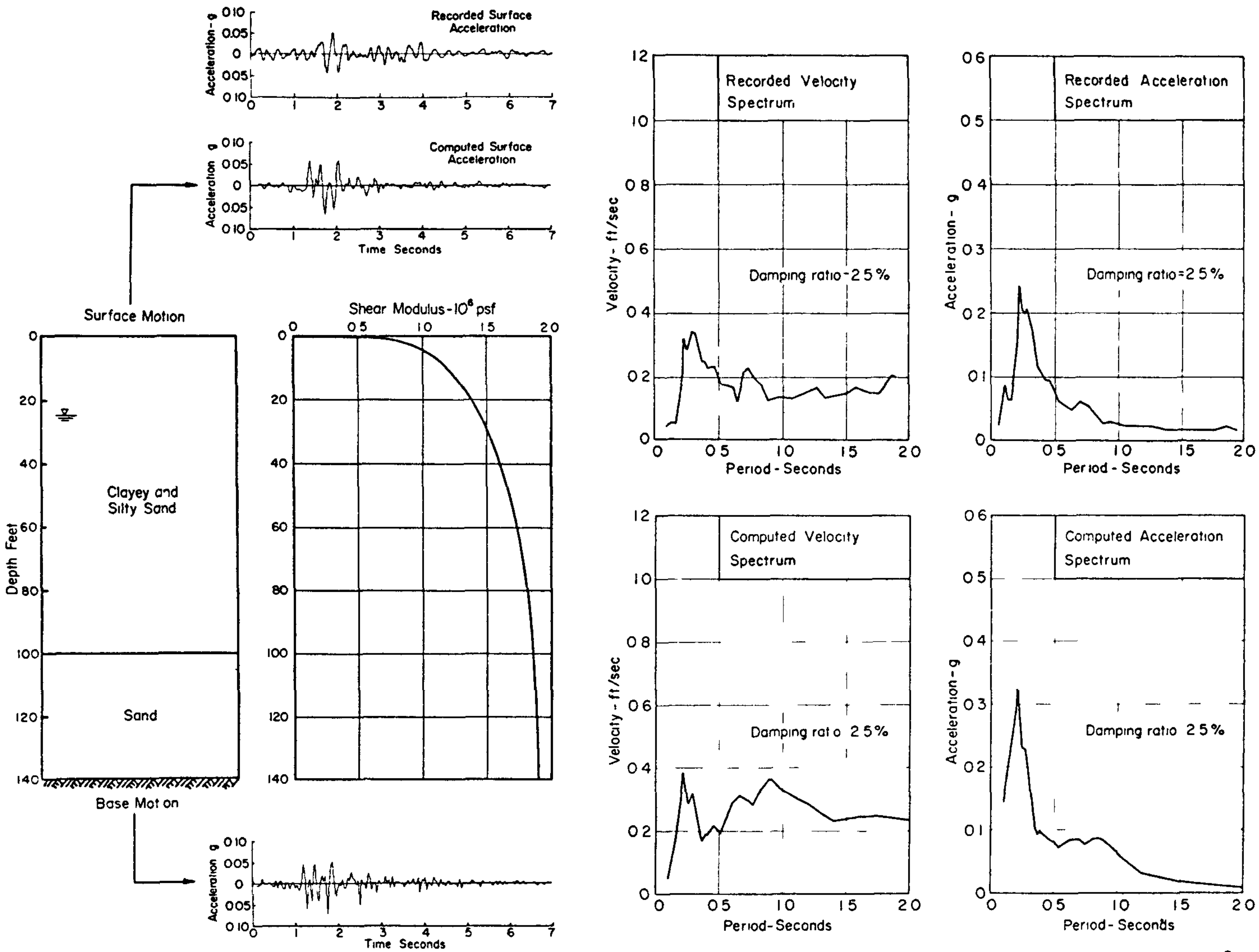

AJA1283

FIGURE 4-6. RESULTS OF SHEAR BEAM ANALYSIS OF GROUND MOTIONS--ALEXANDER BUILDING, SAN FRANCISCO (REFERENCE 4-13)

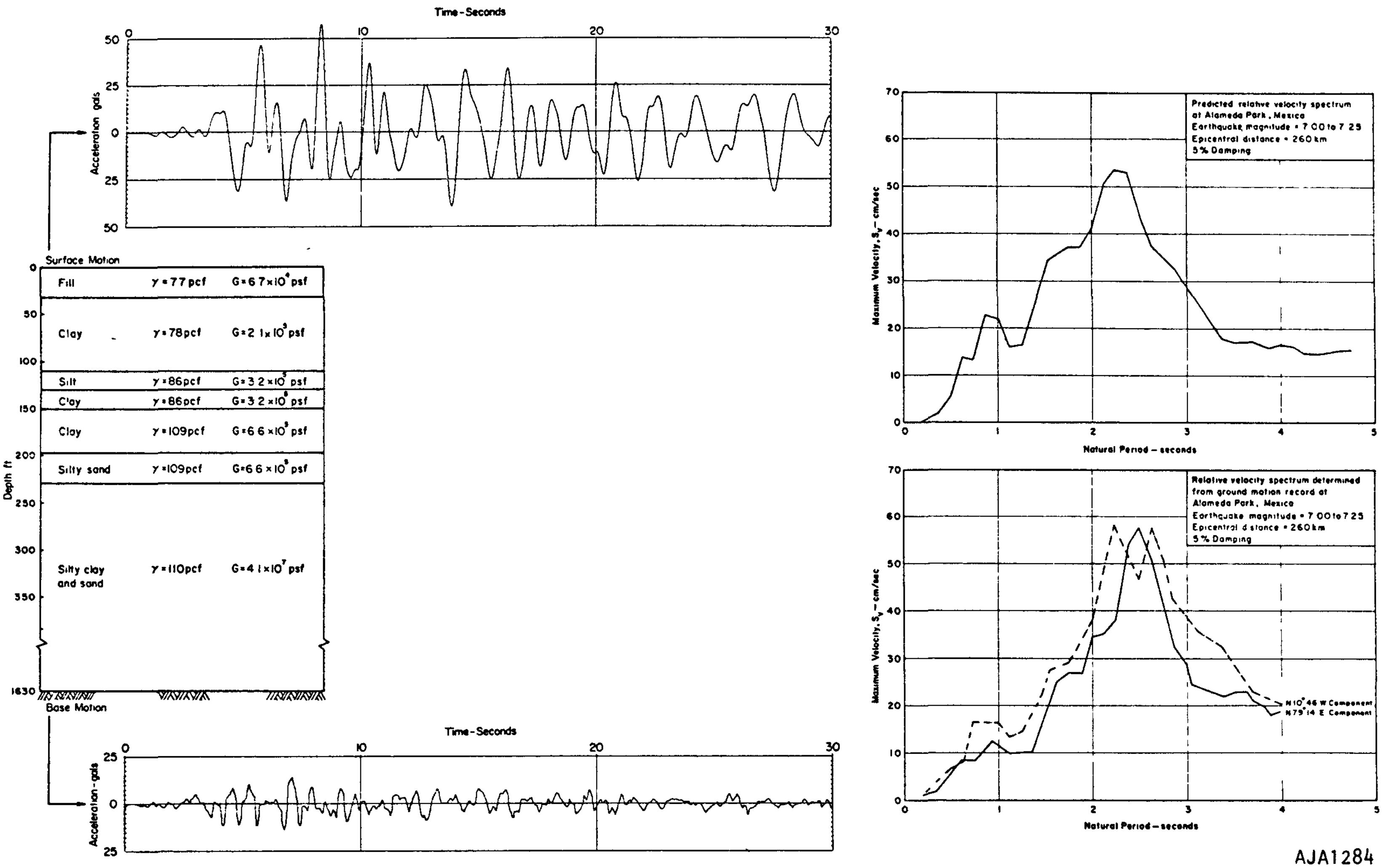

FIGURE 4-7. RESULTS OF SHEAR BEAM ANALYSIS OF SOIL RESPONSE AT SITE IN ALAMEDA PARK, MEXICO CITY (REFERENCE 4-14)

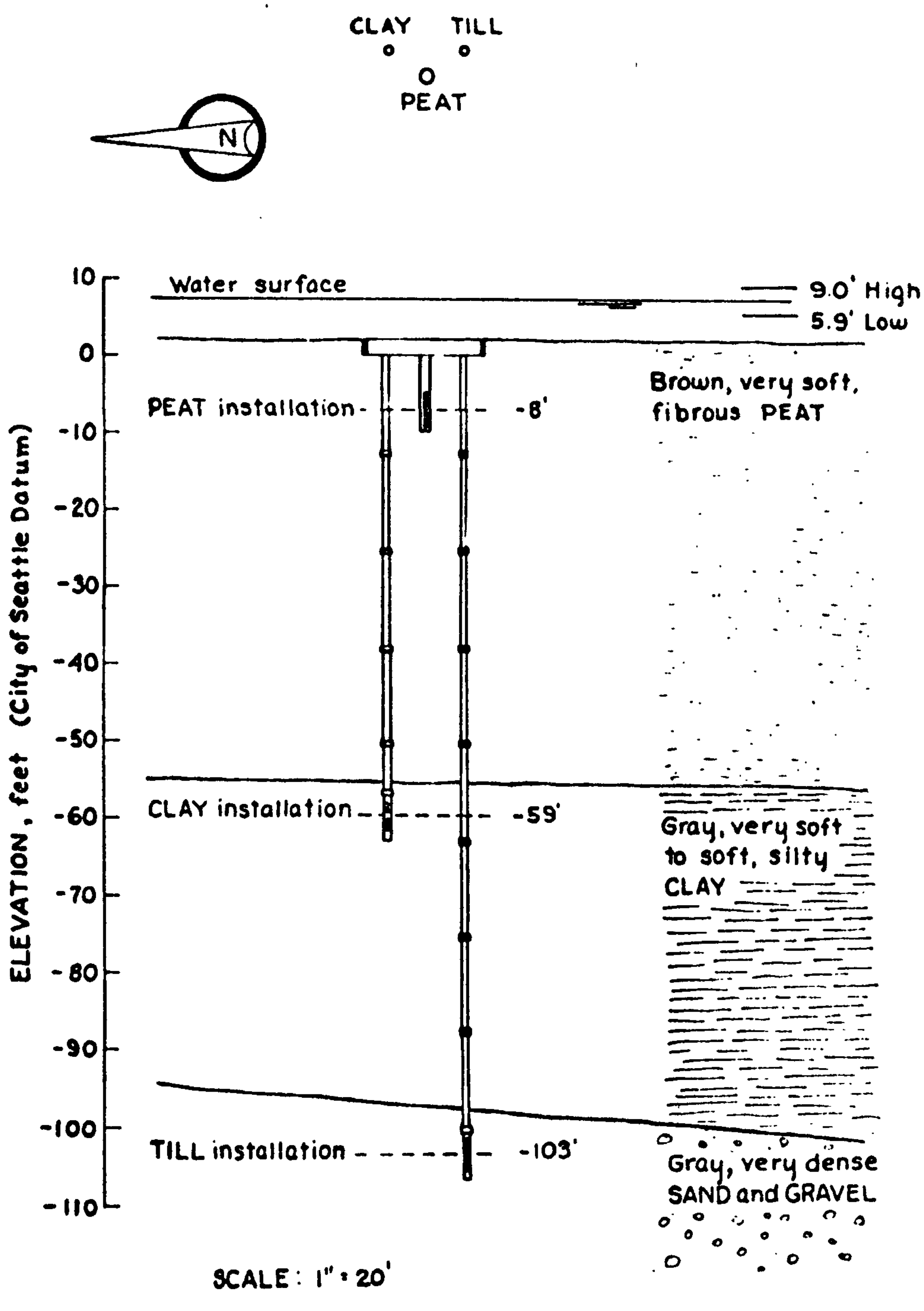

FIGURE 4-8. PRINCIPAL SYSTEM PROFILE THROUGH THE SEISMOMETER STATION AT UNION BAY (REFERENCE 4-11)

used by Tsai in these calculations was first to calculate the spectral density functions of the measured motions at the till and clay installations. The till-clay transfer function was computed from the ratio of these spectral density functions, and a shear beam model with the characteristics of this transfer function was determined. The measured time history at the till installation then was input to the base of the shear beam model. As shown in Figure 4-9, the response at the clay installation computed by the shear beam model compared closely with the measured response.

In summary, the work of Seed and Idriss and of Tsai indicate that if the input base motions and material parameters of the shear beam model are properly defined, the shear beam is capable of predicting surface motions that compare well with measured data at sites for which the above conditions are valid.

If a deposit has irregular or sloping boundaries, or is subjected to a shallow focus earthquake for which the response of the site is essentially two dimensional, the shear beam approach discussed above is no longer valid. For these conditions, more complex analytical procedures which incorporate the two-dimensional aspects of the problem are required. It is noted that the computer costs involved in these two-dimensional calculations will generally be substantially greater than those of the one-dimensional shear beam models.

An appropriate method for two-dimensional analyses is the finite element technique, in which a continuous medium is idealized as an assemblage of finite elements of appropriate sizes and shapes. These elements are interconnected at a number of nodal points as shown in Figure 4-10, and the strain distribution in each element is such that compatibility of deformations at the interface of adjacent finite elements is assured. Hence, material properties can be specified uniquely for each of the individual elements in the finite element grid, and variations in geometry and layering characteristics can be readily accommodated.

To date, no comparisons of the seismic response of soil deposits as predicted by the finite element technique with measured earthquake data are available in the published literature. However, this method gives results

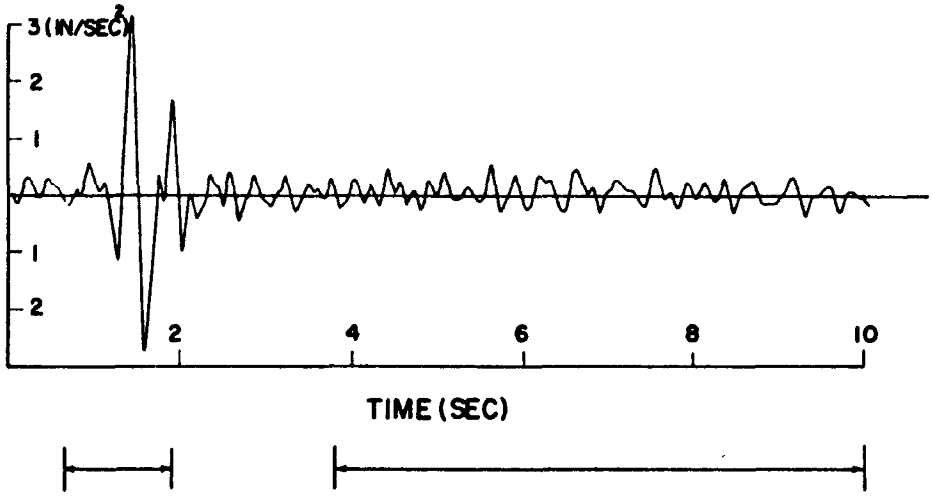

(1) EW CLAY, RECORDED (FIRST 10 SECONDS)

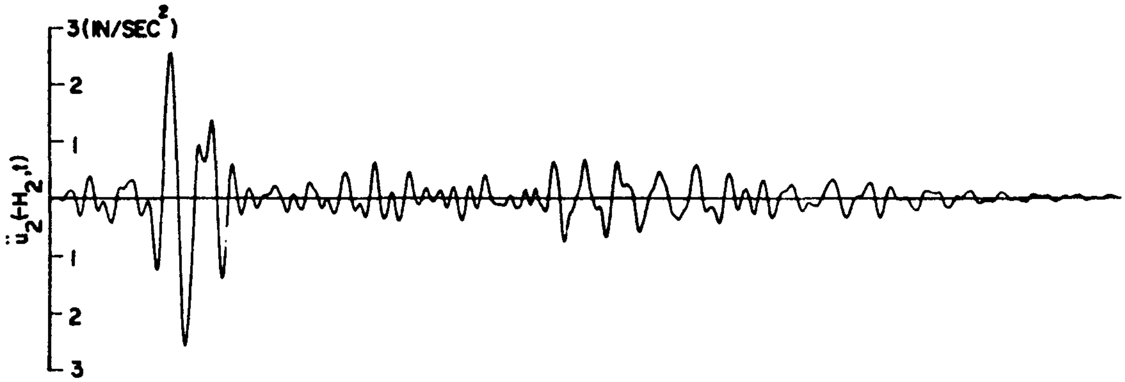

(2) EW CLAY, COMPUTED

(a) RECORDED AND COMPUTED ACCELEROGRAMS IN CLAY (EW)

FIGURE 4-9. COMPARISON OF SHEAR BEAM CALCULATIONS WITH MEASURED RESPONSE AT UNION BAY, WASHINGTON (REFERENCE 4-11)

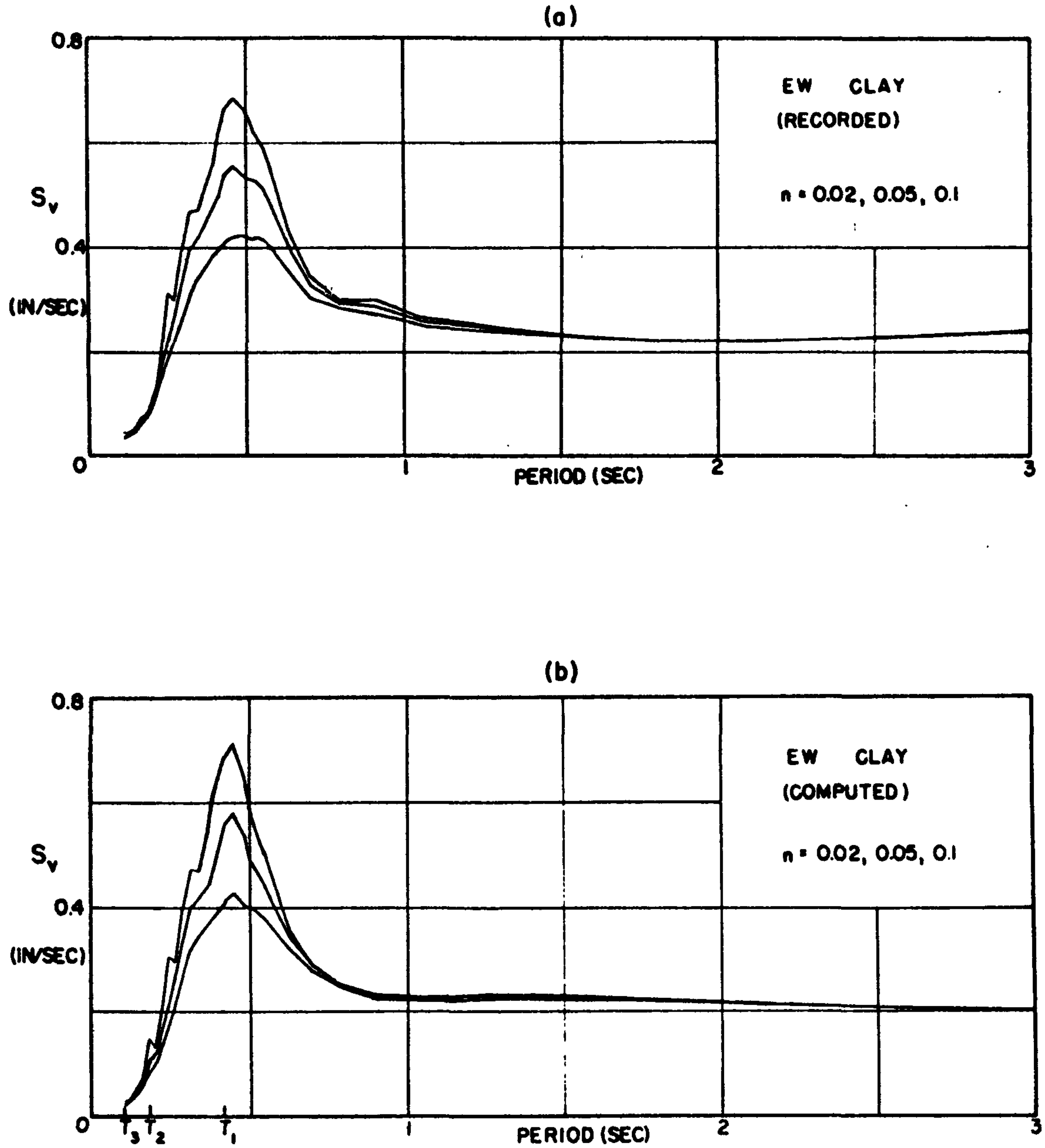

(b) VELOCITY SPECTRA FOR RECORDED AND COMPUTED CLAY ACCELEROGRAMS (EW)

FIGURE 4-9. (CONTINUED)

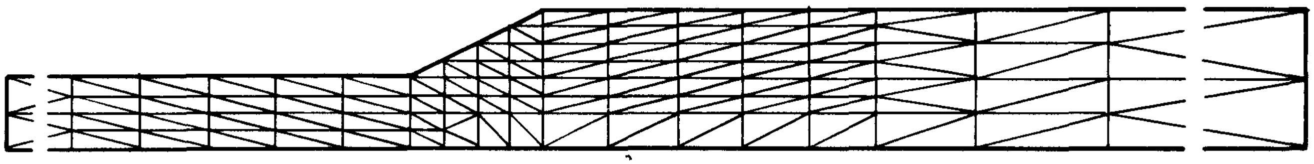

(a) IDEALIZATION OF EARTH BANK

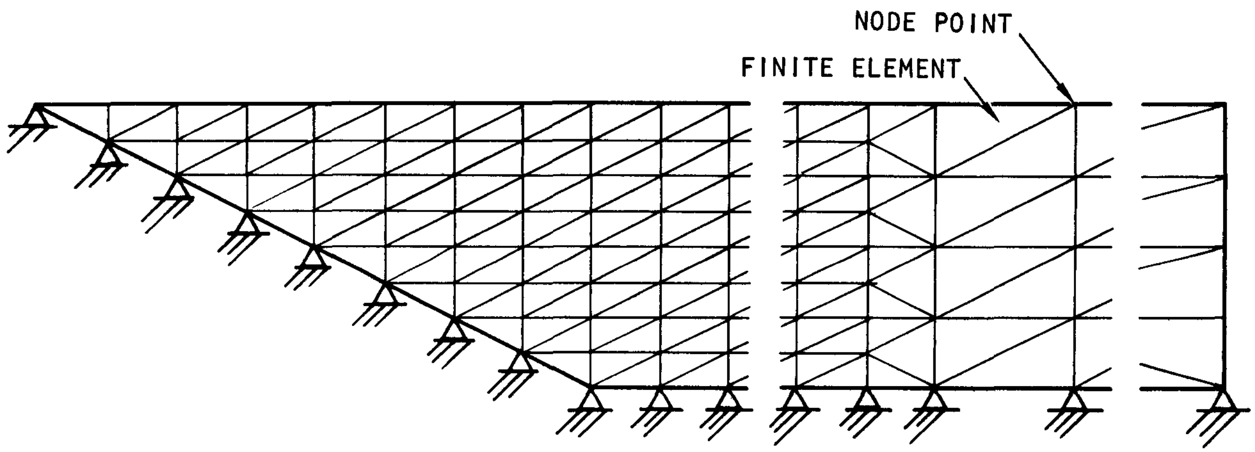

(b) IDEALIZATION OF SOIL DEPOSIT UNDERLAIN BY INCLINED ROCK SLOPE

FIGURE 4-10. FINITE ELEMENT REPRESENTATION FOR TWO-DIMENSIONAL SEISMIC RESPONSE ANALYSIS OF SOIL PROFILES (REFERENCE 4-15) in agreement with those computed using one-dimensional theories at sites with horizontal boundaries, and as indicated previously, these latter calculations show reasonable agreement with observed ground motions (Reference 4-15). Therefore, the finite element approach appears reasonable for use in two-dimensional seismic analyses of site profiles.

One of the objectives of this study is to provide seismic response calculations for a number of soil profiles, and thereby identify trends regarding the effect of site properties on earthquake ground motions. To achieve this goal within the time and budget limitations of this study, only site profiles for which the seismic response arises primarily from vertical shear wave propagation have been considered in these calculations. For these sites, a one-dimensional linear-viscoelastic shear beam model is used throughout.

4.4.2 CONTINUOUS AND DISCRETE MASS SHEAR BEAM MODELS

Since a one-dimensional shear beam model of a site profile is used in the calculations contained in this study, it is pertinent at this time to discuss various methods for representing a shear beam subjected to a seismic excitation at its base. As indicated in Reference 4-15, two general approaches have been used:

a. Solution of the One-Dimensional Wave Equation. For this case, the site profile is assumed to have linear viscoelastic properties, and the motion in the underlying bedrock is considered to be a superposition of harmonic motions of different frequencies. The response of the profile at the surface is computed for a range of bedrock motion frequencies, thereby producing a transfer function of the soil profile. The response at the ground surface is obtained by determining the inverse transform of the product of the Fourier transform of the base excitation and the transfer function of the profile.

b. Discrete Mass Representation of the Site Profile. In this technique, the site profile is represented by a series of discrete masses interconnected by shear springs, with properties determined from the stress-strain relationships of the layers, and by viscous dashpots, with characteristics determined from the energy dissipation characteristics of the soil media. An additional dashpot mechanism that simulates radiation damping at the base may also be provided.

A number of investigations comparing these two approaches have been made. In Reference 4-16, analytical procedures corresponding to each of the above general methods have been formulated and compared. It was shown that both methods for determining the dynamic behavior of the soil are essentially equivalent if appropriate values of the parameters are selected for each one. A conclusion of Reference 4-16 is that the choice of one of these methods for a given application depends primarily on the relative efficiency (i.e., calculation time for a given prescribed accuracy) and flexibility for that application.

Comparisons of the results of the continuous and discrete approaches for deposits on both a firm rock base and on flexible rock have been made in References 4-11 and 4-17. In Reference 4-11, the two shear beam models shown in Figure 4-11 were utilized. In the first model, energy dissipation is provided by a dashpot between the base and the layered system, whereas in the second model no energy dissipation into the base of the profile is allowed. In Figure 4-12, it is seen that amplification functions (i.e., transfer functions) obtained using each of the shear beam models compare well with those of the continuous solution for the same site. In the shear beam model with the rigid base, however, high modal damping factors (10 percent of critical in the first mode) were required in order to obtain this close correlation. Similar results have been noted in Reference 4-17.

From these results and others indicated in the above references, it is concluded that for cases where the one-dimensional model is appropriate, either a continuous solution to the wave equation or a discrete shear beam approach may be used.

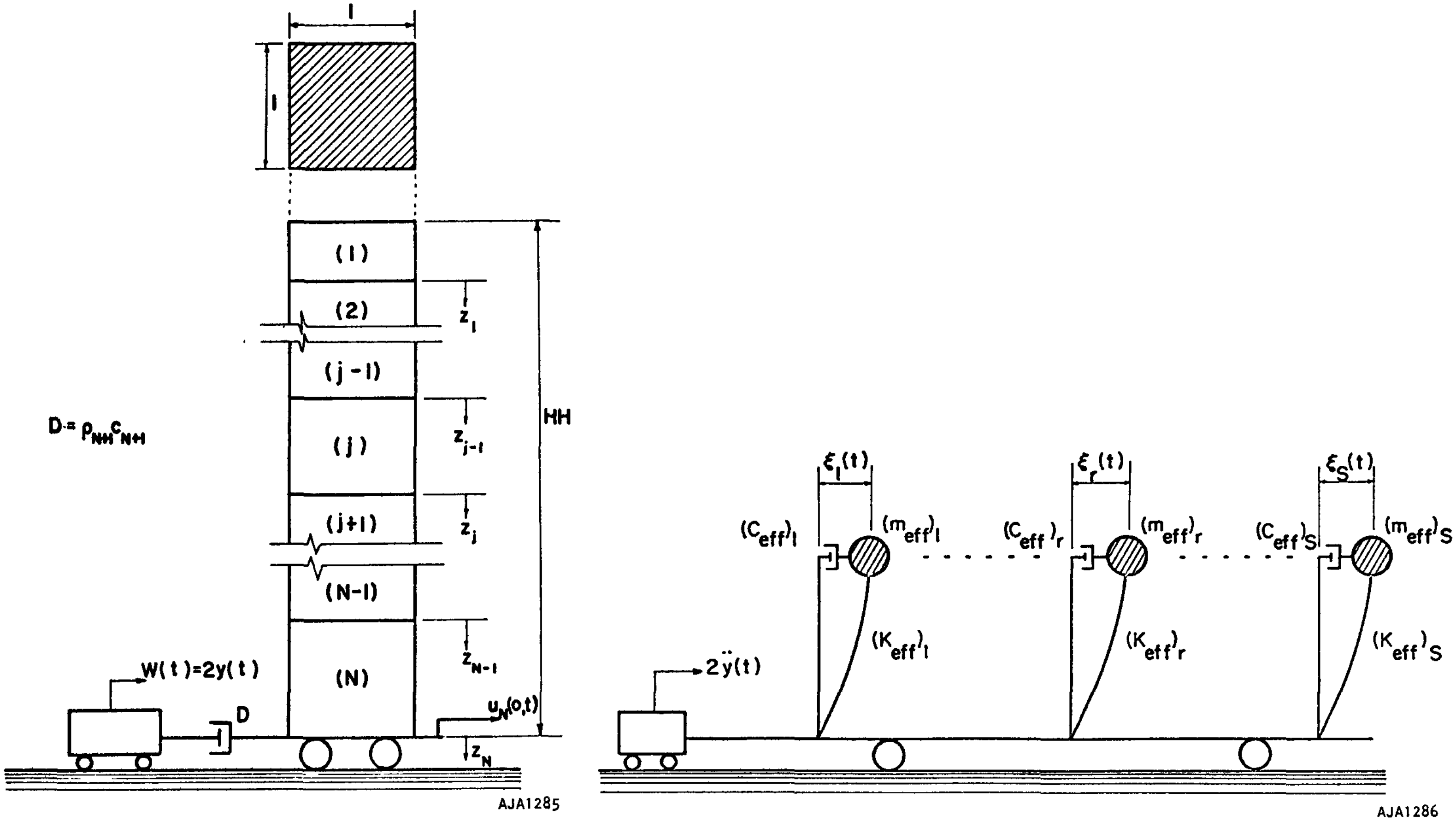

(a) THE FIRST SHEAR BEAM MODEL

(b) AN S-MODE REPRESENTATION OF THE SECOND SHEAR BEAM MODEL

FIGURE 4-11. SHEAR BEAM MODELS OF REFERENCE 4-11

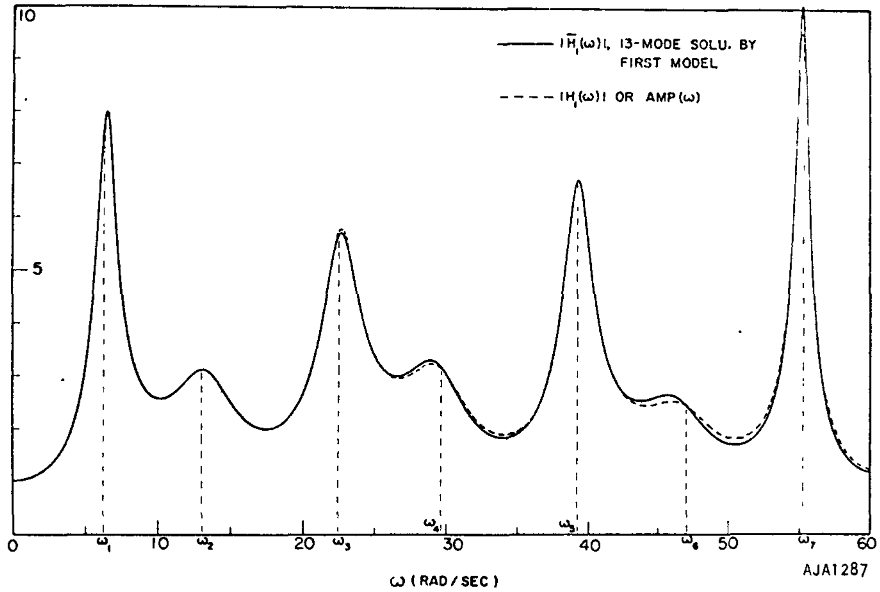

(a) COMPARISON OF RESULTS USING FIRST SHEAR BEAM MODEL WITH THOSE OF EXACT SOLUTION

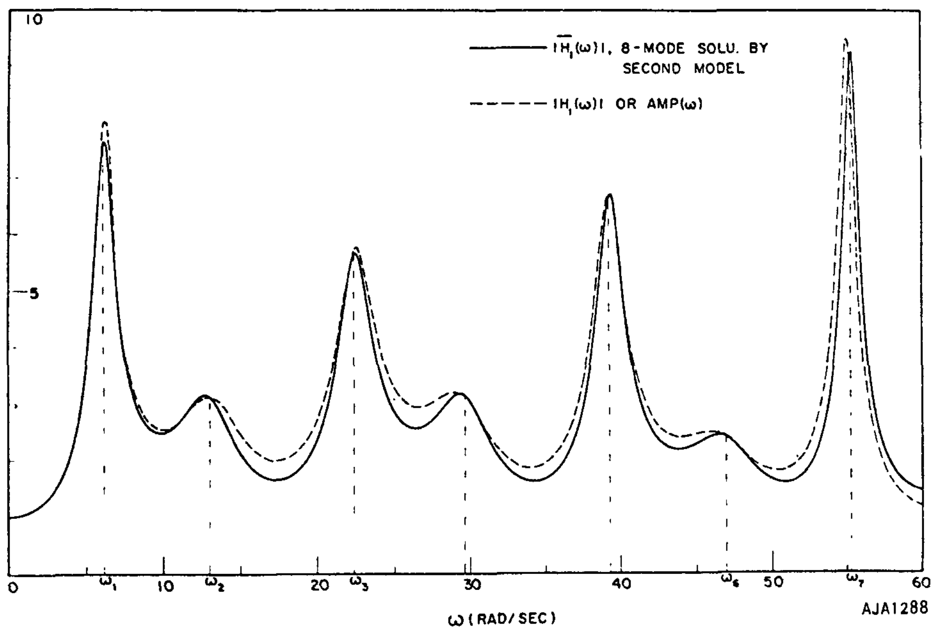

(b) COMPARISON OF RESULTS USING SECOND SHEAR BEAM MODEL WITH THOSE OF EXACT SOLUTION

FIGURE 4-12. AMPLIFICATION FUNCTION COMPARISONS (REFERENCE 4-11)

4.4.3 DESCRIPTION OF SHEAR BEAM MODEL USED IN THIS STUDY

The discrete mass shear beam approach developed by Seed and Idriss (Reference 4-12) has been adopted for use in this this study. As noted in Subsection 4.4.1, computations using this approach have shown reasonable agreement with measured earthquake responses of the ground surface.

In this approach, the stiffness and damping characteristics of each layer in the site are represented by linear-viscoelastic properties. Some strain dependent stiffness and damping characteristics for clays, silts, and sands have been recommended for use by Seed and Idriss (Reference 4-14), and are shown in Figure 4-13. It is noted that stiffness and damping characteristics other than those of Figure 4-13 can be readily incorporated into the computer program.

Each layer in the site is idealized into a series of discrete masses, interconnected by shear springs, and with damping of both absolute and relative motion. The equations of motion of the entire system of layers in matrix form is

$$[M]\{\ddot{x}\} + [C]\{\dot{x}\} + [K]\{x\} = \left\{R(t)\right\} \tag{4-2}$$

where $[M]$, $[C]$, and $[K]$ are the mass, damping, and stiffness matrices of the system, $\{x\}$ is the relative displacement vector, and $\left\{R(t)\right\}$ is the forcing function arising from the seismic input at the base of the shear beam.

The damping matrix for each sublayer is taken to be a combination of absolute damping and relative damping, and is expressed in the following form:

$$[C]_j = \alpha_j[M]_j + \beta_j[K]_j \tag{4-3}$$

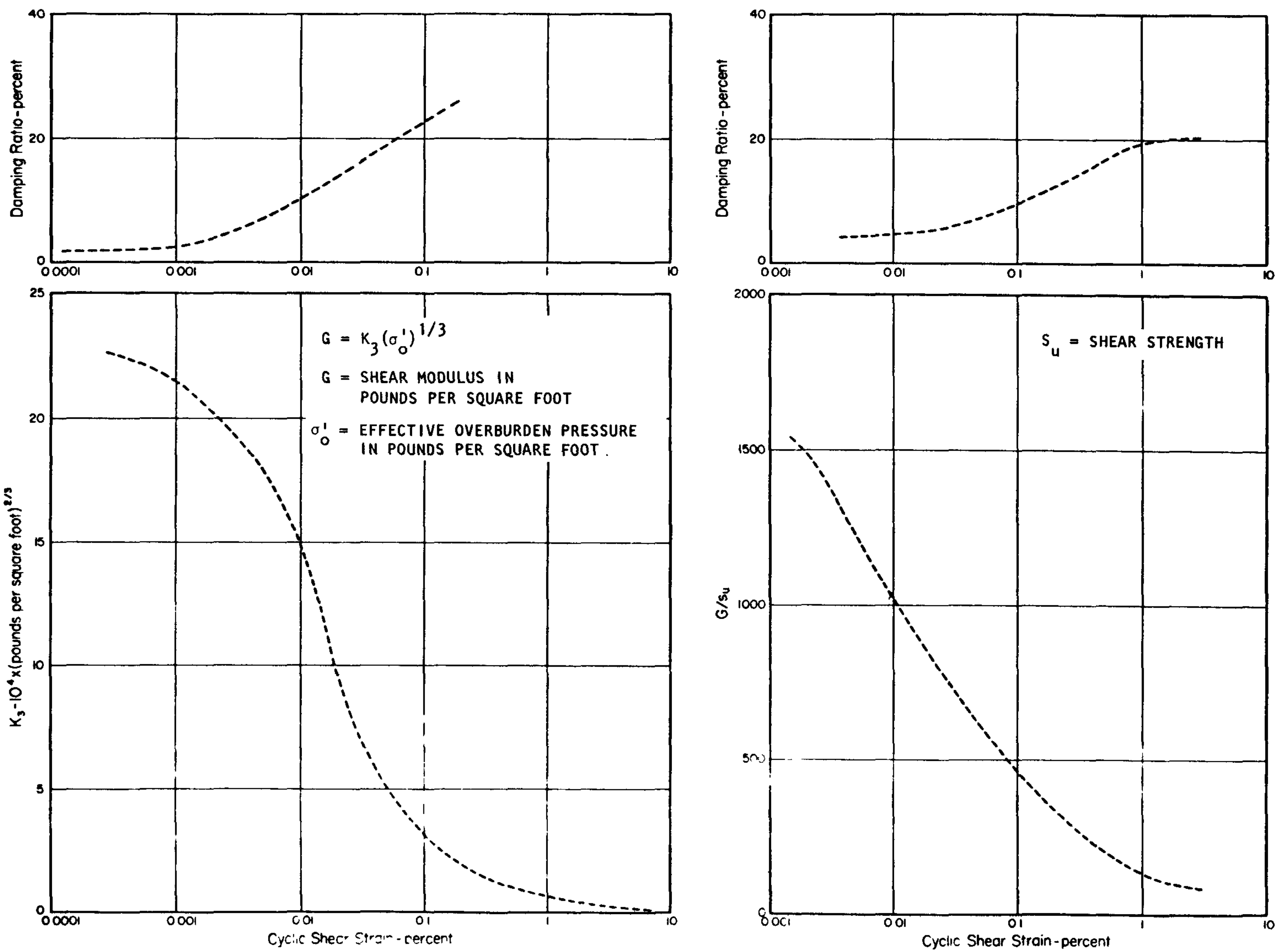

(a) MODULI AND DAMPING RATIOS FOR MEDIUM SANDS--RELATIVE DENSITY--80 PERCENT

(b) MODULI AND DAMPING RATIOS FOR SATURATED CLAYS

FIGURE 4-13. SOME RECOMMENDED MODULI AND DAMPING RATIOS FOR SHEAR BEAM ANALYSIS (REFERENCE 4-14) where

$\alpha_j [M]_j$ = Absolute damping term

$\beta_j [K]_j$ = Relative damping term

$[M]_j$, $[K]_j$ = Mass matrix and stiffness matrix of the layer

α_j = $\lambda_j \cdot \omega_j$

β_j = λ_j / ω_j

$$\omega_j = \frac{\pi}{2H_j}\sqrt{\frac{G_j g}{\gamma_j}} \qquad (4\text{-}4)$$

and

λ_j = Damping ratio

G_j = Shear modulus

γ_j = Unit weight

H_j = Thickness of the sublayer

g = Acceleration of gravity

The matrix $[C]_j$ is a tridiagonal submatrix of order n_j, where n_j is the number of discrete masses considered for the j^{th} sublayer. The damping matrix for the entire system, $[C]$, which is also tridiagonal, is obtained by addition of the appropriate components of the submatrices $[C]_j$ for all the sublayers comprising the deposit. The damping matrix $[C]$ for the entire system thus incorporates the variations of damping with depth because it is based on the damping ratios of the various sublayers of the deposit (Reference 4-12). However, some limitations are inherent in assuming the damping to be of the form indicated in Equations 4-3 and 4-4. These limitations are discussed in later paragraphs of this subsection.

An iterative procedure is used in the numerical integration of the coupled equations of motion of the layered site. At the start of the problem, a set of initial shear moduli and damping factors are chosen for each layer. From this, a first estimate of the damping and stiffness matrices of the system are obtained and the response of each discrete mass in the shear beam is computed using a linear acceleration, step-by-step numerical integration procedure. A set of equivalent cyclic strains are then computed for each layer, and by using curves such as those in Figure 4-13, a new set of shear modulus and damping properties consistent with these peak strains are obtained for each layer. The responses are then recomputed using the revised stiffness and damping properties. This iteration process is repeated until convergence between the assumed and computed shear moduli and damping factors has occurred. It is noted that although the time history calculations within a given iteration cycle are for a linear-viscoelastic shear beam, the variations in properties between successive cycles, based on the computed cyclic soil strains, accounts for the nonlinearities inherent in the soil materials in an approximate manner.

It remains to examine the nature of the damping mechanism in the Seed-Idriss model. First, it is noted that the frequency of the n^{th} mode of a homogeneous shear beam of height H_j is

$$\omega_n = \frac{(2n - 1)\pi}{2H_j}\sqrt{\frac{G_j g}{\gamma_j}} \tag{4-5}$$

where G_j and γ_j are the shear modulus and the density of the soil. Comparing Equations 4-4 and 4-5, it is seen that the quantity ω_j, as given in Equation 4-4, is the fundamental frequency of a homogeneous cantilevered shear beam with the properties of the j^{th} layer.

To investigate the significance of λ_j, consider a homogeneous shear beam with properties G_j and γ_j. The equations of motion for free vibration of this shear beam are

$$[M]\{\ddot{x}\} + \Big[\alpha[M] + \beta[K]\Big]\{\dot{x}\} + [K]\{x\} = 0 \tag{4-6}$$

where the damping matrix form indicated in Equation 4-3 has been assumed. To expand Equation 4-6 into normal modes, assume

$$\{x\} = [\phi]\{\zeta\} \tag{4-7}$$

In this, $[\phi]$ is a matrix of mode shapes (eigenvectors) that have been normalized so that

$$[\phi]^T[M][\phi] = [I], \qquad [\phi]^T[K][\phi] = \left[\diagdown \omega_n^2 \right] \tag{4-8}$$

where $[I]$ is the identity matrix and $\left[\diagdown \omega_n^2 \right]$ is a diagonal matrix of the modal frequencies. Substituting Equation 4-7 into 4-6 and premultiplying through by $[\phi]^T$ gives a series of N decoupled equations of motion for the N modes of vibration of the shear beam. These equations are:

$$\ddot{\zeta}_n + \left(\alpha + \beta\omega_n^2\right)\dot{\zeta}_n + \omega_n^2\zeta_n = 0 \qquad n = 1,2,\text{---}N \tag{4-9}$$

Now, if α and β take the form specified by Equation 4-4, the modal equations of motion become:

$$\ddot{\zeta}_n + \lambda\left(\omega_1 + \frac{\omega_n^2}{\omega_1}\right)\dot{\zeta}_n + \omega_n^2\zeta_n = 0 \qquad n = 1,2,\text{---}N \tag{4-10}$$

The standard form of the modal equation of motion, including damping, is

$$\ddot{\zeta}_n + 2\psi_n\omega_n\dot{\zeta}_n + \omega_n^2\zeta_n = 0 \tag{4-11}$$

where ψ_n is the percent of critical damping in the n^{th} mode. Comparing the coefficients of $\dot{\zeta}_n$ in Equations 4-10 and 4-11 shows that the shear beam code used in this study, if applied to a homogeneous shear beam, implies modal damping of the form:

$$\psi_n = \frac{\lambda}{2}\left[\frac{\omega_1}{\omega_n} + \frac{\omega_n}{\omega_1}\right] \qquad n = 1,2,\text{---}N$$

or (4-12)

$$\frac{\psi_n}{\lambda} = \frac{1}{2}\left[\frac{1}{2n-1} + (2n-1)\right] \qquad n = 1,2,\text{---}N$$

As will be seen below, the two terms in the brackets in Equation 4-12 refer to the contributions of the absolute and relative damping mechanisms, respectively. For the first mode $(n = 1)$ these two mechanisms contribute equally to the damping in the Seed-Idriss model; however, for higher modes, the second term in Equation 4-12 dominates the value of ψ_n.

Equation 4-12 is plotted in Figure 4-14, and indicates that the higher modes are essentially damped out using this particular technique. Also, it is noted that the quantity λ is the percent critical damping in the first mode of the homogeneous shear beam.

As a more general case, consider a continuous shear beam with the two most commonly assumed types of damping, namely:

a. Absolute damping

$$F_a = C_1 \frac{\partial x}{\partial t}$$

b. Strain rate (or relative) damping

$$F_d = -C_2 \frac{\partial^3 x}{\partial t \partial z^2}$$

where z refers to the axial dimension of the shear beam model and C_1 and C_2 are determined from the material properties.

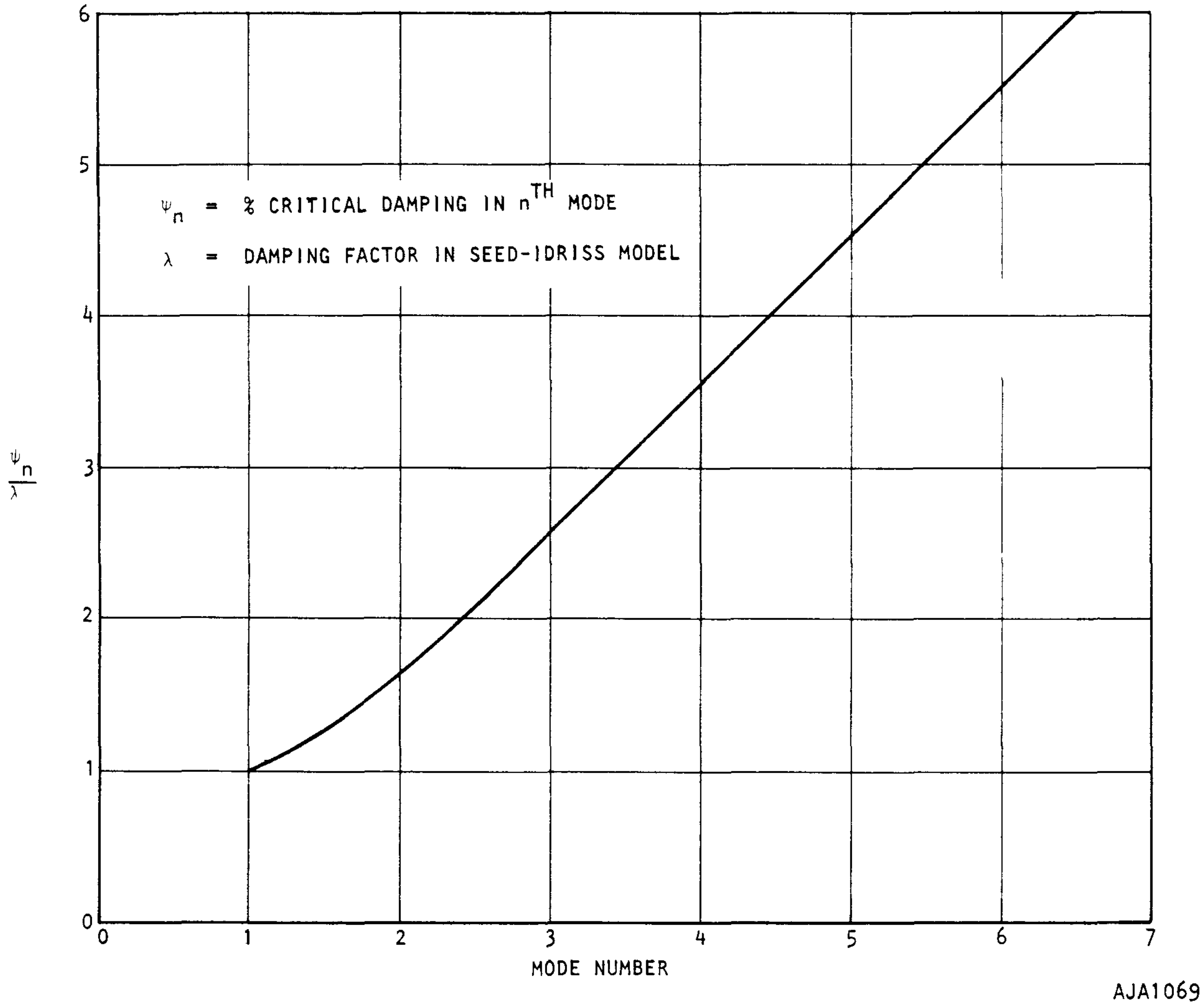

FIGURE 4-14. PERCENT CRITICAL DAMPING FOR EACH MODE OF A HOMOGENEOUS SHEAR BEAM--SEED-IDRISS VARIABLE DAMPING MODEL

Now, as shown in Appendix B, if both absolute and relative damping are present in a homogeneous shear beam, the percent critical damping in the n^{th} mode is

$$\psi_n = \frac{C_1}{2\omega_n \rho A} + \frac{C_2 \omega_n}{2GA} \tag{4-13}$$

where ρ is the mass density and A is the cross section area of the shear beam.

A comparison of coefficients of $1/\omega_n$ and ω_n in Equations 4-12 and 4-13 indicates that

$$\lambda = \frac{C_1}{\omega_1 \rho A} = \frac{C_2 \omega_1}{GA} \tag{4-14}$$

This implies that

$$\frac{C_2}{C_1} = \frac{1}{\omega_1^2} \frac{G}{\rho}$$

in order for Equations 4-12 and 4-13 to be equivalent.

In summary, it has been shown that the Seed-Idriss shear beam model is one particular case of more general damping. By a different choice of the constants α and β, damping values substantially different from those given in Figure 4-14 can be obtained, resulting in substantial differences in the transfer function of the soil profile and in the computed earthquake motions. The determination of a damping model that will simulate all energy dissipation mechanisms that might exist at a site is one of the prime difficulties of this shear beam model. However, it is noted that similar difficulties are encountered in any analytical technique that uses a viscous damper to represent the energy dissipation mechanisms inherent in soils. This indicates the need for more research work in this area.

4.5 COMPARISON OF SHEAR BEAM CALCULATIONS WITH MEASURED DATA

A series of shear beam calculations were made in this study using profile characteristics that represent, in an approximate manner, the site of the 1940 El Centro earthquake. The purpose of these calculations has been to compare the computed results with measured data and thereby assess the effects of uncertainties in estimating site profile characteristics and bedrock motions on the calculated surface motions.

It is noted that the factors that can influence the surface motions at a site are (Reference 4-18):

a. The nature of the source mechanism; the dimensions and orientation of the slipped area of fault; the stress drop; the nature of the fault movement, its amplitude, direction, time, and history.

b. The travel path of the seismic waves; the physical properties of the rock including discontinuities, etc.

c. Local geology; physical properties of soil layers and sedimentary rock; vertical and horizontal dimensions of bodies of soil and rock; orientations of bedding planes, etc.

The mathematical model of the site profile can only account for the effects of local geology on the ground motions (Item c above) whereas the effects of the nature of the source mechanism and the travel path of the seismic waves must be considered in the estimates of the input motions to the mathematical model. As indicated in Reference 4-11, the local geology may not always produce a significant effect on the earthquake motions at a site, while the source mechanism and travel path of the seismic waves may, on the other hand, play an important role in determining the general characteristics of the ground spectra.

With this in mind, rms accelerations and response spectra of the two measured components of the 1940 El Centro earthquake have been compared to records obtained using the shear beam analysis. The first 15 sec of the El Centro records have been chosen for comparison with the shear beam calculations, since the dominant portion of the ground surface motion has occurred within this duration. The earthquake has a magnitude 7.0.

The El Centro site was assumed to be a uniform clay site extending to a depth of 100 ft. At this level, bedrock motions were input into a shear beam model of the top 100-ft clay profile. This depth at which the input motions are applied is consistent with that used in previous analyses of this site (Reference 4-3), and, because of time and budget limitations, was not varied in this study. It is felt, however, that variations in the depth at which the input motions are applied could affect the resulting surface motion calculations and should be investigated in future studies.

An important step in the estimation of earthquake induced ground motions at a site is the careful determination of representative soil properties for use in the mathematical model. Past experience has indicated the existence of a number of potential sources of considerable uncertainty in the determination of soil properties, such as:

- Disturbances imparted to the soil samples during the boring and extraction of the samples from the ground.

- The determination of a representative set of properties from a number of different borings at the site.

- Differences between laboratory test procedures and the actual loading and constraint conditions to which the soil will be subjected during an earthquake.

In order to consider the uncertainties described above, three sets of profile characteristics have been considered in this set of calculations, namely:

- A profile having the basic shear modulus and damping properties given in Reference 4-3 and termed G_o and λ_o
- A soil profile having a shear modulus of $1.33G_o$ and a damping ratio of $0.67\lambda_o$ (assumed upper bound stiffness properties)
- A profile with a shear modulus of $0.67G_o$ and a damping ratio of $1.33\lambda_o$ (assumed lower bound stiffness properties)

The strain-dependent shear moduli and damping factors for the El Centro site are illustrated in Figure 4-15. The spread between the dynamic characteristics of the ground motions corresponding to each of the above sites, and the comparison of these results to the measured El Centro record, will give an indication of the effects of uncertainties in the soil property estimates on calculated ground motions at a site. The density and shear strength properties used in the calculations correspond to those indicated in Reference 4-3, and are shown in Figure 4-15.

The uncertainties involved in estimating the dynamic characteristics of the subsurface bedrock motions have been discussed in Subsection 4.2. In order to investigate the effects of variations in the bedrock record on the ground surface motions, three sets of base motion input records are considered:

a. In Reference 4-3, Seed et al. utilized a scaled verions of the North-South component of the 1940 El Centro earthquake as input at the base of his shear beam model. In this, the acceleration and time axes of the original record were scaled using factors that are dependent on the earthquake magnitude

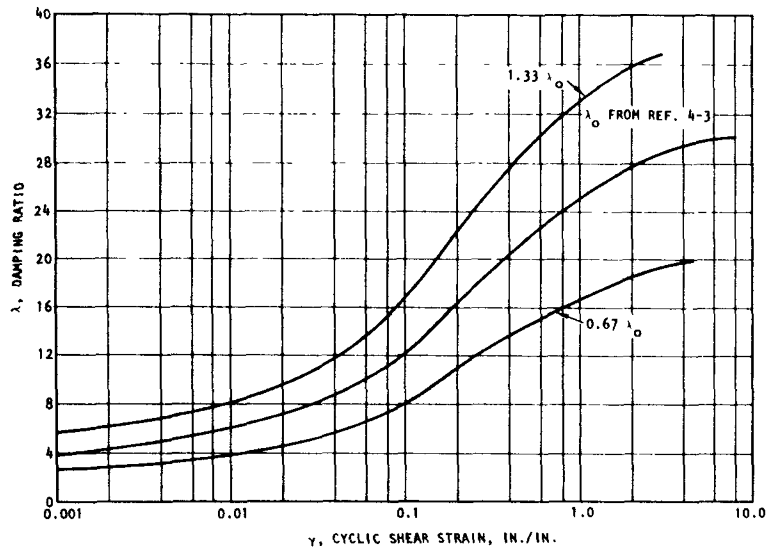

(a) DAMPING CURVE FOR SATURATED CLAY

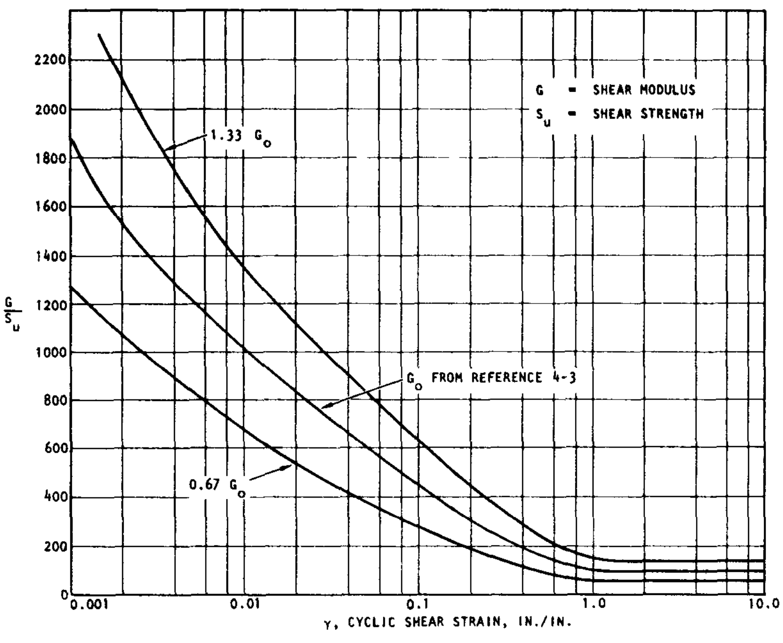

(b) MODULUS CURVES FOR SATURATED CLAY

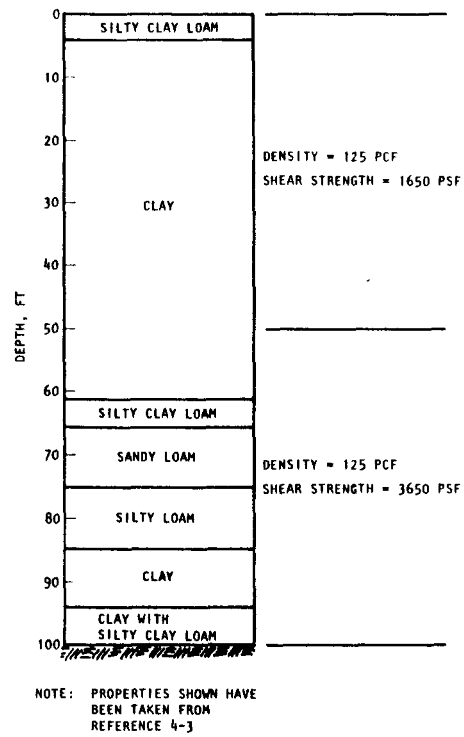

(c) ASSUMED SOIL PROFILE AT EL CENTRO

FIGURE 4-15. SOIL PROPERTIES USED IN EL CENTRO SITE ANALYSIS and the causative fault distance. The factors used by Seed, et al., for this case are:

$$a_s = 0.636a_{EC}$$

$$t_s = 0.545t_{EC}$$

where a_s, t_s are the acceleration and time of the scaled record, and a_{EC}, t_{EC} are the acceleration and time of the original El Centro record.

b. For purposes of comparison with the scaled North-South El Centro record suggested by Seed, et al., for use as base motion, the actual El Centro record, with unaltered acceleration and time scales, was also used as base motion input.

c. Band-limited white noise samples, with acceleration amplitudes scaled to provide surface motions comparable to the El Centro measured records.

The results of the calculations on the El Centro site are summarized in Table 4-1 and in Figures 4-16 through 4-18. From these results, the following observations can be made:

a. The spectral characteristics of the two measured components of the actual El Centro record differ considerably, especially at the long period end of the spectrum, as shown in Figure 4-18. This suggests that factors not included in the shear beam model, such as the source mechanism, the travel path of the seismic waves, or unidentified nonhomogeneities in the soil, may have had a major effect on the measured records at El Centro.

TABLE 4-1. RMS ACCELERATIONS OF EARTHQUAKE MOTIONS AT EL CENTRO SITE

Case No.	Material Properties	Calculated rms Acceleration, (in./sec^2)	$\frac{(\text{rms})\text{calc}}{(\text{rms})\text{input}}$	$\frac{(\text{rms})\text{calc}}{(\text{rms})\text{actual}}$	Subsurface Bedrock Input Motion	Comments
1	$G = G_o$ $\lambda = \lambda_o$	21.0	1.14	0.71	Scaled El Centro (N-S component) Accel. scale = 0.636 Time scale = 0.545 (as indicated in Reference 4-3)	rms acceleration (input) = 18.4 in./sec^2 rms acceleration (actual N-S component) = 29.4 in./sec^2
2	$G = 1.33G_o$ $\lambda = 0.67\lambda_o$	28.2	1.53	0.96		
3	$G = 0.67G_o$ $\lambda = 1.33\lambda_o$	16.6	0.91	0.57		
4	$G = 0.67G_o$ $\lambda = 1.33\lambda_o$	31.9	1.08	1.08	Actual El Centro (N-S component)	The soil profile has resulted in some amplification of the base motion rms acceleration.
5	$G = 1.33G_o$ $\lambda = 0.67\lambda_o$	44.0	1.50	1.50		
6	$G = 0.67G_o$ $\lambda = 1.33\lambda_o$	22.1	0.76	0.92(E-W) 0.75(N-S)	Scaled white noise No. 1	rms acceleration of bedrock = 29.0 in./sec^2
7	$G = 1.33G_o$ $\lambda = 0.67\lambda_o$	33.9	1.17	1.41(E-W) 1.15(N-S)		
8	$G = 1.33G_o$ $\lambda = 0.67\lambda_o$	36.4	1.26	1.52(E-W) 1.23(N-S)	Scaled white noise No. 2	Calculated rms acceleration of actual record: E-W = 24.0 in./sec^2 N-S = 29.4 in./sec^2
9	$G = 0.67G_o$ $\lambda = 1.33\lambda_o$	20.9	0.73	0.87(E-W) 0.71(N-S)		

AJA1087

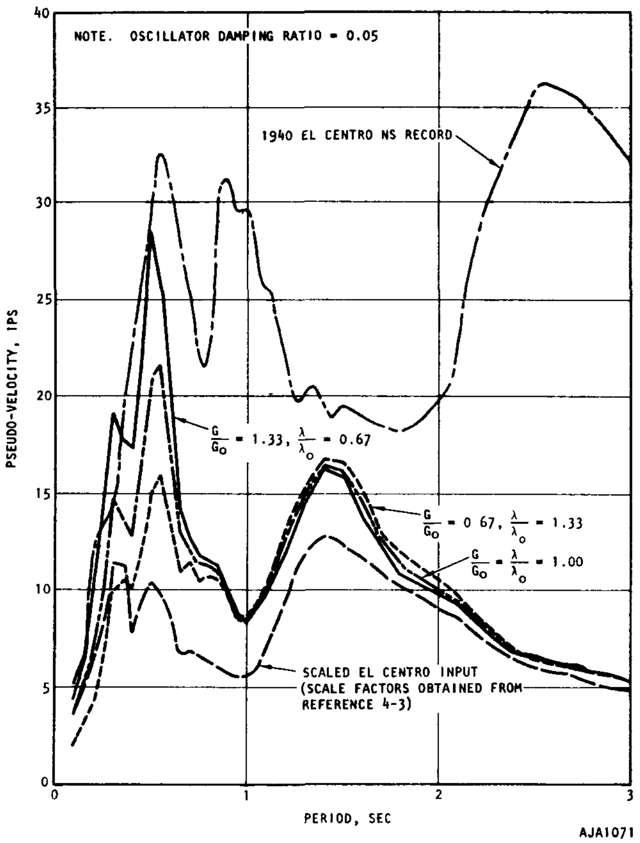

(a) INPUT = SCALED EL CENTRO NS RECORD

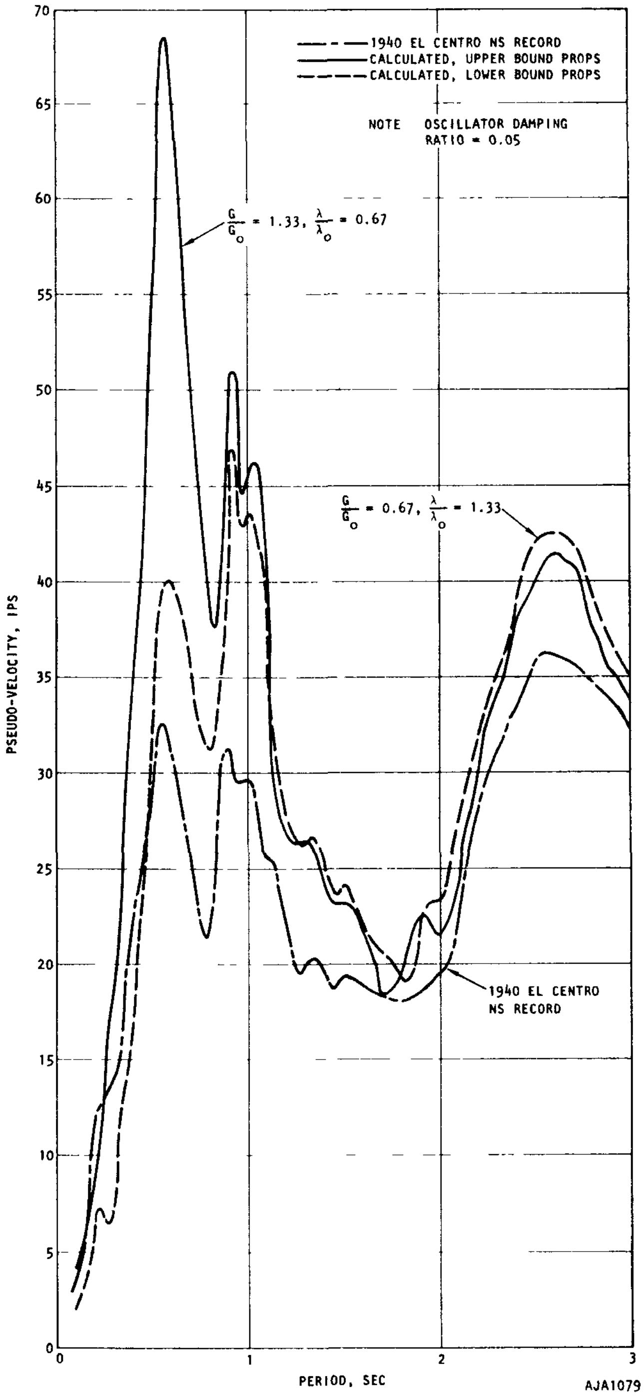

(b) INPUT = ACTUAL EL CENTRO NS RECORD

FIGURE 4-16. EL CENTRO SITE--SPECTRA OF SHEAR BEAM RESULTS WITH SCALED AND UNSCALED EL CENTRO NS RECORD INPUT AT BASE

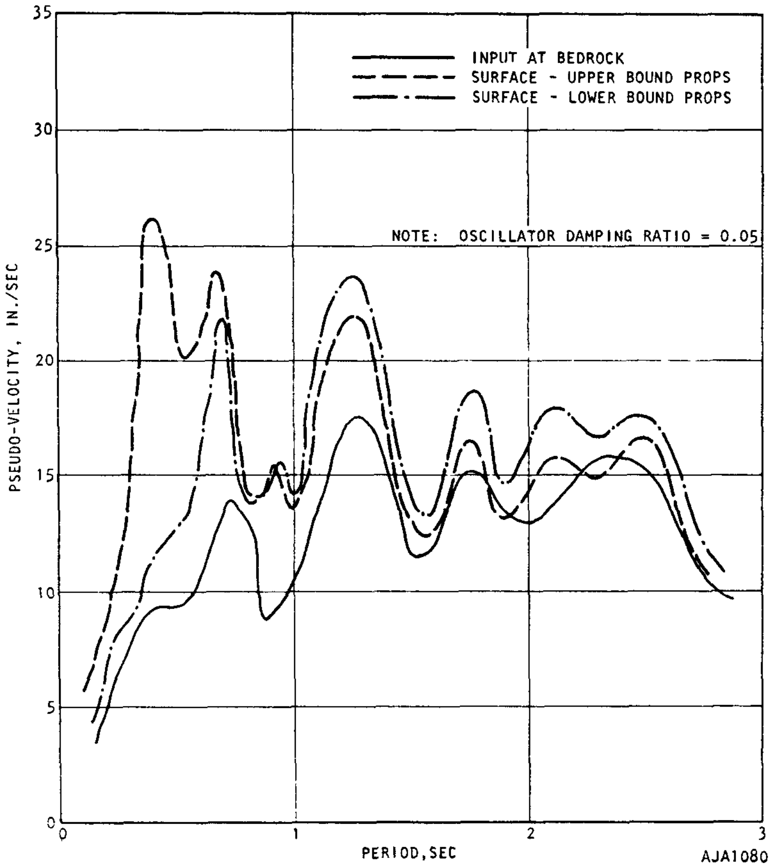

(a) WHITE NOISE RECORD NO. 1

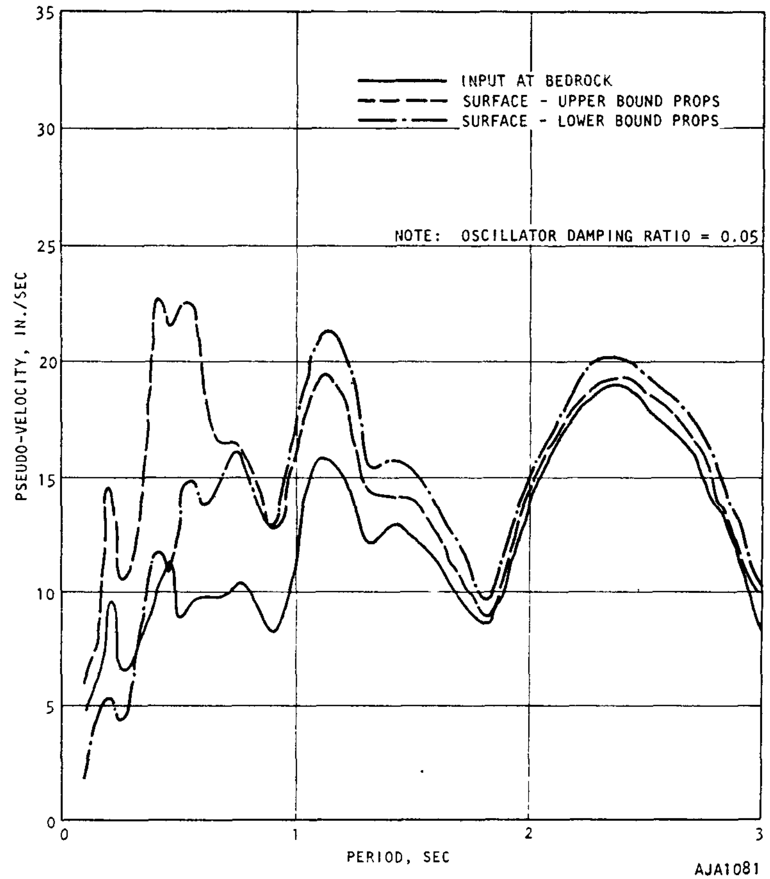

(b) WHITE NOISE RECORD NO. 2

FIGURE 4-17. EL CENTRO SITE--SPECTRA OF SHEAR BEAM RESULTS WITH BAND LIMITED WHITE NOISE INPUT

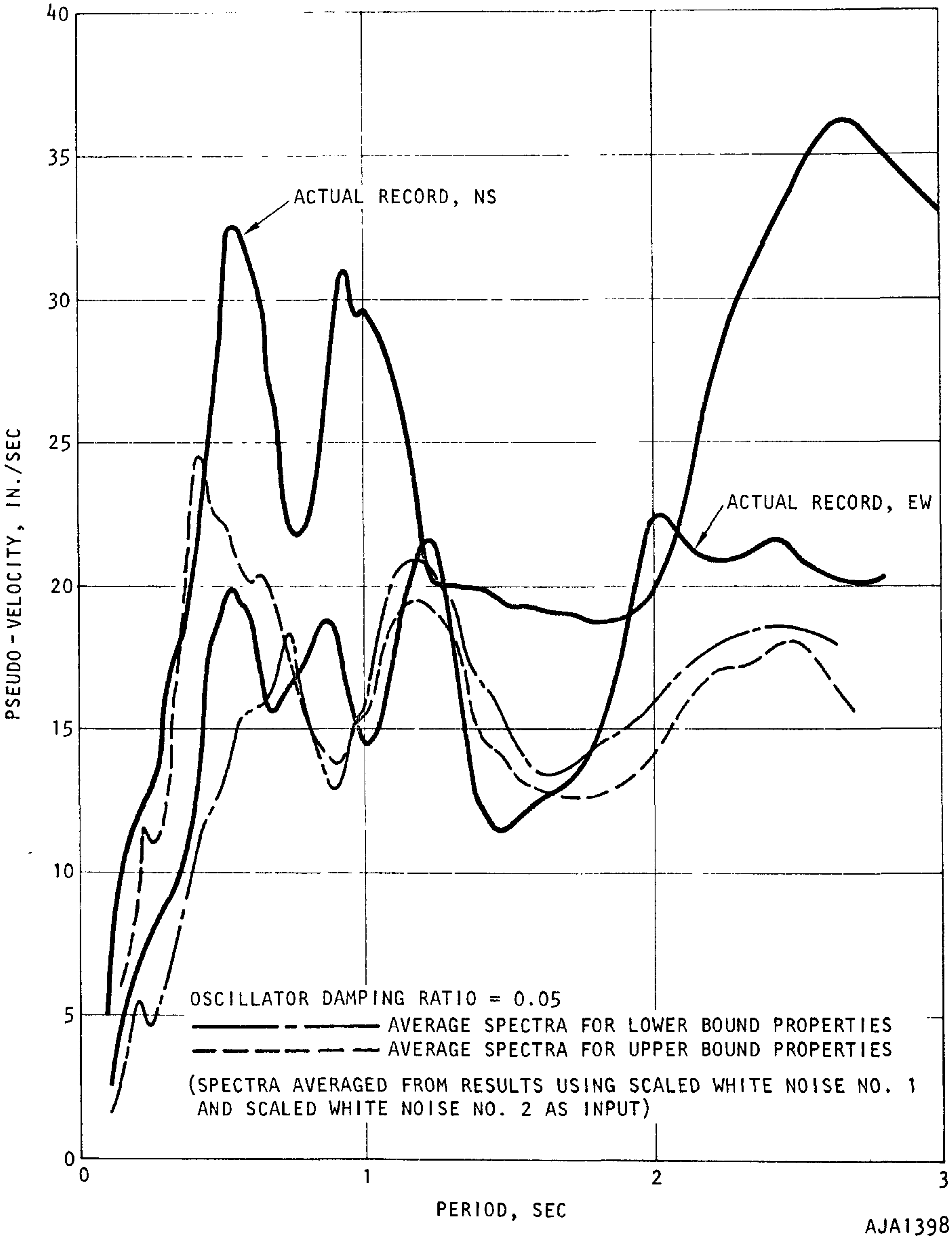

FIGURE 4-18. EL CENTRO SITE--COMPARISON OF AVERAGE CALCULATED SPECTRA (USING WHITE NOISE INPUT) WITH SPECTRA OF MEASURED RECORDS

b. Amplification of the subsurface input motion by the soil profile at this site occurs only at the low-period end of the pseudo-velocity spectra, and is strongly dependent on the soil properties in this period range. For periods greater than about 1 sec, the spectral characteristics of the calculated surface motions are nearly equal to those of the subsurface input record and are essentially independent of the soil properties assumed for this site.

c. The rms accelerations of the surface motions are strongly dependent on the soil properties and input motions used. The calculated amplification factors and a comparison of strength levels of the real and calculated surface records are shown in Table 4-1.

d. When the scaled N-S El Centro record is used as input to the El Centro site model shown in Figure 4-15, the pseudo-velocity spectra of the calculated surface motions do not compare well with that of the North-South component of the measured surface motion, especially at the high period end of the spectrum (Figure 4-16(a)). It appears that this has resulted from the fact that the time scale of the scaled El Centro input record is compressed from that of the actual record. This will shift the input spectrum uniformly toward the lower periods, as indicated by Tsai in Reference 4-19. This shift becomes quite apparent when it is noted that the range of large pseudo-velocities that exist in the spectrum of the actual record at periods of 2.5 to 3.0 sec occurs in the spectra of the calculated records and of the input motion at periods of about 1 to 2 sec.

e. The pseudo-velocity spectra and rms accelerations obtained when the unaltered N-S component of the El Centro record is used as input are shown in Figure 4-16(b) and Table 4-1, respectively. These results clearly demonstrate that the amplification effect of this site is concentrated in the periods ranging from 0.3 to 1.0 sec, and depends on the soil properties used in the calculation. A comparison of Figure 4-16(a) to 4-16(b) indicates the dependence of the long period end of the spectrum on the characteristics of the base input motion.

f. Two different band limited white noise records (Nos. 1 and 2 in Figure 4-1(a) and (b)) have been used as input base motions to both the upper bound and lower bound profiles for the El Centro site. These input records were scaled so that their rms acceleration was 29 in./sec^2. As indicated in Table 4-1, the rms accelerations of the computed ground surface records bounded the rms accelerations of the two measured El Centro components, and were dependent on the soil properties used in the calculations. The average spectra obtained from the computed surface records also depend on soil properties (in the short period range), but generally fall below the average of the spectra from the two measured components. These discrepancies are especially noticeable in the long periods where factors unrelated to the local geology of the site (such as the source mechanism or the seismic wave travel path) may have caused the spectra of the East-West and North-South components to deviate from one another.

The results of the comparisons of the shear beam calculations with the 1940 El Centro earthquake records are summarized as follows:

a. When used in conjunction with the El Centro site model of Figure 4-15, the method indicated by Seed, et al., in Reference 4-3, did not lead to good correlation between velocity spectra of measured and calculated results. However, as indicated in Figure 4-15, bedrock motions were applied to the shear beam at a depth of 100 ft. Variations in this depth could affect the resulting surface motion spectra and should be investigated in future studies.

b. Variations of ±30 percent in the material properties for this particular shear beam model of the El Centro site resulted in substantial variations in the rms accelerations and short period spectral characteristics of the resulting computed ground motions. The longer period components of the computed motions (greater than about 1 sec) were more dependent on the characteristics of the input base motions, and were not strongly influenced by these variations in soil properties.

c. Only a limited number of shear beam calculations were made using band-limited white noise as input at the subsurface bedrock level. Therefore, no definitive statements can be made regarding the overall correlation of this approach with measured data. The few calculations made using band-limited white noise as input showed that reasonable comparisons with the rms acceleration level of the 1940 El Centro records could be obtained. However, this same white noise input produced spectra that fell below those of the actual El Centro records, especially in the long period regions of the spectra. It is noted that the spectra of the two measured components of the 1940 El Centro earthquake differ considerably in the long period region; therefore, factors not related to the local site properties considered in the shear beam analysis may be affecting these frequency components of the measured records.

4.6 PARAMETRIC INVESTIGATION OF SOIL PROFILE EFFECTS

4.6.1 DESCRIPTION OF PROCEDURES AND MATRIX OF CASES

The next series of calculations in this study have used the shear beam model to investigate earthquake motions at two profiles that are typical of sites where nuclear reactors have been built. These profiles are shown in Figure 4-19, and represent a site with a lower fundamental frequency (Site 1) and a site with a higher fundamental frequency (Site 2).

The matrix of cases for the analysis of these sites is shown in Table 4-2. For each site, a high magnitude earthquake (7.5) and a moderate-magnitude earthquake (5.5) have been considered. Each of these magnitudes has, in turn, been investigated for a site near a causative fault (5 miles) and farther from a causative fault (50 miles). The input data at the base of the shear beam is band-limited white noise whose duration and strength are obtained from Figures 4-2 and 4-4(b), respectively. For each of these cases, the dynamic characteristics of the ground surface response at Sites 1 and 2 have been calculated in terms of acceleration time histories, rms accelerations, and pseudo-velocity spectra.

4.6.2 DISCUSSION OF RESULTS

The computed acceleration time-histories at the ground surface, and the rms acceleration of these records are shown in Figures 4-20(a) through 4-20(d) and in Table 4-3 for each case considered in the parametric investigation. From this, it is seen that, for a given base motion input, the stiffer site (Site 2) has generally resulted in higher peak accelerations and rms accelerations at the ground surface. Also, from Table 4-3, it is seen that the amplification factor for rms acceleration tends to increase as the strength of the base motion input decreases. This is attributed to the fact that the equivalent shear moduli and damping ratios used in the shear beam model are strain dependent quantities (see Subsection 4.4.3). Hence, as the rms acceleration of the subsurface bedrock motion increases, the peak strains in each layer of the sites will, in

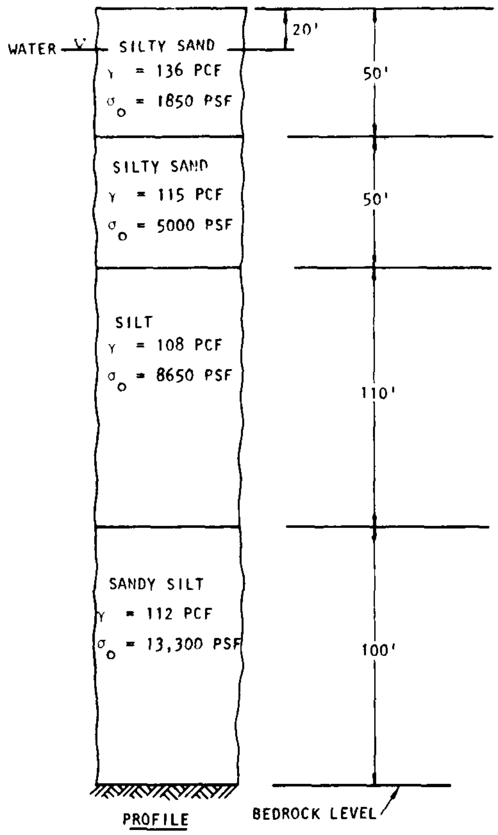

(a) SITE NO. 1--LOWER FREQUENCY SITE

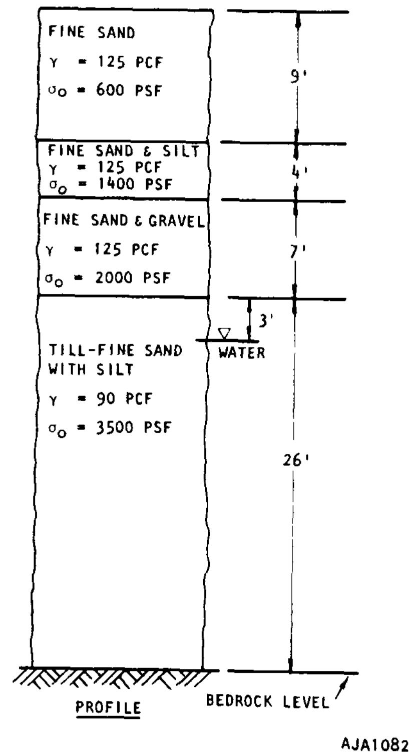

(b) SITE NO. 2--HIGHER FREQUENCY SITE

FIGURE 4-19. SITES CONSIDERED IN PARAMETRIC INVESTIGATION (NOTE DIFFERENT SCALES)

TABLE 4-2. MATRIX OF CASES FOR PARAMETRIC INVESTIGATION

Case No.	Site No.	Earthquake Magnitude	Distance from Fault, miles	rms Acceleration of Bedrock Motion, ft/sec^2*	Duration of Bedrock Motion, sec*
10	1	7.5	5	4.0	30
11			50	0.85	30
12		5.5	5	0.91	10
13			50	0.09	10
14	2	7.5	5	4.0	30
15			50	0.85	30
16		5.5	5	0.91	10
17			50	0.09	10

*Duration and rms acceleration of bedrock motion are obtained from Figures 4-2 and 4-4(b), respectively.

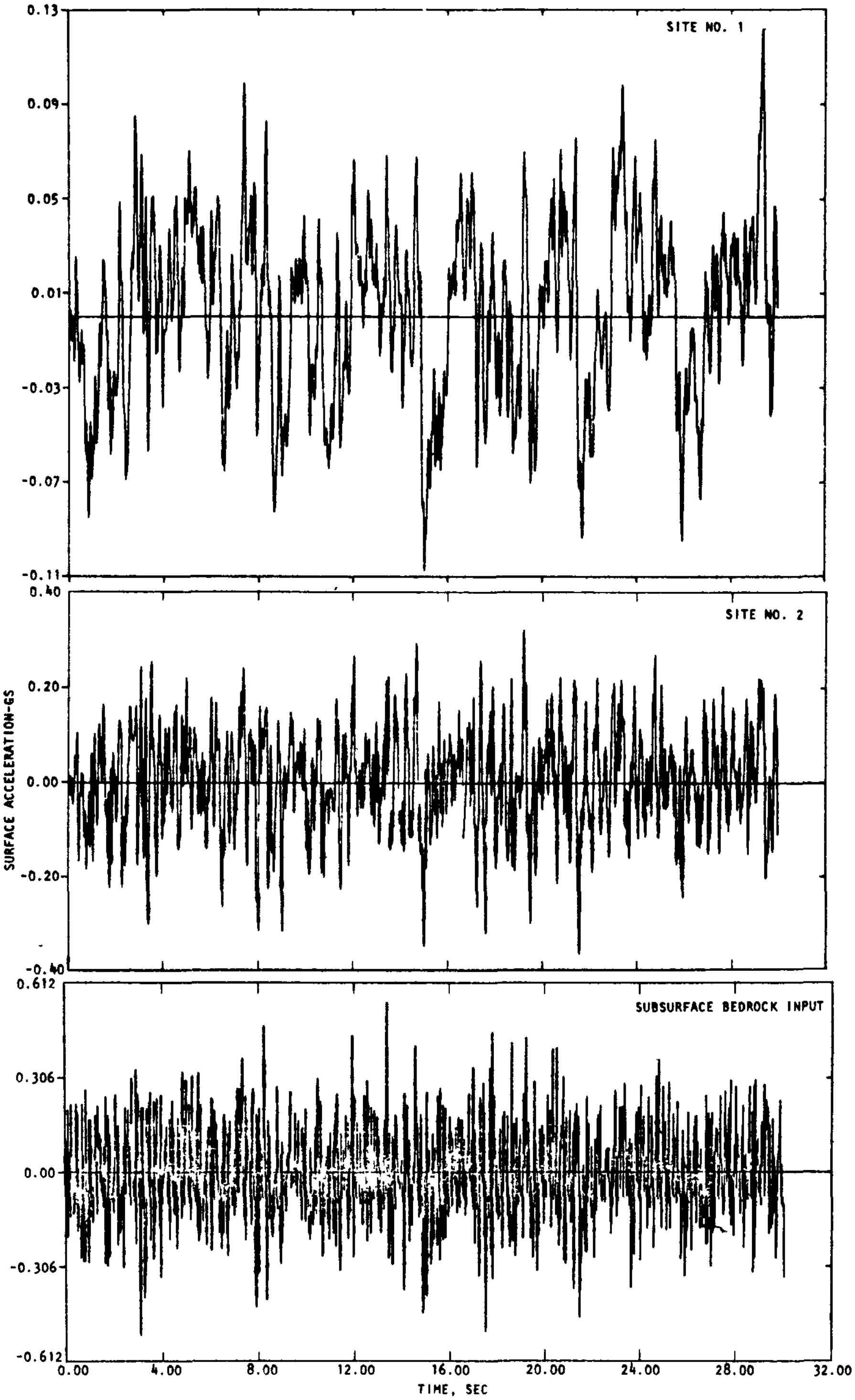

(a) MAGNITUDE 7.5 EARTHQUAKE--5 MILES FROM CAUSATIVE FAULT

FIGURE 4-20. ACCELERATION TIME HISTORIES FROM PARAMETRIC INVESTIGATION OF SOIL PROFILE EFFECTS (NOTE DIFFERENT SCALES)

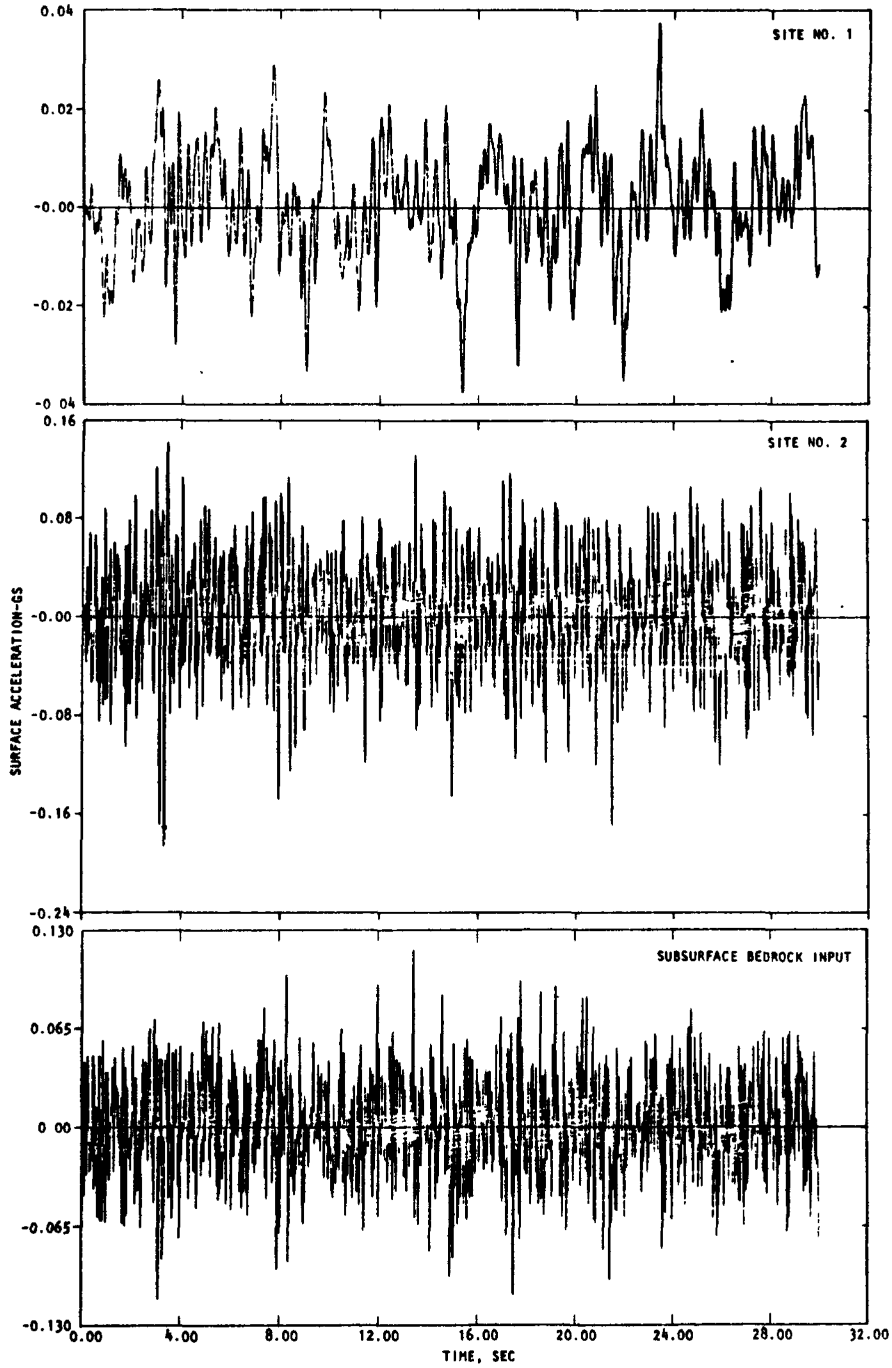

(b) MAGNITUDE 7.5 EARTHQUAKE--50 MILES FROM CAUSATIVE FAULT

FIGURE 4-20. (CONTINUED)

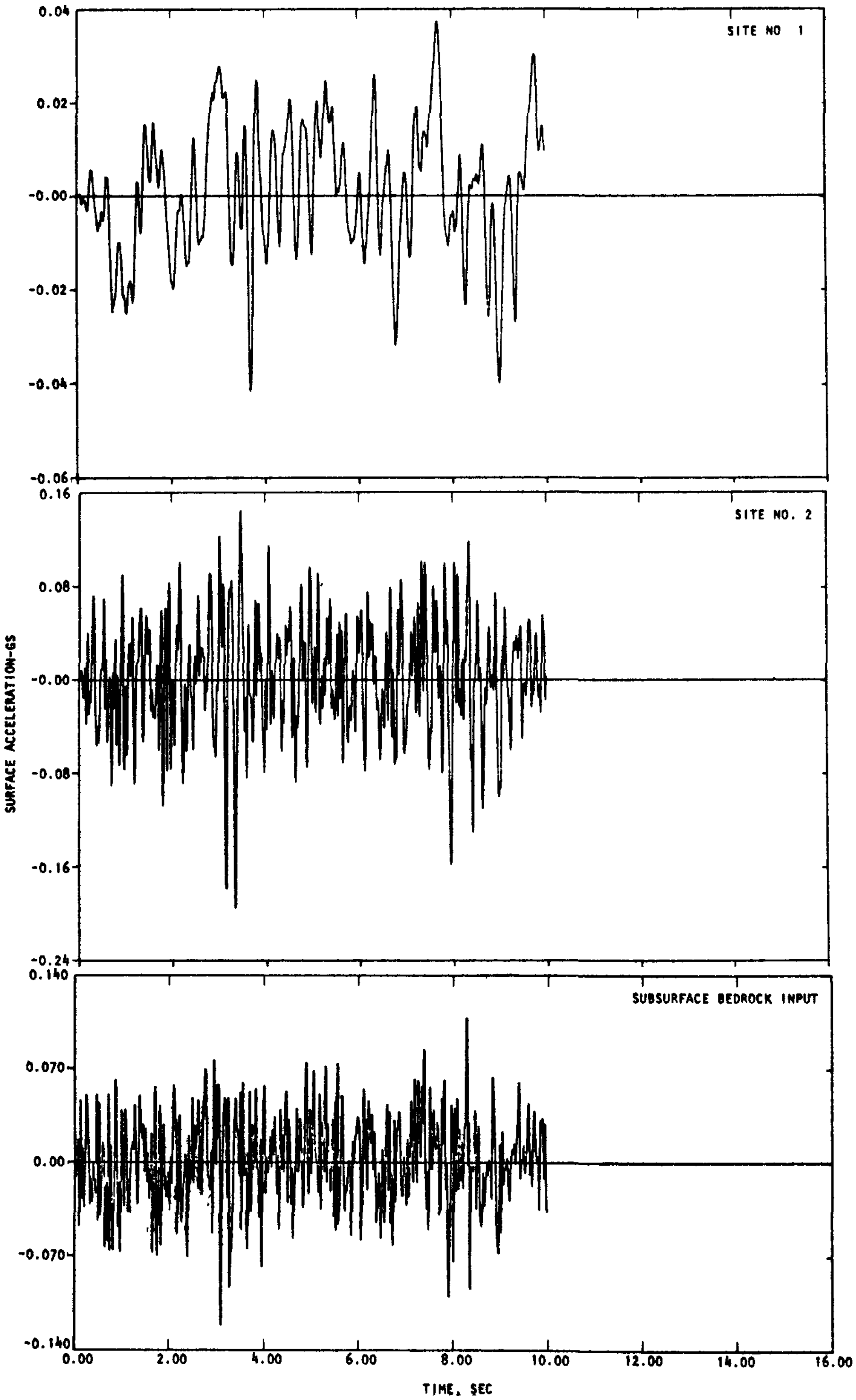

(c) MAGNITUDE 5.5 EARTHQUAKE--5 MILES FROM CAUSATIVE FAULT

FIGURE 4-20. (CONTINUED)

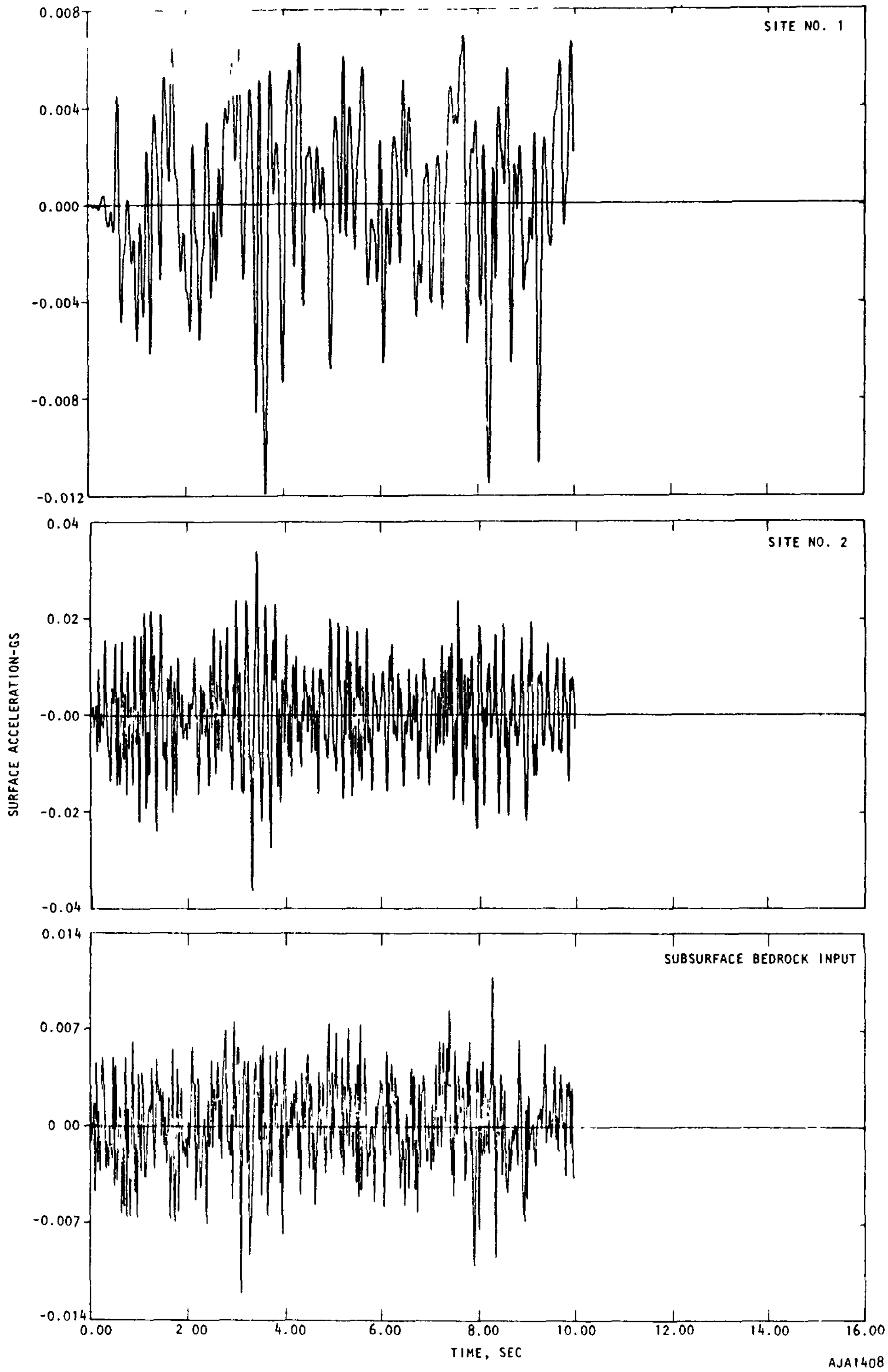

(d) MAGNITUDE 5.5 EARTHQUAKE--50 MILES FROM CAUSATIVE FAULT

FIGURE 4-20. (CONTINUED)

TABLE 4-3. SUMMARY OF STRENGTH LEVELS OF SURFACE GROUND MOTIONS--PARAMETRIC INVESTIGATION OF SOIL PROFILE EFFECTS

Earthquake Magnitude	Distance from Fault, miles	Input Parameters: rms, Acceleration in./sec^2	Input Parameters: Duration, sec	Results for Site 1: rms, Acceleration in./sec^2	Results for Site 1: $\frac{rms(Site\ 1)}{rms(Input)}$	Results for Site 2: rms, Acceleration in./sec^2	Results for Site 2: $\frac{rms(Site\ 2)}{rms(Input)}$	$\frac{rms(Site\ 2)}{rms(Site\ 1)}$
7.5	5	48.0	30	14.4	0.30	40.0	0.87	2.78
	50	10.2	30	4.35	0.43	15.6	1.53	3.57
5.5	5	10.8	10	5.46	0.51	18.7	1.73	3.44
	50	1.1	10	1.30	1.18	3.26	2.96	2.50

NOTE: Site 1 corresponds to a site with a lower characteristic frequency, whereas Site 2 corresponds to a site with a higher characteristic frequency. The actual frequency characteristics of each site are dependent on the peak strains induced in each layer of the profile, which, in turn, are dependent on the strength level of the subsurface bedrock record.

AJA1411

general, increase also, resulting in a decrease in the equivalent layer moduli and an increase in the equivalent damping factor for each layer (Figure 4-13). The increased damping and reduced stiffness will, in turn, tend to reduce the amplification of the rms acceleration of the base motion record by the soil profile. The dependence of the equivalent moduli and damping ratios on the rms acceleration level of the base motion is indicated in Figure 4-21.

The effects of the rms acceleration of the input bedrock motion on the 5 percent damped velocity spectra of the ground surface record are illustrated in Figures 4-22(a) through (d). As expected from the basic layer geometries and material properties of the sites, the Site 1 results show an amplification at the longer period regions of the spectra, whereas, for Site 2, the shorter period spectral components are amplified. Also, these figures indicate that, as the rms acceleration of the base motion increases, (1) the amplification of the base motion spectra by the soil profile tends to decrease and, (2) the magnitudes of the natural periods over which the base motion spectra are amplified tend to increase somewhat. These trends can be related to the strain dependence of the soil properties discussed in the previous paragraph.

The dependence of the ground surface motion velocity spectra on the earthquake magnitude and on the distance of the site from the causative fault is shown in Figures 4-23 and 4-24, respectively. These figures indicate that, for a given site, an increase in the magnitude of the earthquake from 5.5 to 7.5 results in a significant increase in the velocity spectrum of the ground surface record over much of the period range. Likewise, it is seen that for a given earthquake magnitude, as the distance of the site from the causative fault increases from 5 miles to 50 miles, the velocity spectrum of the resulting ground surface record decreases greatly over most of the period range, with the exception of the very short periods.

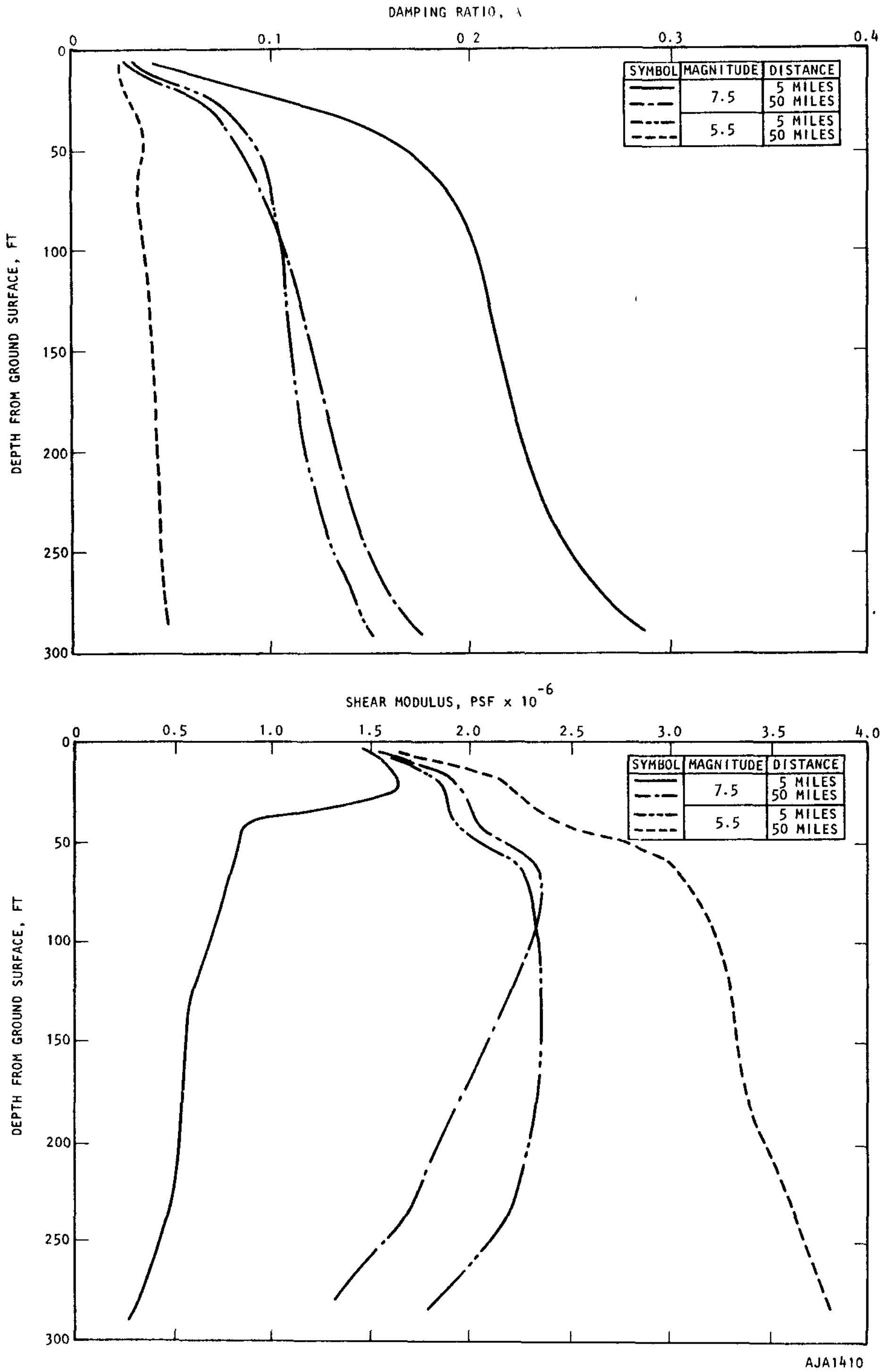

(a) SITE NO. 1

FIGURE 4-21. VARIATION IN MATERIAL PROPERTIES WITH DEPTH

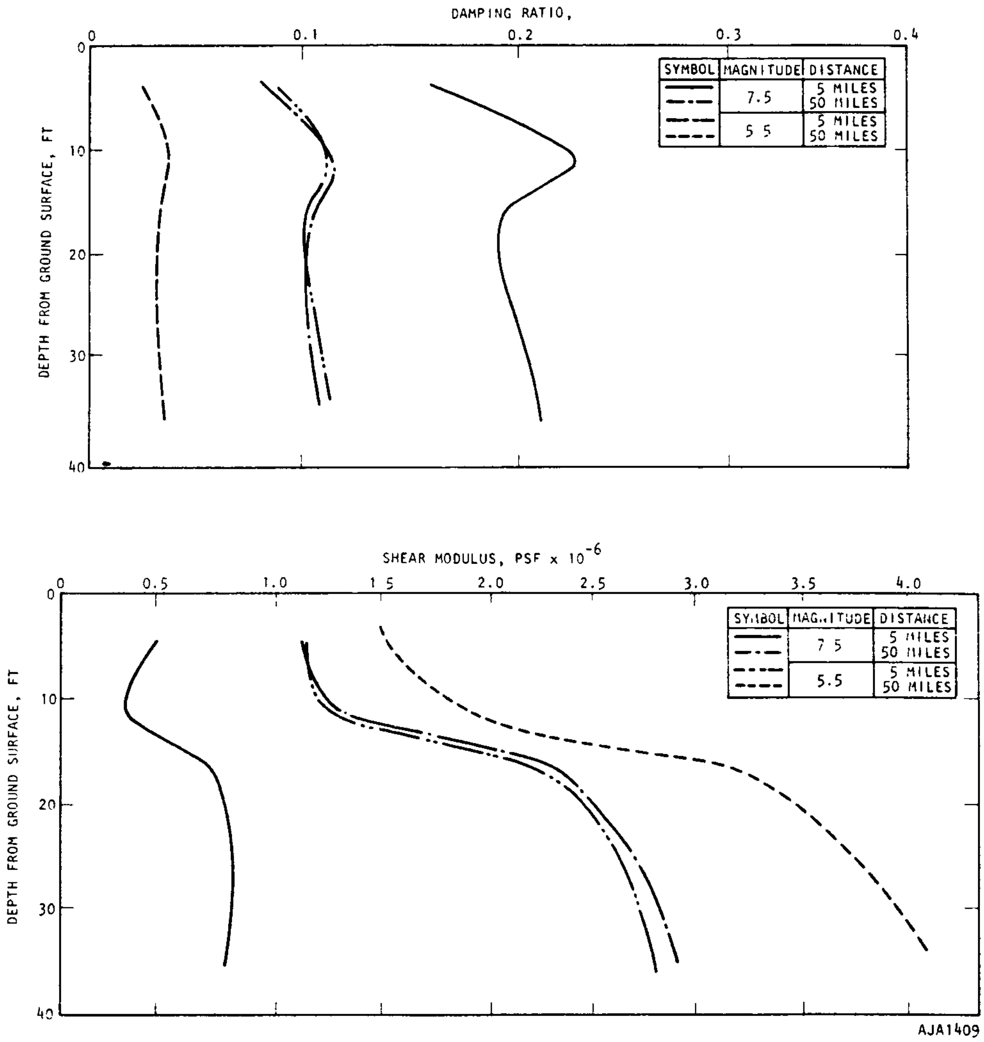

(b) SITE NO. 2

FIGURE 4-21. (CONTINUED)

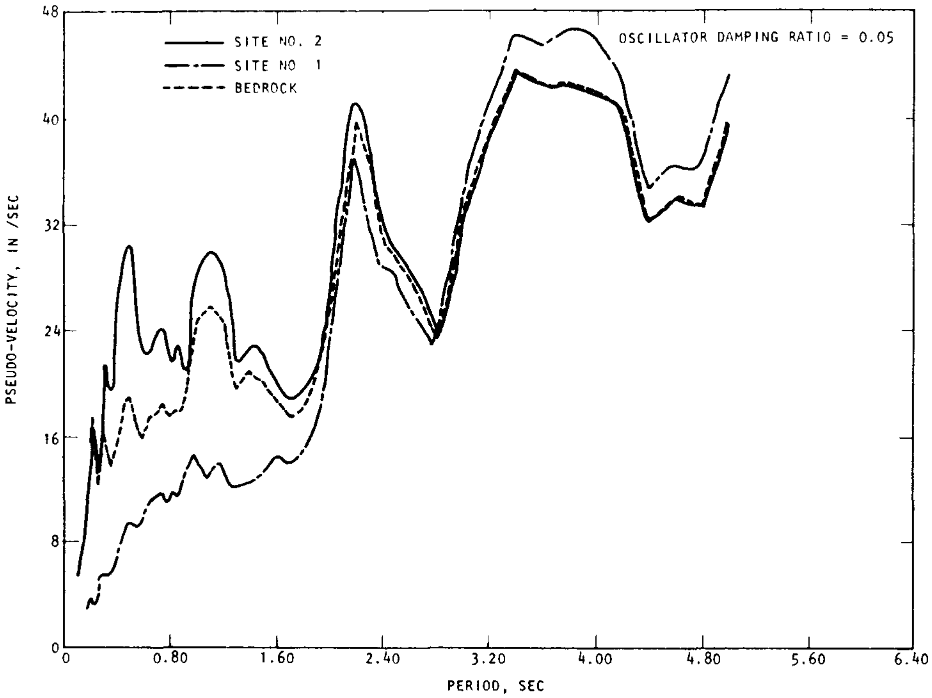

(a) MAGNITUDE 7.5, DISTANCE = 5 MILES

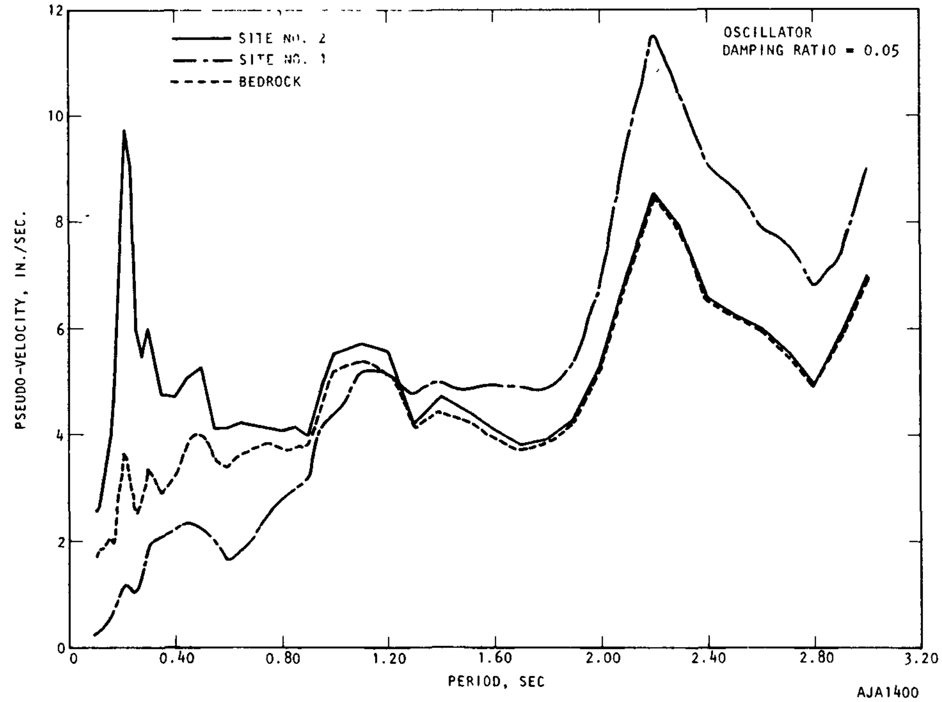

(b) MAGNITUDE = 7.5, DISTANCE = 50 MILES

FIGURE 4-22. DEPENDENCE OF GROUND SURFACE VELOCITY SPECTRA ON STRENGTH OF BASE MOTION INPUT (NOTE DIFFERENT SCALES)

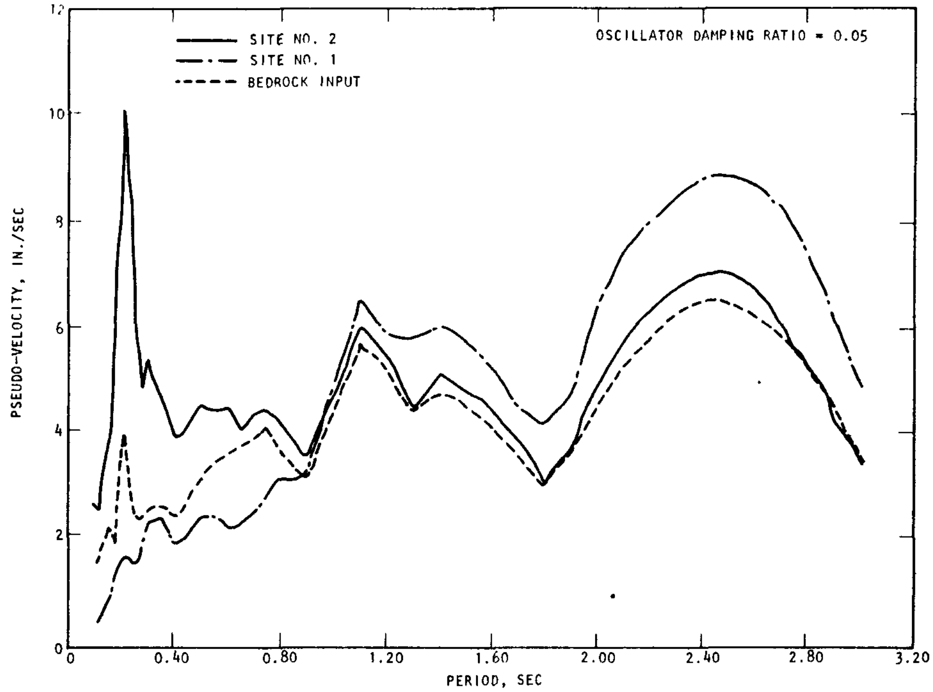

(c) MAGNITUDE = 5.5, DISTANCE = 5 MILES

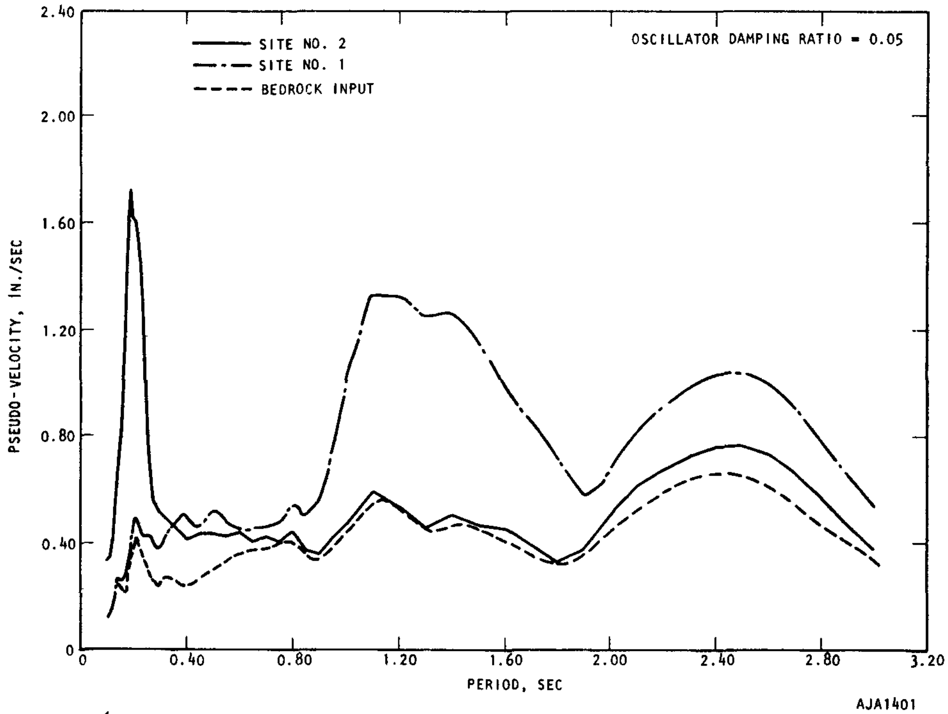

(d) MAGNITUDE = 5.5, DISTANCE = 50 MILES

FIGURE 4-22. (CONTINUED)

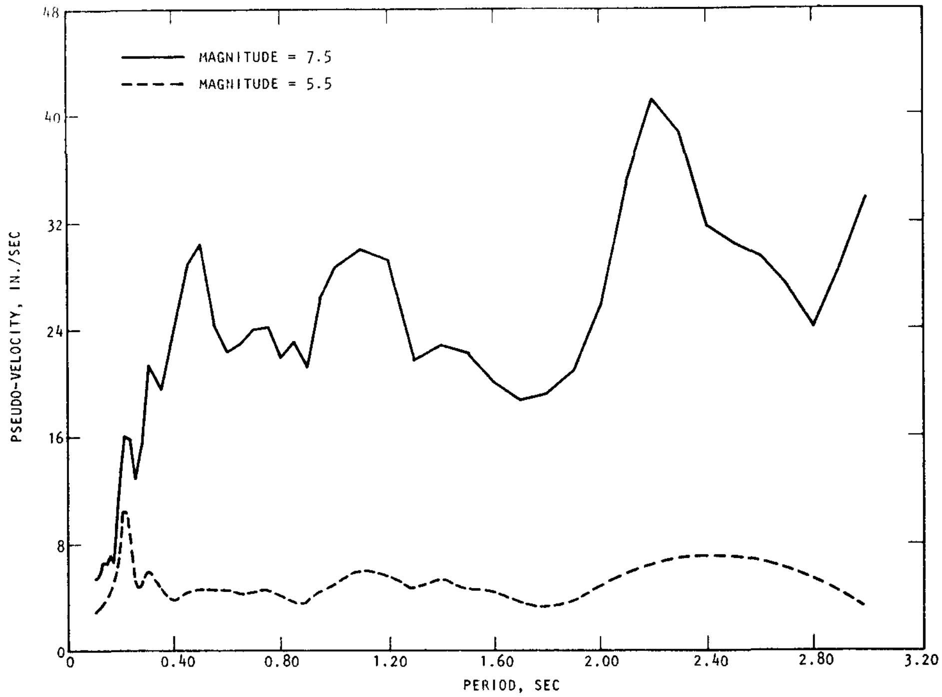

(a) SITE NO. 2--5 MILES FROM FAULT

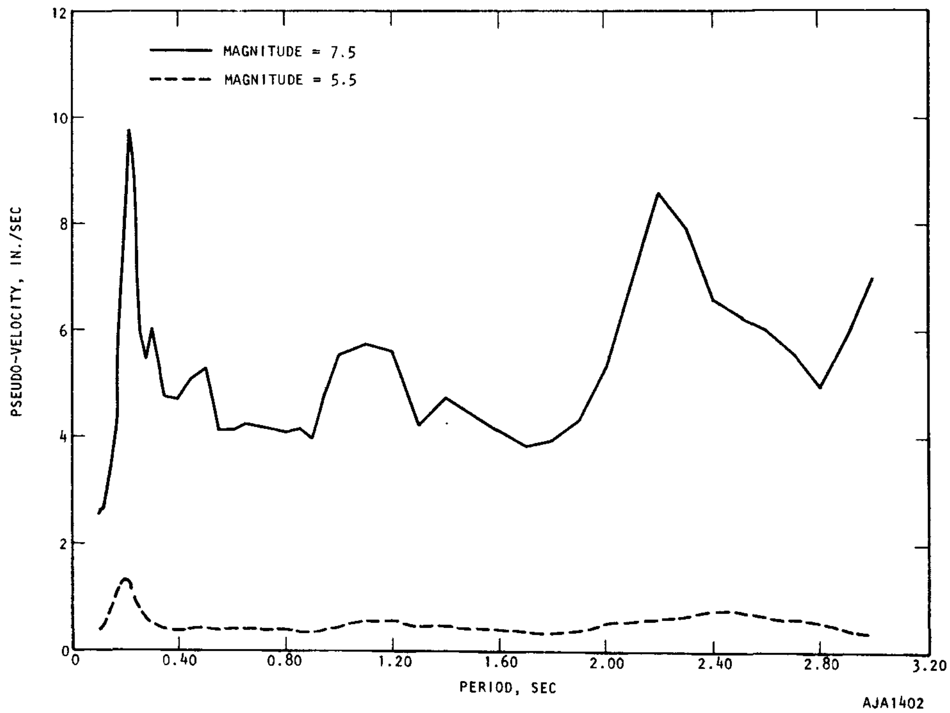

(b) SITE NO. 2--50 MILES FROM FAULT

FIGURE 4-23. EFFECT OF EARTHQUAKE MAGNITUDE ON RESPONSE SPECTRUM AT GROUND SURFACE (NOTE DIFFERENT SCALES)

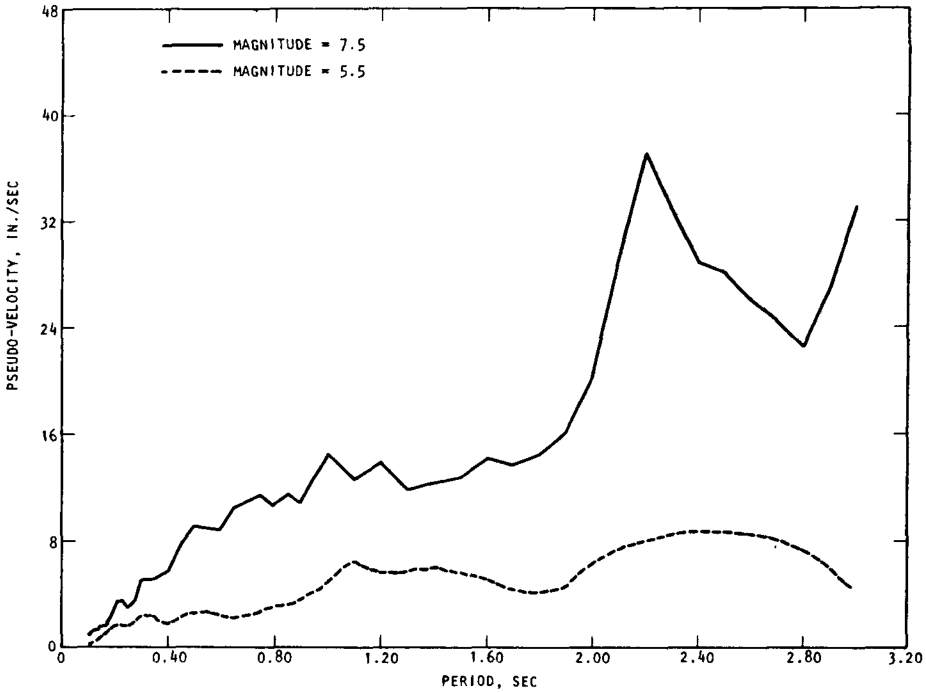

(c) SITE NO. 1--5 MILES FROM FAULT

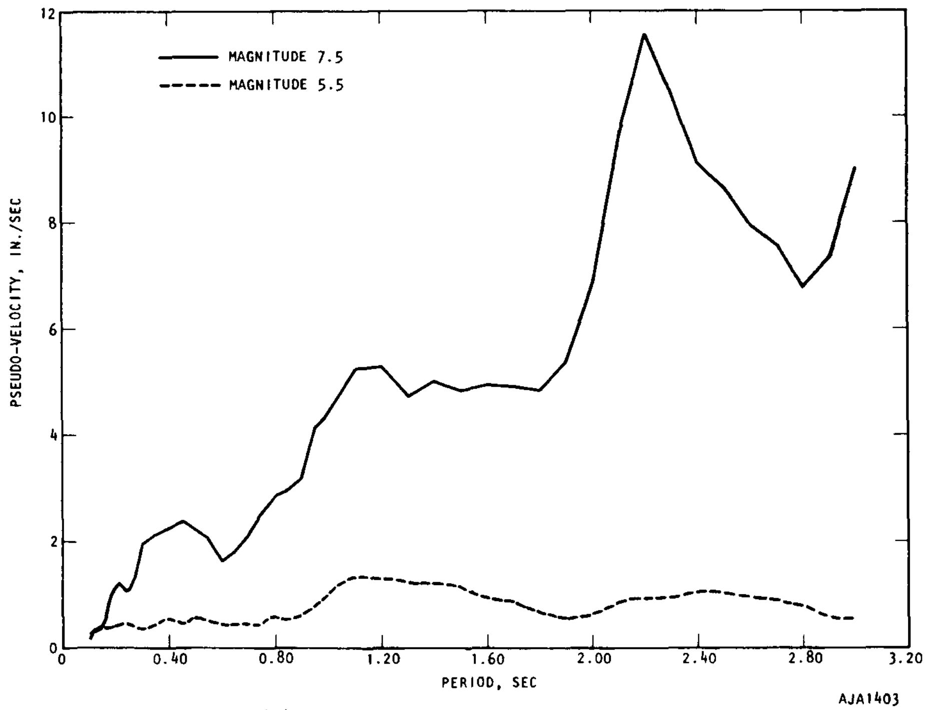

(d) SITE NO. 1--50 MILES FROM FAULT

FIGURE 4-23. (CONTINUED)

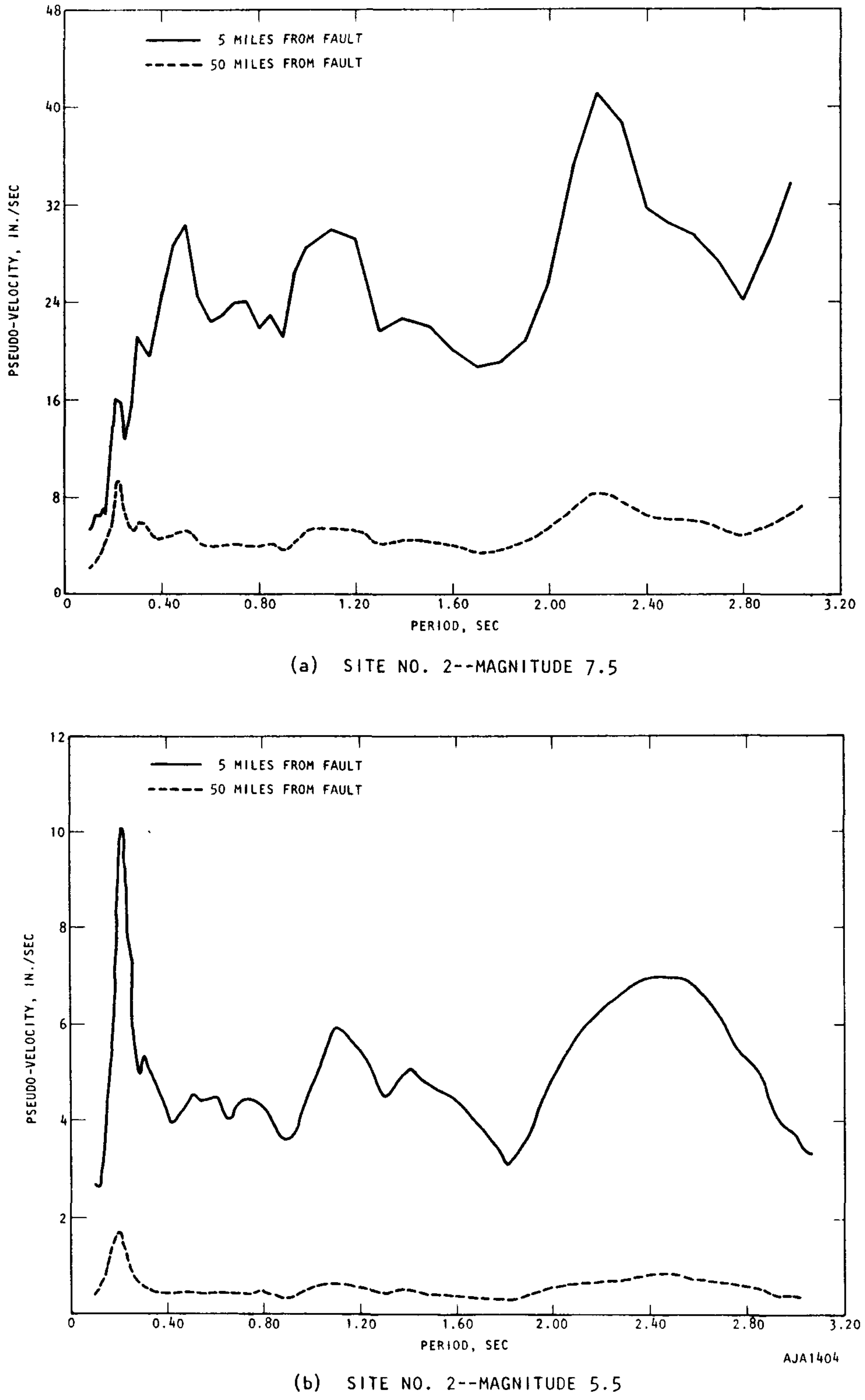

FIGURE 4-24. EFFECT OF DISTANCE FROM CAUSATIVE FAULT ON SURFACE EARTHQUAKE MOTIONS (NOTE DIFFERENT SCALES)

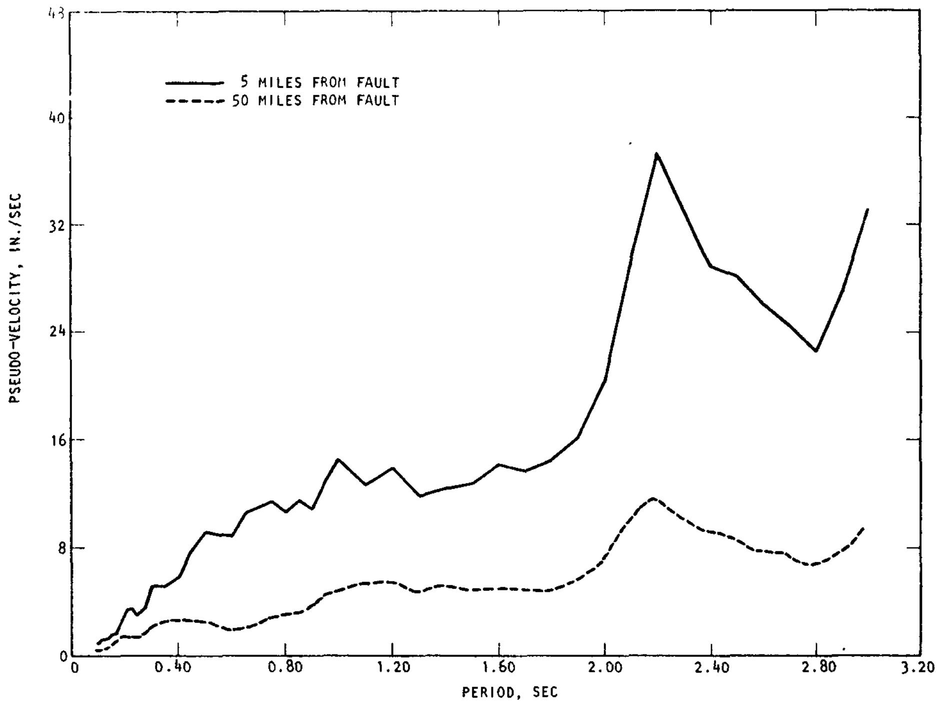

(c) SITE NO. 1--MAGNITUDE 7.5

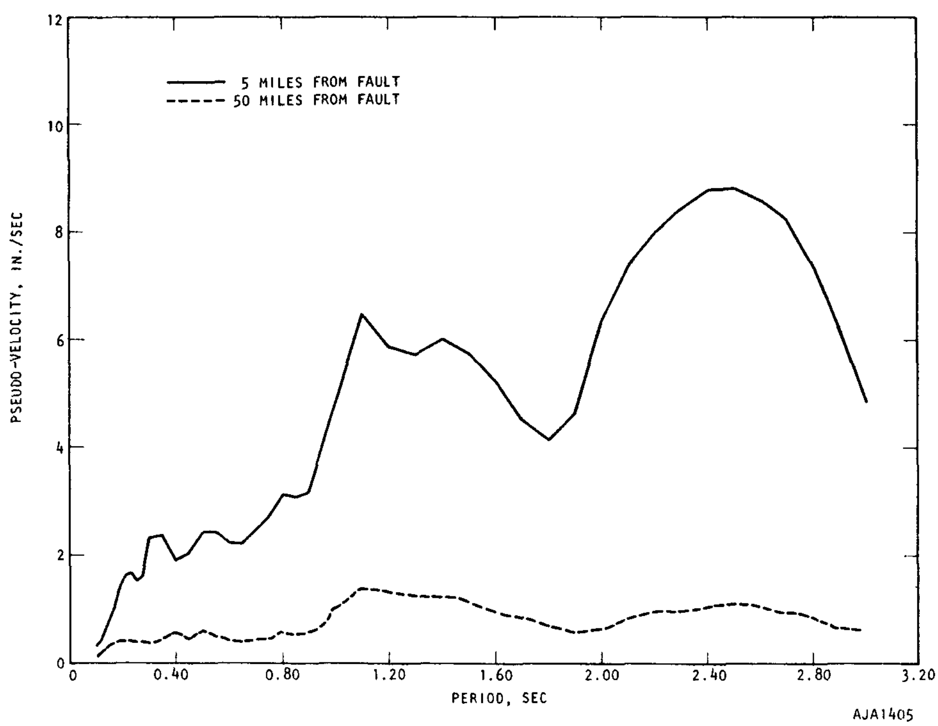

(d) SITE NO. 1--MAGNITUDE 5.5

FIGURE 4-24. (CONTINUED)

4.6.3 COMPARISON OF CALCULATED RESULTS WITH OTHER APPROACHES

It is of interest to compare some of the results of the above parametric investigation with the results of other approaches for selecting earthquake motions at a site.

The first approach that has been compared with the calculated results was suggested by N. M. Newmark and W. J. Hall in Reference 4-20. This consists of peak response levels specified for a "standard" earthquake, a "very intense" earthquake, and a "minimum" earthquake. Spectra can be constructed for each of these earthquakes, and amplification factors are provided for scaling these spectra to correspond to a site consisting of either competent rock, firm sediment (or soft rock), or soft sediment. The Newmark-Hall spectra for firm sediment have been considered in this comparison.

The second approach selected for comparison is the first-level approach, and is based on a set of average spectra obtained by G. W. Housner from the spectral characteristics of measured strong motion records (Reference 4-5). These spectra can be scaled to correspond to peak acceleration levels suggested in Table A-5 of Appendix A in regions of either high, moderate, low, or minimal seismicity. This approach is similar to that suggested by Housner in Reference 4-21, except that the basis for scaling the spectra has been modified somewhat.

In Figures 4-25(a) and (b), spectra from each of these approaches have been compared to the spectra of Site No. 1 and Site No. 2 from (1) the magnitude 7.5 earthquake for a site 5 miles from the fault, and (2) the magnitude 5.5 earthquake for a site 50 miles from the fault. These earthquake magnitude-causative fault distance combinations correspond to the maximum and minimum earthquake strength levels considered in the parametric investigation. Periods from 0.1 to 3.0 sec are included in the comparison since this is the period range of interest for most structures.

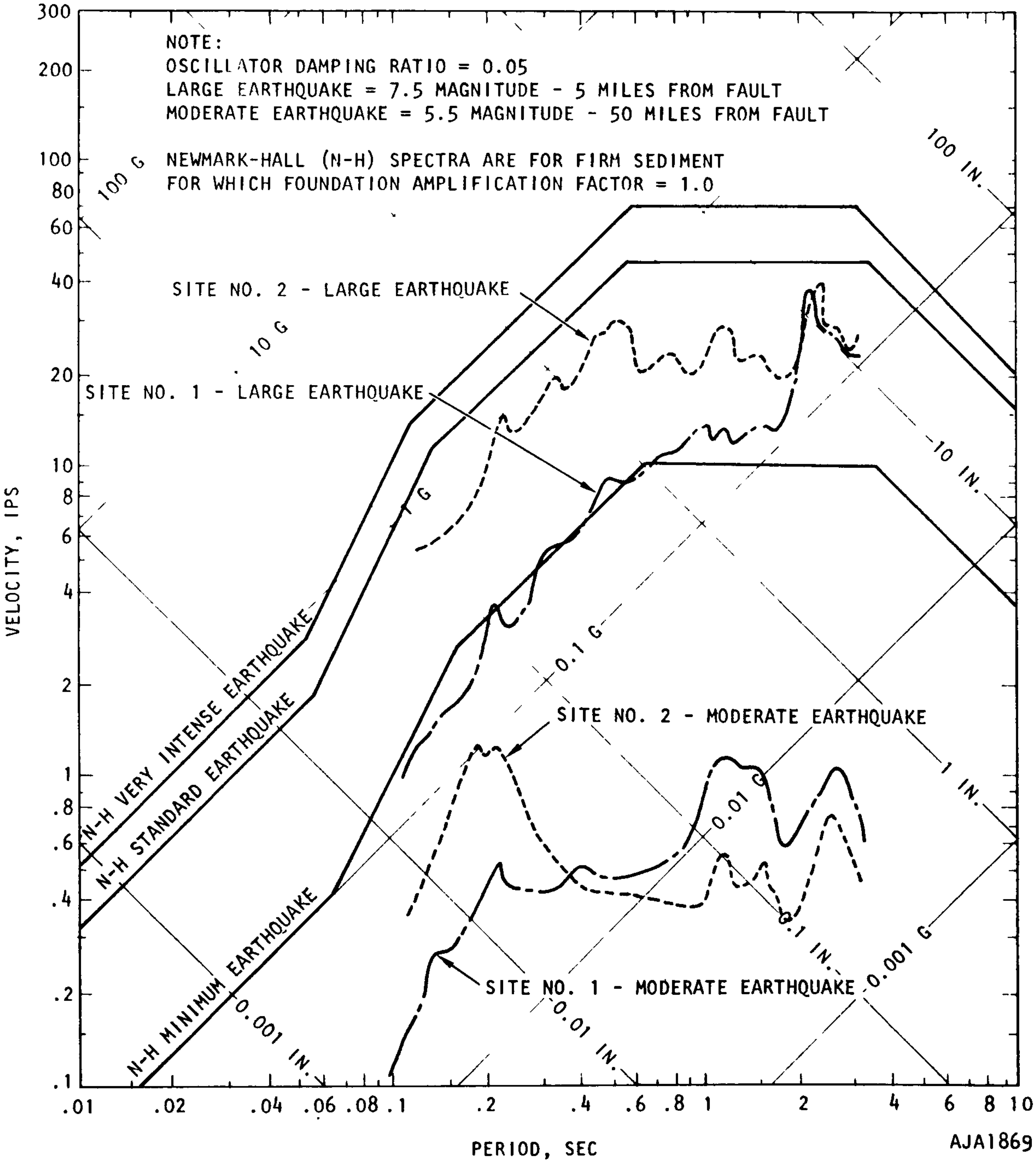

(a) COMPARISON OF CALCULATED SPECTRA WITH SPECTRA FROM NEWMARK-HALL APPROACH (REFERENCE 4-20)

FIGURE 4-25. COMPARISON OF CALCULATIONS WITH RESULTS FROM EXISTING APPROACHES

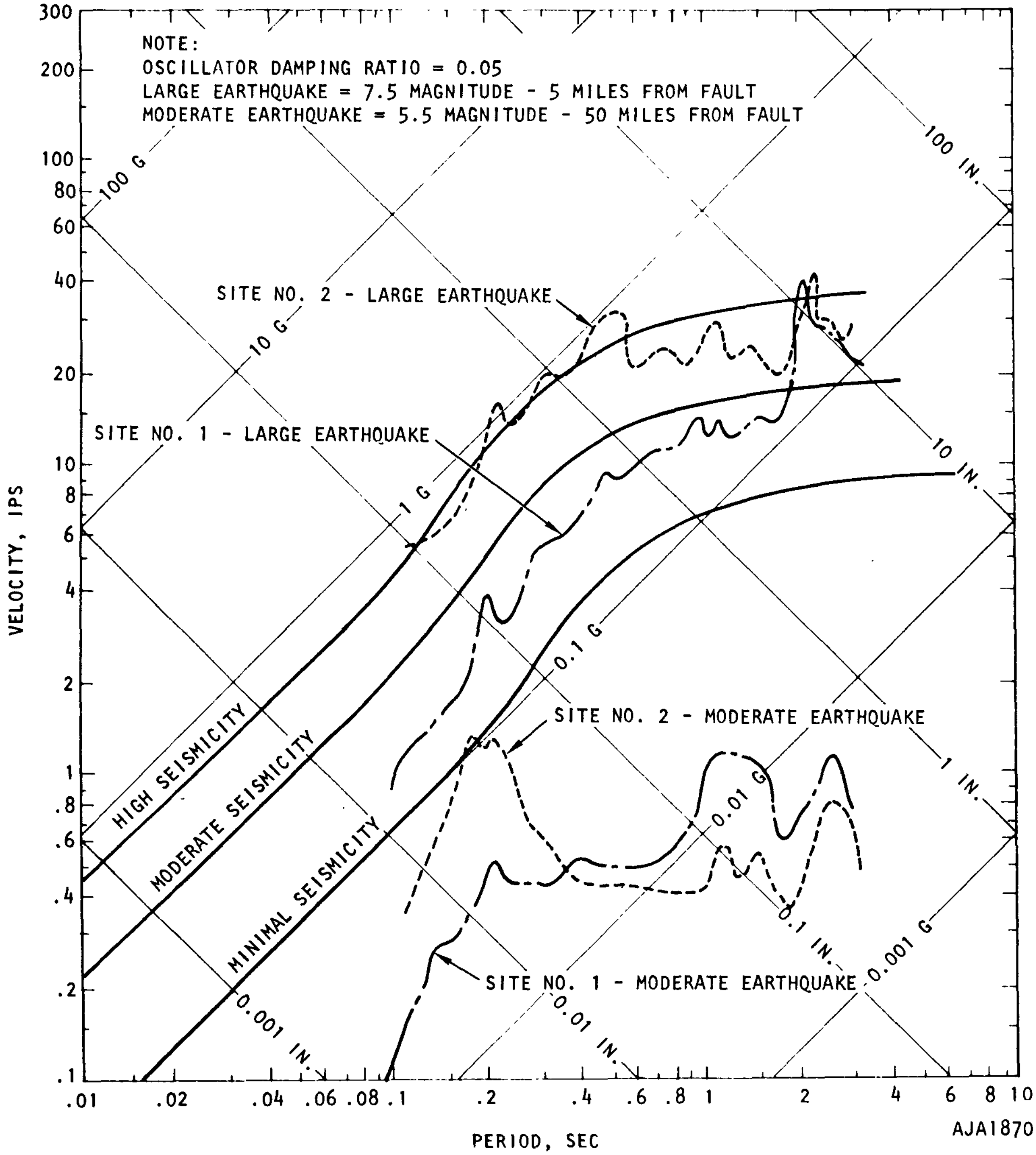

(b) COMPARISON OF CALCULATED SPECTRA WITH SPECTRA PROVIDED IN FIRST-LEVEL APPROACH

FIGURE 4-25. (CONTINUED)

The comparisons shown in Figures 4-25(a) and (b) indicate the following results:

a. The lower bound spectra for the Newmark-Hall approach (applied to firm sediment) and for the first-level approach each represent a more conservative approach to the design of structures than do the results of these shear beam calculations for a magnitude 5.5 earthquake at a site 50 miles from the causative fault.

b. The very intense earthquake spectrum and standard earthquake spectrum recommended by Newmark-Hall for a site consisting of firm sediment each represent a more conservative approach to the design of structures to resist large earthquakes than do the results of these shear beam calculations for a magnitude 7.5 earthquake at a site 5 miles from the causative fault.

c. The spectrum recommended in the first-level approach for a highly seismic region provides a fairly close correlation with the computed results for Site No. 2, when the site is located 5 miles from the fault and is subjected to a magnitude 7.5 earthquake. It is noted that the spectra recommended in the first-level approach corresponds to representative, not maximum, conditions in each seismic region. Therefore, since the maximum credible earthquake in a highly seismic region is generally considered to have a magnitude of greater than 8, it is consistent for the upper bound spectrum from the shear beam calculations (corresponding to a magnitude 7.5 earthquake) and the upper bound spectrum from the first-level approach to exhibit about the same strength levels.

REFERENCES

4-1. Tamura, C., "Characteristics of Earthquake Motion on the Rocky Ground," *Proceedings of the Fourth World Conference on Earthquake Engineering*, Santiago, Chile, January 1969.

4-2. Coon, R. F., *Recommended Construction Procedures for Hardened Facility Test Structures at Cedar City, Utah*, A. A. Mathews, Inc., Construction Report No. 569, January 1969.

4-3. Seed, H. B., and I. M. Idriss, *Characteristics of Rock Motions During Earthquakes*, EERC 68-5, University of California at Berkeley, 1969.

4-4. Bycroft, G. N., "White Noise Representation of Earthquakes," *Journal of the Engineering Mechanics Division*, ASCE, Vol. 86, No. EM2, April 1960.

4-5. Housner, G. W., "Behavior of Structures During Earthquakes," *Journal of the Engineering Mechanics Division*, ASCE, Vol. 85, No. EM4, October 1959.

4-6. Housner, G. W., and P. C. Jennings, "Generation of Artificial Earthquakes," *Journal of the Engineering Mechanics Division*, ASCE, Vol. 90, No. EM1, February 1964.

4-7. Liu, S. H., and D. P. Jhaveri, "Spectral Simulation and Earthquake Site Properties," *Journal of the Engineering Mechanics Division*, ASCE, Vol. 95, No. EM5, October 1969.

4-8. Housner, G. W., "Intensity of Earthquake Ground Shaking Near a Causative Fault," *Proceedings of the Third World Conference on Earthquake Engineering*, Aukland and Wellington, New Zealand, January 1965.

4-9. Liu, S. H., "On Intensity Definitions of Earthquakes," *Journal of the Structural Division*, ASCE, Vol. 95, No. ST5, May 1969.

4-10. Housner, G. W., *Requirements of Seismic Analysis and Pesearch Needs*, paper presented at Annual and Environmental Meeting of American Society of Civil Engineering, October 1969.

4-11. Tsai, N. C., *Influence of Local Geology on Earthquake Ground Motion*, Ph. D. Thesis, California Institute of Technology, Pasadena, California, 1969.

4-12. Idriss, I. M., and H. B. Seed, "Seismic Response of Soil Deposits," *Journal of the Soil Mechanics Division*, ASCE, Vol. 96, No. SM2, March 1970.

REFERENCES (CONTINUED)

4-13. Idriss, I. M., and H. B. Seed, "An Analysis of Ground Motions During the 1957 San Francisco Earthquake," *Bulletin of the Seismological Society of America*, Vol. 58, No. 6, December 1968.

4-14. Seed, H. B., and I. M. Idriss, "Influence of Soil Conditions on Ground Motions During Earthquakes," *Proceedings of the American Society of Civil Engineers*, Vol. 95, No. SM1, January 1969.

4-15. Seed, H. B., *The Influence of Local Soil Conditions on Earthquake Damage*, paper presented at the Seventh Conference on Soil Mechanics and Foundation Engineering, Soil Dynamics Specialty Conference, Mexico City, August 1969.

4-16. Roesset, J. M., and R. V. Whitman, *Theoretical Background for Amplification Studies*, Research Report R69-15, Soils Publication No. 231, Department of Civil Engineering, Massachusetts Institute of Technology, Cambridge, Massachusetts, March 1969.

4-17. Hagmann, A. J., and R. V. Whitman, *Comparison of Methods for Analyzing Soil Deposits During Earthquakes*, Research Report R69-29, Soils Publication No. 238, Department of Civil Engineering, Massachusetts Institute of Technology, Cambridge, Massachusetts, June 1969.

4-18. Housner, G. W., "Strong Ground Motion," article appearing in *Earthquake Engineering*, edited by R. L. Wiegle, Prentice-Hall, 1970.

4-19. Tsai, N. C., "Transformation of Time Axes of Accelerograms," *Journal of the Engineering Mechanics Division*, ASCE, Vol. 95, No. EM3, June 1969.

4-20. Newmark, N. M., and W. J. Hall, "Seismic Design Criteria for Nuclear Reactor Facilities," *Fourth World Conference on Earthquake Engineering*, Santiago, Chile, January 1969.

4-21. Housner, G. W., "Design of Nuclear Power Reactors Against Earthquakes," *Second World Conference on Earthquake Engineering*, Tokyo, Japan, July 1960.

SECTION 5

SOIL-STRUCTURE INTERACTION ANALYSIS TECHNIQUES

5.1 OBJECTIVES AND SCOPE

The objective of this task was to review and assess soil-structure interaction analysis techniques suitable for application to nuclear power plants subjected to earthquake ground motions. The ability of these techniques to predict the peak structure motions and stresses as well as response time histories at selected points in the structure has been considered. In addition, more complex aspects of the problem have been examined, such as soil-structure interface conditions, three-dimensional effects, and inelastic material behavior.

To facilitate this review, the soil-structure interaction techniques are categorized as follows:

- Closed-form solutions
- Discrete element representations of interaction effects at the soil-structure interface
- Finite difference methods
- Finite element methods

Representative analysis techniques are described for each of these general approaches to illustrate their available capabilities in predicting interaction effects. In view of the limited scope of the present undertaking, only the pertinent aspects of each analysis, rather than detailed descriptions, are included. Where possible, comparisons are made to indicate the advantages and disadvantages of the various methods.

5.2 GENERAL DISCUSSION OF SOIL-STRUCTURE INTERACTION

The bedrock-soil-structure interaction problem has been considered by R. V. Whitman (Reference 5-1) as composed of the following two effects:

a. As the earthquake motions in bedrock (u_1 in Figure 5-1) are propagated up to the ground surface, they are modified by the soil to a ground motion indicated by u_2 in Figure 5-1. This modification is observed even if the structure is not present.

b. As the earthquake motions are propagated upward to a region in the vicinity of a structure, they are changed to a form denoted by u_3 in Figure 5-1. This modification is caused by soil-structure interaction.

If the depth to bedrock is equal to or less than the width of the structure, the above effects are coupled, and any structural response that considers interaction should include these coupled effects. However, if the depth to bedrock is large compared to the width of the structure, the two effects listed above can be decoupled. For this case, the modified motion u_2 (due to the soil profile characteristics) is termed the free field motion, and is studied using closed-form solutions, a discrete shear beam approach, and finite element techniques. The shear beam technique has been used in Task 1 of this study to obtain the free field motion, u_2.

The second effect indicated above is termed soil-structure interaction. For flexible structures, tests have shown that soil-structure interaction may have little effect in modifying the free field ground motions (References 5-2, 5-3). However, for stiff structures, such as containment structures for large nuclear reactors, soil-structure interaction effects will, in general, have a significant influence in modifying the free field ground motions in the vicinity of the structure.

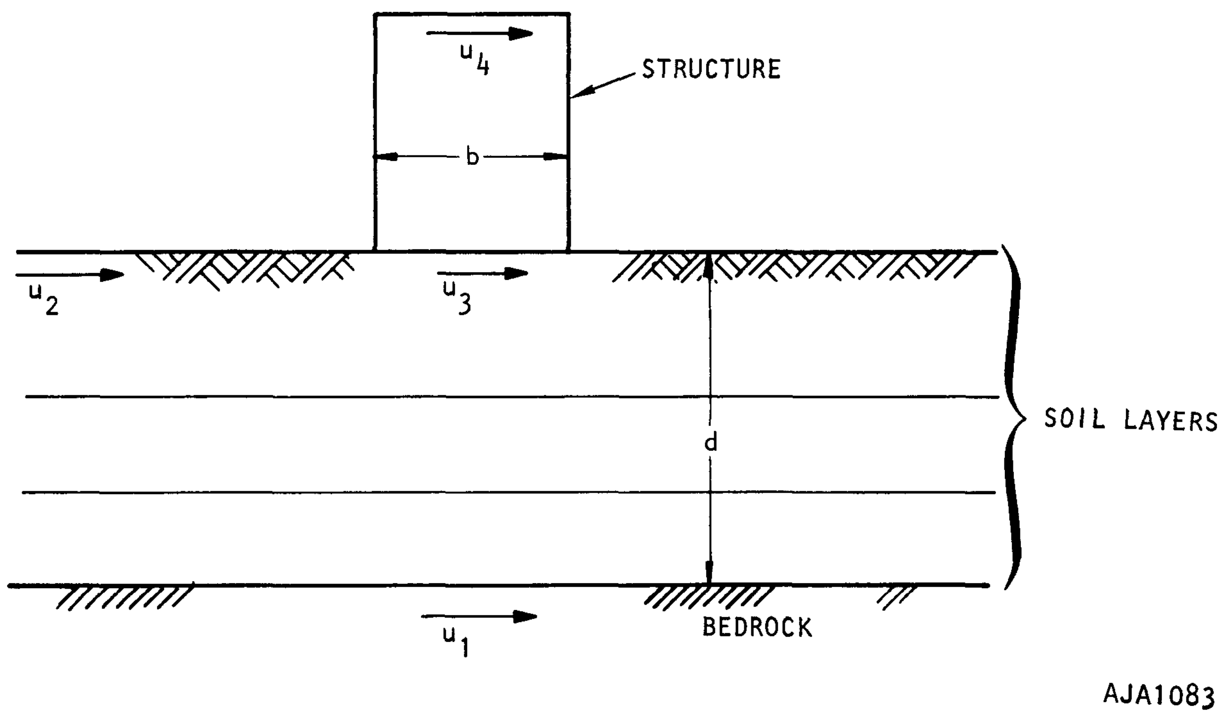

FIGURE 5-1. BEDROCK-SOIL-STRUCTURE INTERACTION EFFECTS

5.3 SUMMARY OF REPRESENTATIVE TECHNIQUES

5.3.1 ANALYSES BASED ON CLOSED-FORM SOLUTIONS

A number of techniques using closed-form solutions have been used to investigate soil-structure interaction phenomena. These range from closed-form solutions for a rigid plate on an elastic half-space to multimass structure models coupled to an elastic half-space. A number of such closed-form solutions are summarized in Table 5-1.

The approaches described in References 5-4 through 5-8 deal with closed-form solutions of a rigid plate on a linear elastic, homogeneous, isotropic half-space. The forcing functions considered in these analyses are either periodic or harmonic in nature. These solutions are suited for investigation of the forced vibration of a simple rigid structure on an elastic solid, and appear to be particularly oriented toward the dynamics of machine foundations.

Several investigators have extended the half-space solutions cited above to accommodate a more refined representation of the structure and earthquake excitation. For example, R. W. Parmelee has analyzed a three-degree-of-freedom structure coupled to an elastic half-space model of the soil; in this the system is subjected to earthquake ground motions at the soil-structure interface (Reference 5-9). The results of this analysis identified the shear wave velocity of the soil medium as the most important parameter affecting the coupling of the response of the soil and structure.

Other researchers also have used analytical techniques of this type for particular structures. B. G. Korenev, et al. (Reference 5-10), investigated the earthquake response of tower-like structures coupled to an elastic half-space and concluded that, for tall, slender structures, the horizontal displacements at the base of the structure are small when compared to its rocking motions. A. K. Chopra and P. R. Perumalswami (Reference 5-11) performed a finite element planar analysis of a dam structure coupled to an

AJA

TABLE 5-1. REPRESENTATIVE ANALYSES BASED ON CLOSED FORM SOLUTIONS OF THE WAVE EQUATION

Type	Representative Techniques	
	Approach	Description
Rigid Circular Mass on Elastic Half-Space	Reissner (Reference 5-4) Sung (Reference 5-5)	Vertical motion of rigid circular mass resting on elastic semi-infinite medium and subjected to periodic vertical force.
	Toriumi (Reference 5-6) Bycroft (Reference 5-7)	Vertical translation, horizontal translation, and rotation of harmonically loaded circular plate on elastic half-space.
Rectangular Rigid Plate on Half-Space	Kobori (Reference 5-8)	Vertical motion of dynamically loaded rectangular base on elastic half space. Results for square plate compared well with those of Reissner for circular base of same area.
Multi-mass Structure Model Coupled to Elastic Half-Space	Parmelee (Reference 5-9) (see Figure 5-2(a))	Structure model has 3 degrees of freedom: horizontal translation of base, m_o, horizontal translation of top, m_2, and rocking about point b in Figure 5-2(a). Half-space analysis based on Bycroft steady state solution of Reference 5-7. Seismic waves propagate vertically upward through half-space to soil structure interface. Only horizontal motion of foundation is considered.
	Korenov, et al., (Reference 5-10) (see Figure 5-2(b))	Analysis of effects of foundation inertia on vibrations of tower like structure subjected to base motions. Foundation modelled as homogeneous elastic half space and was analyzed using the approach of Bycroft (Reference 5-7.) Seismic input either stationary random process or deterministic record.
	Chopra, et al., (Reference 5-11) (see Figure 5-2(c))	Analysis of soil-structure interaction of a dam structure during earthquake loading. Finite element model of dam and elastic homogeneous half-space analyses of soil medium was used. Radiation damping is represented since infinite extent of foundation is considered in formulation.
	Scavuzzo (Reference 5-12) (see Figure 5-2(d))	Analysis of effects of interaction during earthquake excitation on response spectrum at base of simplified model of nuclear reactor structure.
Rigid Foundation in Elastic Layered Site	Tajimi (Reference 5-13) (see Figure 5-2(e))	Rigid circular foundation resting on one elastic stratum and surrounded by a second elastic stratum. Rocking of structure and amplification of motions by upper stratum considered. Requires continuity between foundation and soil strata.
Three Dimensional Analysis of Rigid Block on Elastic Half-Space	Hsieh (Reference 5-15)	Three dimensional analysis of rigid block on homogeneous, elastic, isotropic medium. Showed solution of this problem to be analogous to that using "spring-dashpot" analogy.

AJA1319

elastic, homogeneous half-plane model of the soil medium. They showed that: (1) the elasticity of the soil may have an important influence on the natural frequencies and mode shapes of the dam, and (2) for the homogeneous site considered, radiation damping resulted in significant energy dissipation as a result of wave propagation into the soil medium. The earthquake response of a simplified discrete mass model of a nuclear reactor coupled with a two-dimensional, elastic half-space analyses (Figure 5-2(d)) was investigated by R. J. Scavuzzo, et al. (Reference 5-12). The Alexander Building site in San Francisco was investigated and, for this site, the response spectrum of the free field ground motions was reduced significantly due to interaction with a short structure having significant mass. However, interaction with a tall flexible building was shown to result in a slight increase in the base response spectrum and the lateral accelerations.

H. Tajimi has investigated the dynamic response of a rigid circular cylinder resting on one elastic stratum and surrounded by a second elastic stratum (Reference 5-13 and Figure 5-2(e)). This solution, which provides significant insight into the response of a structure embedded in a layered site, has indicated two aspects of the coupling between the structure and the upper stratum: a restraining effect and a driving effect. The driving effect results from the free field ground motion at the top of the upper stratum, which is greater than the ground motion applied to the base of the structure. For the cases considered by Tajimi, the driving effect was shown to be more significant than the restraining effect of the upper stratum. Thus, neglecting the presence of the upper soil stratum in the analysis of an embedded structure may not be conservative, since the effect of the soil surrounding the structure may be to increase the structural motions. As indicated by Whitman (Reference 5-14), the work of Tajimi indicates the need for further study of the dynamic earth stresses against the sides of an embedded structure.

A three-dimensional analysis of a rigid block resting on a homogeneous, isotropic, elastic half-space has been provided by T. K. Hsieh in Reference 5-15. This work treated the coupled six degrees of freedom of

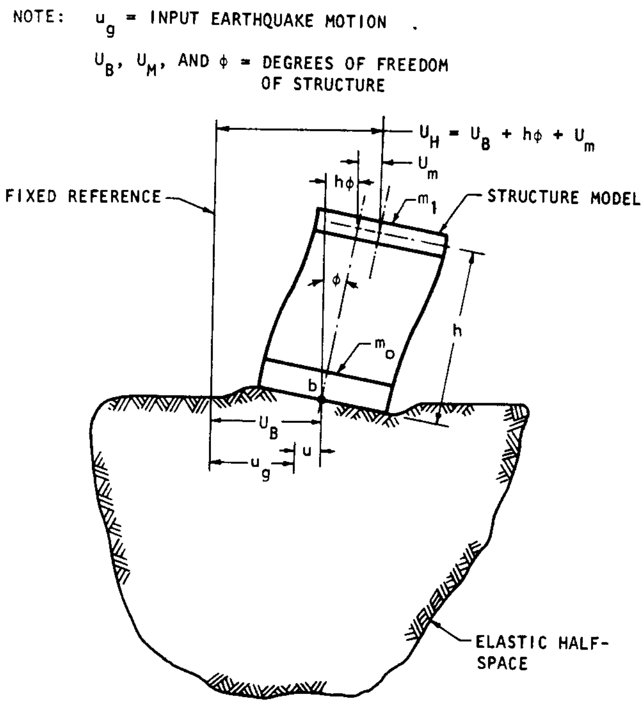

(a) MODEL OF THREE DOF STRUCTURE ON ELASTIC HALF-SPACE (REFERENCE 5-9)

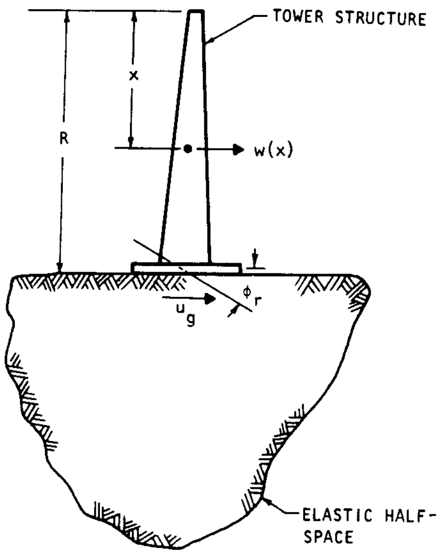

(b) MODEL OF TOWER STRUCTURE ON ELASTIC HALF-SPACE (REFERENCE 5-10)

AJA1429

FIGURE 5-2. MODELS USED IN CLOSED FORM ANALYSES

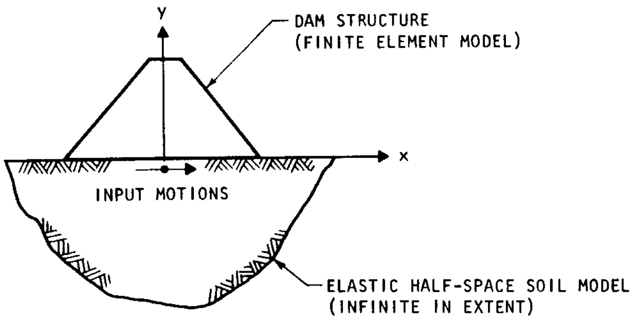

(c) MODEL OF DAM STRUCTURE AND SOIL HALF-SPACE (REFERENCE 5-11)

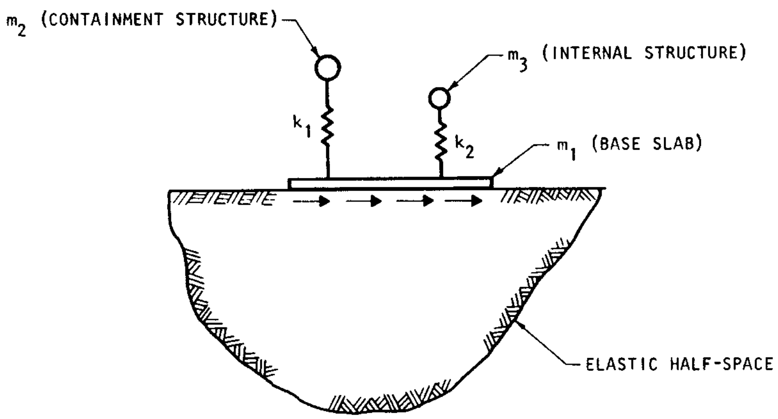

(d) MODEL OF NUCLEAR REACTOR AND SOIL HALF-SPACE (REFERENCE 5-12)

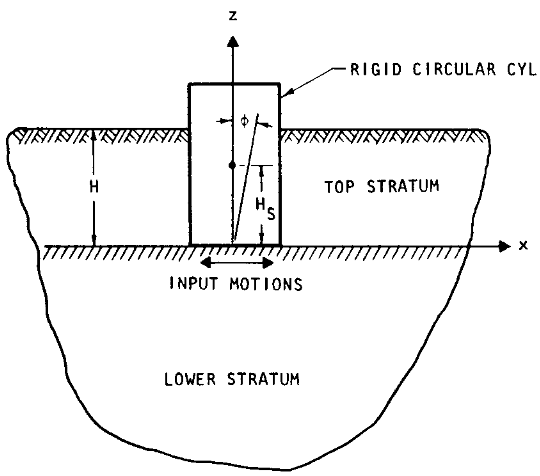

(e) MODEL OF EMBEDDED STRUCTURE (REFERENCE 5-13)

AJA1778

FIGURE 5-2. (CONTINUED)

the block, and showed that the solution to this problem is analogous to the spring-dashpot analogy. Expressions for the "spring" and "dashpot" constants are provided in terms of the soil properties, the dimensions of the block, and the frequency of the impressed vibration.

In summary, analyses based on closed-form solutions provide a means for indicating the nature of the soil-structure interaction problem, and identify the important parameters and their effects in cases of simplified geometries and material properties. However, this class of analytical techniques seems limited to simplified structural geometries, and to soil properties which are generally represented by a linear elastic, homogeneous, isotropic semi-infinite half-space. Since these simplifications are often far from actual siting conditions, it appears that closed-form solutions of the type discussed herein are appropriate only for preliminary interaction evaluations at an actual site.

4.3.2 USE OF DISCRETE ELEMENTS AT SOIL-STRUCTURE INTERFACE TO REPRESENT INTERACTION EFFECTS

A popular method of analyzing interaction effects in structures subjected to earthquake motions is through simple arrangements of springs and dashpots located at various points along the soil-structure interface; a model of this type is shown in Figure 5-3.

The springs and dashpots simulate the stiffness and energy-loss characteristics of the soil in the vicinity of the structure. In additon, the inertia of the soil is often simulated by an effective soil mass that is considered to be constant with time and is superimposed onto the structure mass (References 5-16 and 5-17).

Three typical discrete element models have been considered in this subsection and are indicated in Table 5-2. The first of these models is the simple normal force interaction mechanism described in Reference 5-18. This interaction mechanism imparts a force to the structure, F, which is given by the following expression:

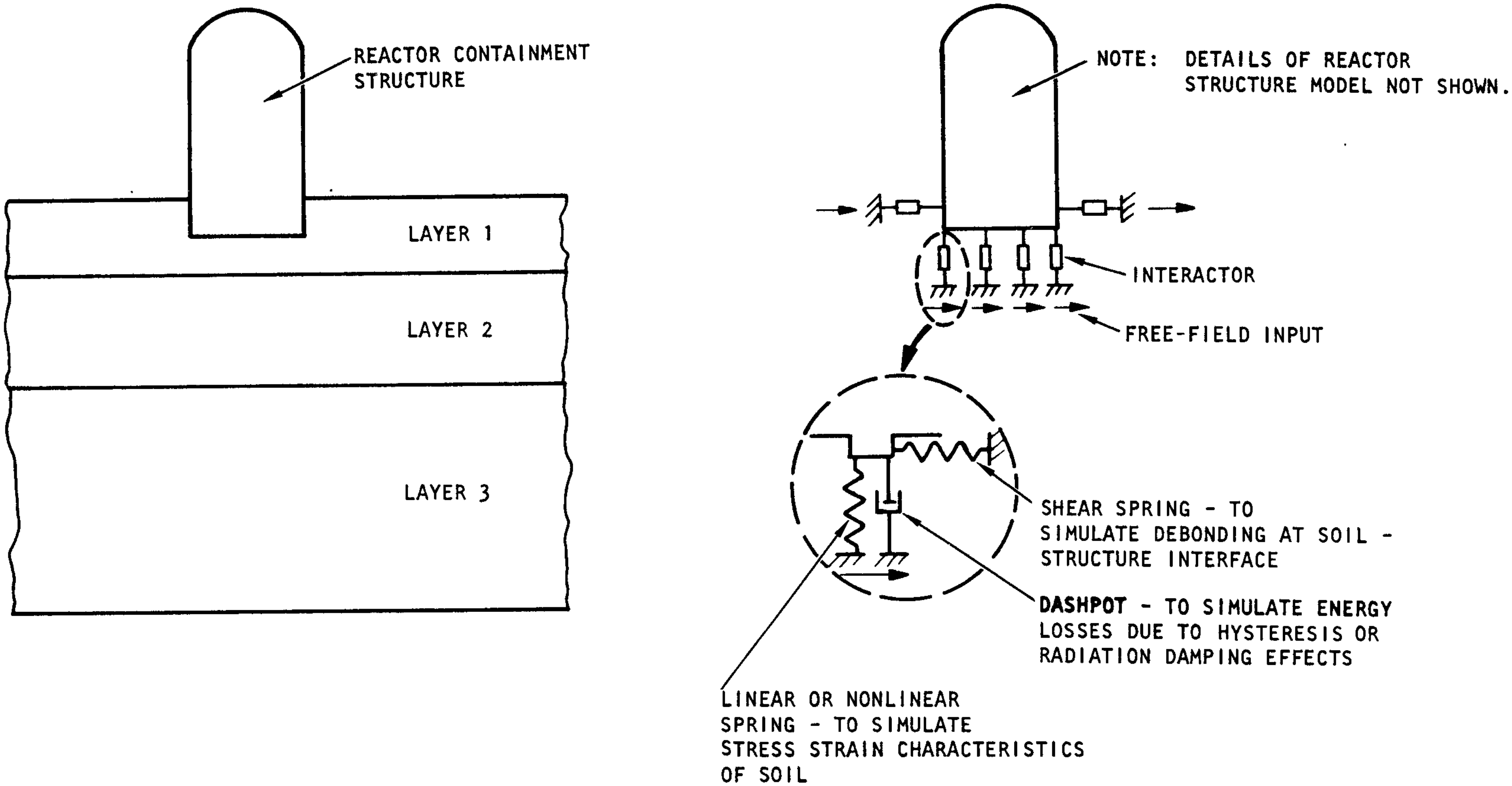

(a) ACTUAL SITE

(b) SPRING-DASHPOT MODEL

AJA1075

FIGURE 5-3. SPRING-DASHPOT REPRESENTATION OF SOIL-STRUCTURE INTERACTION AT A NUCLEAR REACTOR SITE

TABLE 5-2. REPRESENTATIVE DISCRETE ELEMENT MODELS OF SOIL-STRUCTURE INTERACTION

Type	Mechanism	Description
Simple Normal Force Interaction Model (Reference 5-18)	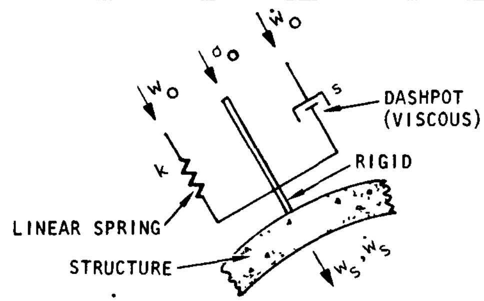 σ_o, w_o, $\dot{w}_o$ = Free-field stress, displacement, velocity w_s, $\dot{w}_s$ = Structure displacements, velocity	Medium represented by spring and dashpot at structure-soil interface. Spring and dashpot forces are superimposed onto free-field stress to give resultant interaction stress. Does not transmit shear waves.
Normal and Shear Interaction Mechanism (Reference 5-20)	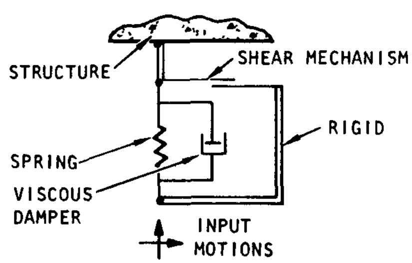	Medium represented by transverse nonlinear spring and viscous damper in parallel, and a shear mechanism that can simulate debonding at soil-structure interface.
Equivalent Lumped Model for Structure on Soil Layer of Limited Depth (Reference 5-1)	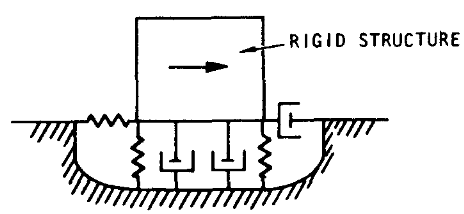	Examination of effect of depth of soil layer on selection of equivalent spring constants, masses, damping ratios. Closed form solutions for response of elastic stratum used as a guideline in selecting discrete element parameters.

AJA1320

$$F = \sigma_o + s(\dot{w}_o - \dot{w}_s) + k(w_o - w_s)$$

where σ_o, $\dot{w}_o$, and w_o are the free field stress, velocity, and displacement of the free field, and $\dot{w}_s$ and w_s are the velocity and displacement of the structure. It has been shown in Reference 5-19 that the term $\sigma_o + s(\dot{w}_o - \dot{w}_s)$ $- \dot{w}_s)$ has its origin in the study of the response of a structure encased has its origin in the study of the response of a structure encased in an acoustic medium and subjected to a transverse shock wave. The additional term $k(w_o - w_s)$ attempts to account for the influence of the solid ality factor s is considered to represent the effects of hysteretic and radiation damping in the soil profile, and k is a function of the compressive stress-strain characteristics of the site in the vicinity of the structure.

This model gives satisfactory correlation with experimental results for soft soils. However, as noted in Reference 5-19, the model cannot transmit shear waves and will, therefore, not provide satisfactory results when these motions are important.

A second, recently developed, interaction model consists of a tangential shear spring in addition to a transverse spring and viscous damping element (Reference 5-20). The normal spring element is nonlinear and can accommodate permanent deformations; the viscous dashpot element simulates radiation damping in the soil profile. The shear element is linear up to a stress level corresponding to the debonding stress at the soil-structure interface. This debonding stress is a function of the cohesion and angle of internal friction of the soil. The inertia of the soil is represented by an equivalent soil mass; the selection of this mass is based on experimental work by Funston and Hall (Reference 5-21).

Although this model is quite general in nature, the techniques used to select the various model parameters have not yet been finalized. This will be done eventually through comparisons with finite element calculations, as well as with experimental results.

A third discrete element technique that has been examined is an equivalent lumped model for a structure on a soil layer of limited depth (Reference 5-1). In this technique, Whitman has used a closed-form solution for the horizontal response of a rigid structure on an elastic stratum of limited depth and subjected to a periodic base motion. The fundamental frequency of the soil-structure system obtained from the closed-form solution guided the choice of the parameters for use in an equivalent discrete element system.

The results of this study are indicated in Figure 5-4 for various ratios of the soil stratum depth H to the structure radius r. These results are summarized as follows:

- $H/r > 4$ — The stratum acts as a half-space of infinite extent (Figure 5-4(a)).
- $4 > H/r > 0.5$ — The soil and structure are modeled as a two-degree-of-freedom system (Figure 5-4(b)).
- $H/r < 0.5$ — A simple single-degree-of-freedom model is suggested (Figure 5-4(c)).

As noted above, this work has considered only horizontal translation motions of the structure. The extension of this work to treat rocking effects should be of considerable value.

The discrete element approach has been widely used in the treatment of soil-structure interaction effects during an earthquake. The primary advantage of this approach lies in its relatively short computation time requirements and in its familiarity within the engineering community. Also, it is noted that the discrete element approach is readily applicable to three-dimensional analyses, as illustrated in Figure 5-5. However, there are a number of shortcomings of the discrete element approach, as pertains to its

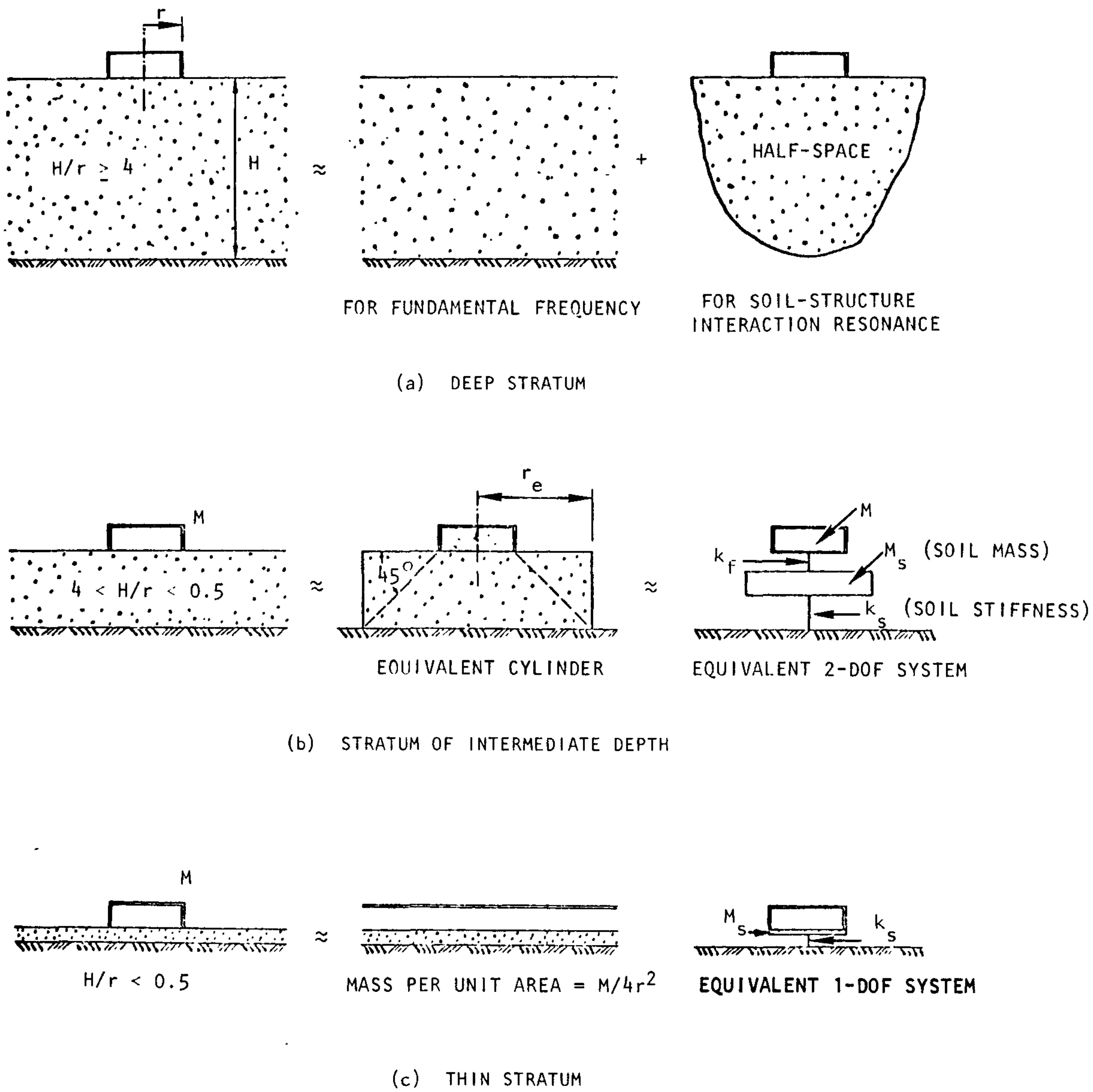

FIGURE 5-4. RESPONSE OF RIGID STRUCTURE ON ELASTIC STRATUM OF LIMITED DEPTH (REFERENCE 5-1)

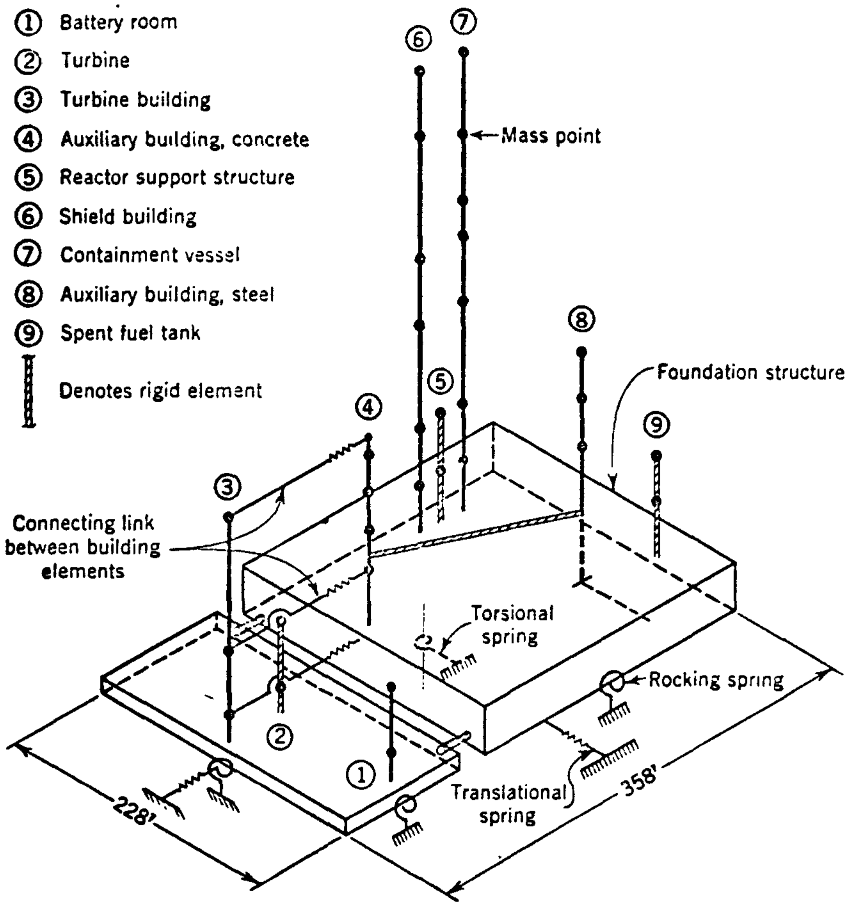

NOTE: TRANSLATIONAL, ROTATIONAL, AND TORSIONAL SOIL SPRINGS OBTAINED FROM GEOTECHNICAL SOIL PROPERTIES AND THROUGH COMPARISON WITH FINITE ELEMENT OR CLOSED FORM SOLUTIONS.

FIGURE 5-5. DISCRETE ELEMENT MODEL FOR THREE-DIMENSIONAL ANALYSIS OF SOIL-STRUCTURE INTERACTION IN A NUCLEAR POWER PLANT (REFERENCE 5-22) capabilities in representing the physical characteristics of the soil-structure system:

a. The effective mass of the soil acting with the structure during the earthquake is usually assumed to be constant with time, whereas it is actually a time-dependent parameter.

b. The procedure for selecting ground motion input in a manner consistent with the definition of the discrete element parameters is not yet established. For example, the soil spring constant is generally based on an average stiffness of the entire profile extending to the subsurface bedrock level, whereas the earthquake motions at the ground surface are usually used as input to the analysis.

c. A consistent approach for the selection of spring constants, damping coefficients, and an effective soil mass for a layered site is not known.

In view of these limitations, the finite element and finite difference techniques provide a more realistic representation of the distributed soil and structure properties than does the discrete element approach (Subsections 5.3.3 and 5.3.4). However, the discrete element approach appears useful in preliminary analyses, in parametric studies, and in evaluating three-dimensional soil-structure interaction effects (since three-dimensional finite difference and finite element approaches have not yet been developed to the point where they represent usable techniques for the evaluation of soil-structure interaction effects in nuclear power plants).

5.3.3 FINITE DIFFERENCE METHODS

The solution of complex problems of wave propagation in a continuum by the classical theories of elasticity and plasticity almost invariably involves considerable analytical difficulties. These problems can sometimes be resolved by expressing the partial differential equations of motion of the continuum as a set of equivalent finite difference equations. The solution to this set of equations then can be obtained using numerical procedures.

Classical finite difference procedures have been applied to a variety of problems involving wave propagation in a continuum. These involve approaches ranging from equivalent discrete element models (References 5-23 to 5-28) to highly complex techniques of wide applicability, (References 5-29 to 5-33). Some representative finite difference techniques are described in Table 5-3.

A. H.-S. Ang has proposed the two-dimensional discrete element representation of an elastic or elastic-plastic continuum shown in Figure 5-6(a) (References 5-23 to 5-26). This model is mathematically equivalent to a finite difference representation of the differential equations of motion for the corresponding continuum and has also been applied to elastic-plastic wave propagation problems. As noted in Figure 5-6(a), the Ang model consists of mass points and stress points arranged along a uniformly spaced grid network of finite size which is oriented at 45 degrees relative to the boundaries. A set of axial springs, shear springs, and moment (rotational) springs interconnect adjacent mass points, and equations of motion are developed for the displacement of the mass points along each of the inclined axes. The stresses are computed at designated stress points in the model. A "quiet" boundary capability, in the form of damping elements along the side and bottom boundaries of the continuum model, has been added to reduce the intensity of waves reflected from these artificial boundaries and thereby more realistically simulate the half-space solution. Although the Ang model was originally developed to study wave propagation in an elastic or elastoplastic continuum, it has been used in Reference 5-27 by M. E. Agabien, et al., as the basis for the study of interaction between a rigid-plate structure and a soil continuum during an earthquake (Figure 5-6(b)).

TABLE 5-3. REPRESENTATIVE FINITE DIFFERENCE ANALYSIS TECHNIQUES

Type	Representative Techniques	
	Approach	Description
Plane Strain Analysis of Linear Elastic or Elastic-Plastic Media	Ang, et al., (References 5-23 to 5-26) Agabien, et al., (Reference 5-27) Parmelee (Reference 5-28)	Original version (by Ang) designed for analysis of free-field response to a nuclear weapon. Extension by Agabien, et al., is capable of treating interaction between soil continuum and rigid plate structure. Viscous dashpot quiet boundary adaptation has been developed. Among the simplest to understand.
Plane Strain or Axisymmetric Analysis of Hydrodynamic Elastic-Plastic Media	Wilkins (Reference 5-29) Godfrey, et al., (Reference 5-30) Bjork and Kreyenhagen (Reference 5-31)	Codes included here (HEMP, PIPE, & SHEP Codes) originally developed to treat problems of hypervelocity impact and the propogation of shock waves from nuclear or chemical explosions. Basic capability appropriate for analysis of earthquake soil structure interaction problems. Several materials may be considered, and laminated media, inclusions bounded by coordinate surfaces are easily treated.
Two-Dimensional (Planar or Axisymmetric) Continuum System with Nearly Arbitrary Material Properties	Trulio (References 5-32 and 5-33)	Designed to treat nuclear explosion problems. The calculation proceeds in a continuous flow without rezoning, since grid points may be moved in an arbitrary, non-Lagrangian manner. Several materials may be included; regions defined by other than coordinate surfaces may be treated. Quiet boundary adaptation for elastic waves has been developed in axisymmetric version. Flexibility of code, complexity of derivation makes this among most difficult codes to understand and use.

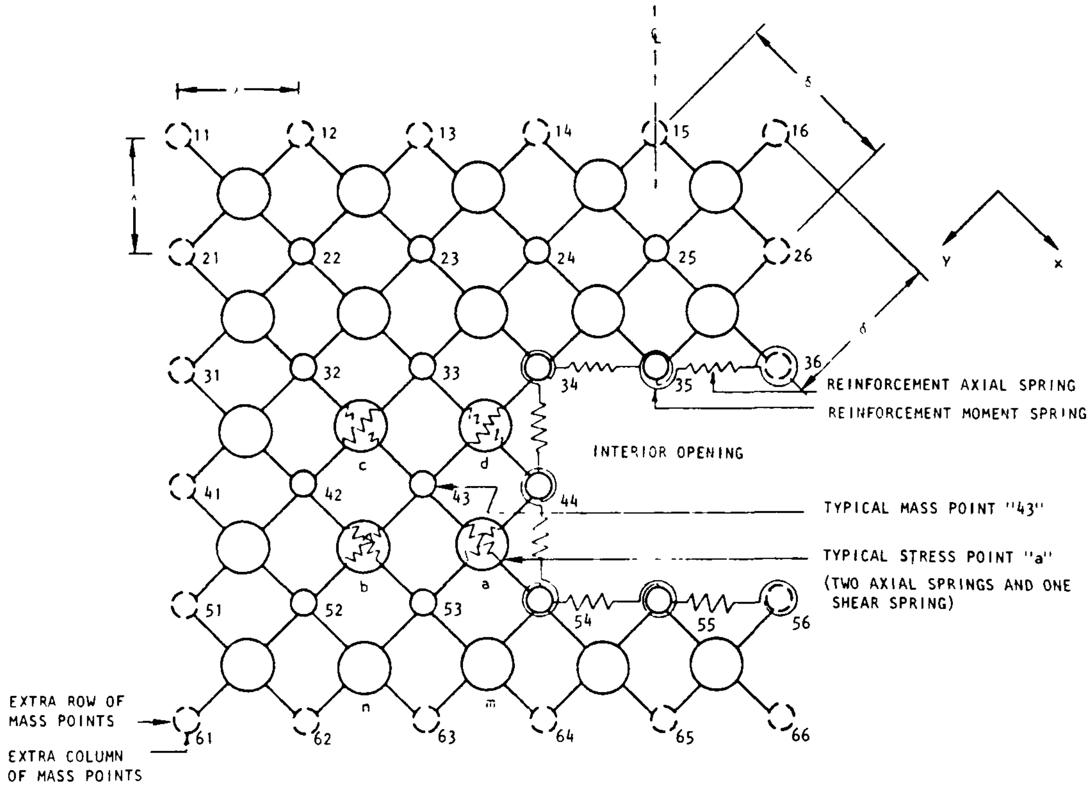

(a) THE DISCRETE MODEL (REFERENCE 5-23)

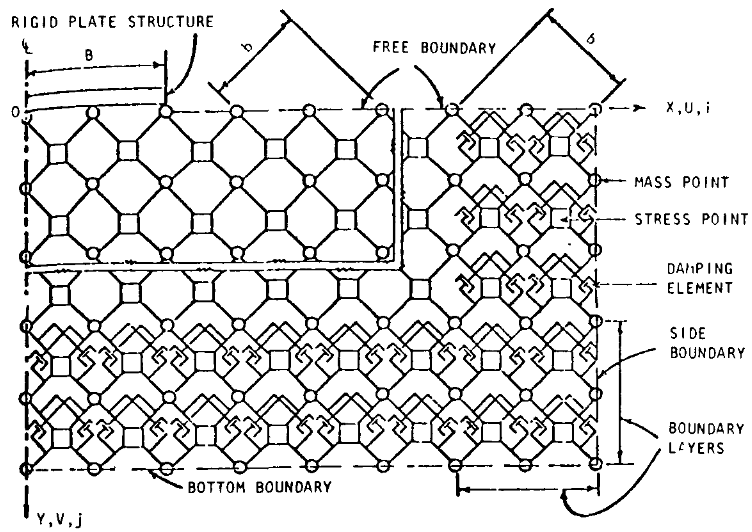

(b) LUMPED PARAMETER MODEL FOR VIBRATORY MOTION OF A BODY ON AN ELASTIC HALF PLANE (REFERENCE 5-27)

FIGURE 5-6. APPLICATION OF ANG MODEL TO SOLUTION OF WAVE PROPAGATION PROBLEMS

A number of more general finite difference codes have been applied to a wide variety of elastic and inelastic wave propagation problems, and could conceivably be used to investigate soil-structure interaction effects resulting from an earthquake (Table 5-3). An example of an analysis technique of this type is the AFTON Code, in which the soil structure could be simulated as a two-dimensional planar or axisymmetric continuum system with nearly arbitrary material properties (References 5-32 and 5-33). Several different materials can be included, and either welded or slip contact at the interfaces can be specified. "Quiet" boundaries have been developed for the axisymmetric case. The AFTON Code has been used to examine the transient response of non-uniform axisymmetric structures embedded in layered soils when subjected to uniform time-dependent pressure pulses, (Reference 5-34), and to study the response of a multilayered planar soil system to moving, time-dependent surface loads (Reference 5-35). However, due to the generality and resulting complexity of this code, it will require significant engineering and computer time for a typical analysis.

A number of other finite difference techniques are available that, although less complex than the AFTON Code, are sufficiently general to handle most soil-structure interaction problems that might arise. For example, the HEMP, PIPE, and SHEP Codes have been developed to treat the plane-strain or axisymmetric response of a hydrodynamic, elastic-plastic continuum (Table 5-3). The SHEP Code has been used to examine the interaction between complex structures typical of space vehicles under shock loading (Reference 5-31).

Three-dimensional, finite difference codes have been developed (see, for example, Reference 5-36) but, because of machine core storage limitations, the available capability is not particularly helpful. The STRIDE Code (Reference 5-36) can treat 8000 cells, approximately 20 in each direction. This limitation prevents a detailed description of structures and limits the domain free from boundary reflected signals. The useful finite difference capability is truly indicated by the representative two-dimensional codes described briefly in Table 5-3.

The application of finite difference analyses to the study of soil-structure interaction effects in an earthquake has not generally been as widespread as the discrete element, finite element, or closed-form-solution approaches. However, finite difference analysis techniques, ranging from the relatively simple Ang model to the highly complex AFTON Code, appear to have merit for this application, since, for two-dimensional analyses, they are capable of representing the mass distribution, stiffness, and energy dissipation characteristics of the soil and structure in a relatively realistic manner. The extension of these approaches to include three-dimensional effects should be studied as computers with larger core storage capabilities become available.

5.3.4 FINITE ELEMENT TECHNIQUES

A powerful tool appropriate for use in the analysis of soil-structure interaction effects is the finite element method. The major advantage of this method lies in the fact that continua of arbitrary shapes and variations of properties can be approximated as a system of finite elements having simple shapes and simply varying properties. A set of interpolation functions appropriate to the chosen finite element shapes will represent the displacements in completely arbitrary soil-structure systems. To retain favorable bounding and convergence properties, it is necessary that the interpolation functions include rigid body displacements and uniform strain states, and that they maintain displacement compatibility along inter-element and exterior boundaries (Reference 5-37). An example finite element representation of a soil-reactor structure system is shown in Figure 5-7.

A number of representative finite element techniques, suitable for use in analyzing interaction effects between the soil and a nuclear reactor structure, are described briefly in Table 5-4. The available techniques range from a two-dimensional, elastic, plane-strain model to a pseudo-three-dimensional representation of a continua having nonlinear material properties. As noted in Subsection 5.3.2, three-dimensional, dynamic,

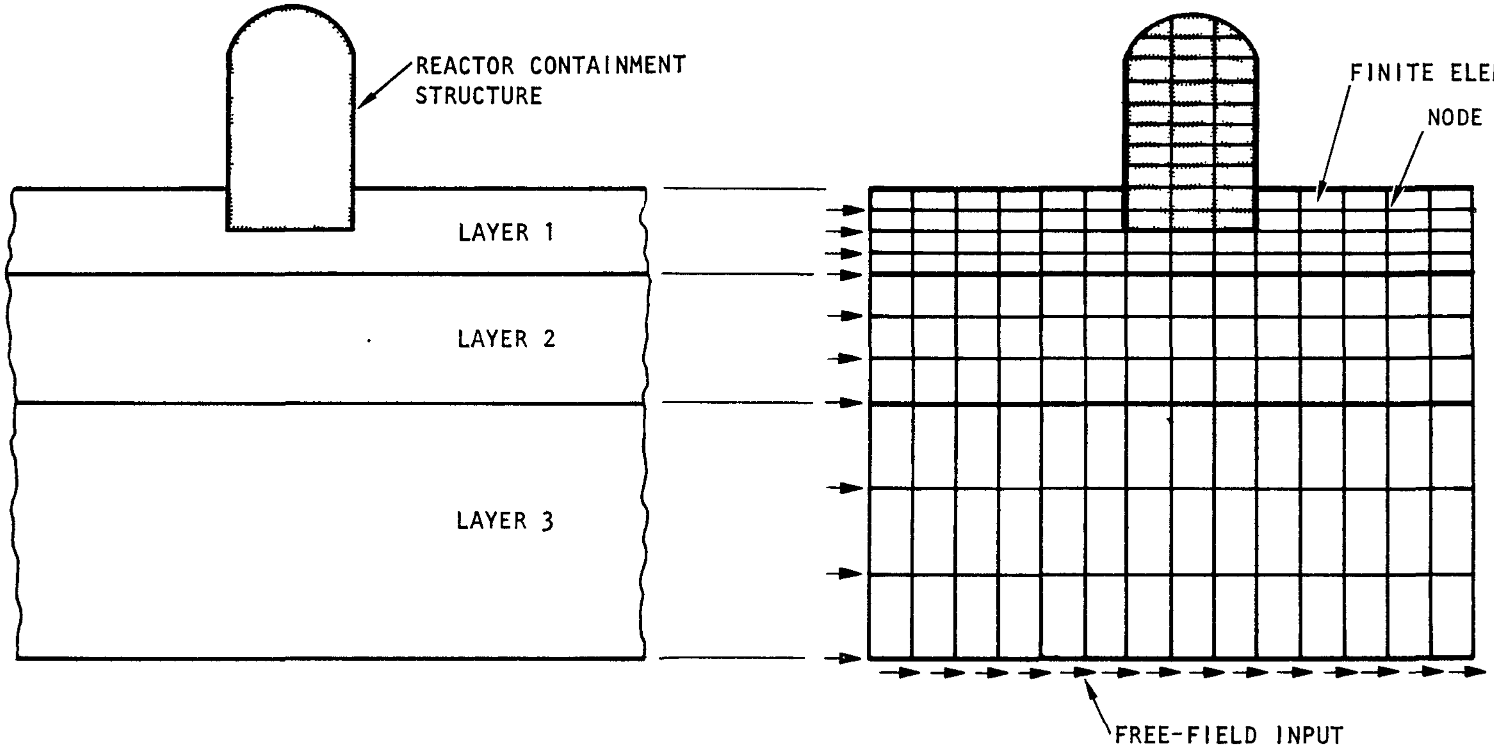

(a) ACTUAL SITE

(b) FINITE ELEMENT MODEL

AJA1074

FIGURE 5-7. FINITE ELEMENT REPRESENTATION FOR THE STUDY OF SOIL-STRUCTURE INTERACTION FOR A NUCLEAR REACTOR

TABLE 5-4. REPRESENTATIVE FINITE ELEMENT ANALYSIS TECHNIQUES

Type	Representative Techniques	
	Approach	Description
Two-Dimensional, Elastic, Plane Strain	WILSON Code (Reference 5-38)	Originally developed for analysis of underground structures Accepts only force excitations, no quiet boundary Relatively poor damping model, uses average Raleigh damping for entire system rather than individual damping properties for each material
	DEPS Code (Reference 5-39)	Original WILSON Code modified to include (1) kinematic, as well as force inputs, (2) increased capacity of program, and (3) approximate one-dimensional "quiet boundary" technique Same damping model as for original WILSON Code
Asixymmetric-Elastic	Ghosh and Wilson (Reference 5-40)	Original WILSON Code modified to treat axisymmetric elastic structures subjected to antisymmetric dynamic loading Damping model same as for WILSON Code, no quiet boundary Used for pseudo-three-dimensional analyses of nuclear power plants
Two-Dimensional Planar Response with Nonlinear Material Properties	Dibaj and Penzien (Reference 5-41)	Finite element formulation of nonlinear dynamic response of general earth dam structures to earthquake excitation Extension of Drucker-Prager yield criterion to include work hardening effects was developed Earthquake excitation giver in form of either uniform or nonuniform base motions
	INDEPS Code (Reference 5-42)	Inelastic, dynamic, plane strain analysis suited to analysis of soil-structure interaction under earthquake loading Material properties represented in form of bulk and shear moduli which may vary with stress, strain, stress and strain history, or strain rate General yield criterion developed, which may correspond to any differentiable function of stress components Prandtl-Reuss or plastic potential type flow rule given Force or velocity type excitations
Pseudo-Three-Dimensional Response with Nonlinear Material Properties	FEAT Code (Reference 5-43)	Attempts consideration of several real-life aspects of interaction problem, namely (1) three-dimensionality of soil-structure system, (2) nonideal material behavior, such as compaction, cracking, elastic-plastic behavior, (3) specification of more realistic interface conditions, such as debonding and controlled slip Geared toward blast analysis of buried or partially buried cylindr cal structures

finite element codes have not yet been developed to the extent that they represent usable techniques for the analysis of soil-structure interaction in nuclear power plants.

A significant first effort in the finite element analysis of a soil-structure system is the two-dimensional finite element code written by Wilson (Reference 5-38). From Table 5-4, it is seen that the original code is somewhat limited in its ability to analyze soil-structure interaction effects under earthquake loading; however, this code has been subsequently used as the basis for other more general analyses. For example, in Reference 5-39, the original WILSON Code has been modified to include kinemetic input and an approximate "quiet" (energy-absorbing) boundary capability. Also, an axisymmetric version of the original WILSON Code has been used in the analysis of nuclear power plants under earthquake loading (Reference 5-40).

Since typical soils are far from being ideal elastic materials, efforts have been directed toward the development of a finite element analysis including nonlinear material properties. These analyses commonly employ a yield criterion (such as prepared by von Mises or Coulomb, for example) and a plastic flow rule to update the system stiffness matrix on an incremental step-by-step basis. This is done to account for yielding in various regions of the soil-structure system. The calculation times for the nonlinear finite element codes are generally much greater than for the linear viscoelastic finite element analyses.

Two examples of finite element analyses that incorporate nonlinear material properties are described in Table 5-4. The work of Dibaj and Penzien (Reference 5-4) is oriented toward the seismic response of earth dam structures and uses a Drucker-Prager yield criterion that has been extended to include work hardening. Another recently completed code suited to the analysis of soil-structure interaction under earthquake loading is the INDEPS Code (Reference 5-42). This analysis uses a general yield criterion which may be any differentiable function of the stress.

An analysis technique that considers pseudo-three-dimensional effects in an approximate manner, nonideal material behavior, and debonding, is termed the FEAT Code (Reference 5-43). However, only a small number of checkout problems have been completed at this time; therefore, the applicability of this code to the problem of soil-structure interaction under earthquake excitation has not yet been evaluated.

The use of finite element techniques to predict soil-structure interaction effects has increased significantly in recent years. This has resulted in the development of increased capabilities and experience in this field. Like the finite difference method, the finite element approach can provide a relatively realistic model of the soil-structure system. Therefore, it should be considered as a feasible method for evaluating interaction effects in a nuclear reactor structure. Its principal drawback is its limited capability to treat problems which are essentially three-dimensional in character. This problem is presently being investigated, however, and significant progress should soon be made in this direction.

5.4 SUMMARY

The application to interaction problems of closed-form solutions, discrete element models, finite difference techniques, and finite element methods has been discussed in this section. From each of these general approaches, representative techniques have been described to illustrate their capability in predicting soil-structure interaction effects in the response of a nuclear reactor structure to earthquake motions.

Some advantages and disadvantages of each approach are summarized in Table 5-5. From this summary, it appears that finite difference and finite element techniques, despite the increased computer time and technical effort required for their use, provide the most realistic model for use in the two-dimensional analysis of earthquake-induced interaction effects. The principal drawback in the use of these approaches is their present inability to treat problems that are three-dimensional in nature. Closed-form solutions and discrete element models, because of their simplicity, appear feasible for use in the preliminary analysis and design stages for parametric studies, and for estimating three-dimensional effects in a soil-structure system.

AJA

TABLE 5-5. SUMMARY OF ASSESSMENT OF SOIL-STRUCTURE INTERACTION TECHNIQUES

Approach	Advantages	Disadvantages
Closed Form Solution	Valuable for indicating trends regarding the effects of various parameters on soil-structure interaction under earthquake loading. Some three-dimensional problems have been solved.	Solutions limited to simplified representations of structure geometry, soil material properties, and loading conditions.
Discrete Element Representations of Interaction Effects at Soil-Structure Interface	Simple, inexpensive, calculation for estimate of soil-structure interaction effects. Widely used procedure in earthquake response calculations. Mathematically exact for some simple structure geometrics and soil properties, if moduli or equivalent soil mass are frequency dependent.	Inertia of soil in layered sites not properly represented. The procedure for selecting input for response calculations is not clearly defined. Also, representation of layered sites not clearly known. Guidelines for selecting nonlinear spring-dashpot parameters not yet established.
Finite Difference Techniques	Attractive approach for studying soil-structure interaction. Can accommodate complicated boundaries, partial loading, nonlinear material properties, and layered sites. Satisfactory model of soil mass and stiffness is provided. Quiet boundary adaptations currently being developed.	Displacements, stresses defined by interpolation except at finite number of points. Increased computer run time and associated technical effort required for analysis. Many refined finite difference codes, although widely used in nuclear weapons effects problems, have never been applied to earthquake problems. At present, practical use in dynamic problems is limited to two-dimensional idealizations.
Finite Element Techniques	Same advantages as indicated above for finite difference technique. Generally, wider application to earthquake response calculations than many finite difference techniques.	Unless quiet boundary techniques are available, radiation damping not accounted for. Except for some nonlinear codes, internal damping simulated by approximate viscous damping mechanism. Increased computer run time and associated technical effort required for analysis. Relatively few studies of convergence of solution. At present, practical use in dynamic problems is limited to two-dimensional idealizations.

AJA1421

REFERENCES

5-1. Whitman, R. V., "Equivalent Lumped System for Structure Founded upon Stratum of Soil," *Fourth World Conference on Earthquake Engineering*, Santiago, Chile, January 1969.

5-2. Richart, F. E., and R. V. Whitman, "Comparison of Footing Vibration Tests with Theory," *Journal of the Soil Mechanics Division,* ASCE, Vol. 93, No. SM6, November 1967.

5-3. Jennings, P. C., and J. H. Kuroiwa, "Vibration and Soil Structure Interaction Tests of a Nine Story Reinforced Concrete Building," *Bulletin of the Seismological Society of America*, Vol. 58, No. 3, June 1968.

5-4. Reissner, E., "Stationäre, axialsymmetrische, durch eine schütteinde Masse erreqte Schwingungen eines homogenen elastichen Halbraumes," *Ingenieur-Archiv*, Vol. 7, 1936, pp. 381-396.

5-5. Sung, Tse Yung, "Vibrations in Semi-Infinite Solids Due to Periodic Surface Loading," *Special Technical Publication No. 156*, ASTM, Symposium on Dynamic Testing of Soils, 1953, pp. 35-68.

5-6. Toriumi, I., *Vibrations in Foundations of Machines*, Technology Reports of Osaka Univ., No. 146, Vol. 5, 1955, pp. 103-126.

5-7. Bycroft, G. N., "Forced Vibrations of a Rigid Circular Plate on a Semi-Infinite Elastic Space and on an Elastic Stratum," *Philosophical Transactions*, Royal Society of London, Vol. 248, A 948, January 1956.

5-8. Kobori, T., "Dynamic Response of Rectangular Foundations on an Elastic-Space," *Proceedings of Japan National Symposium on Earthquake Engineering*, Tokyo, Japan, 1962, pp. 81-86.

5-9. Parmelee, R. A., "Building-Foundation Interaction Effects," *Journal of the Engineering Mechanics Division*, ASCE, Vol. 93, No. EM2, April 1967.

5-10. Korenev, B. G., et al., "Oscillations of Tower-Like Structures with Account of Inertia and Elasticity of Solid Medium," *Fourth World Conference on Earthquake Engineering*, Santiago, Chile, January 1969.

5-11. Chopra, A. K., and P. R. Perumalswami, "Dam-Foundation Interaction During Earthquakes," *Fourth World Conference on Earthquake Engineering*, Santiago, Chile, January 1969.

5-12. Scavuzzo, R. J., et al., *Lateral Structure-Foundation Interaction of Nuclear Power Plants During Earthquake Loading*, USAEC Contract No. AT-(40-1)-382, Technical Report No. 1, The Research Foundation, University of Toledo, August 1969.

REFERENCES (CONTINUED)

5-13. Tajimi, H., "Dynamic Analysis of a Structure Embedded in an Elastic Stratum," *Fourth World Conference on Earthquake Engineering,* Santiago, Chile, January 1969.

5-14. Whitman, R. V., *Summary Reports, Fourth World Conference on Earthquake Engineering-Soil Mechanics and Soil-Structure Interaction*, Report No. NSF-UCEER, Conference on Earthquake Engineering Research University of California, Berkeley, California, March 1969, pp. 19-26.

5-15. Hsieh, T. K., "Foundation Vibrations," *Proceedings of the Institution of Civil Engineers*, Volume 22, 1962.

5-16. Barkan, D. D., *Dynamics of Bases and Foundations*, McGraw-Hill Book Co., Inc., New York, 1962.

5-17. Lycan, D. L., and N. M. Newmark, "Effect of Structure and Foundation Interaction," *Journal of the Engineering Mechanics Division*, ASCE, Vol. 87, No. EM5, Proc. Paper 2960, 1961, pp. 1-31.

5-18. Costantino, C. J., et al., "A Simplified Soil-Structure Interaction Model to Investigate the Response of Buried Silos and Cylinders," *Proceedings of the Symposium on Soil-Structure Interaction*, University of Arizona, Tuscon, Arizona, September 1964.

5-19. Applied Theory, Inc., and Agbabian-Jacobsen Associates, *Review and Assessment of Medium-Structure Interaction Analysis Techniques for Study of Free-Field Ground Motion for Beneficial Facility Siting*, ATI-AJA R-6819-101, prepared for AFSWC, September 1968.

5-20. Agbabian-Jacobsen Associates, *Dynamic Analyses of Sentinel Structures*, Technical Progress Report No. 1, Los Angeles, California, January 1969.

5-21. Funston, N. E., and W. J. Hall, "Footing Vibration with Nonlinear Support," *Journal of the Soil Mechanics and Foundation Division*, ASCE, Vol. 93, No. SM5, September 1967, pp. 191-211.

5-22. Sharpe, R. L. "Earthquake Engineering for Nuclear Reactors, *Civil Engineering ASCE*, Vol. 39, No. 3, March 1969.

5-23. Ang, A. H.-S, "Mathematically Consistent Discrete Models for Simulating Solid Continua," in *Computation of Underground Structural Response*, compiled by A. Ang and N. M. Newmark, Final Report to the Defense Atomic Support Agency, Contract No. DA-49-146-XZ-104, June 1963.

5-24. Ang, A. H.-S., and G. N. Harper, "Analysis of Contained Plastic Flow in Plane Solids," *Journal of Engineering Mechanics*, ASCE, October 1964.

REFERENCES (CONTINUED)

5-25. Ang, A. H.-S., "Numerical Approach for Wave Motions in Nonlinear Solid Media," *Conference on Matrix Methods in Structural Mechanics*, Proc. Volume, Wright-Patterson Air Force Base, Ohio, 26-28 October, 1965.

5-26. Sameh, A. H. M., and A. H.-S. Ang, *Numerical Analysis of Axisymmetric Wave Propagation in Elastic-Plastic Layered Media*, Civil Engineering Studies, Structural Research Series No. 335, University of Illinois, Urbana, Illinois, 1968.

5-27. Agabien, M. E., et al., "A Model for the Study of Soil-Structure Interaction," *8th Congress of International Association for Bridge and Structural Engineering*, New York, N. Y., September 1968.

5-28. Parmelee, R. A., "Earthquake Engineering Research at Northwestern University," *NSF-UCEER, Conference on Earthquake Engineering Research*, University of California, Berkeley, California, March 1969, pp. 96-105.

5-29. Wilkins, M. L., *Calculation of Elastic Plastic Flow*, Report UCRL-7322, Lawrence Radiation Laboratory, University of California, Berkeley California, April 1963.

5-30. Godfrey, C. S., et al., *Calculation of Underground and Surface Explosions*, Technical Report AFWL-TR-65-211, Air Force Weapon Laboratory, June 1966.

5-31. Bjork, R. L., and K. N. Kreyenhagen, *Free-Field Calculations in Rock Media (U)*, Shock Hydrodynamics Inc., Report No. SH6010F, February 1967, (CONFIDENTIAL).

5-32. Trulio, J. G., *Theory and Structure of the AFTON Code*, Technical Report AFWL-TR-66-19, Air Force Weapons Laboratory, June 1966.

5-33. Trulio, J. G., et al., *Numerical Ground Motions Studies Volume III, Ground Motion Studies and AFTON Code Development*, Technical Report AFWL-TR-67-27, Air Force Weapons Laboratory, February 1969.

5-34. Niles, W. J., and V. T. Honda, *Evaluation of Minuteman Hardness (U)*, Report No. ATI-R-69-15-1, Applied Theory Inc., October 1969 (to be released) (SECRET).

5-35. Cooper, H. F., and W. J. Niles, *Free-Field Calculations for HEST Test V, (U)*, Report No. AFWL-TR-68-47, December 1968, (SECRET).

5-36. Read, H. E., *Hardening Technology Studies, Volume II, STRIDE, A Three-Dimensional Code*, AFBSD-TR-67-191, August 1967.

REFERENCES (CONTINUED)

5-37. Clough, R. W., "Analysis of Structural Vibrations and Dynamic Response," paper given at Japan-U.S. *Seminar on Matrix Methods of Structural Analysis and Design*, Tokyo, Japan, August 1969.

5-38. Wilson E. L., *A Computer Program for the Dynamic Stress Analysis of Underground Structures*, Report No. 68-1, Report to Waterways Experiment Station, U.S. Army Corps of Engineers, Structural Engineering Laboratory, University of California, Berkeley, California, January 1968.

5-39. Agbabian-Jacobsen Associates, *Safeguard BMD System--A Briefing on the Dynamic Response Analysis of the MSR Power Plant*, briefing presented to the SAFSO Air Blast and Shock Vulnerability Working Group, June 1969.

5-40. Ghosh, S., and E. L. Wilson, *Dynamic Analysis of Axisymmetric Structures Under Arbitrary Loading*, Report No. EERC 69-10, University of California, Berkeley, California, September 1969.

5-41. Dibaj, M., and J. Penzien, *Nonlinear Seismic Response of Earth Structures*, Report No. EERC 69-2, Report to the State of California, Department of Water Resources, Earthquake Engineering Research Center, University of California, Berkeley, California, January 1969.

5-42. Isenberg, J., *Interaction Between Soil and Nuclear Reactor Foundation During Earthquakes*, Agbabian-Jacobsen Associates Report No. 6915-1200, prepared for the University of Toledo Research Foundation, Toledo, Ohio, June 1970.

5-43. The Boeing Company, *Structure-Medium Interaction and Design Procedures Study--Analysis Method*, First Technical Report, Vol. 1, Contract No. F04694-67-C-0084, July 1968.

APPENDIX A

FIRST-LEVEL APPROACH TO DEFINING SEISMIC INPUT

A.1 PURPOSE AND SCOPE

In this appendix, a first-level approach to the definition of seismic input at a nuclear reactor site is described. The purpose of this approach is as follows:

- To provide a simplified method for choosing representative seismic ground motions based on the dynamic characteristics of existing strong motion records.

- To provide a starting point and reference base for the more detailed approach described in Section 4.

In this first-level approach, some suggested criteria spectra are provided. These spectra are based on the dynamic characteristics of existing strong motion earthquake records and are intended to represent average (rather than envelope) strength levels for a region of either high, moderate, low, or minimal seismicity. Next, real and artificial earthquake records that are appropriate for use in conjunction with the criteria spectra as a representative ensemble of seismic input time histories are provided. In addition, suggested scaling procedures and scale factors are applied to the ensemble of earthquake records so that these accelerograms correspond to the seismic characteristics of the region in which the site is located. Finally, a discussion of the response statistics is provided so that the criteria spectra and the ensemble of time histories can be interpreted in a consistent manner for a given earthquake strength level.

A.2 BASIS OF CHOICE FOR CRITERIA SPECTRA

The basis for the formulation of the suggested first-level approach for choosing seismic input at a site will be described in this subsection. This basis has consisted of a review of past design practices, and a consideration of the characteristics of real and artificial earthquake records.

A.2.2 PAST DESIGN PRACTICE

A.2.2.1 Operating Basis and Design Basis Earthquakes

In the past, seismic design of nuclear reactors has been based on two strength levels for earthquakes at a site: (1) Operating Basis Earthquakes and (2) Design Basis Earthquakes.

The Design Basis Earthquake (DBE) defines the strength and duration of the most severe earthquake that might be conceived as occurring at the site at any time in the future. This earthquake defines the peak strength level for which a safe shutdown of the reactor must be achieved.

An Operating Basis Earthquake (OBE) defines the strength and duration of an earthquake which might realistically be experienced by a structure during its economic life. The OBE defines the maximum input strength level which the reactor is able to withstand and continue to operate at full efficiency. The structure is required to remain elastic when subjected to the OBE. The OBE is typically half as strong as the design basis earthquake.

A.2.2.2 Seismic Risk Maps

In the past, seismic risk maps have been widely used in the earthquake design of nuclear power plants and other structures. Therefore, it is pertinent at this time to discuss various seismic maps currently in existence.

In 1947, the United States Coast and Geodetic Survey (USCGS) prepared a Seismic Probability Map of the United States showing zones of seismic risk. These zones were described in terms of damage to structures with Zone 0 indicating no damage, and Zones 1 through 3 indicating minor damage, moderate damage, and major damage, respectively. Although withdrawn by the USCGS, this map was adopted by the Pacific Coast Building Officials Conference for inclusion in the 1952 edition of the Uniform Building Code.

The Seismic Probability Map, as shown in Figure A-1(a), has been the basis for the establishment of lateral force requirements for buildings and has not been changed since adopted in 1952. It has had wide circulation and is a familiar document to those structural engineers required to design structures located in highly seismic regions of the United States.

In 1969, Algermissen (Reference A-1) prepared the Seismic Risk Map shown in Figure A-1(b). This map is an interim revision of the 1947 USCGS Probability Map, and is not intended to represent the final form of a risk map for the United States. The 1969 map has been based on the following factors: (1) Distribution of Modified Mercalli intensities associated with the known seismic history of the United States, (2) strain release in the United States since 1900, and (3) the association of strain release patterns with large-scale geologic features believed to be related to recent seismic activity.

At this time, no seismic risk map has been sanctioned by the USCGS as being appropriate for use in defining the strength of earthquake motions in a region. Therefore, the first-level approach described in this appendix defines strength levels for regions of either high, moderate, low, or minimal seismicity; the classification of a region into one of these four categories should be based on a careful seismic and geologic investigation by qualified geologists and engineers.

A.2.2.3 Existing Design Approaches

In this subsection, two existing approaches for estimating earthquake input are described briefly and compared.

G. W. Housner (Reference A-2) suggested an approach based on dynamic characteristics of strong earthquake motion measurements on competent soil. Some averaged normalized spectra that reflect these dynamic characteristics (Reference A-3 and Subsection A.2.2.1) are scaled to correspond to earthquake strength levels estimated for the seismic zones

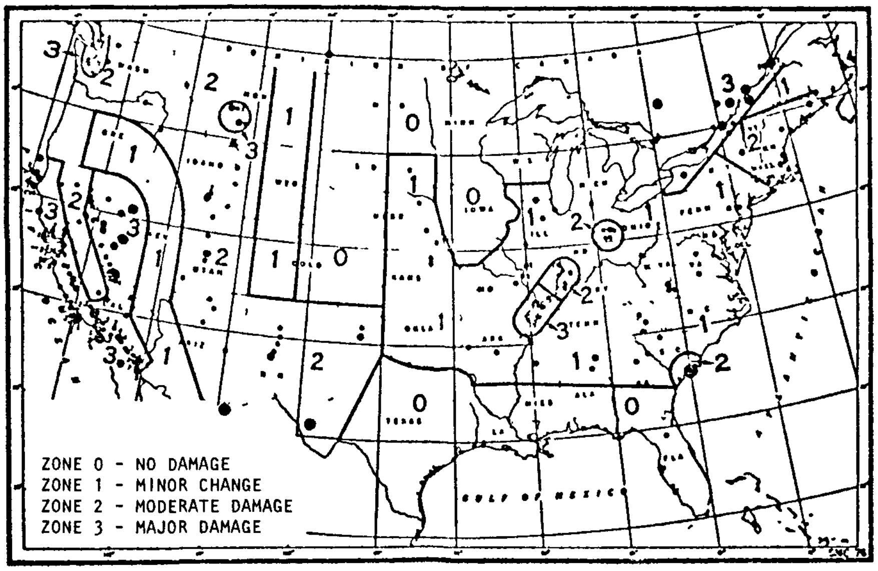

(a) SEISMIC MAP--1947 EDITION

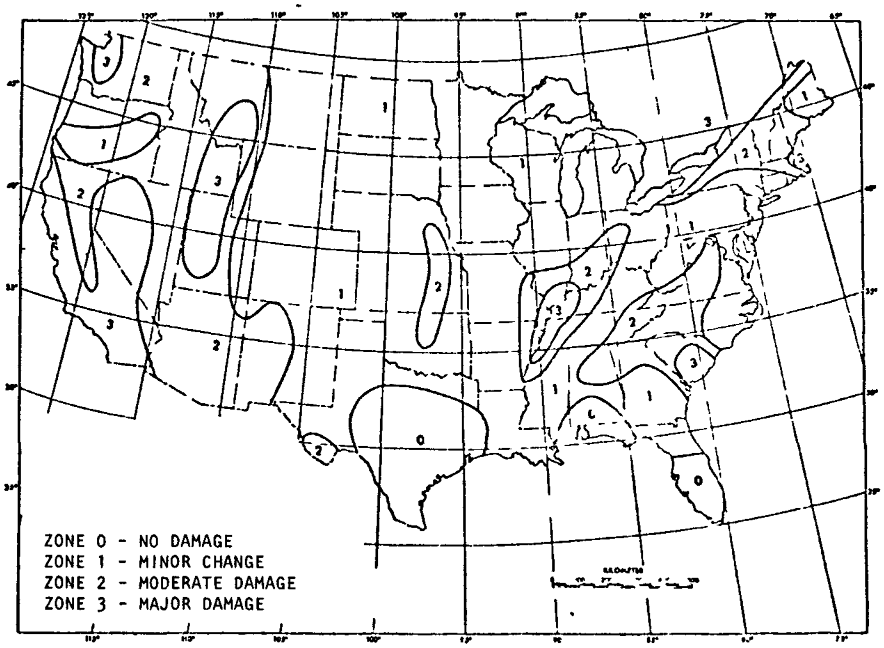

(b) SEISMIC MAP--1969 EDITION

AJA1873

FIGURE A-1. U.S. COAST AND GEODETIC SURVEY SEISMIC MAPS in the 1947 USCGS Seismic Risk Map. The strength ratios suggested by Housner are shown in Table A-1. It is noted that no Zone 0 criterion has been specified by Housner since factors other than earthquake considerations will govern the structure design in these regions of low seismicity.

TABLE A-1. STRENGTH LEVELS FOR EARTHQUAKE GROUND MOTIONS SUGGESTED IN REFERENCE A-2.

Seismic Zone	Strength of OBE / Strength of El Centro	Strength of DBE / Strength of El Centro
3	1.0	2.0 to 3.0
2	0.5	1.0 to 2.0
1	0.25	0.5 to 0.75

N. M. Newmark and W. J. Hall have suggested an approach to the problem of selecting seismic input at a site for which specific seismicity or soils information is unavailable (Reference A-4). This approach is based on some estimated ground motions for a "standard" earthquake in competent soil; as indicated in Table A-2, these standard earthquake motions are 50 percent more severe than the ground motions recorded during the 1940 El Centro earthquake. Newmark and Hall have also estimated the peak ground response that might occur in competent soil during a "very intense" earthquake and during a "minimum" earthquake. In addition, amplification factors that account for foundation conditions other than a competent soil are also provided.

The following general comparisons can be made between the approach suggested by Newmark-Hall and that selected by Housner:

a. Housner's approach uses spectra that are based on the *average* dynamic characteristics of strong earthquake motions on competent soil, and otherwise are independent of the soil properties at a site. The Newmark-Hall approach is based on the spectra *envelopes* from strong motion earthquakes, and

TABLE A-2. CRITERIA BASED ON STANDARD EARTHQUAKE (REFERENCE A-4)

(a) EARTHQUAKE STRENGTH LEVELS

Condition	Maximum Values of Ground Motion		
	Acceleration, g	Velocity, in./sec	Displacement,* in.
"Standard" Relative Values	0.5	24	18
Typical Maxima			
El Centro, 1940, Horizontal	0.33	16	12
El Centro, 1940, Vertical	0.22	11	8
**Minimum, Horizontal	0.10	5	4
**Minimum, Vertical	0.07	3	3
Very Intense Earthquake	0.75	36	27

*Transient motion not involving permanent fault displacement

**Minimum values recommended for use in the design of nuclear reactors in any region, even where earthquakes are not considered probable.

(b) SPECTRUM AMPLIFICATION FACTORS

Percent of Critical Damping	Amplification Factor		
	Displacement	Velocity	Acceleration
0	2.5	4.0	6.4
0.5	2.2	3.6	5.8
1	2.0	3.2	5.2
2	1.8	2.8	4.3
5	1.4	1.9	2.6
7	1.2	1.5	1.9
10	1.1	1.3	1.5
20	1.0	1.1	1.2

(c) FOUNDATION AMPLIFICATION FACTORS

Competent Rock	Soft Rock or Firm Sediment	Soft Sediment
0.67	1.0	1.5

has provided foundation amplification factors that should be used only in the absence of more detailed soils data.

b. The Housner approach is based on the use of a seismic risk map in selecting the strength of earthquake ground motions at a site. However, in the Newmark-Hall approach, the specification of strength levels for an earthquake at a site is left to engineering judgment, based on the seismicity and geology of the region.

To serve as a basis for further comparison, some 5 percent damped spectra from the Housner approach and from the Newmark-Hall approach for a soil profile containing firm sediment are shown in Figure A-2. The Newmark-Hall spectra have incorporated the spectrum amplification factors shown in Table A-2 and have been constructed according to the procedures described in Reference A-4. The comparisons indicate that the Newmark-Hall "very intense" earthquake has a more severe spectrum than does the Housner Zone 3 DBE. Also, the Newmark-Hall "standard" earthquake spectrum is more severe than that of the Housner Zone 3 DBE in the long-period end of the spectrum, and is less severe than the Housner Zone 3 DBE in the short-period region. In addition, the spectrum for the Newmark-Hall "minimum" earthquake is more severe than that of the Housner Zone 1 OBE. Finally, it is noted that the ratio of the peak spectral acceleration to the zero period spectral acceleration is greater in the Newmark-Hall spectra than in the Housner spectra.

A.2.3 CHARACTERISTICS OF REAL AND ARTIFICIAL EARTHQUAKE RECORDS

In this subsection, the dynamic characteristics of a number of real and artificial earthquake records are discussed. This discussion provides a basis for the choice of an ensemble of records suitable for this first-level approach for specifying seismic input to a nuclear reactor.

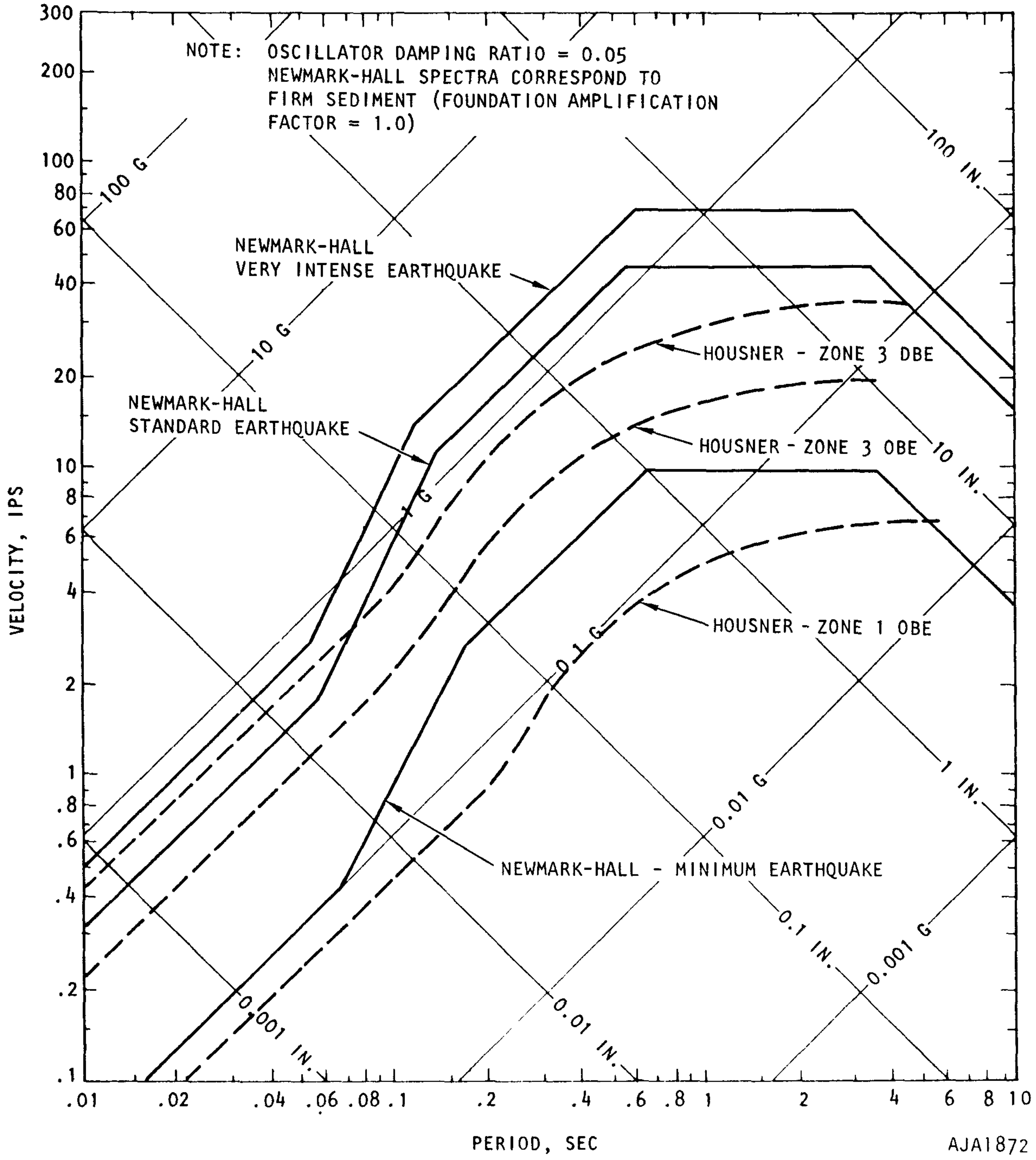

FIGURE A-2. COMPARISON OF SEISMIC INPUT SPECTRA FROM HOUSNER AND FROM NEWMARK-HALL APPROACHES

A.2.3.1 Real Strong Motion Earthquake Records

A number of measurements of strong earthquake motions have been obtained from some highly seismic regions in the western United States. Among the records most widely used for structural design purposes are the following strong motion earthquake accelerograms:

- 1940 El Centro
- 1934 El Centro
- 1952 Taft
- 1949 Olympia

Time histories of one component of the motion and the seismic characteristics for each of these records are indicated in Figure A-3 and Table A-3, respectively. It is noted that these records are from the four strongest ground motions yet recorded.

In Reference A-3, Housner has formulated a set of averaged, normalized spectra for the two components of each of the four strong motion earthquakes listed above. These average spectra, which have been smoothed, are shown in Figure A-4. Scale factors, by which the amplitudes of the normalized spectra can be multiplied so that their spectrum intensities are in agreement with those of the individual strong motion records, are also shown in Figure A-4.

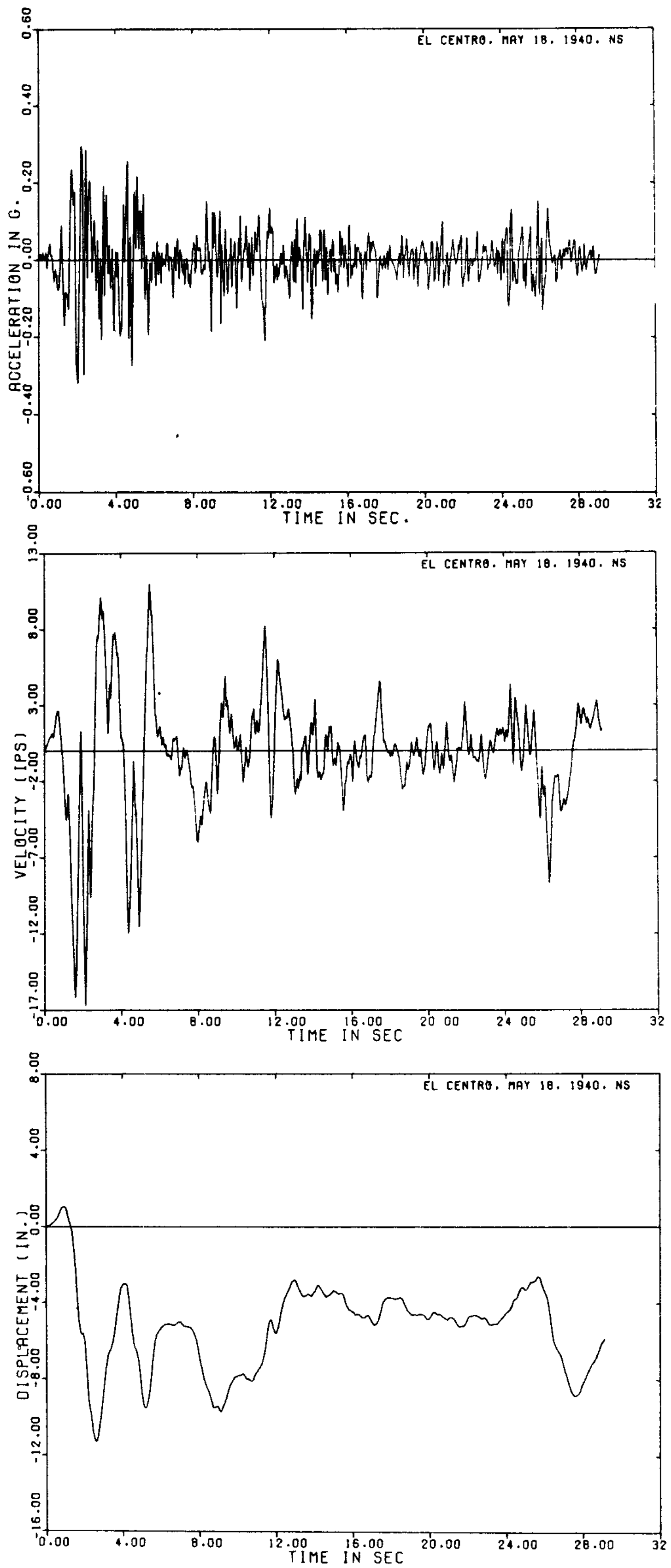

(a) 1940 EL CENTRO NS-COMPONENT

FIGURE A-3. STRONG MOTION EARTHQUAKE RECORDS

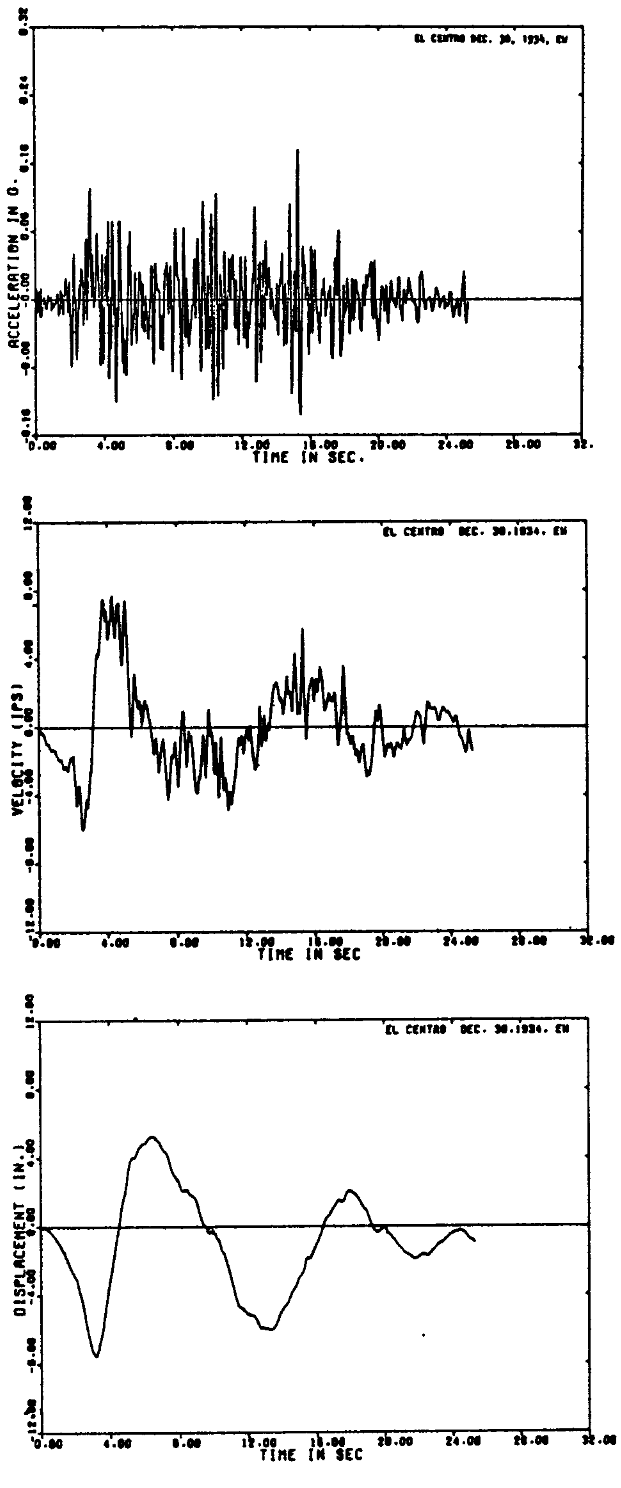

(b) 1934 EL CENTRO--EW COMPONENT

FIGURE A-3. (CONTINUED)

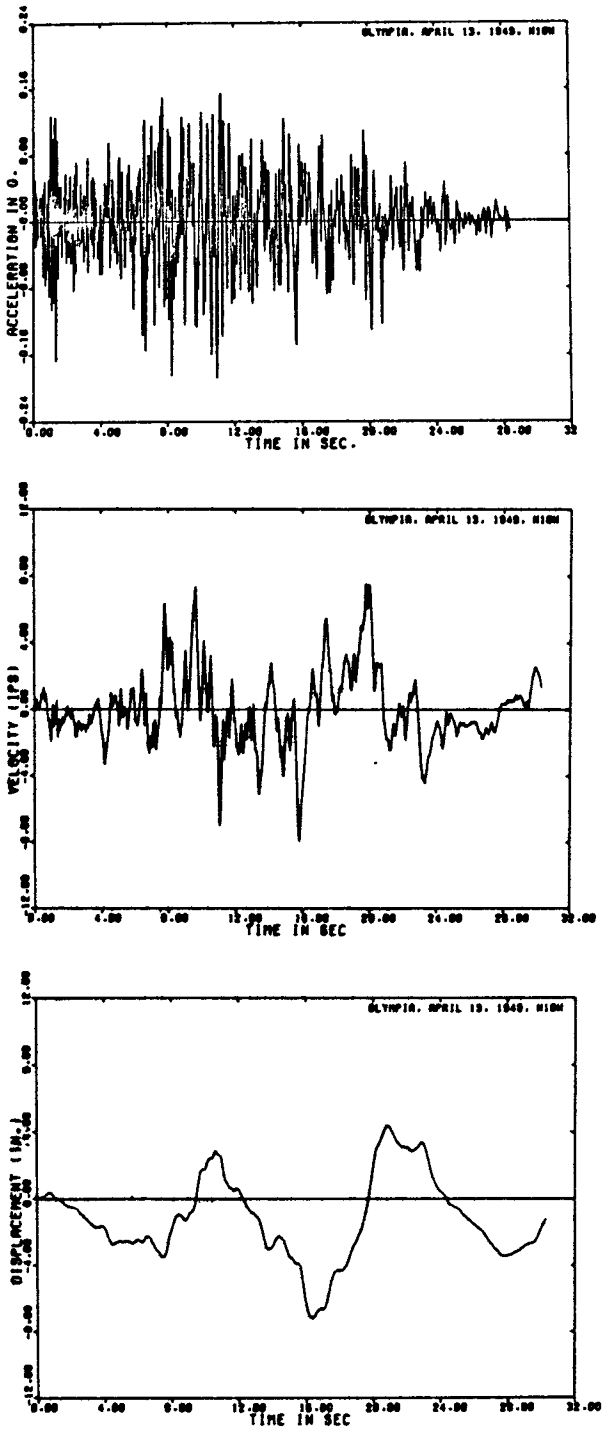

(c) OLYMPIA 1949 'U F ONENT

FIGURE A-3. (CONTINUED)

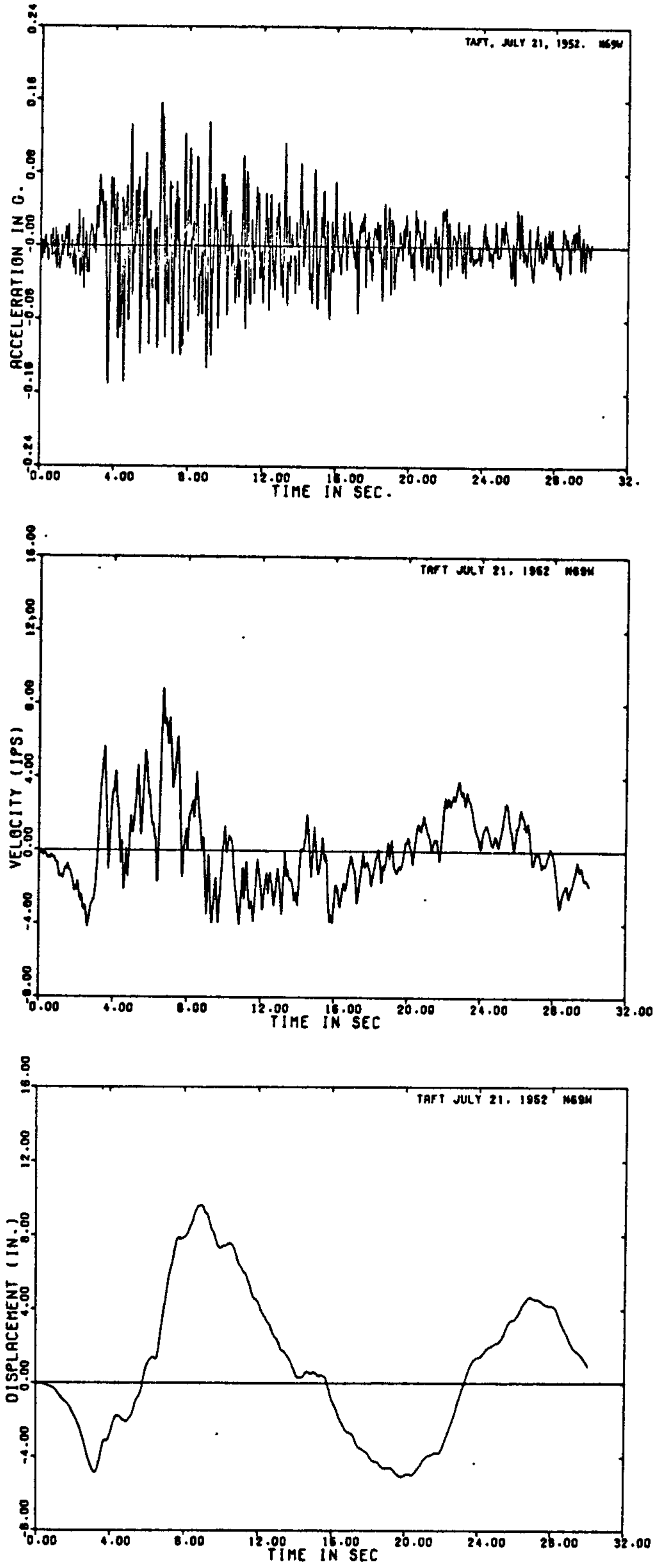

(d) TAFT 1952--S 69 E COMPONENT

FIGURE A-3. (CONTINUED)

TABLE A-3. SEISMIC CHARACTERISTICS OF STRONG MOTION EARTHQUAKES (Reference A-5)

Record	Richter Magnitude	Distance From Center of Slipped Length of Fault	Spectrum Intensity
1940 El Centro	7.0	10-15 miles	2.9
1949 Olympia	7.1	25 miles	2.3
1952 Taft	7.7	40 miles	2.0
1934 El Centro	6.5	35 miles	2.2

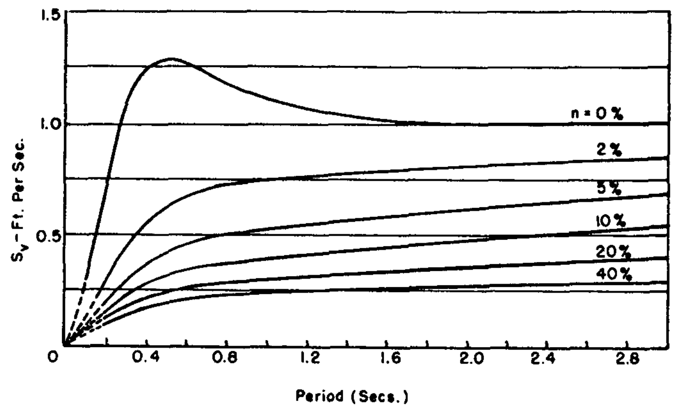

(a) AVERAGE VELOCITY SPECTRUM CURVES

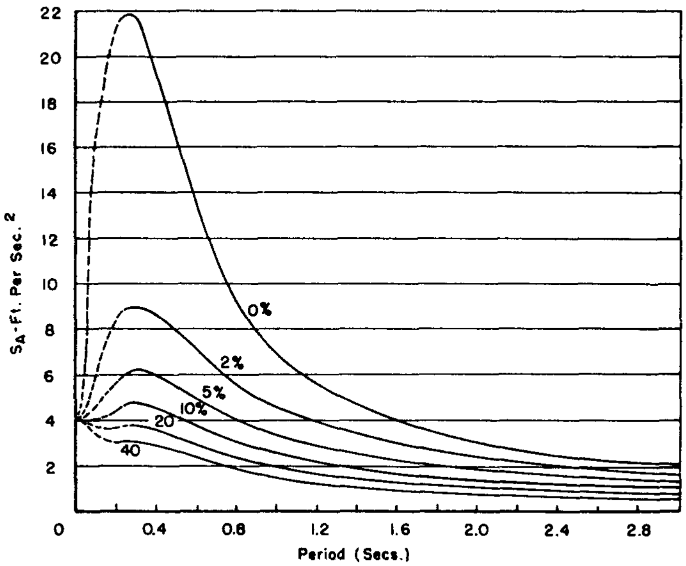

(b) AVERAGE ACCELERATION SPECTRUM CURVES

Scale Factors (related to spectrum intensity ratios)

1940 El Centro	2.7
1934 El Centro	1.9
1949 Olympia	1.9
1952 Taft	1.6

FIGURE A-4. STRONG MOTION EARTHQUAKE SPECTRA (REFERENCE A-3)

A.2.3.2 Artificial Earthquakes

In order to compensate for the scarcity of measured earthquake records, artificial earthquake records have been generated which have the basic dynamic characteristics observed in actual earthquake measurements. These artificial earthquakes are intended to furnish a larger sample of records of a given Richter magnitude; this increased sample size will, in turn, provide a basis for the consideration of the effect of statistical fluctuations in intensity, duration, and frequency content of earthquakes on the dynamic response of a structural system. Two sets of artificial earthquake records that have been formulated at Caltech will now be briefly described.

In Reference A-6, an ensemble of stationary artificial earthquakes have been simulated from sections of a stationary Gaussian process. In this approach, a series of white noise records were passed through a mathematical filter; the characteristics of this filter were such that the spectra of the resulting output records corresponded to the average strong motion earthquake response spectra obtained by Housner (Figure A-4). The velocity spectra for the ensemble of eight artificial earthquakes obtained in this way are shown in Figure A-5. It is noted that the resulting stationary artificial earthquake records are feasible for modeling strong motion earthquakes; however, these records are not appropriate for modeling less intense earthquakes which typically exhibit significant nonstationarities.

Reference A-7 describes the simulation of earthquake records showing nonstationarities. To do this, a special type of nonstationary random process has been utilized in which the artificial earthquake record $\ddot{z}(t)$ is given by:

$$\ddot{z}(t) = E(t)\ddot{x}(t)$$

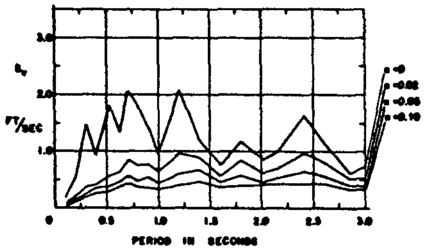

VELOCITY SPECTRA OF ARTIFICIAL EARTHQUAKE NO. 1

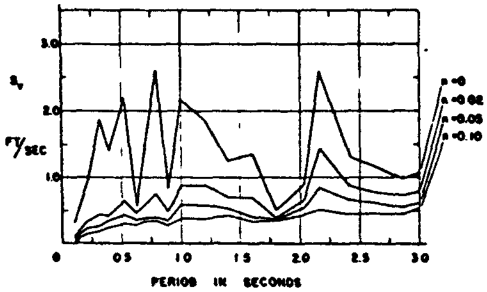

VELOCITY SPECTRA OF ARTIFICIAL EARTHQUAKE NO. 2

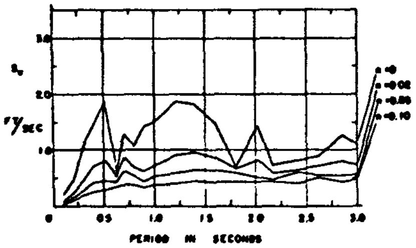

VELOCITY SPECTRA OF ARTIFICIAL EARTHQUAKE NO. 3

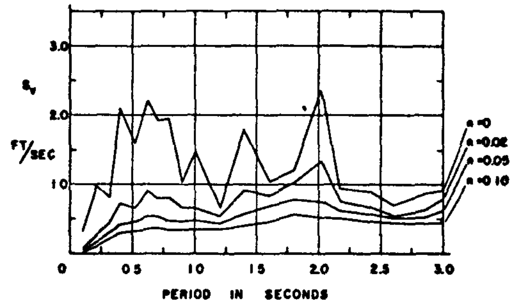

VELOCITY SPECTRA OF ARTIFICIAL EARTHQUAKE NO. 4

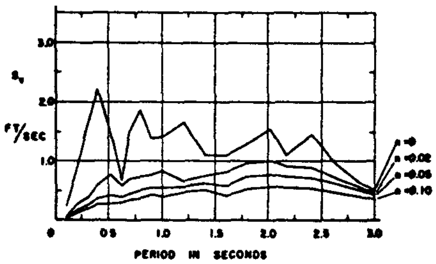

VELOCITY SPECTRA OF ARTIFICIAL EARTHQUAKE NO. 5

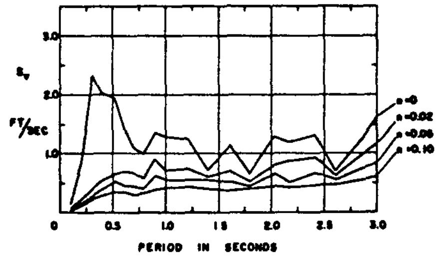

VELOCITY SPECTRA OF ARTIFICIAL EARTHQUAKE NO. 6

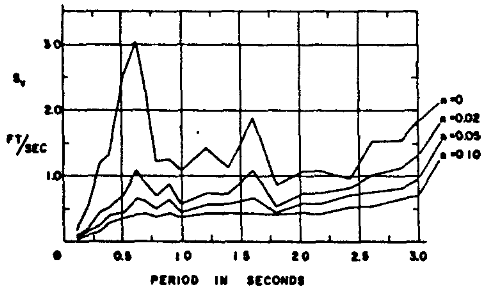

VELOCITY SPECTRA OF ARTIFICIAL EARTHQUAKE NO. 7

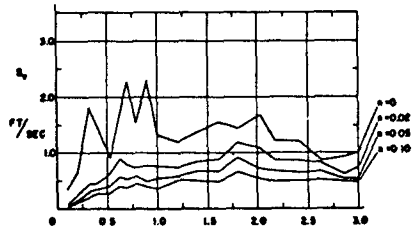

VELOCITY SPECTRA OF ARTIFICIAL EARTHQUAKE NO. 8

FIGURE A-5. DAMPED VELOCITY SPECTRA FOR STATIONARY ARTIFICIAL EARTHQUAKES (REFERENCE A-6) in which

$\ddot{x}(t)$ = Stationary random process

$E(t)$ = Time dependent envelope function

The envelope functions utilized are shown in Figure A-6. Segments of the resulting nonstationary earthquake records are described in Table A-4 and Figure A-7.

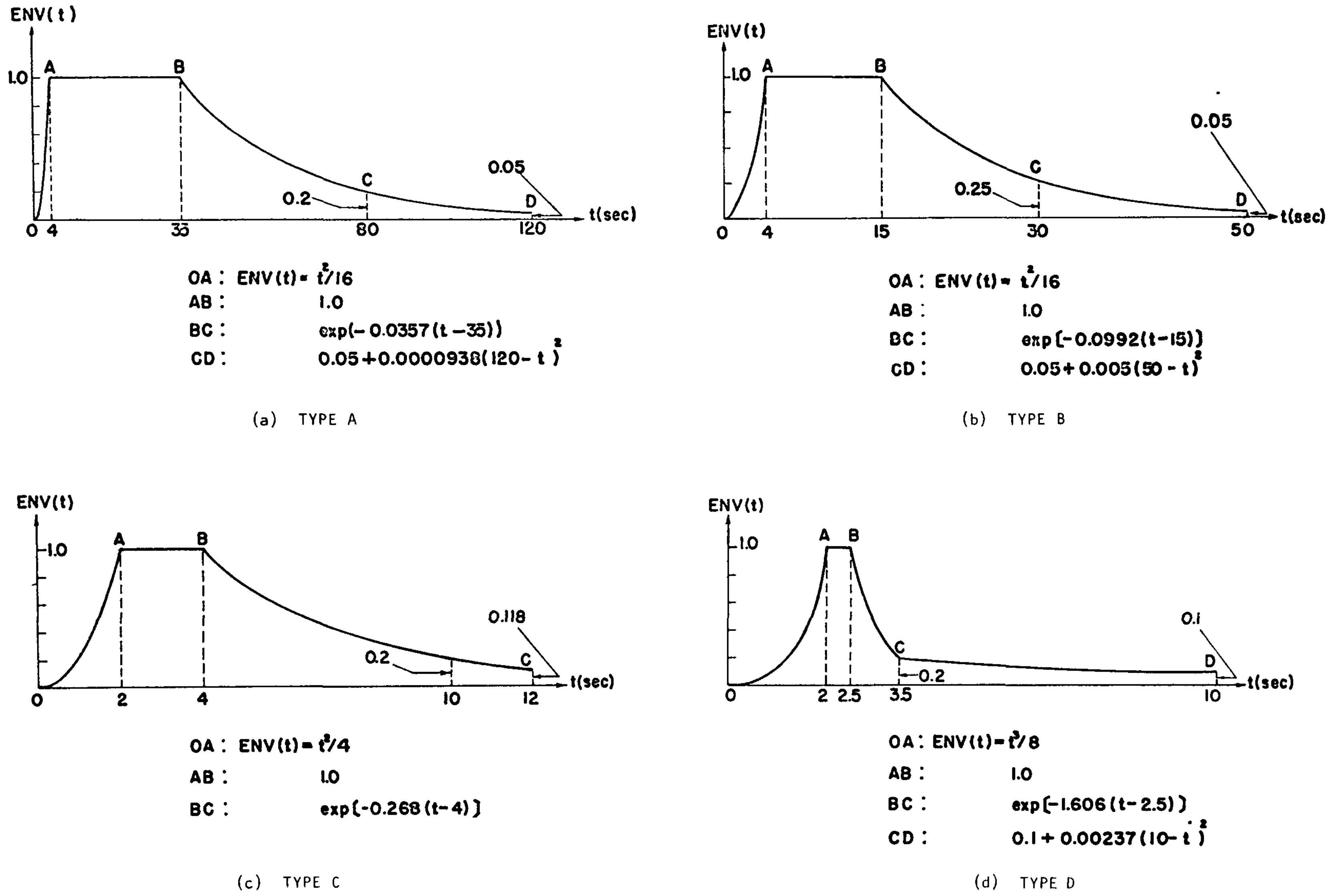

FIGURE A-6. ENVELOPE FUNCTIONS FOR NONSTATIONARY EARTHQUAKES (REFERENCE A-7)

TABLE A-4. DESCRIPTION OF NONSTATIONARY ARTIFICIAL EARTHQUAKE RECORDS (REFERENCE A-7)

Simulated Earthquake Type	Type of Earthquake Motion	Spectrum Intensity of Earthquake (Damping ratio = 0.2)	Total Duration, sec	Duration of Strong Motion, sec
A	Represents upper bound for ground motions expected near causitive fault during earthquake having Richter Magnitude 7-8.	150 percent as strong as average spectrum intensity of 1940 El Centro records.	120	29
B	Models shaking close to fault in Magnitude 7 earthquake (e.g., 1940 El Centro and 1952 Taft).	Equal to average spectrum intensity of 1940 El Centro records.	50	11
C	Simulates motion expected in epicentral region of Magnitude 5.5-6.0 shock (e.g., 1957 San Francisco and 1935 Helena, Montana).	Equal to average spectrum intensity of 1957 Golden Gate records.	12	2
D	Models shaking close to fault of very shallow Magnitude 4.5-5.5 earthquake (e.g., 1966 Parkfield, California).	Maximum acceleration scaled to be equal to that of Parkfield record (0.5 g).	10	0.5

Notes:

(a) Intensity of earthquakes is measured by spectrum intensity for Earthquakes A, B, C, and by peak accelerations in Earthquake D. Spectrum intensity defined as

$$SI_n = \int_{0.1}^{2.5} S_v(n,T)\,dT$$

S_v = Velocity spectrum as function of period T and critical damping ratio, n. For scaling purposes, n = 0.2 was chosen.

(b) Envelopes for Earthquakes A-D are given in Figure A-6.

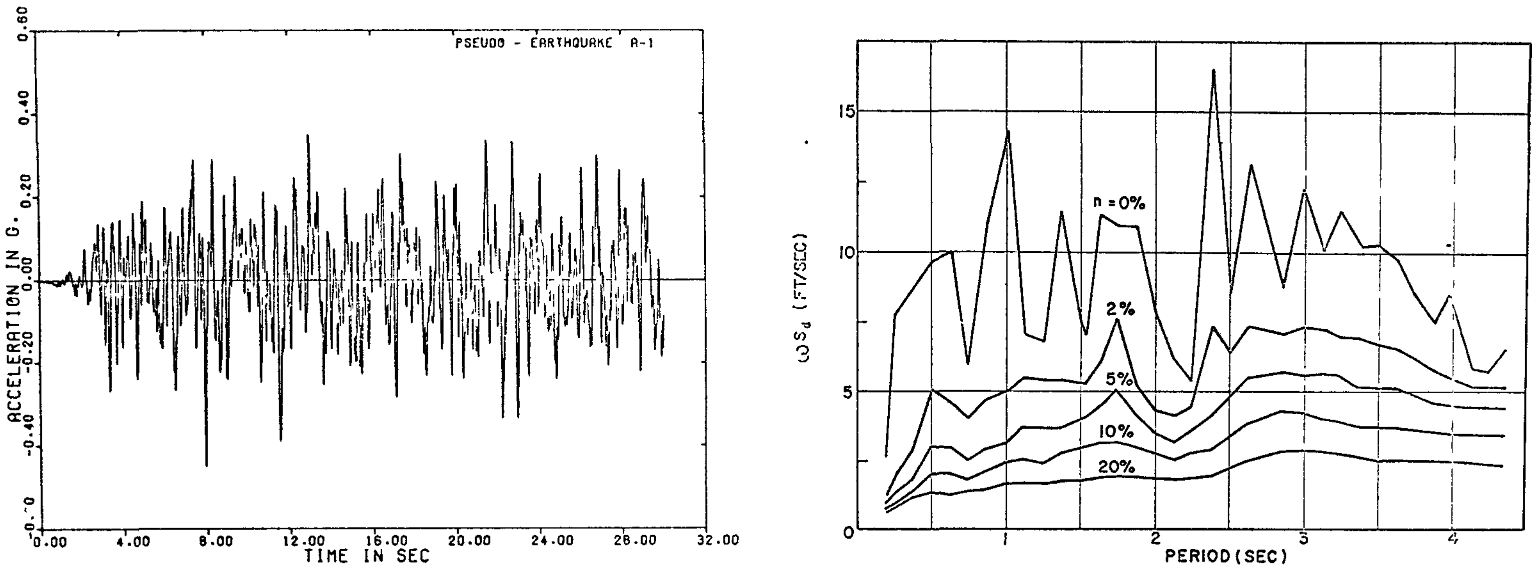

(a) EARTHQUAKE A-1

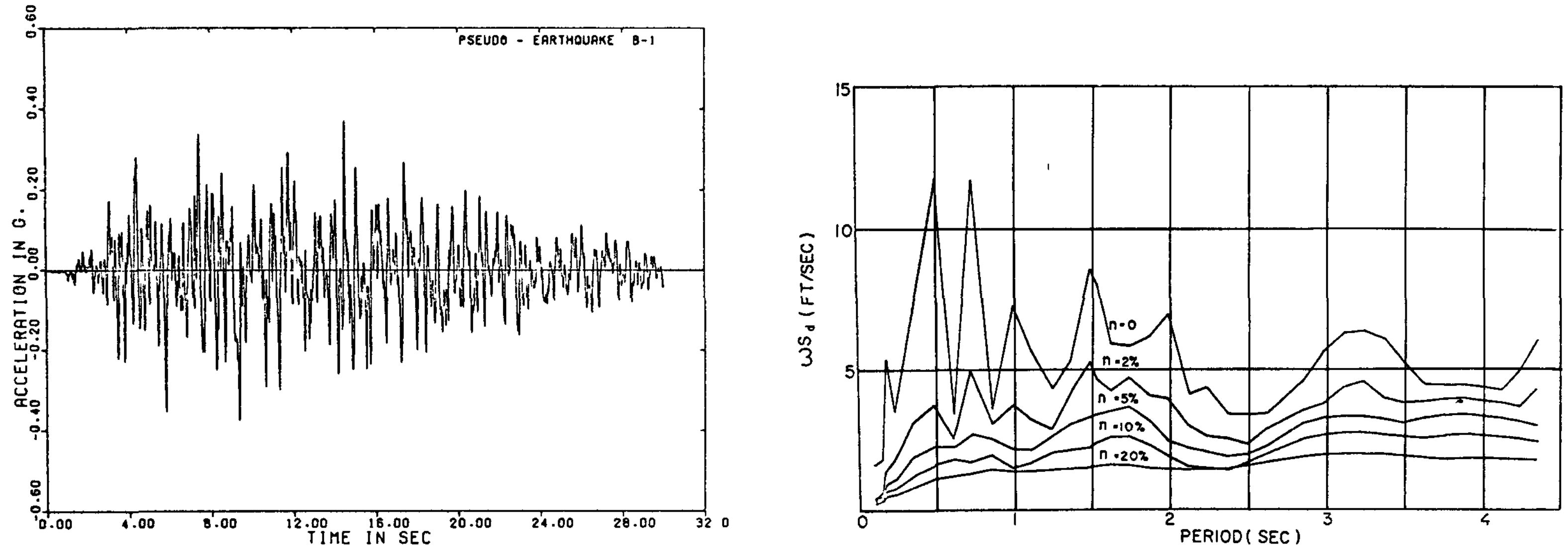

(b) EARTHQUAKE B-1

FIGURE A-7. ACCELEROGRAMS AND RESPONSE SPECTRA OF NONSTATIONARY EARTHQUAKES (REFERENCE A-7)

R-6914-925

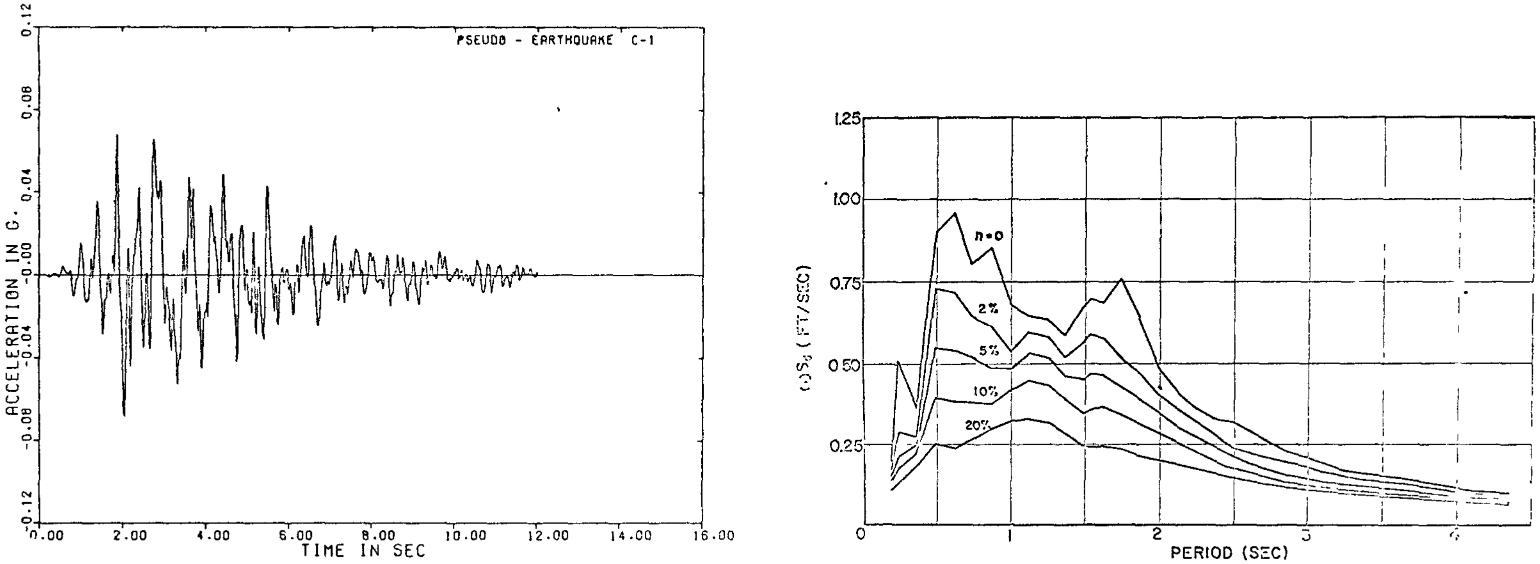

(c) EARTHQUAKE C-1

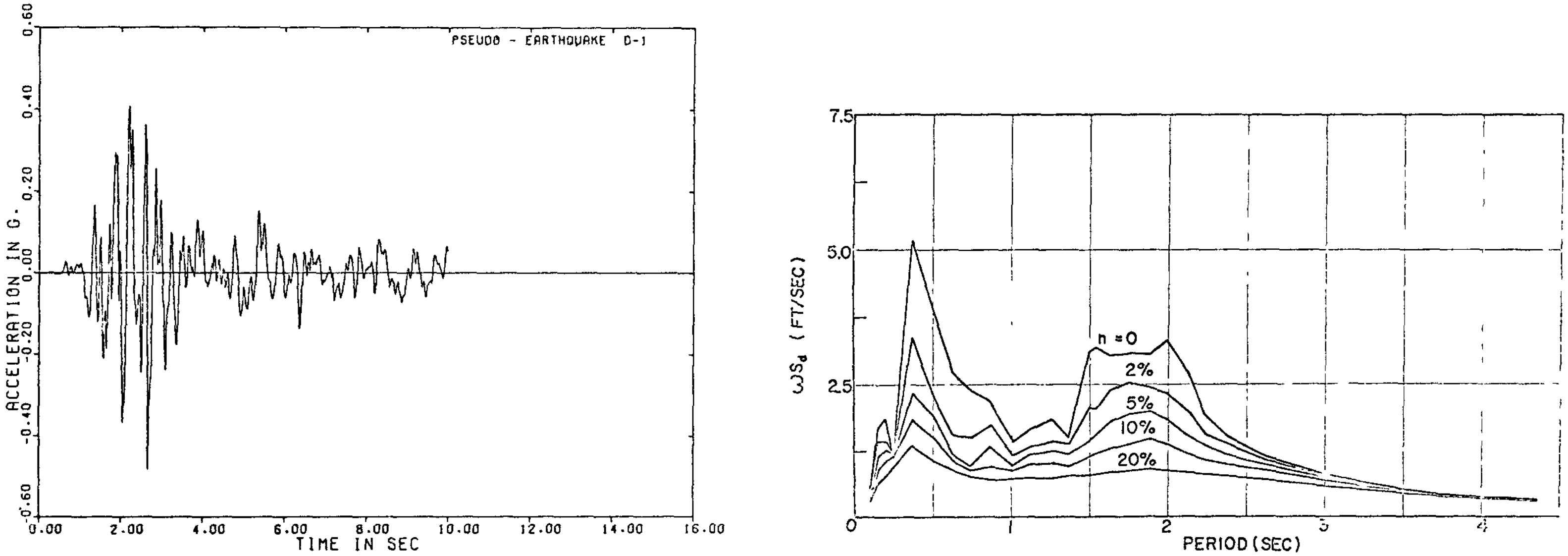

(d) EARTHQUAKE D-1

FIGURE A-7. (CONTINUED)

A.3 SUGGESTED FIRST-LEVEL APPROACH

Based on the discussion in the preceding sections, a first-level approach for the selection of seismic input at a site is now suggested. Criteria spectra have been chosen to represent average strength levels for regions of high, moderate, low, and minimal seismicity. In addition, an ensemble of earthquake records, whose dynamic characteristics correspond to those of the criteria spectra, have been provided. These records, when properly scaled, can be used as input into a calculation of the response time history of the power plant (including soil-structure interaction effects).

A.3.1 CRITERIA SPECTRA FOR SEISMIC REGIONS

The criteria spectra suggested for this first-level approach are shown in Figures A-9(a) and (b). It is noted that the spectra indicated correspond to the Design Basic Earthquake (DBE) average strength levels for regions of high, moderate, low, or minimal seismicity. The seismicity classification for a nuclear reactor site should be selected after careful study by qualified geologists and engineers.

The criteria spectra have the shape of the average spectra obtained by Housner for strong motion earthquakes (Figure A-4). These spectra are for an oscillator damping ratio of 0.05, since this appears to be a reasonable estimate of the damping levels anticipated for the rocking mode in nuclear reactor structures (Reference A-4). Other damping levels, which are not shown, can be scaled from Figure A-4. The DBE criteria spectra have been scaled to correspond to the peak accelerations specified in Table A-5.

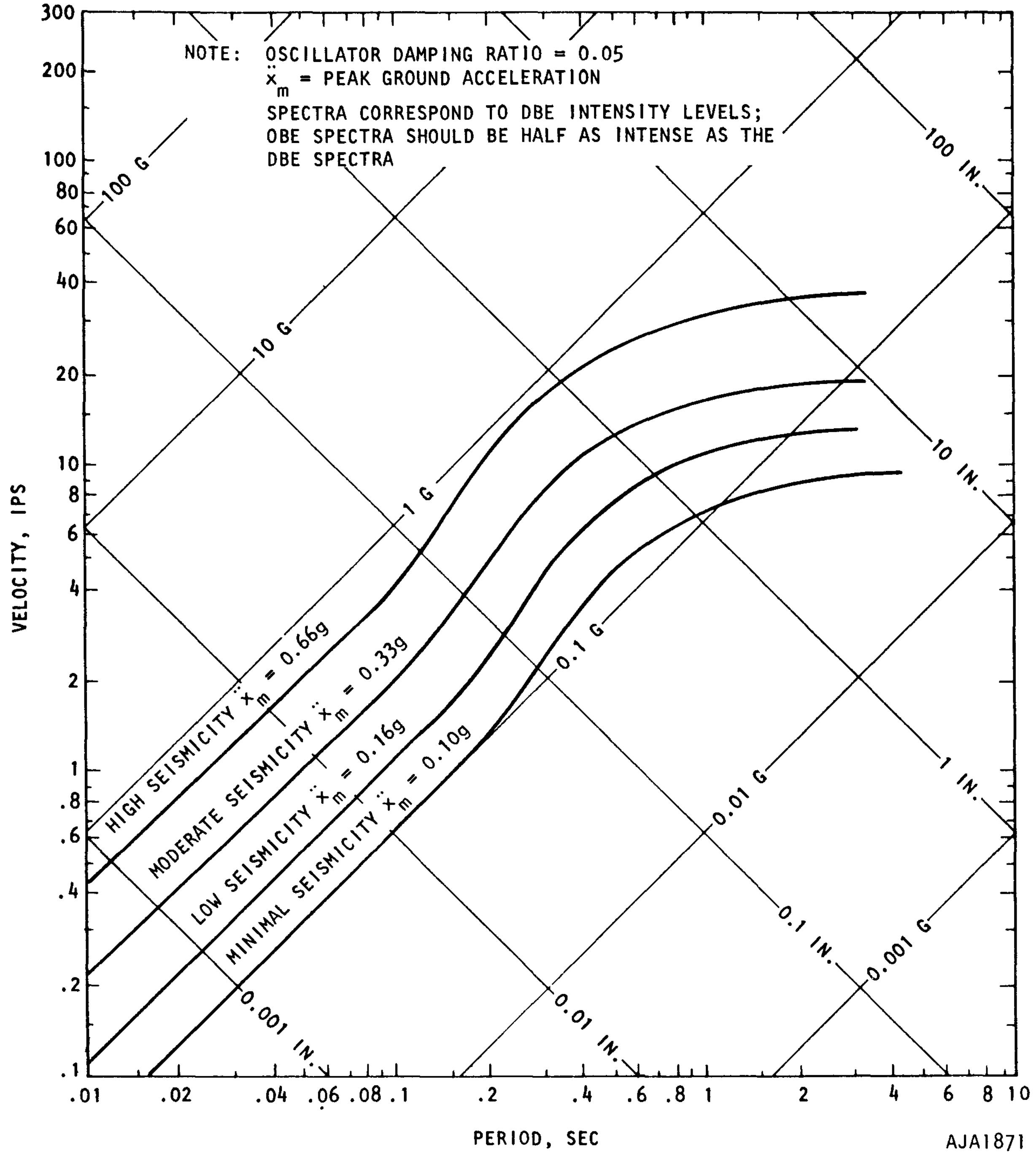

(a) TRIPARTITE PLOT

FIGURE A-8. DESIGN BASIS EARTHQUAKE CRITERIA SPECTRA

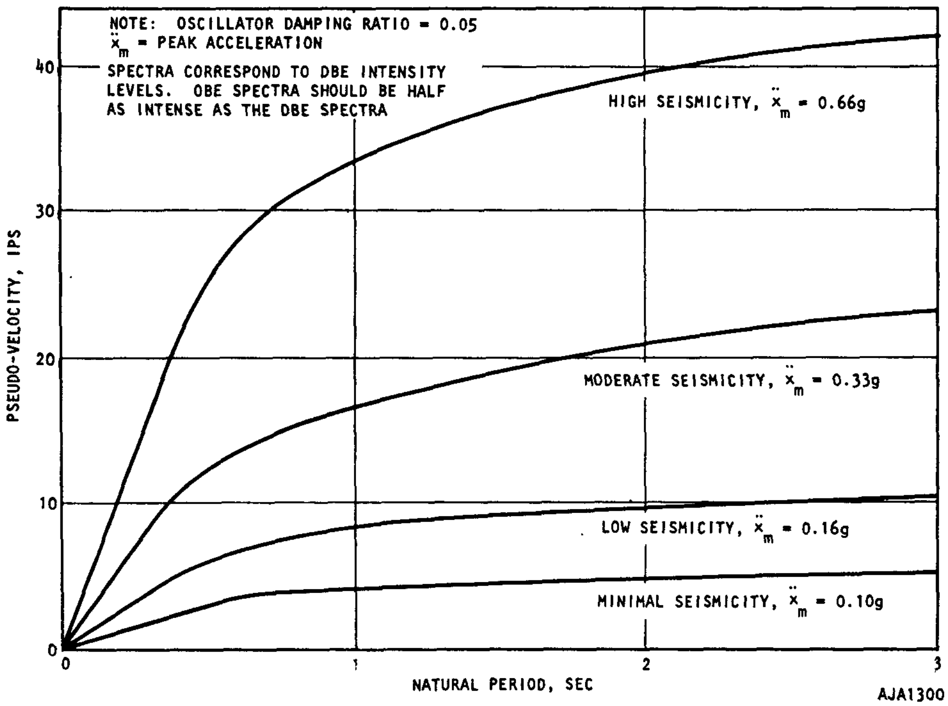

(b) ARITHMETIC SCALE PLOT

FIGURE A-8. (CONTINUED)

TABLE A-5. SUGGESTED DBE PEAK ACCELERATION LEVELS FOR FIRST-LEVEL APPROACH

Seismicity of Region	Peak Acceleration in g's
High	0.66
Moderate	0.33
Low	0.16
Minimal	0.10

Note: OBE peak acceleration levels are half those indicated above for the DBE.

The strength, frequency content, and duration of strong earthquake motions at a site are dependent on the local site properties as well as on the seismicity of the region. An analysis technique that considers the effects of localized soil properties should therefore be used to estimate earthquake motions at a reactor site. However, there are a number of uncertainties inherent in the scaling procedures and in the mathematical models currently available for this purpose. Therefore, it is intended that the results of the first-level approach, which are based on existing strong motion earthquake measurements, should serve as a basis for comparison with analytical techniques used for predicting site-dependent earthquake ground motions.

A.3.2 ENSEMBLE OF RECORDS FOR FIRST-LEVEL APPROACH

It was judged that an ensemble of at least four earthquake records would be needed to model statistical characteristics of the earthquake motions in an adequate manner. Therefore, the following strong motion accelerograms have been chosen:

a. 1940 El Centro, N-S Component

b. 1934 El Centro, E-W Component

c. 1949 Olympia, S10E Component

d. 1952 Taft, S69E Component

In general, these particular components of each of the strong motion earthquakes were chosen on the basis of the smoothness of the 5 percent damped response spectra. The acceleration, velocity and displacement waveforms of these earthquake components are shown in Figures A-3(a) through (d).

The minimum size ensemble given above is a sampling of strong motion earthquake records. Other records can be used in addition to these four records to form a larger sample of the statistical process being considered in this first-level approach. Some records feasible for use in this manner are:

a. The other horizontal component of the strong motion earthquake records indicated above

b. The stationary artificial earthquakes described in Reference A-6

c. The Type B nonstationary artificial earthquakes described in Reference A-7

The scaling of the above ensemble is based on a comparison of the spectrum intensity of each member to that of the various criteria spectra. The spectrum intensity of an earthquake has been defined by Housner to be the area under its pseudo-velocity spectrum between periods of 0.1 to 2.5, as indicated in Table A-4.

As shown in Reference A-8, a linear relationship exists between the scaling of the acceleration ordinates of an earthquake record and the scaling of the amplitudes of its response spectrum. This linear scaling relationship has been used to scale each record in the ensemble so that its spectrum intensity equals the spectrum intensity of the criteria spectra for each seismic zone. The 5-percent damped pseudo-velocity spectra for each record in the ensemble are shown in Figure A-9 and the resulting scale factors are given in Table A-6.

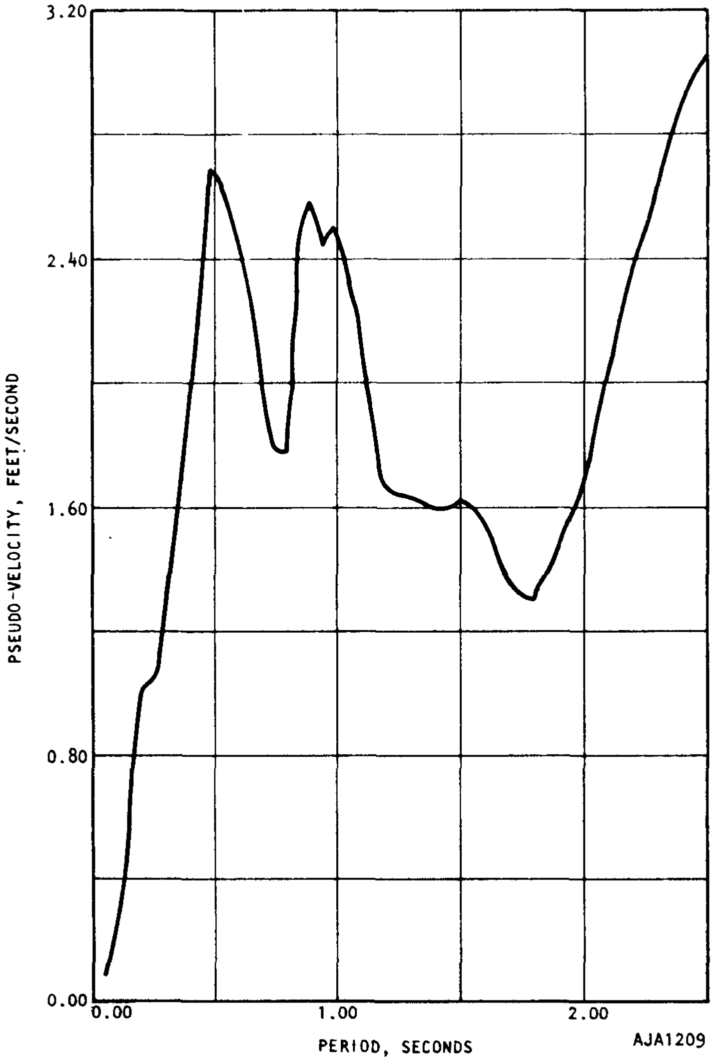

(a) 1940 EL CENTRO, NS

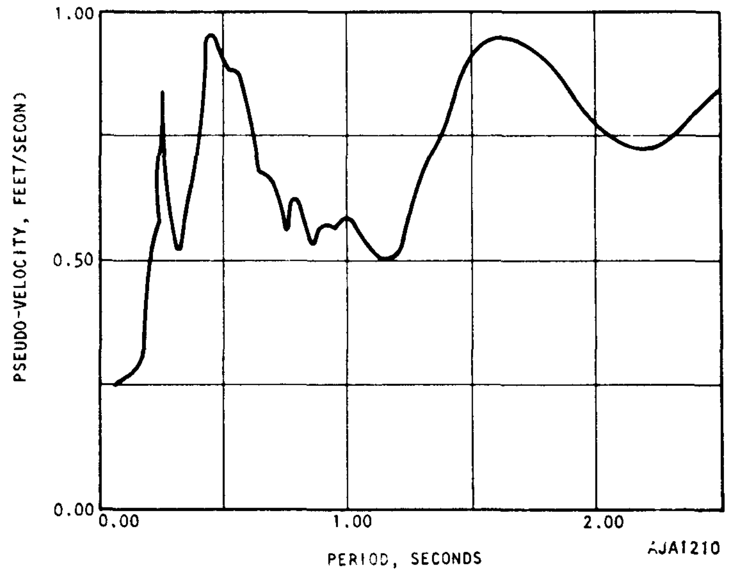

(b) 1934 EL CENTRO, EW

FIGURE A-9. RESPONSE SPECTRA OF SUGGESTED MINIMUM SIZE ENSEMBLE (OSCILLATOR DAMPING RATIO = 0.05)

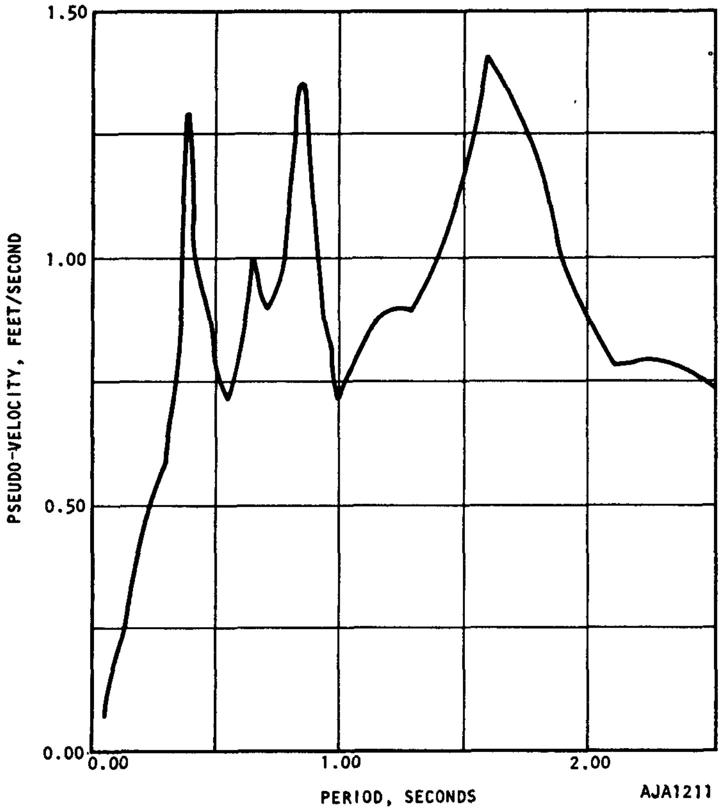

(c) 1952 TAFT, S69E

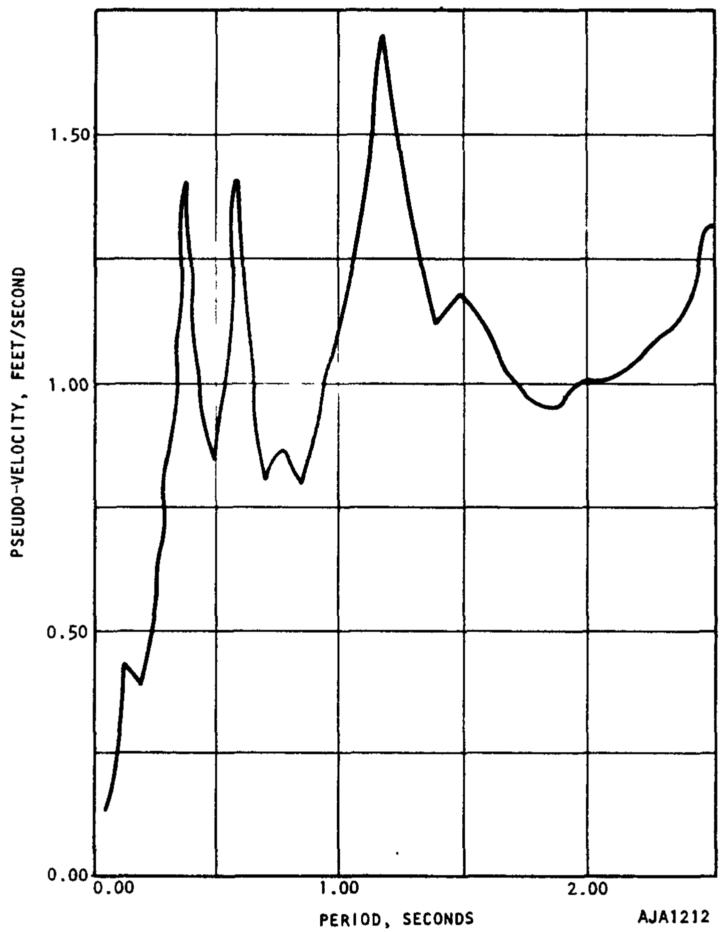

(d) 1949 OLYMPIA, S10E

FIGURE A-9. (CONTINUED)

AJA

TABLE A-6. SCALE FACTORS FOR EARTHQUAKE ENSEMBLE IN FIRST-LEVEL APPROACH

Earthquake Record	Spectrum Intensity, in.	Scale Factors for Design Basis Earthquake			
		High Seismicity	Moderate Seismicity	Low Seismicity	Minimal Seismicity
1940 El Centro, NS Component	50.2	1.59	0.80	0.38	0.19
1934 El Centro, EW Component	21.6	3.70	1.86	0.88	0.44
1949 Olympia S10E Component	33.0	2.42	1.22	0.58	0.29
1952 Taft S69E Component	27.0	2.96	1.48	0.72	0.36

Note:

- Spectrum Intensities of Design Basis Earthquakes in Each Seismic Region:

  High Seismicity: 80 in. ($\ddot{x}_m$ = 0.66 g)

  Moderate Seismicity: 40 in. ($\ddot{x}_m$ = 0.33 g)

  Low Seismicity: 19.2 in. ($\ddot{x}_m$ = 0.16 g)

  Minimal Seismicity: 9.6 in. ($\ddot{x}_m$ = 0.10 g

- Scale Factors for the OBE in each seismic region should be reduced by a factor of 2 from those indicated above for the DBE.

R-6914-925

A.4 INTERPRETATION OF RESPONSE STATISTICS

Both the criteria spectra and ensemble of scaled time histories are intended to represent the expected properties of the ground motion at a site. The approaches are somewhat different, however, and some interpretation is necessary to make them consistent with each other for a given level of earthquake strength.

The design spectra shown in Figure A-8 provide an overall level of structural strength that varies with frequency in the same manner as the average properties of strong earthquakes; this structural strength level is adjusted to represent the seismic hazard at the site. Statistical fluctuations do not arise directly in using this approach, nor for that matter, when using the static loading approach embodied in the seismic loading sections of building codes.

When using the time histories in response calculations, however, the statistical nature of the earthquake problem will confront the engineers in a direct manner. The time histories have been scaled to have the same spectrum intensity as the design spectra, so there will be portions of the spectra of the individual time histories which are above, and others below, the smooth curves of Figure A-8.

In this first-level approach, consistency is maintained between the spectral and time history approaches by requiring the structure to meet the *average* response from the ensemble with the same stress levels that are appropriate for the smooth spectra of the same level, whether it is the OBE or the DBE. It is not required, then, that stress and deflection limits be met for each member of the ensemble, but only for the ensemble average response. To require the stress and deflection limits to be met for each member of the ensemble would specify an average level of resistance significantly greater than that required by the smooth spectra of Figure A-8 with the same spectrum intensity.

In summary then, for both the OBE and DBE levels, only the average values of response, averaged over the four records, should be used in determining the strength of the structure when using the time-history approach. With this interpretation, the design spectrum and time-history methods suggested here in this first-level approach will be consistent. Of course, the statistical fluctuations in response, if interpreted correctly, will give the design engineers additional insight into the earthquake behavior of his proposed design.

APPENDIX A

REFERENCES

A-1. Algermissen, S. T., "Seismic Risk Studies in the Unites States," *Fourth World Conference on Earthquake Engineering*, Santiago, Chili, January, 1969.

A-2. Housner, G. W., "Design of Nuclear Power Reactors Against Earthquakes," *Second World Conference on Earthquake Engineering*, Tokyo, Japan, July 1960.

A-3. Housner, G. W., "Behavior of Structures During Earthquakes," *Engineering Mechanics Division, Proceedings of American Society of Civil Engineers*, Vol. 85, No. EM4, October 1959.

A-4. Newmark, N. M., and W. J. Hall, "Seismic Design Criteria for Nuclear Reactor Facilities," *Fourth World Conference on Earthquake Engineering*, Santiago, Chile, January 1969.

A-5. Berg, G. V., and G. W. Housner, "Integrated Velocity and Displacement of Strong Earthquake Ground Motion," *Bulletin of the Seismological Society of America*, Vol. 51, No. 2, April 1961.

A-6. Housner, G. W., and P. C. Jennings, "Generation of Artificial Earthquakes," *Engineering Mechanics Division, Proceedings of American Society of Civil Engineers*, Vol. 90, No. EM1, February 1964.

A-7. Jennings, P. C., G. W. Housner, and N. C. Tsai, "Simulated Earthquake Motions for Design Purposes," *Fourth World Conference on Earthquake Engineering*, Santiago, Chile, January 1969.

A-8. Tsai, N. C., "Transformation of Time Axes of Accelerograms," Technical Note, *Engineering Mechanics Division, Proceedings of American Society of Civil Engineers*, Vol. 95, No. EM3, June 1969.

APPENDIX B

ANALYSIS OF DAMPING IN A HOMOGENEOUS SHEAR BEAM

In this appendix, expressions will be formulated for the modal damping ratios in a homogeneous shear beam with absolute damping and relative damping mechanisms. This is intended to provide background information for the discussion contained in Subsection 4.4.3.

B.1 HOMOGENEOUS SHEAR BEAM WITH ABSOLUTE DAMPING

Consider a shear beam with a damping force proportional to velocity, i.e.,

$$F_a = C_1 \frac{\partial x}{\partial t} \tag{B-1}$$

where x is the transverse displacement of the shear beam, t is the time variable, and C_1 is a constant of proportionality. The free vibration equation of motion of the shear beam for this case is

$$\rho A \frac{\partial^2 x}{\partial t^2} + C_1 \frac{\partial x}{\partial t} - GA \frac{\partial^2 x}{\partial z^2} = 0 \tag{B-2}$$

where ρ is the mass density, A the cross section area, G the shear modulus, and z the axial dimension of the shear beam.

Now, let us assume

$$x(z,t) = \sum_{n=1}^{\infty} \zeta_n(t) \sin \frac{(2n-1)\pi z}{2\ell} \tag{B-3}$$

where ℓ is the height of the shear beam. Substituting into Equation B-2, results in a series of equations of motion of the form:

$$\ddot{\zeta}_n + \frac{C_1}{\rho A}\dot{\zeta}_n + \frac{G}{\rho}\left[\frac{(2n-1)\pi}{2\ell}\right]^2 \zeta_n = 0 \qquad (n = 1,2,---) \tag{B-4}$$

where a dot refers to differentiation with respect to time. Now the frequency of the n^{th} mode of a homogeneous shear beam is expressed as

$$\omega_n = \frac{(2n-1)\pi}{2\ell}\sqrt{\frac{G}{\rho}} \tag{B-5}$$

so that Equation B-4 takes the form

$$\ddot{\zeta}_n + \frac{C_1}{\rho A}\dot{\zeta}_n + \omega_n^2 \zeta_n = 0 \qquad (n = 1,2,---) \tag{B-6}$$

The usual form of equation of motion for the n^{th} mode of a multidegree-of-freedom system is

$$\ddot{\zeta}_n + 2\psi_n\omega_n\dot{\zeta}_n + \omega_n^2\zeta_n = 0 \tag{B-7}$$

where ψ_n is the damping ratio for the n^{th} mode.

Comparing coefficients of $\dot{\zeta}_n$ in Equations B-6 and B-7, the modal damping ratio for the n^{th} mode of a homogeneous shear beam with absolute damping takes the form:

$$\psi_n = \frac{C_1}{2\omega_n \rho A} \tag{B-8}$$

B.2 HOMOGENEOUS SHEAR BEAM WITH RELATIVE DAMPING

Consider a shear beam with a damping force proportional to strain rate, i.e.,

$$F_d = -C_2 \frac{\partial}{\partial t}\left(\frac{\partial^2 x}{\partial z^2}\right)$$

For this case, the free vibration equation of motion for a homogeneous shear beam is

$$\rho A \frac{\partial^2 x}{\partial t^2} - C_2 \frac{\partial^3 x}{\partial z^2 \partial t} - GA \frac{\partial^2 x}{\partial z^2} = 0 \qquad \text{(B-9)}$$

If we assume x to be of the form given in Equation B-3, Equation B-9 takes the form:

$$\ddot{\zeta}_n + \frac{C_2}{\rho A}\left(\frac{2n-1}{2\ell}\right)^2 \dot{\zeta}_n + \frac{G}{\rho}\left(\frac{2n-1}{2\ell}\right)^2 \zeta_n = 0$$

or, upon substituting ω_n^2 from Equation B-5

$$\ddot{\zeta}_n + \frac{C_2}{GA}\omega_n^2 \dot{\zeta}_n + \omega_n^2 \zeta_n = 0 \qquad \text{(B-10)}$$

Comparing coefficients of $\dot{\zeta}_n$ in Equations B-7 and B-10, the modal damping ratio for the n^{th} mode of a homogeneous shear beam with relative damping takes the form,

$$\psi_n = \frac{C_2 \omega_n}{2GA} \qquad \text{(B-11)}$$

B.3 SUMMARY

The damping ratio for the n^{th} mode of a homogeneous shear beam with absolute and relative damping is seen from Equations B-8 and B-11 to take the form

$$\psi_n = \frac{C_1}{2\omega_n \rho A} + \frac{C_2 \omega_n}{2GA}$$

This corresponds to Equation 4-13 in Subsection 4.4.3.